Synthesis of Rotaxanes and Pseudorotaxanes as Intermediates towards Molecular Cages

by

Damian Franz Weske

A thesis submitted to the University of Birmingham for the degree of

Doctor of Philosophy

School of Chemistry

University of Birmingham

January 2013

Abstract

The work described in this thesis concerns the synthesis of novel rotaxanes and pseudorotaxanes as intermediates towards molecular cages. The area of rotaxanes and cage molecules was reviewed and selected examples discussed in detail.

Three main strategies to synthesise a fumaramide thread were investigated, however these were unsuccessful. By changing the templating station and the stopper groups, several novel azo-dicarboxylate threads were synthesised, as well as their [2]- and [3]rotaxanes. Unusual reductions of the azo-dicarboxylate stations during the clipping processes were observed and these were studied in detail.

A couple of different stopper groups from those initially used, provided several novel double fumaramide threads and rotaxanes in high yields

Linking reactions of the two macrocycles of the newly synthesised [3]rotaxanes to form a molecular cage were investigated. However, reduction of the macrocycles was required, which led to deslipping of the macrocycles. Therefore, new routes to generate rotaxanes with bulkier stopper groups were explored.

In the final section, novel pseudorotaxanes were synthesised and detected via ^{1}H NMR spectroscopy and mass spectrometry. By linking the two macrocycles of a [3]pseudorotaxane, a molecular cage was formed.

Acknowledgments

First of all I would like to thank Professor Nigel S. Simpkins for the opportunity to undertake a PhD in his laboratory, for the interesting and challenging project, as well as for his guidance over the past three years.

Secondly, I would like to thank the School of Chemistry and the University of Birmingham for their financial support. I would also like to thank the Analytical Facility, specially to Graham Burns, Peter Ashton, Dr. Neil Spencer, Dr. Louise Male and Dr. Chi Tsang for their hard work.

I would like to thank the past and present members of the Simpkins group. Special thanks go to Fred, Bick, Ilias, Pete, Matt, Giorgio, Bhaven, Shamim, Luke, Bene, Lucia, Carlos, Andrea, Luca and Sebastien for all the good times together.

I am grateful to Dr. Richard Grainger and Dr. Jim Tucker for their advice during my project and keeping always an open door for my questions.

I would also like to thank Mike, Tom, Dave, Huy, Bhaven and Natalia for their help at some point during my PhD.

A big thanks to Jenna and Chris for the nice days out and to Mark and Amanda for a great trip across Scotland and their overwhelming hospitality.

I would like to express my deepest gratitude to Carina, Nora, Katharina and my mum, for their love and support during all my life.

Last but not least, I would like to thank Natalia for making my life incredibly amazing, for all her support, love and humour that made my time in Birmingham the best of my life.

Table of Contents

Glossary

aq.	aqueous
BtH	benzotriazole
cat.	catalyst, catalytic
conc.	concentrated
CuAAC	copper(I)-catalysed azide-alkyne cycloaddition
Da	dalton
DBU	1,8-diazabicyclo[5.4.0]undec-7-ene
decomp.	decomposition
DFT	density functional theory
DMAP	4-(dimethylamino)pyridine
DMF	*N*,*N*-dimethylformamide
DMSO	dimethylsulfoxide
DNA	deoxyribonucleic acid
EDC	1-ethyl-3-(3-dimethylaminopropyl)carbodiimide
EI	electron impact
eq.	equivalent

ES+	electrospray, positive ionisation mode
ES-	electrospray, negative ionisation mode
HATU	1-[bis(dimethylamino)methylene]-1*H*-1,2,3-triazolo[4,5-*b*] pyridinium 3-oxid hexafluorophosphate
HOAt	1-hydroxy-7-azabenzotriazole
HoBt	hydroxybenzotriazole
HPLC	high pressure liquid chromatography
IBCF	isobutyl chloroformate
IR	infrared spectroscopy
Lit.	literature value
MALDI	matrix assisted laser desorption ionisation
m.p.	melting point
MS	mass spectrometry
NBS	*N*-bromosuccinimide
NMM	*N*-methylmorpholine
NMR	nuclear magnetic resonance
pet	petroleum ether
ppm	parts per million

py	pyridine
RT	room temperature
R_t	retention time
TLC	thin layer chromatography
ToF	time of flight
Å	Angström (10^{-10} meters)
ν	frequency

Chapter 1: Introduction

1.1 Supramolecular chemistry

In 1987 the Nobel prize in chemistry was awarded to Cram, Pedersen and Lehn. Jean-Marie Lehn is still one of the leading proponents in the area of supramolecular chemistry and defined it as "chemistry beyond the molecule".[1] The most important attribute of a supramolecular system is that several components (host and guest) are held together via reversible intermolecular interactions. In contrast to supramolecular systems, molecular systems are mainly connected via covalent bonds. Supramolecular chemists are able to synthesise covalently bonded molecular building blocks, which are held together by intermolecular forces to create functional architectures.[2] These intermolecular forces can be electrostatic (ion-ion, ion-dipole and dipole-dipole), hydrogen bonding, π-π stacking, van der Waals, hydrophobic or solvatophobic interactions. These non-covalent interactions are generally much weaker than covalent bonds. The combination of several of these weak interactions generates a powerful interlocked system, and thus host molecules are able to selectively recognise a specific guest. As these interactions are reversible, host-guest products can sit either in a local or global thermodynamic energy minimum.

This type of lock and key principle can be compared to that used by Nature itself, *e.g.* in the reaction of a substrate with the active site of an enzyme as described by Emil Fischer in 1894.[3] Base pairing in DNA is another example, where two

antiparallel strands are held together by hydrogen bonds between complementary base pairs.[4] The receptor sites on the host (lock) are sterically and electronically complementary to the guest (key). Therefore, the host is highly selective for only one substrate favouring one single product.

1.2 Rotaxanes and catenanes

Rotaxanes and catenanes are the two main classes of mechanically interlocked molecules.[5] Mechanically interlocked molecules possess two or more separate covalent components. These components are connected via mechanical bonds, which are described as bonds that prevent dissociation. When one of the covalent bonds is cleaved, the components will dissociate. Catenanes are formed of two or more interlocked macrocycles (Figure 1.1)[6], while rotaxanes are made of at least one macrocycle and one thread with two stoppers, which prevent the dissociation of the components (Figure 1.2).[7,8]

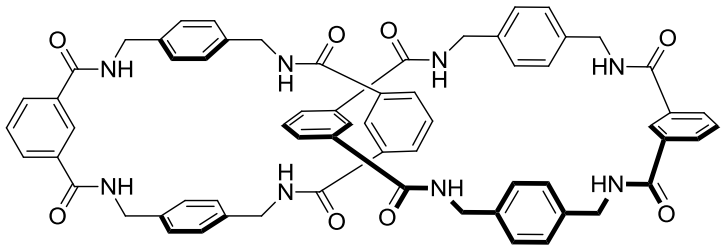

Figure 1.1: Structure of a [2]catenane.[6]

Catenanes are topological isomers and their rings cannot be dissociated without notionally breaking at least one covalent bond. In the other hand, rotaxanes can be separated via deformations of one of the components, *e.g.* a macrocycle can

stretch and this might cause its slipping over the stoppers and therefore dissociation from the thread. In other words, rotaxanes are threaded species stabilised by steric interactions.

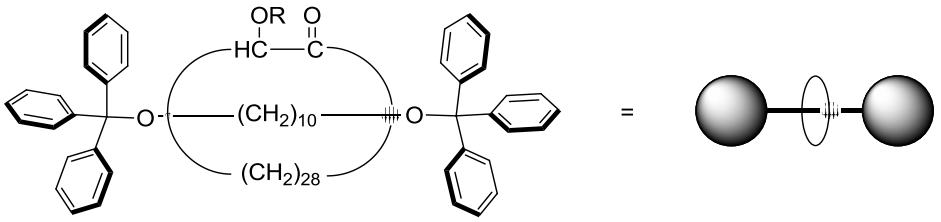

Figure 1.2: First [2]rotaxane synthesised by Harrison and Harrison (left)[9] and the graphical representation of a [2]rotaxane (right).

The term rotaxane was first proposed by Schill and Zollkopf in 1967.[10] The nomenclature used is derived from the Latin where the word *rota* means wheel and the word *axis* means axle. In the same year, Harrison and Harrison synthesised the first [2]rotaxane with an overall yield of 6% (Figure 1.2).[9]

Due to the fascinating structure of rotaxanes, the development of straightforward procedures to synthesise this kind of compounds has been extensively explored, leading to synthetic strategies which generally follow one of three main routes. These three methods involve *threading* followed by *stoppering*, *slipping* or *clipping* (Figure 1.3).[11-19]

In the *threading* method, a preformed macrocycle is first coordinated onto a thread *via* attractive interactions. Stopper groups are then attached to the end of the thread, which prevent dissociation of the newly formed rotaxane.[11] In the *slipping* strategy, a pre-synthesised macrocycle is slipped over an already stoppered thread. The macrocycle and the stoppers have to be of the correct size to allow

the formation of the rotaxane. The rotaxane is formed by applying the right amount of thermal energy, *e.g.* by lowering the temperature, the macrocycle becomes kinetically trapped, thus forming the rotaxane.[19] The third approach is the *clipping* method, where a macrocycle is formed in the presence of a thread.[16] Usually an attractive interaction between the ring forming components and the thread is used to initially entrap the macrocycle to be, followed by a ring-closing reaction to form the rotaxane.

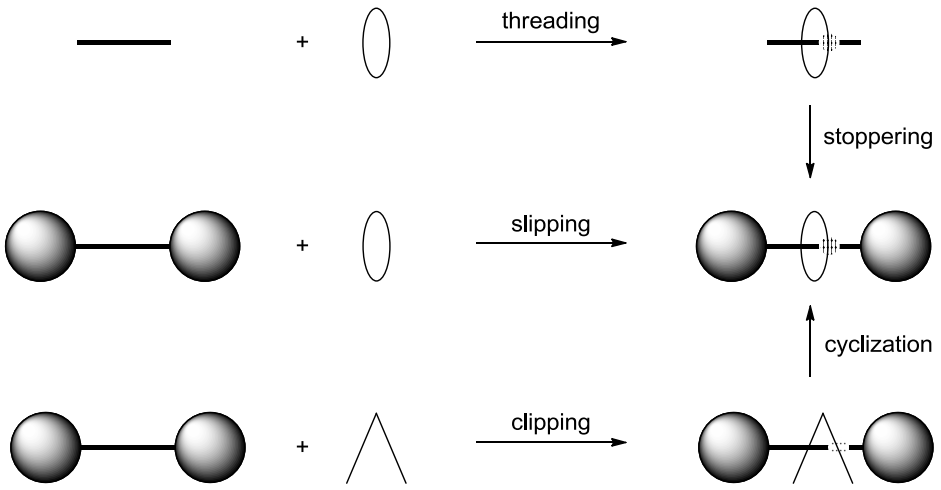

Figure 1.3: The three main methods for rotaxane assembly.

In 2007, Leigh and co-workers developed a new strategy for the synthesis of rotaxanes called the active metal template method, where a metal is used to promote the formation of the thread and the coordination of the preformed macrocycle (Figure 1.4).[20,21] This method was directly inspired by the work of Sauvage.[20]

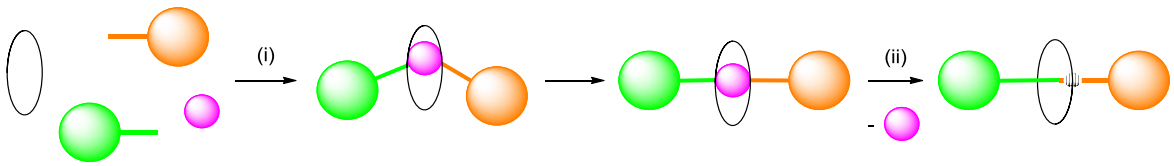

Figure 1.4: Active-metal template method for rotaxane formation; (i) template assembly and covalent bond forming catalysis, (ii) subsequent demetalation.

The two stopper units (shown in green and orange) generate the thread by the aid of the metal (shown in pink). At the same time the metal coordinates through the cavity of the macrocycle (shown in black) via metal to ligand interactions. In many cases, once the rotaxane is formed the metal can bind to another free macrocycle, as this is more favoured and can promote the next threading process.

1.2.1 Nomenclature of rotaxanes

Harrison and Harrison's first rotaxane shows the simplest rotaxane topology (Figure 1.2). It is designated as a [2]rotaxane, where the number in square brackets indicates the number of components, two, that is one macrocycle and one thread.

Generally, an [*n*]rotaxane consists of one thread and (*n* – 1) macrocycles or (*n* - 1) threads and one macrocycle. Figure 1.5 shows some fundamental rotaxane topologies.

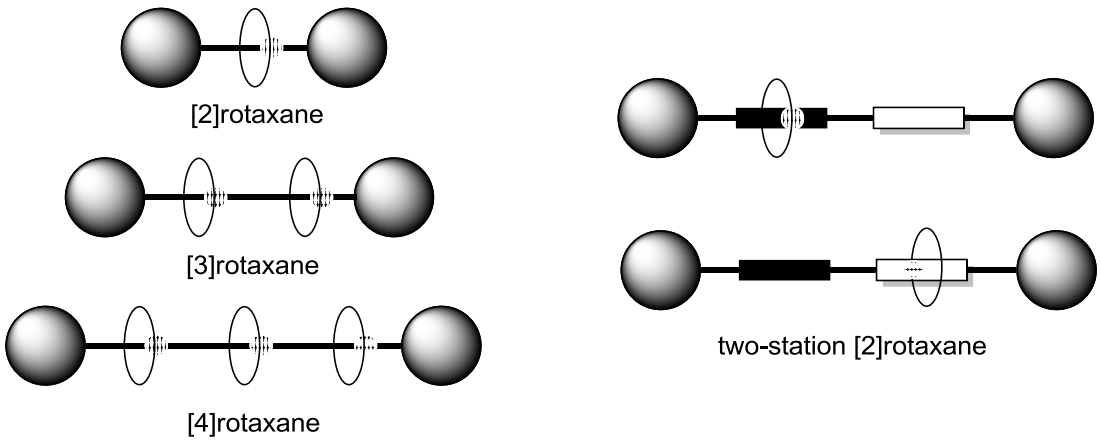

Figure 1.5: Some rotaxanes topologies.

[3]- and [4]rotaxanes are the corresponding higher analogues of the [2]rotaxane, with [3]rotaxanes being more common than [4]rotaxanes.[21,22]

The development of [2]rotaxanes with two separate sites or stations has been an important breakthrough for the synthesis of molecular switches, motors and machines.[23] These two stations, that can be either identical or different, can act as binding sites for the macrocycle. When the two stations are different, they can be addressed selectively using an external input. Hence, chemical, electrochemical, or photochemical stimulation can induce changes in the binding site by generating repulsive or attractive supramolecular interactions and therefore, the macrocycle can be 'shuttled' between the two stations along the thread (see Section 1.2.4). This induced discrimination process between the two stations is not possible when the two sites are identical, however shuttling can still occur.[24]

1.2.2 Hydrogen bonding based rotaxanes

Hydrogen bond interactions are known to assemble and stabilise various supramolecular complexes, such as catenanes and rotaxanes.[25] The first example of a hydrogen bond templated catenane was reported by Hunter *et al.* in 1992.[26] High dilution for the macrocyclisation yielded a [2]catenane in 34% yield, accompanied by the expected macrocycle in 51% yield. In 1995, Vögtle *et al.* reported the first example of an amide based [2]rotaxane via a three component threading procedure in a 11% yield.[27] This threading process was later improved by employing a more rigid thread with the preparation of a fumaric thread, which yielded the desired [2]rotaxane in 18% yield.[28] Leigh and co-workers have also described various examples of catenanes and rotaxanes templated via hydrogen bonding interactions. These rotaxanes are produced via a five component clipping reaction, as shown in Scheme 1.1.[29] Reaction of isophthaloyl dichloride and *p*-xylylenediamine forms the intermediate amide **I** in a *syn anti* conformation. In solution, this intermediate can undergo either a dimerisation, as described by Hunter[30] or a catenane formation process, as reported by Leigh.[31] However, in the presence of a suitable template (e.g. peptide thread **1**) a *syn syn* conformation (intermediate **II**) is favoured, as it is stabilised by multicomponent bifurcated hydrogen bonds. The terminal amine and the acid chloride are then close enough and a rapid cyclisation around the thread occurs (Scheme 1.1).[29]

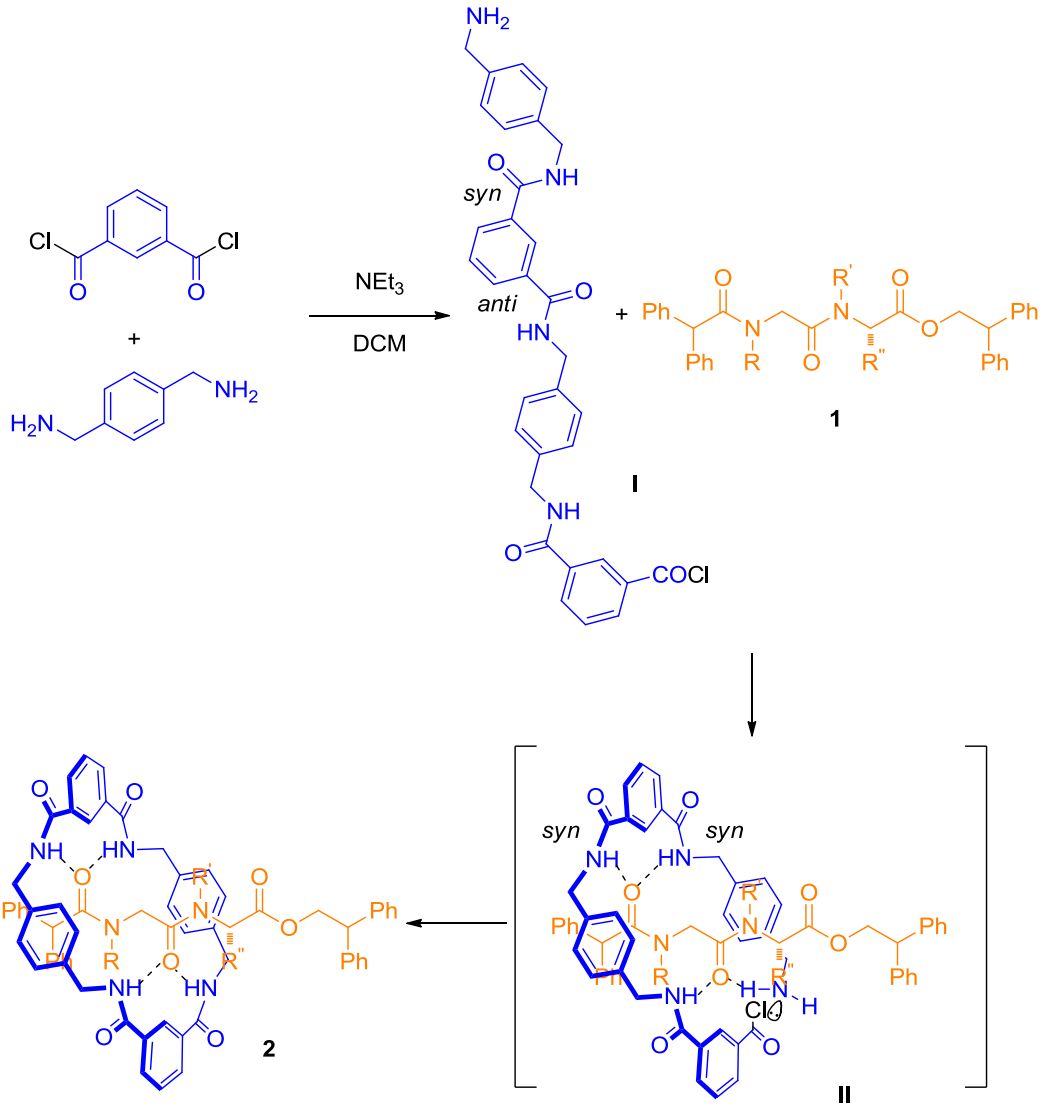

Scheme 1.1: Rotaxane formation around a peptide thread.

Several oligopeptide threads bearing at least one non *N*-terminal glycine residue were also investigated by Leigh and co-workers.[29] Figure 1.6 shows the crystal structures for the obtained Gly-Gly **3**, Gly-Sar **4** and Gly-L-Ala **5** [2]rotaxanes. By comparing the yields of the resulting [2]rotaxanes with the conformational structures of their macrocycles, Leigh rationalised that there is a relationship

between the final rotaxane and the intermediate **II**, which is key for the formation of the resulting rotaxane.

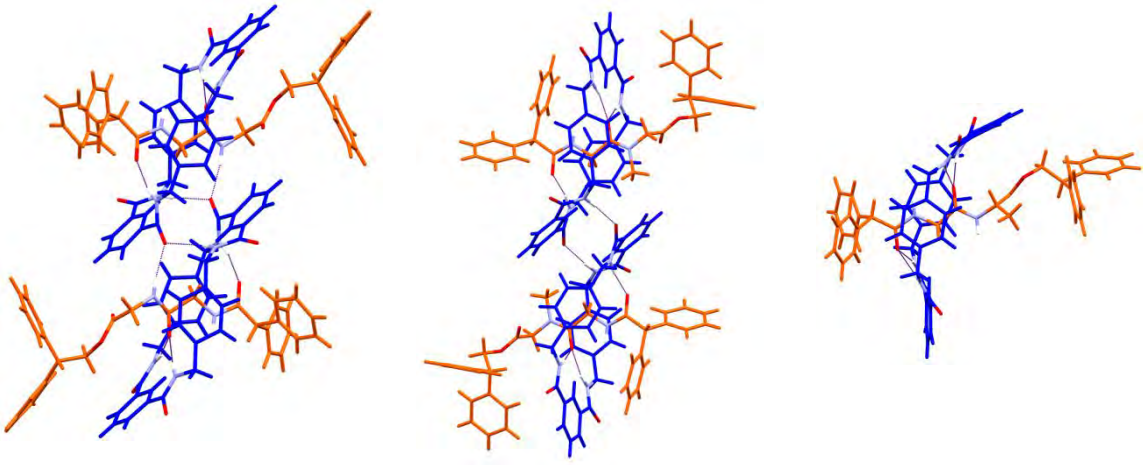

Gly-Gly **3** Gly Sar **4** Gly-L-Ala **5**

Figure 1.6: Crystal structures of three different peptide based [2]rotaxanes.[29]

The Gly-Gly rotaxane **3** has the least steric hindrance for the assembly of the pre-macrocycle around the thread, therefore the most favourable hydrogen bond interaction is realised in the chair conformation and **3** is obtained in a 62% yield. The Gly-Sar rotaxane **4** (60% yield) has an additional methyl group which distorts the hydrogen boding between the macrocycle and the thread and consequently the macrocycle has a half chair / twist boat like conformation. The macrocycle of the Gly-L-Ala rotaxane **5** has an unfavoured boat conformation and this rotaxane is obtained in only 45% yield.[29]

In 2001, Leigh and co-workers reported the first highly efficient template-directed synthesis of an amide based [2]rotaxane.[32] The very rigid fumaric thread **6** is able to template the formation of the [2]rotaxane **7** via clipping reaction of 4 equivalents

of *p*-xylylenediamine and isophthaloyl dichloride in a solvent mixture of chloroform and acetonitrile (9 : 1) (Scheme 1.2). Filtration and spontaneous crystallisation delivered the clean product in 97% yield.[32]

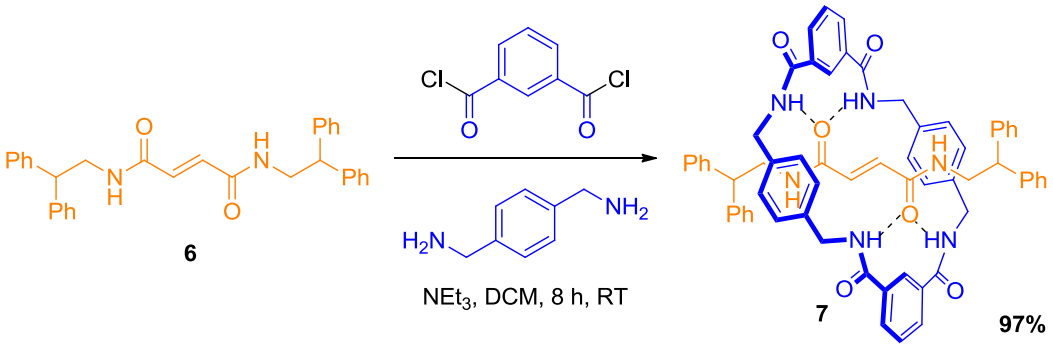

Scheme 1.2: Highly efficient [2]rotaxane formation.

It is believed that the high yield was due to the incorporation of multiple cooperative binding sites on a structurally rigid backbone, facilitating the hydrogen bond assisted synthesis of the rotaxane **7**. The effective templation of the tetraamide macrocycle in a chair conformation around the rigid fumaramide thread **6** maximises the hydrogen bond interactions between the two substrates, making this method one of the most accessible and efficient syntheses described to date.[32]

1.2.3 Higher order rotaxanes

It is more challenging to form [3]- than [2]rotaxanes, for this reason there are fewer examples reported in the literature. Several high yielding [n]rotaxanes, with n = 3-20, were recently reported by the groups of Stoddart and Cronin.[33]

The threads (**8** - **10**), with n = 0-2, were synthesised in a short four step synthesis shown in Scheme 1.3. For the longer threads a protecting group strategy was applied.

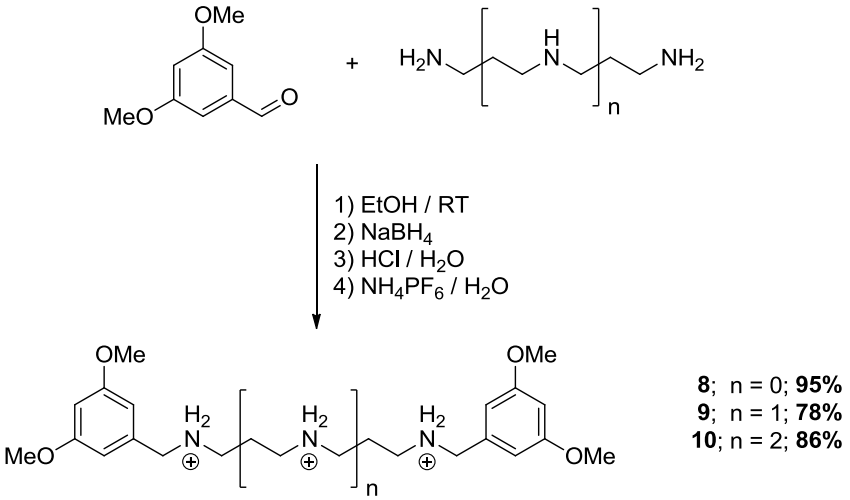

Scheme 1.3: Thread synthesis in four steps.

The rotaxanes (**11** - **13**) were synthesised via a clipping process (Scheme 1.4). The quaternary ammonium cation templating station proved to be very effective for the formation of the polyether macrocycles.

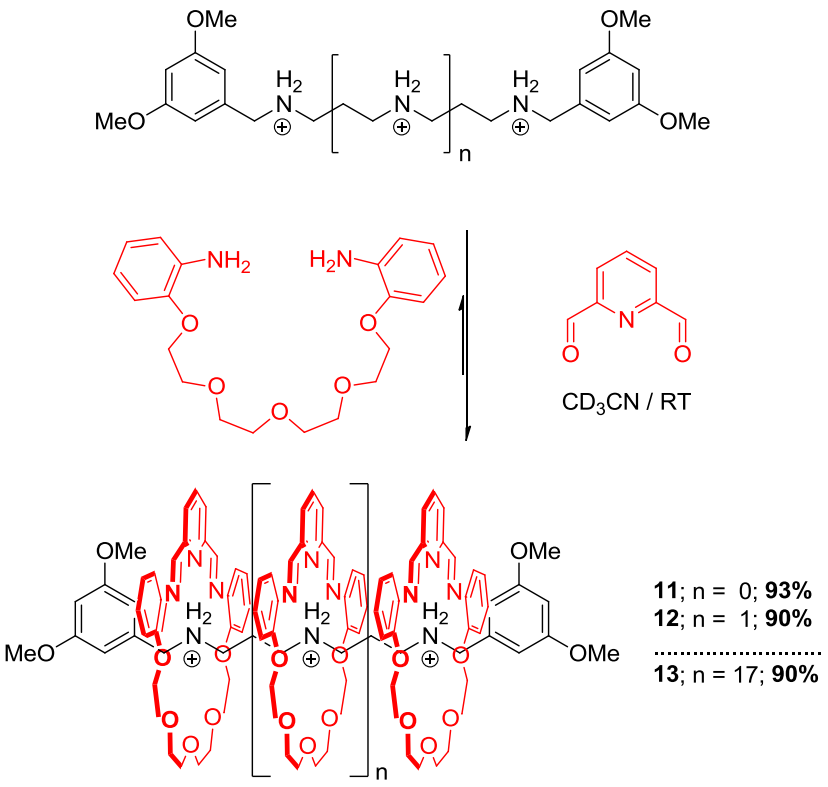

Scheme 1.4: Templated [n]rotaxane formation with NH_2^+ as station.

The aromatic rings of each macrocycle facilitate the formation of the adjacent macrocycle via π-π stacking. The [3]- to [20]rotaxanes (**11** - **13**) were formed in yields ranging from 90 – 93%.

1.2.4 Shuttling

One of the key properties of rotaxanes is the possibility to shuttle the macrocycle along the thread. Shuttling can occur when the thread has more stations than macrocycles. The stations can be the same or different, as mentioned in Section 1.2.1.

The first molecular shuttle was synthesised by the Stoddart group in 1991 (Scheme 1.5).[24] The rotaxane was obtained via the clipping method of the macrocycle around one of the stations. The two stations were identical and in deuterated acetone the macrocycle shuttled 500 times per second between the two stations.

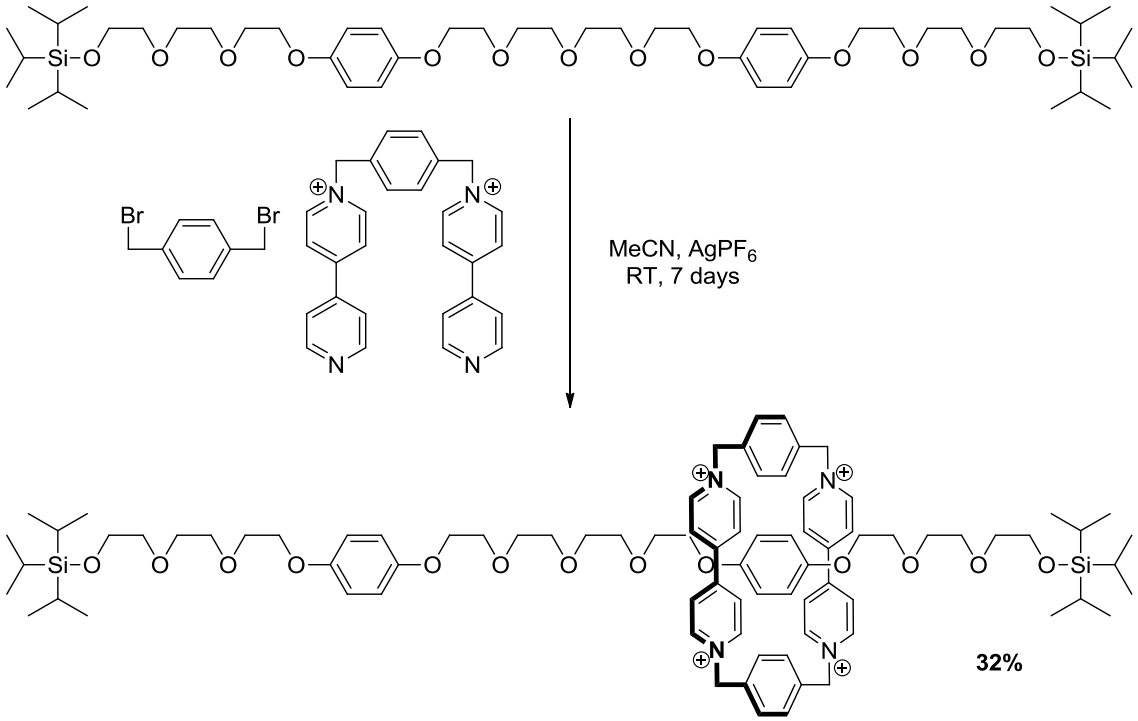

Scheme 1.5: First molecular shuttle synthesised by Stoddart and co-workers.

Stoddart reasoned that a switch to a rotaxane with two different stations would result in the opportunity to control the shuttling process of the macrocycle.[34] In 1997, Fyfe and Stoddart reported the first switchable [2]rotaxane incorporating a benzidine and a biphenol unit.[35]

The Leigh group has also formed several symmetrical [2]rotaxanes with two identical stations (Figure 1.7).[36] The amide macrocycle can shuttle fast between

the stations in deuterated chloroform, hence only one pair of signals is observed in the ^{1}H NMR spectrum. When cooling the sample, the macrocycle slows down until it stops, resulting in a splitting of the ^{1}H NMR signals for the CH_2 protons adjacent to the amide carbonyl on the thread.

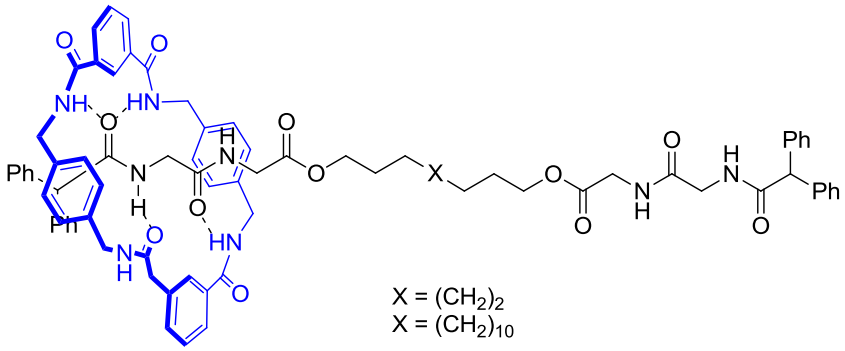

Figure 1.7: A symmetrical [2]rotaxane with a tetraamide macrocycle and a peptide thread.

At room temperature and in deuterated methanol the binding interactions are weakened and therefore the rate of shuttling is increased, while in deuterated DMSO the shuttling stops completely. In the latter case, the macrocycle is located on the hydrophobic part of the thread, enabling the peptide stations to maximise their hydrogen bonding interactions with the solvent.

In 2004, Leigh *et al.* reported the first pH-switchable amide based molecular shuttle (Scheme 1.6).[37] At room temperature the amide macrocycle is located over the succinamide station. When adding a suitable base, such as potassium *tert*-butoxide, the phenol ring gets deprotonated and forms an anion. This anion is more attracted to the macrocycle and the shuttling occurs. The majority of the macrocycle is then over the phenolate anion. Addition of TFA results in the

protonation and reshuttling of the macrocycle to the now more favoured succinamide station. A solvent effect was also observed for the rate of shuttling as as described in the previous example. This system works in optimal conditions with non competing solvents, such as deuterated chloroform.

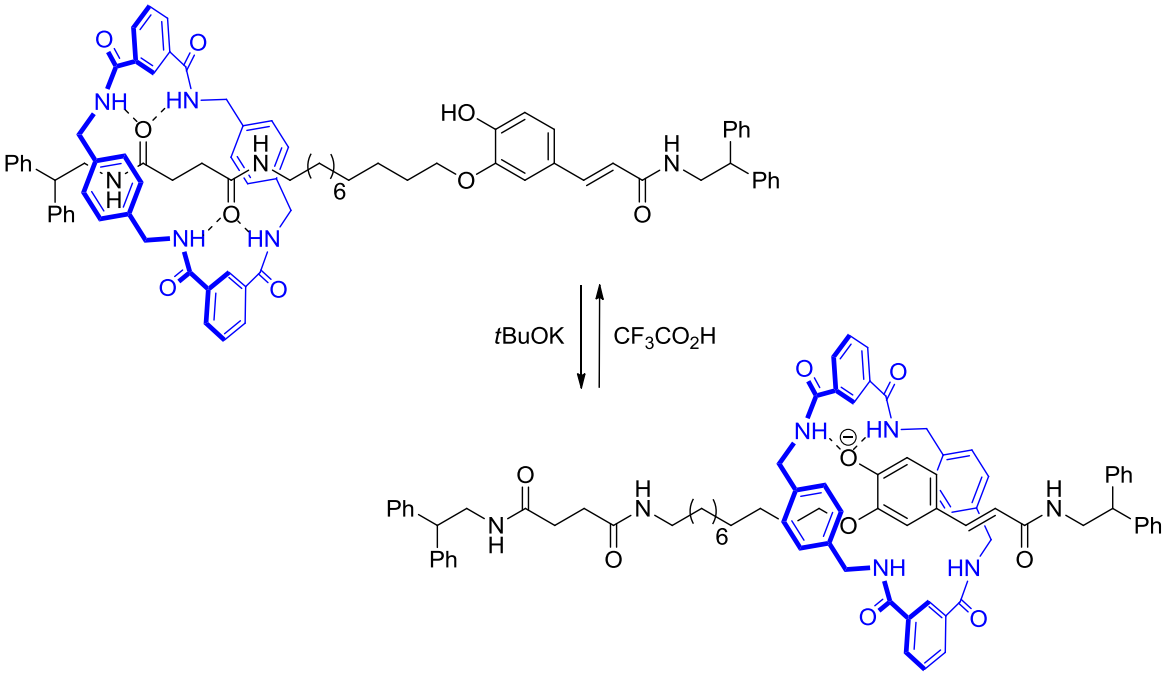

Scheme 1.6: First pH-switchable amide-based molecular shuttle.

These are some of the most outstanding examples of shuttling processes in rotaxanes, however more examples can be found in the literature.[38-40] The rate of shuttling is determined by the attractive interactions between the macrocycle and the station. When the interactions between the macrocycle and one station are strong, the ring does not shuttle and is mainly located on this particular station. When the interactions are weak due to repulsive forces, or solvent effects, or there are similar strong attractions on the two stations, the macrocycle can shuttle to and fro along the thread.

1.2.5 Rotaxanes used for sensing

Another main application of rotaxanes is the recognition and binding of ions.[41] Beer *et al.* has recently reported a sulphate-selective binding and sensing [3]rotaxane (Scheme 1.7).[42]

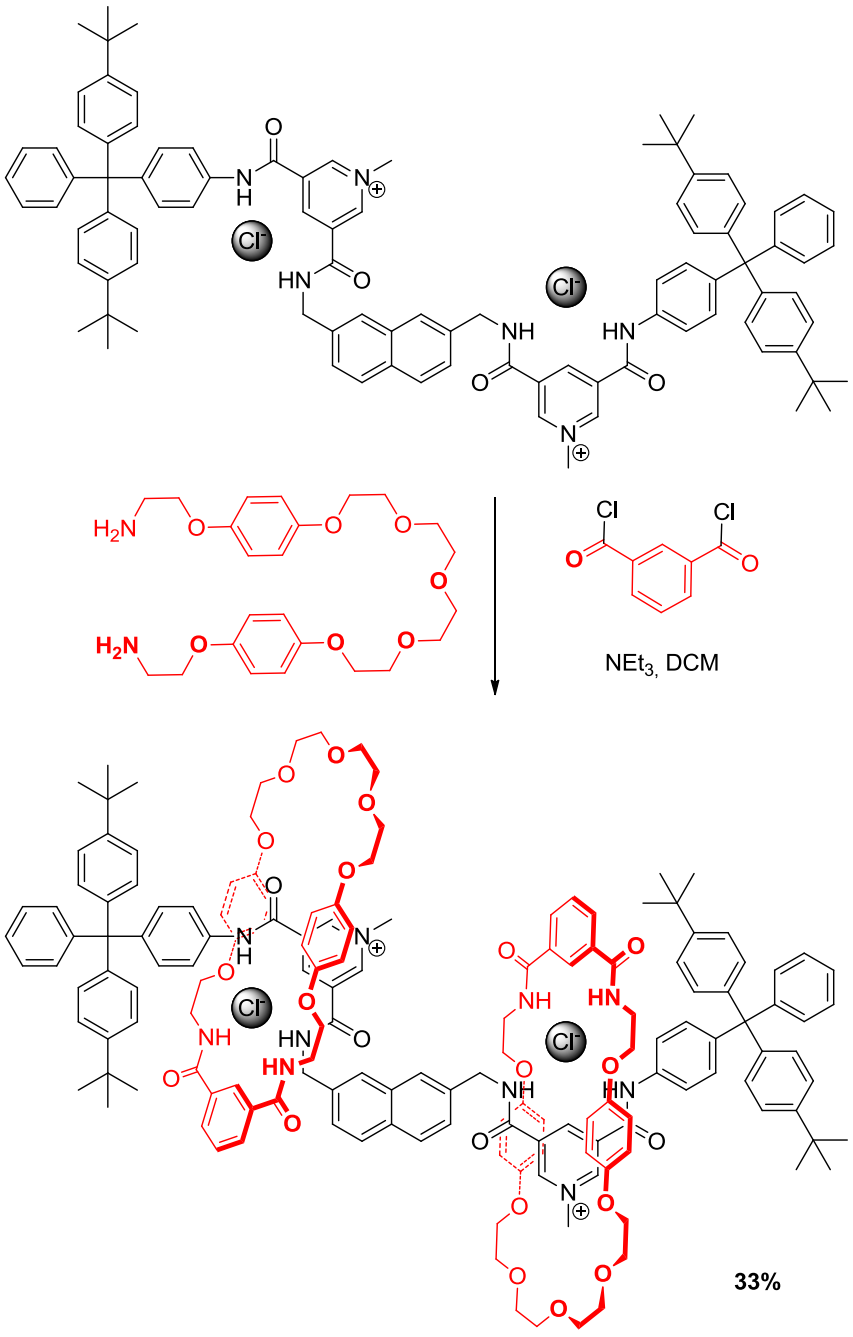

Scheme 1.7: Anion templated synthesis of a [3]rotaxane.

This rotaxane was synthesised via the anion template clipping process in 33% yield. The incorporation of the naphthalene group allows the rotaxane to exhibit room temperature fluorescence. The chloride counter-ions were exchanged by PF_6^- anions to enable an easier conversion to other anions. When replacing just one of the PF_6^- anions with one SO_4^- anion, the fluorescence was quenched. However, exchange of the second PF_6^- anion resulted in an enhancement of the emission. The reason for the quenching and enhancement of the emission lies in the structural changes that the rotaxane suffers. The first SO_4^- anion causes the rotaxane to bend both macrocycles towards the anion. When the second PF_6^- anion is exchanged by a SO_4^- anion, each macrocycle captures one SO_4^- anion and the rotaxane returns to its linear geometry.

Catenanes can also be synthesised via the ion template clipping technique and these catenanes can sense and bind to various ions.[43]

1.2.6 Threaded structures with cross-linked macrocycles

Stoddart has also explored other interlocked structures beyond catenanes and rotaxanes.[44] This new class, of anthropomorphic molecules were named suitanes, which consist of two independent compounds: the ‘body’ and the ‘limbs’. The body could be compared to an unstoppered thread and the limb to a macrocycle. The number between suit and ane indicates how many limbs were used to form the suitane, e.g. a suit[2]ane has one torso and two limbs and a suit[3]ane has one torso and three limbs.

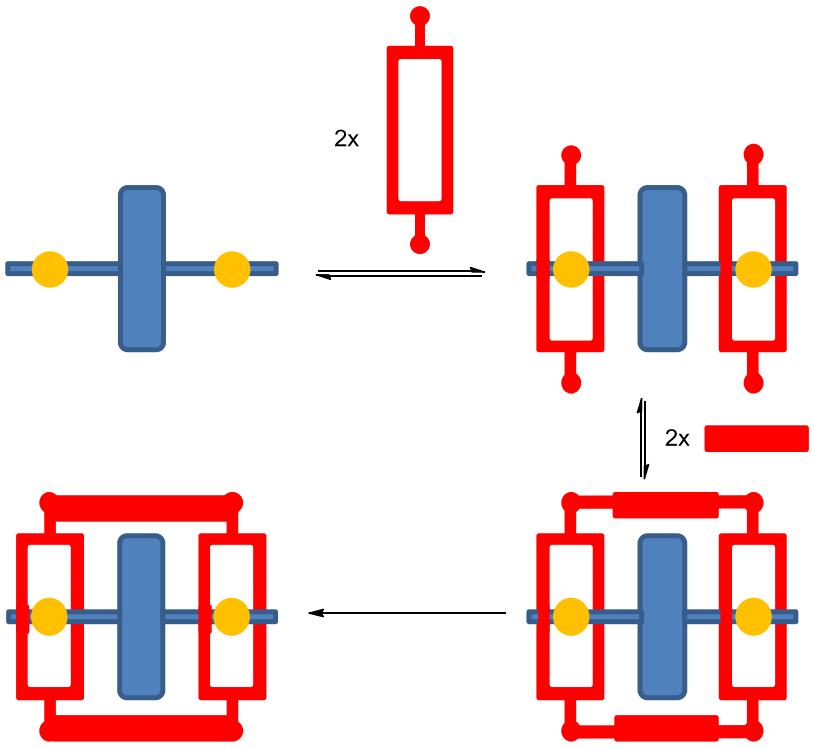

Scheme 1.8: The three steps for the synthesis of a suit[2]ane.

Suitanes are usually formed in three steps (Scheme 1.8). In the first step a torso-limb complex is formed. The torso (illustrated in blue) requires at least two stations (shown in yellow). These stations are capable of interacting with the limbs, which are highlighted as red squares. The limb components are then covalently linked under thermodynamic control. In the final synthetic step, the "suit" is kinetically fixed, which does not allow the components of the suitane to disassemble.

In order to synthesise the suit[2]ane **14**, three components are required (Scheme **1.9**). For this synthesis, Stoddart and co-workers used a dynamic covalent protocol, which they developed in 2004.[45]

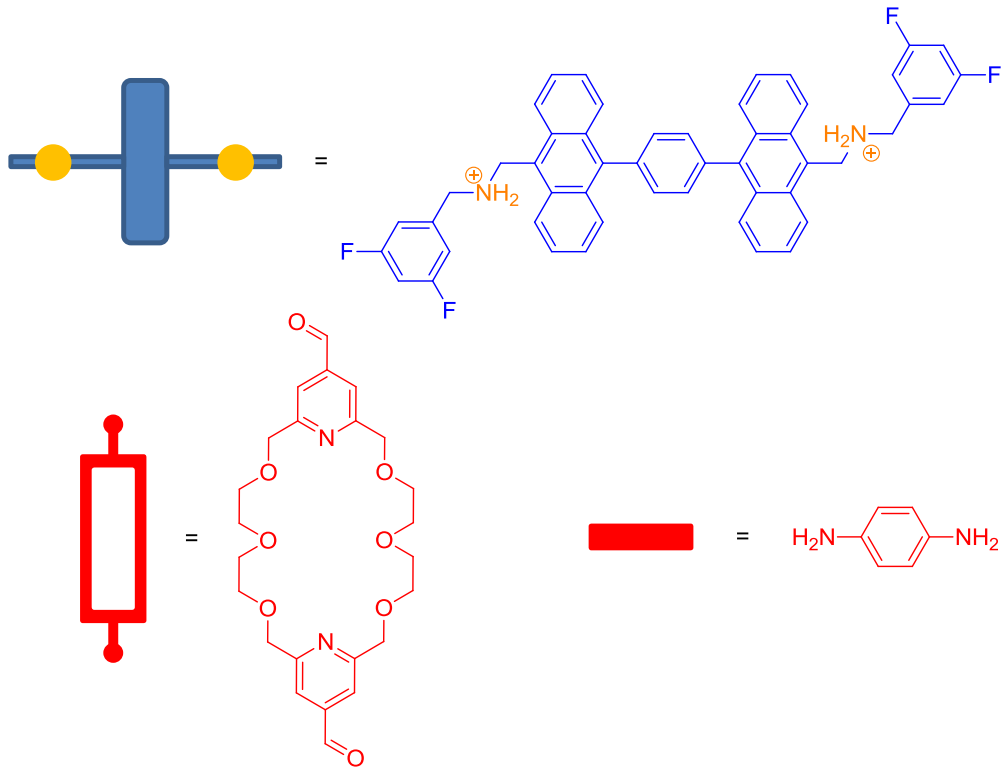

Scheme 1.9: Components used to form the first suit[2]ane.

Computer calculations suggested that the polyether macrocycles recognise the NH_2^+ stations and form a pseudo[3]rotaxane.[†] This pseudo[3]rotaxane can be captured via imine condensation of *p*-phenylenediamine and the two aldehydes, which are located on top of each macrocycle, to form the suit[2]ane **14** (Figure **1.8**). Even when the imines were not reduced to amines, it was found that imine **14** was very stable and could be considered a suit[2]ane. To ensure that the suitane is in fact an interlocked structure, the sample was heated in deuterated acetonitrile for 30 days at 70 °C and no change was observed in the ^{1}H NMR spectrum. Suitanes could be considered as a threaded cage-like molecule.

[†]Pseudorotaxanes are unstoppered rotaxanes. By adding stoppers at the ends of the pseudorotaxanes, they become rotaxanes.

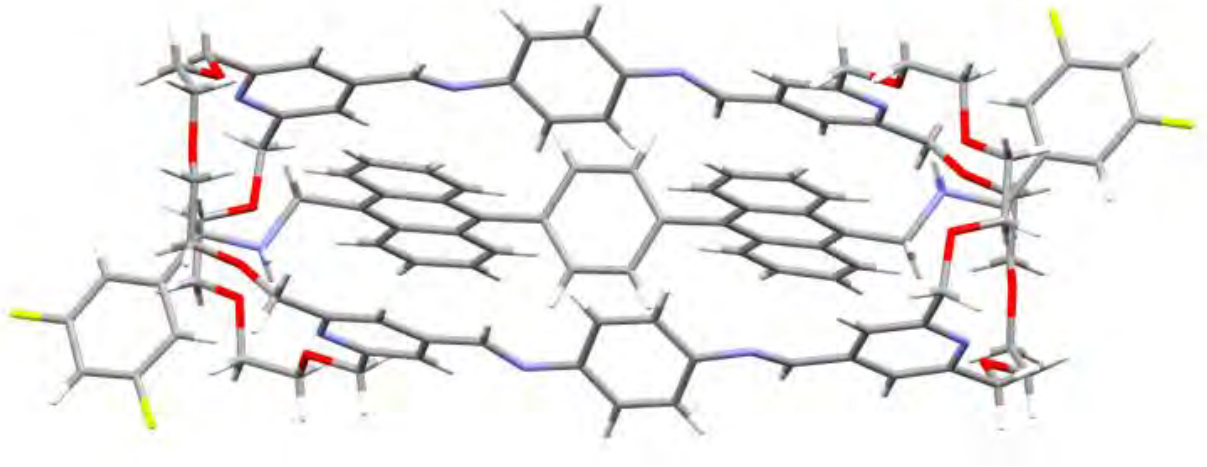

Figure 1.8: Crystal structure of suit[2]ane **14**.[44]

Another method to cross-link two macrocycles was described by Vögtle *et al.* in 1996.[46,47] An initial sulfonamide [3]rotaxane was synthesised in 4% yield via a three component clipping process (Scheme 1.10).

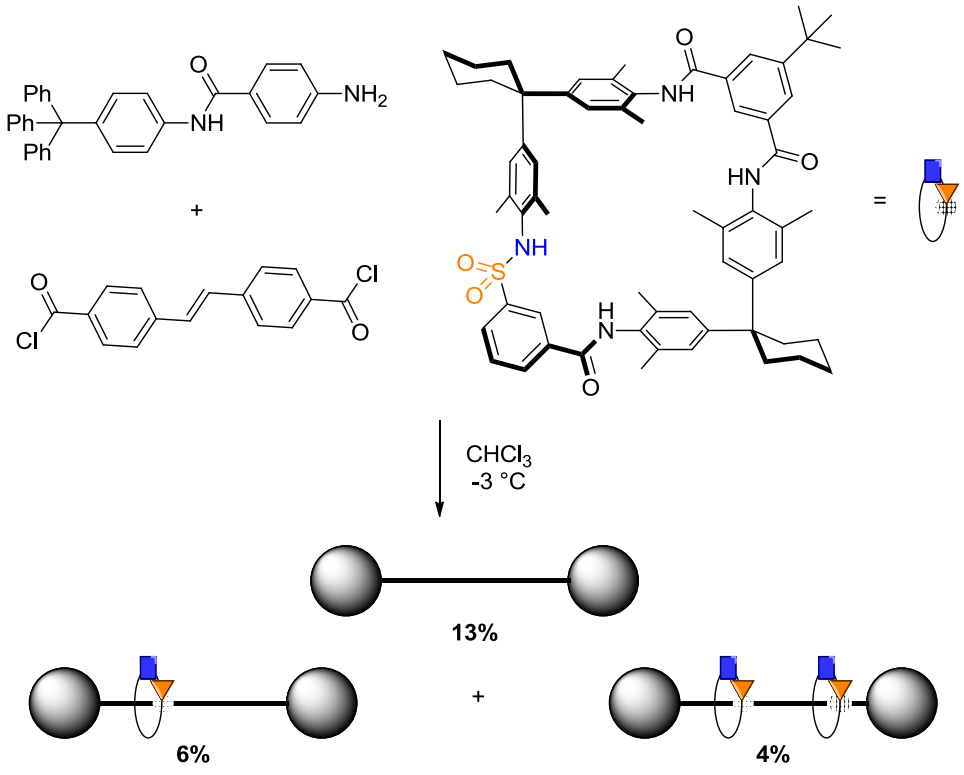

Scheme 1.10: Synthesis of a sulfonamide [3]rotaxane.

This [3]rotaxane can then be cross-linked on the sulfonamide units of the two macrocycles using flexible or rigid halide containing chains (Scheme 1.11).

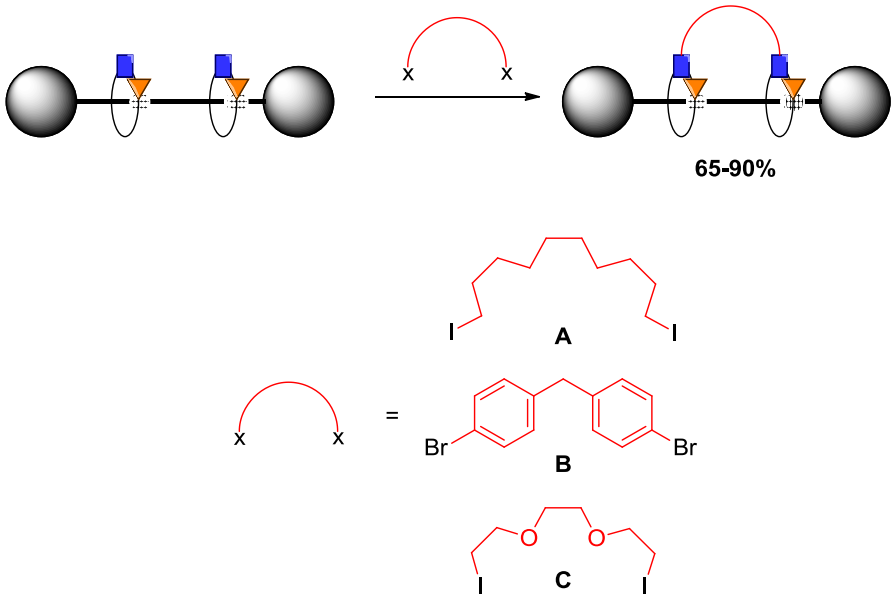

Scheme 1.11: Cross-linking event to form bonnanes.

This newly formed architectures can be obtained in yields ranging from 65 - 90% and are called bonnanes.

1.3 Cage structures

Cage molecules have received great attention over the last decades, driven by the surge in 'bottom-up' strategies to create small and defined supramolecular devices. These devices can then be modified for specific purposes and as a result there are many reports of novel syntheses in the literature.

1.3.1 Metal organic cages

In 1996, Fujita postulated that transition metals could coordinate compounds to form definite structures. The coordinated product is therefore the result of a templated synthesis and this can be controlled by the structure and size of the building blocks.[48] Following these principles, Fujita has described a self-assembled nanometre-sized organic host framework (Scheme 1.12).[49]

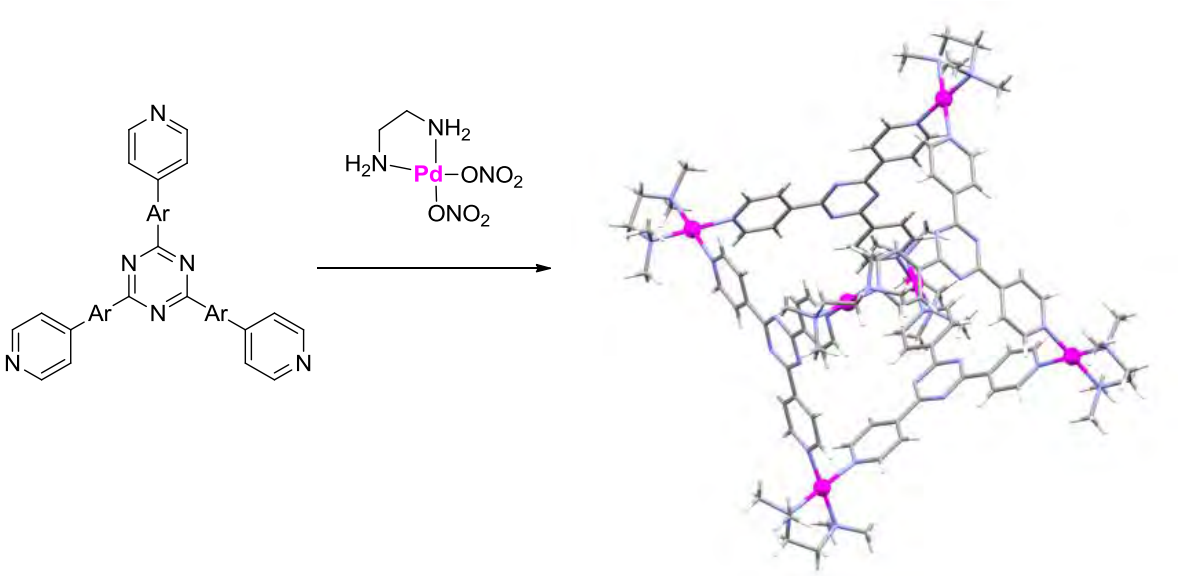

Scheme 1.12: Self-assembled nanometre-sized organic host framework synthesised by Fujita.

More recently, Fujita and co-workers showed that these compounds are able to function as molecular flasks and help to perform unusual reactions.[50] One of such unusual reaction is the naphthalene Diels-Alder reaction (Scheme 1.13). These reactions normally require very harsh conditions (e.g. high temperature) due to the lack of reactivity of the naphthalene molecule. However, quantum-mechanical calculations showed that this reaction is exothermic. Therefore, the entropic cost of the multi-centered reaction is important. The molecular flask (shown as a circle)

pre-organises the reactants and greatly reduces the entropic cost, allowing the Diels-Alder reaction to occur.

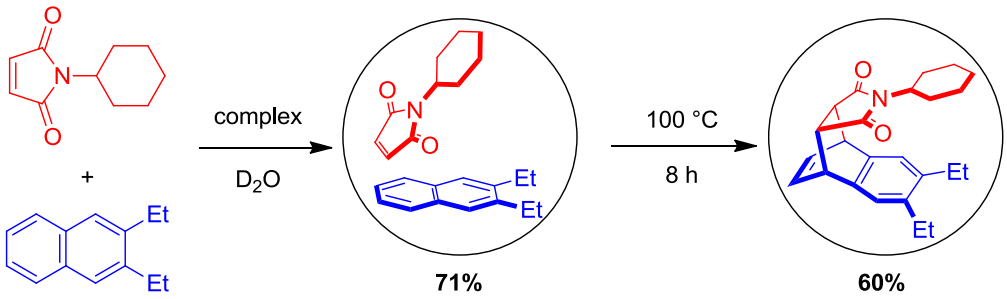

Scheme 1.13: Unusual Diels-Alder reaction promoted by Fujita's cage.

The reaction profile was changed from a bimolecular pathway to a pseudo-intramolecular one.

1.3.2 Boronic ester based cages

Boronic acids are very powerful motifs to assemble molecular and polymeric nanostructures.[51] The condensation reaction of 1,2- and 1,3-diols with boronic acids is reversible and the equilibrium is established very quickly.[52]

In 2008, Kobayashi and co-workers reported a self-assembled boronic ester based cage.[53] The tetraboronic acid **15** and the di-catechol linker **16** formed the cage **17** via a condensation reaction in quantitative yield (Scheme 1.14). The cage **17** is capable of encapsulating several guest molecules, such as biphenyl or anthracene derivatives. This encapsulation process is solvent dependent, e.g. by removal or addition of methanol, an on/off switch was observed.

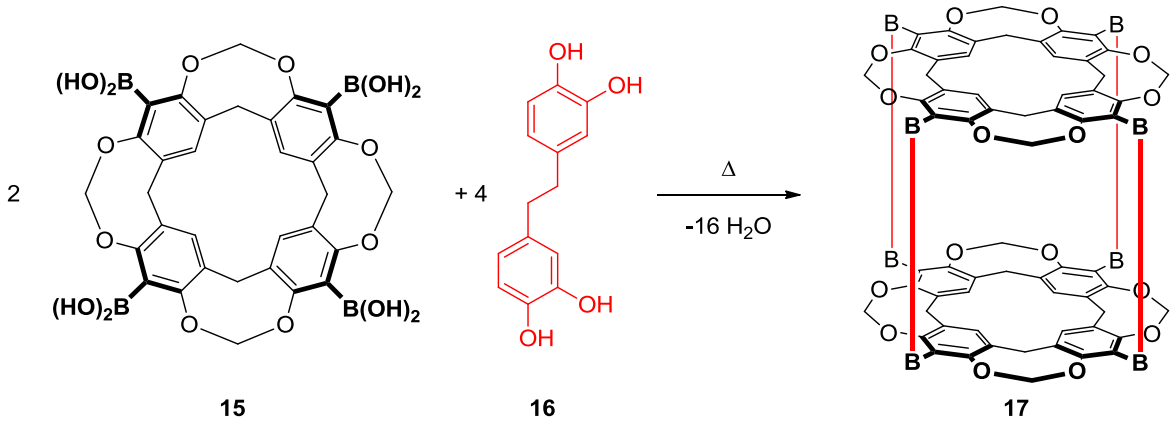

Scheme 1.14: Synthesis of the boronic ester cage **17**, being **16** the four edges of the cage.

Severin *et al.* recently reported the first example of a molecular cage with dative B-N bonds (Scheme 1.15).[54] Boronate esters are known to be Lewis acidic and therefore the B-atoms are capable of forming dative bonds to N-donors, such as pyridines.

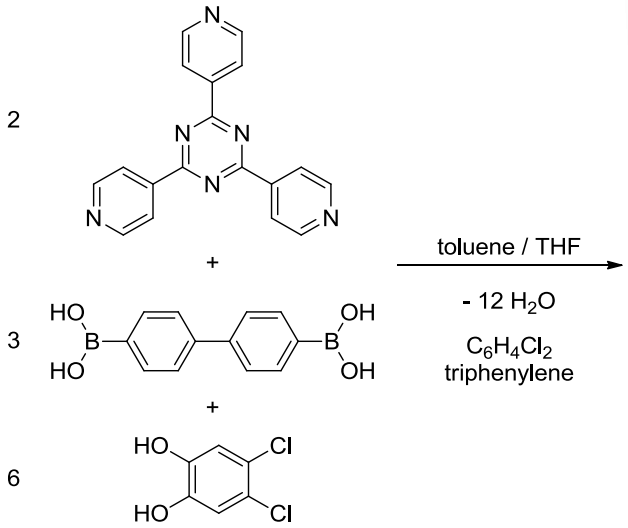

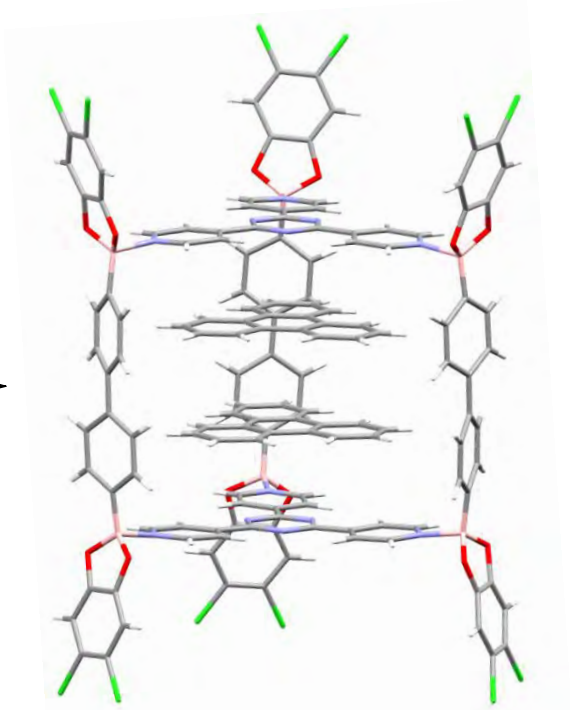

Scheme 1.15: Synthesis of the first boronic ester cage with dative B-N bonds.

These cage molecules were obtained via multicomponent reactions of diboronic acids with catechols and tripyridyl linkers. The cages have six dative B-N bonds and the length of the cages can be varied by the choice of the diboronic acid component. The cages were not particularly stable, however they were capable of encapsulating polyaromatic compounds such as triphenylene.[54]

1.3.3 Imine cages

Recently, Cooper and co-workers have synthesised the imine cage **20** via condensation reaction of the trialdehyde **18** and the diamine **19** (Scheme 1.16).[55] This particular imine cage is able to incorporate (bind) around 12 to 13 water molecules. This result is very impressive given that imine bond formation is reversible by Nature. Even after 4 hours in refluxing water, the cage did not decompose. However, exposure to acidic media led to decomposition of the cage since the equilibrium was shifted to the starting aldehyde and amine.

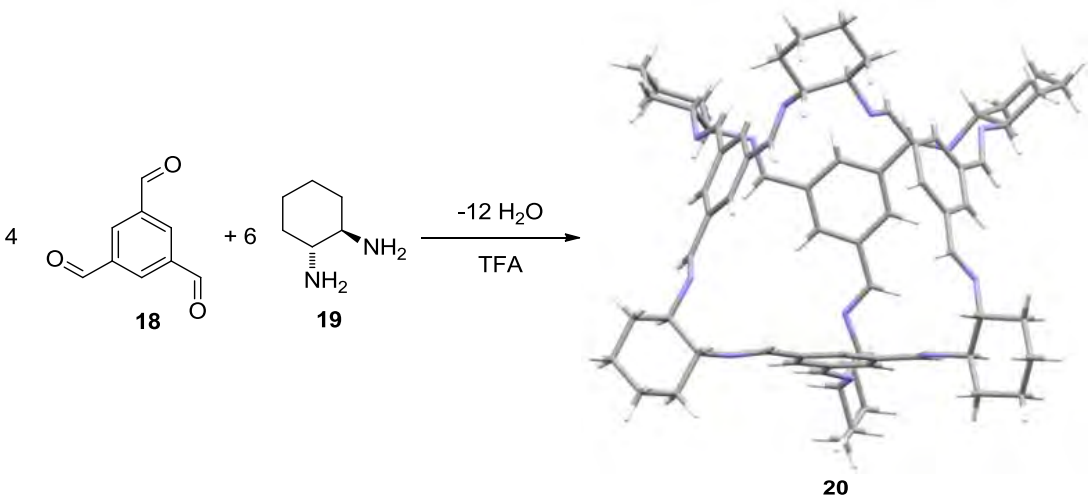

Scheme 1.16: Synthesis of the imine cage **20**.[55]

Cage-like molecular structures are interesting for a number of applications, such as compound separations,[56] catalysis,[57-59] sensing,[60] and drug delivery[61,62]. The thermo- and hydrolytic stability of the cages is the main drawback for these applications.[63] This imine cage **20** addresses the hydrolytic stability issue and might have opened a new pathway that requires further investigation for future applications. A tertiary amine based cage might be able to solve the thermo- and hydrolytic problems.

A great number of examples of cage-like structures more or less closely related to the areas described in this introduction have been reported. Further examples have been reported in the literature and these include MOFs,[64] MORFs,[65] PMOFs,[66] hemicarcerands,[67] hydrogen bond capsules[68,69] and COFs[70].

Chapter 2: Results and Discussion

2.1 Research aims

As discussed in Chapter 1 many research groups have synthesised molecular cages (boxes) via different approaches. The aim of this project is to synthesise a novel molecular box via the construction of a [3]rotaxane as key intermediate.

The first step towards the formation of a molecular box is to access a thread, which should be able to form a [3]rotaxane. Thread **21** is a double fumaric thread with diphenylethyl secondary amides as stopper groups (Figure 2.1).

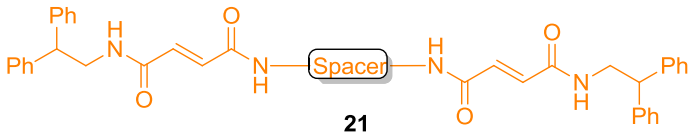

21

Figure 2.1: Double fumaric thread **21**.

Its structure is closely related to that of the fumaric thread used by Leigh and co-workers in 2001, which allowed them to synthesise a [2]rotaxane in high yield (see Section 1.2.2).

In order to build a molecular box, a [3]rotaxane is necessary. If the desired [3]rotaxane **22** (Scheme 2.1) can be synthesised, a cross linking event would be required to connect the two macrocycles. The nitrogen of the amide of the macrocycle or alternative functional groups on the aromatic rings should allow this linking process. If functional groups on the aromatic rings are used, a suitane type

structure would be formed (see Section 1.2.6). Connecting the two macrocycles by using the amide groups would lead to a tertiary amide cage. Reduction of these amides to amines, followed by linking would lead to a tertiary amine cage.

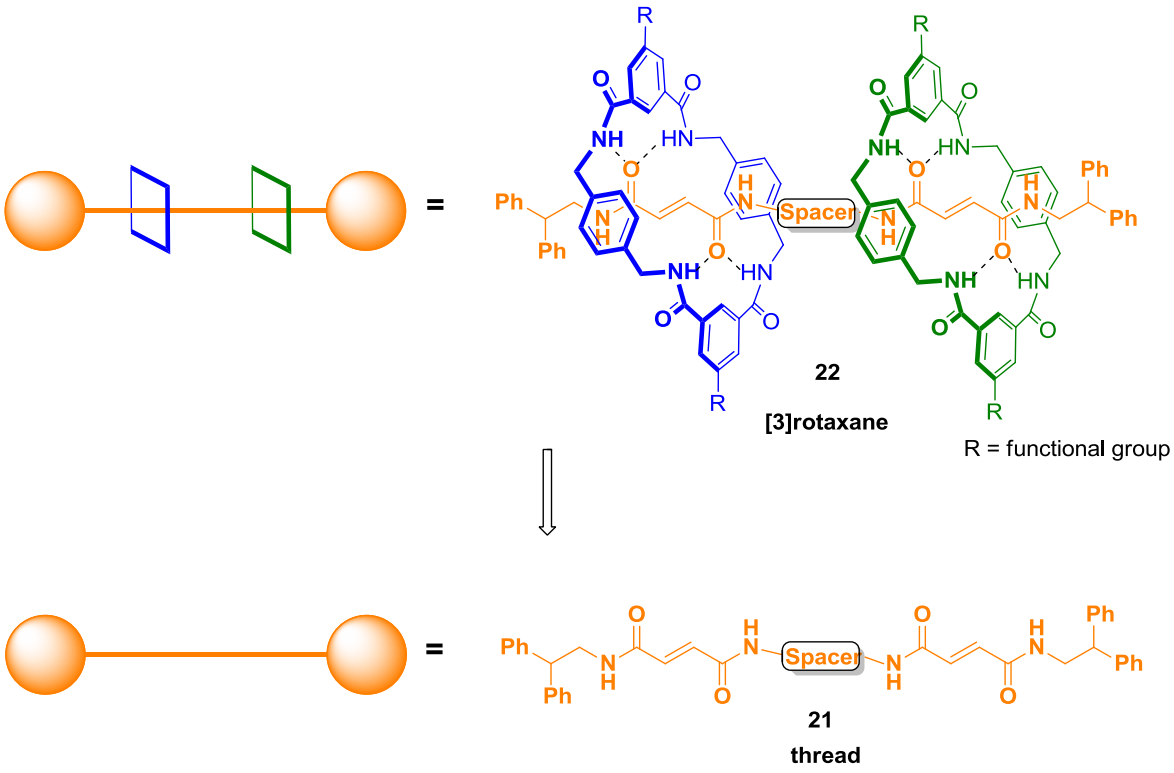

Scheme 2.1: Retrosynthesis for the desired templated [3]rotaxane **22**.

When the two macrocycles are linked, a “threaded box” is formed. A method by which to liberate the box must be then developed (Scheme 2.2).

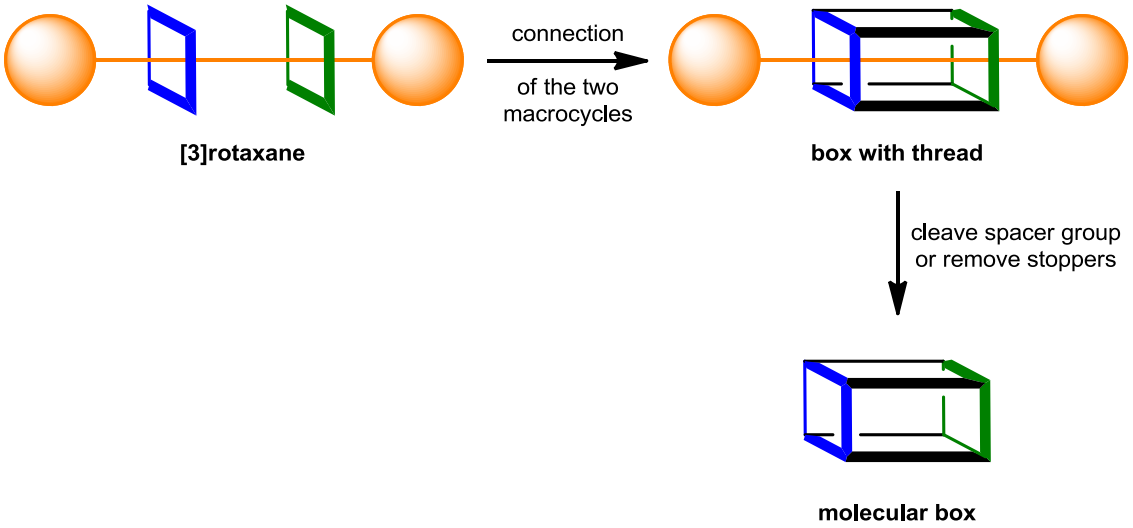

Scheme 2.2: Proposed synthesis of a novel molecular box.

This could be achieved with a cleavable spacer group or by removing the stoppers. This would yield a novel molecular box, synthesised by an unusual route, which hopefully will enable a novel access to even more complex structures.

2.2 Attempted syntheses of the double fumaric thread 21

Three main synthetic routes (A, B and C) towards the synthesis of thread **21** were identified (Figure 2.2).

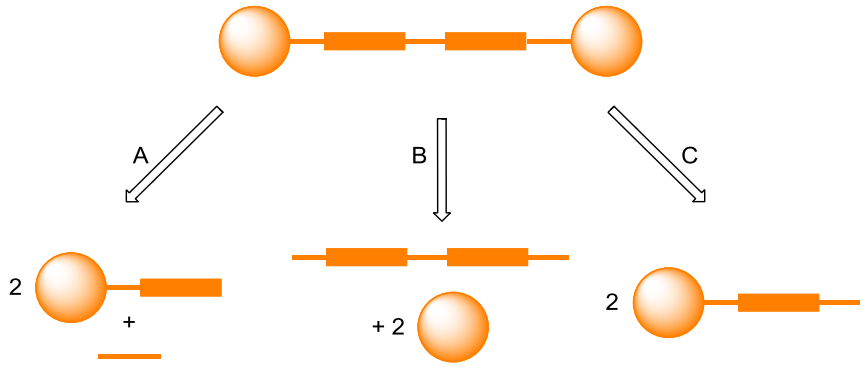

Figure 2.2: The three main synthetic routes (A, B and C) towards the fumaric thread **21**.

Route A involves the synthesis of a stoppered station. Then, two of these stoppered stations have to be connected via a spacer group to from thread **21**. In route B, the two stations are already connected via the spacer group and a stoppering event would afford the desired thread **21**. Route C involves the synthesis of a stoppered half thread, which could be dimerised to form the desired fumaric thread **21**.

2.2.1 Synthetic route A towards thread 21

In the synthetic route A, the desired fumaric thread **21** could be formed by reaction of the known fumaric acid **23** and different diamines in one or two steps (Scheme **2.3**). The fumaric acid **23** could be generated by reaction of the protected acid chloride **25** and 2,2-diphenylethylamine, followed by deprotection of the carboxylic acid.

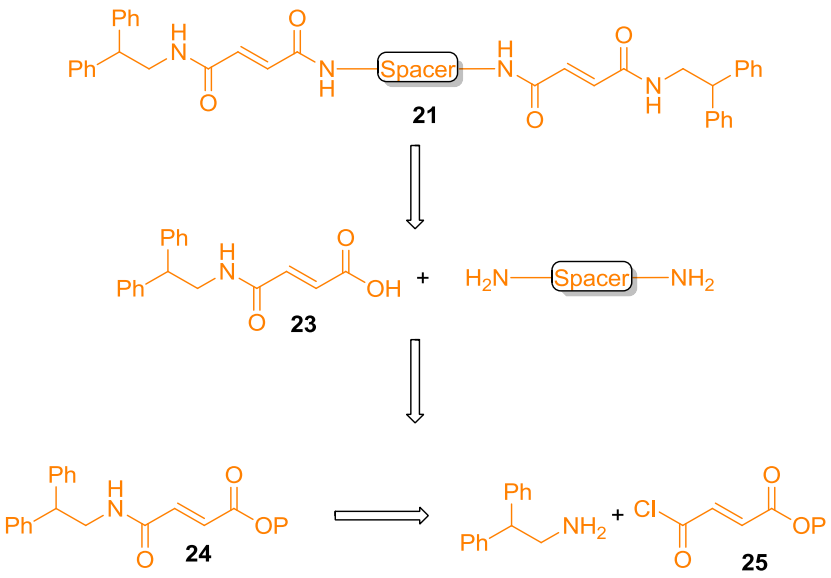

Scheme 2.3: Retrosynthetic analysis of route A towards synthesis of the thread **21**.

Treatment of the acid chloride **26** with 2,2-diphenylethylamine gave the ester **27** in 94% yield. The ester **27** was hydrolysed to afford the fumaric thread precursor **23** in quantitative yield. The acid chloride **26** is commercially available, however it is expensive and it was synthesised in quantitative yield in one step from mono-ethyl fumarate and thionyl chloride under reflux (Scheme 2.4).

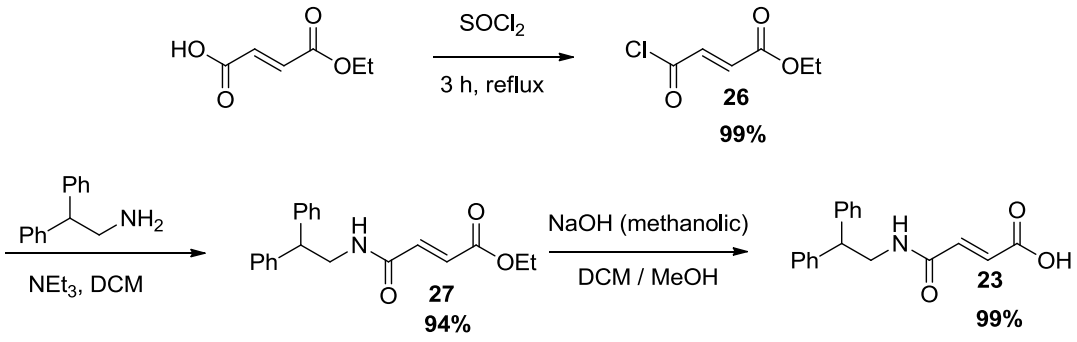

Scheme 2.4: Synthesis of the fumaric thread precursor **23**.

Once the fumaric thread precursor **23** was synthesised several amide coupling reactions were investigated. Since the fumaric thread precursor **23** is a carboxylic acid, it needs to be activated prior the reaction with the diamine.

Computational calculations on the fumaric thread **21** with 1,3-diaminopropane as spacer group showed that four carbon atoms are sufficient to form four linkages between the two macrocycles to build a "threaded box" (Figure 2.3). These calculations[‡] were performed using ArgusLab[71] and optimised from the crystal structure of the [2]rotaxane **2** (see Section 1.2.2) synthesised by Leigh. The results from this calculation were then exported to Mercury[72] to be visualised.

[‡] Molecular mechanics universal force field 1000 steps.

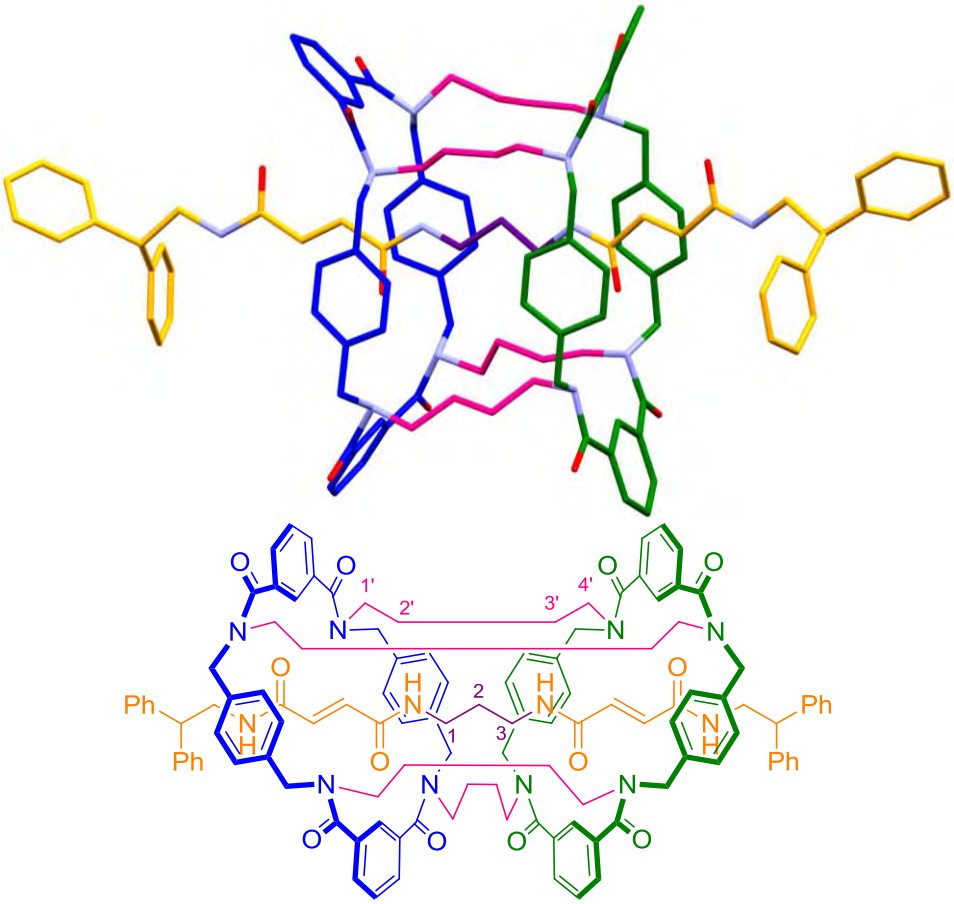

Figure 2.3: Threaded box model created via computational calculations.

Amide coupling reactions are very important in organic chemistry, and therefore they are well established. However, these reactions are not trivial and there are many different coupling reagents commercially available.[73] Unfortunately, there is still not a universal coupling reagent and if the coupling does not occur, different coupling reagents need to be sought.

The fumaric thread **6** was used as a model for the activation of the thread precursor **23** via an amide coupling. The fumaric thread **6** was therefore synthesised using *N,N'*-dicyclohexylcarbodiimide (DCC) as coupling reagent (Scheme 2.5).

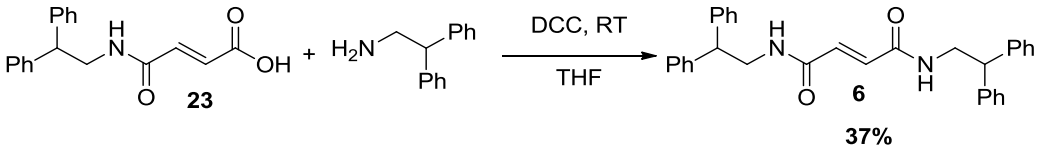

Scheme 2.5: DCC coupling of the thread precursor **23** with 2,2-diphenylethylamine.

Coupling of the fumaric thread precursor **23** with 2,2-diphenylethylamine was successful, however it was low yielding (37%).

Despite the low yield of this test reaction, several diamines (Figure 2.4) were tested in a coupling reaction with the thread precursor **23** (Table 2.1).

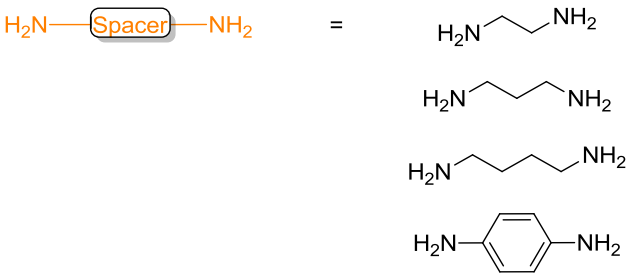

Figure 2.4: Different diamines for use as spacer groups.

None of the conditions tested were suitable for the synthesis of the double fumaric thread **21**.

All reactions with ethylenediamine, 1,3-propyldiamine and 1,4-butyldiamine resulted in a complex mixture of side products or decomposition of the starting materials.

Table 2.1: Different coupling reaction conditions studied.

Entry	Reagent	Additive	Solvent	Time	Temp.	Result
1	DCC	-	THF	48 h	RT	complex mixture
2	DCC	HOBt	THF	48 h	RT	complex mixture
3	HATU	Hünigs base	CH_3CN	24 h	RT	complex mixture
4	HATU	Hünigs base	DCM	24 h	RT	complex mixture
5	EDC	-	MeOH	16 h	RT	50% yield [a)]
6	EDC	HOBt	DCM	16 h	0 °C to RT	complex mixture
7	NMM / IBCF	-	THF	30 min	-15 °C	27% yield [a)]
8	$SOCl_2$	-	neat	3 h	80 °C	- [b)]
9	$SOCl_2$	-	DCM	3 h	80 °C	- [b)]
10	$(COCl)_2$	DMF	DCM	30 min	70 °C	- [b)]
11	DCC	-	DCM	1 h	150 °C	complex mixture

a) Reaction occurred only with *p*-phenylendiamine, however only the mono reacted product **28** was detected (Scheme 2.6). b) Decomposition of the starting materials occurred.

These reactions were followed by Matrix-Assisted Laser Desorption Ionisation (MALDI) and did not show the expected mass peaks. Figure 2.5 shows the general principle behind MALDI-ToF mass spectrometry. A sample of analyte (shown in red) dispersed within a highly absorbing matrix is irradiated by a UV laser beam. The most commonly used UV lasers for MALDI spectrometry are nitrogen lasers (337 nm) and Nd:YAG lasers (355 nm and 266 nm). During the irradiation, a thin upper layer of matrix gets ablated. This method of energy transfer is very mild and excessive energy, which could lead to decomposition, is not required. The matrix must absorb the UV laser light extensively and 2,5-dihydroxy benzoic acid, also called gentisic acid, is used for this purpose.

Gentisic acid can work in a mass range from 500 to 3,000 dalton (Da). Below 500 Da, signals corresponding to the matrix can be observed.

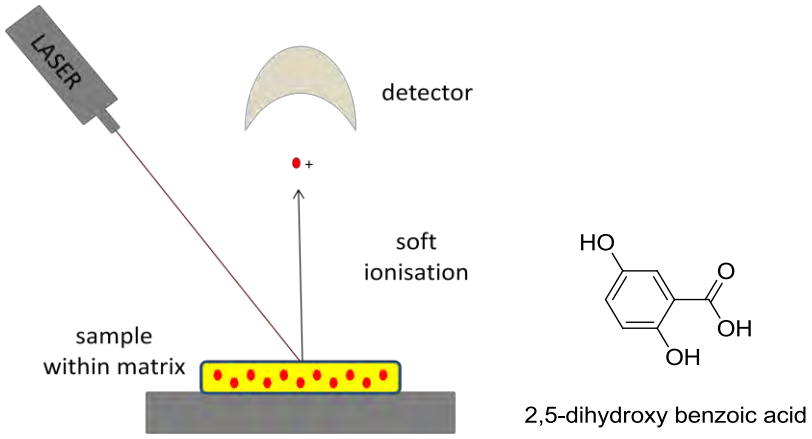

Figure 2.5: Schematic representation of MALDI spectrometer.

The mono reacted product **28** was obtained in two different reaction conditions when using *p*-phenylenediamine as diamine. Coupling of **23** with 1-ethyl-3-(3-dimethylaminopropyl)carbodiimide (EDC) resulted in the mono reacted product **28** in 50% yield (Scheme 2.6). *N*-methylmorpholine (NMM) and isobutyl chloroformate (IBCF), which forms a mixed anhydride of the carboxylic acid, gave **28** in 27% yield.

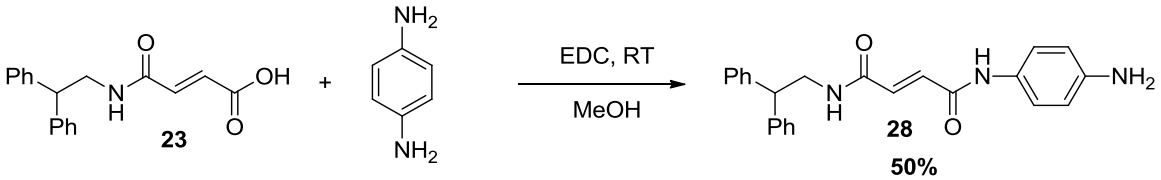

Scheme 2.6: EDC mediated amide coupling to the mono reacted product **28**.

Unfortunately, it was not possible to transform the mono reacted product **28** into the desired double fumaric thread **29** despite screening a number of peptide

coupling reagents (Scheme 2.7). Instead, only the starting material **28** was recovered.

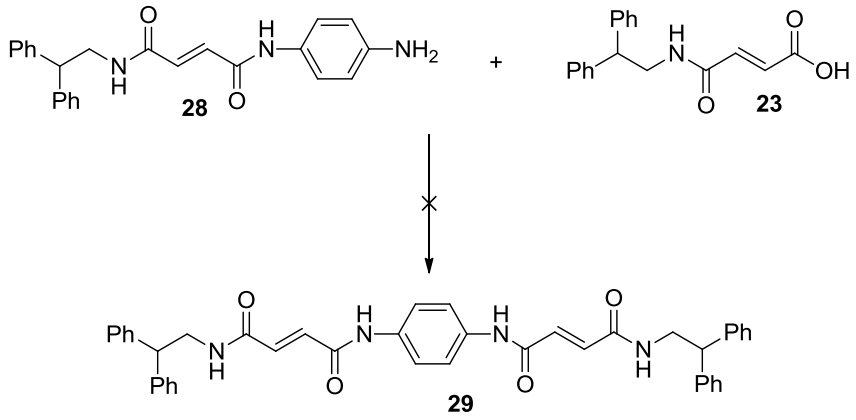

Conditions: NMM/IBCF; DCC; EDC; $(COCl)_2$.

Scheme 2.7: Attempted reactions towards the synthesis of the double fumaric thread **29**.

After the failure of route A to provide the desired thread **21**, route B was investigated, whereby the diamine component is introduced in the first step.

2.2.2 Synthetic route B towards thread 21

In synthetic route B, the proposed retrosynthetic analysis involves the reaction of the diamine **30** with the protected fumaric acid chloride **25** to yield the diamide **31**, which could be deprotected and coupled with 2,2-diphenylethylamine to afford the fumaric thread **21** (Scheme 2.8).

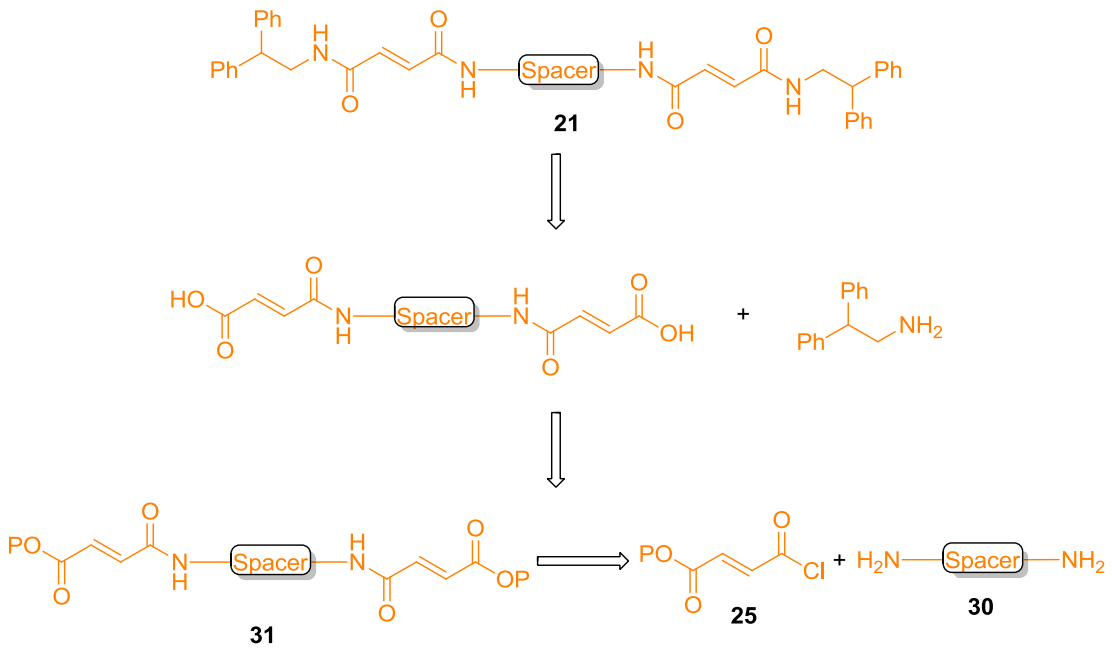

Scheme 2.8: Retrosynthetic analysis of route B towards the synthesis of the thread **21**.

The reactions between ethyl fumaroyl chloride and different diamines were optimised easily by varying the amount of solvent, reaction time and amount of base. Optimisation allowed access to the diamides (**32** - **34**) in yields ranging from 42% to 65% (Scheme 2.9).

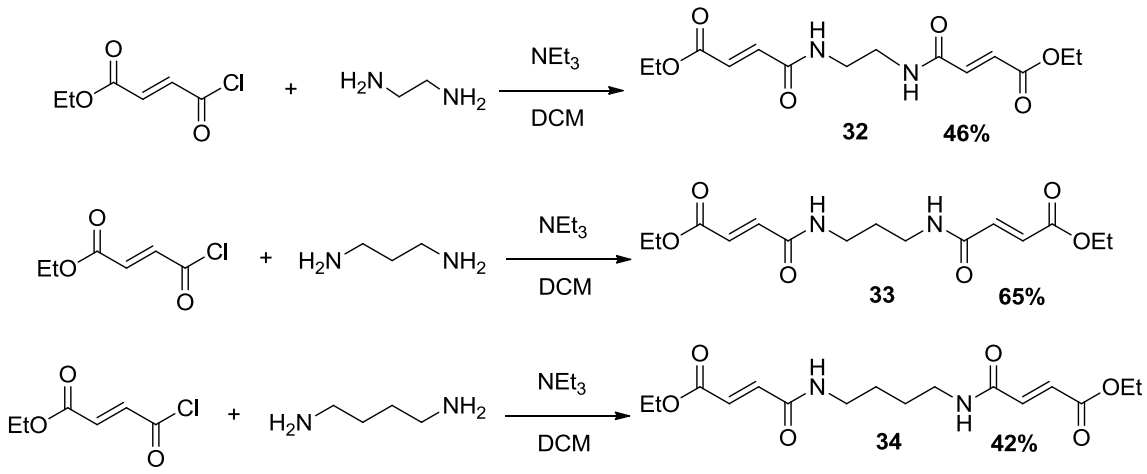

Scheme 2.9: Synthesis of diamide thread precursors.

These diamides could potentially form pseudorotaxanes (see Section 2.6).

Considering the moderate yields for the reactions of the diamide thread precursors, an alternative synthetic approach was investigated.

Katrizky *et al*. have reported the formation of amides mediated by NEt_3 starting from benzotriazole and an amine.[74] As shown in Scheme 2.10 the synthesis of the benzotriazole **35** was high yielding. Unfortunately, the reaction with ethylendiamine proceeded in only 33% yield.

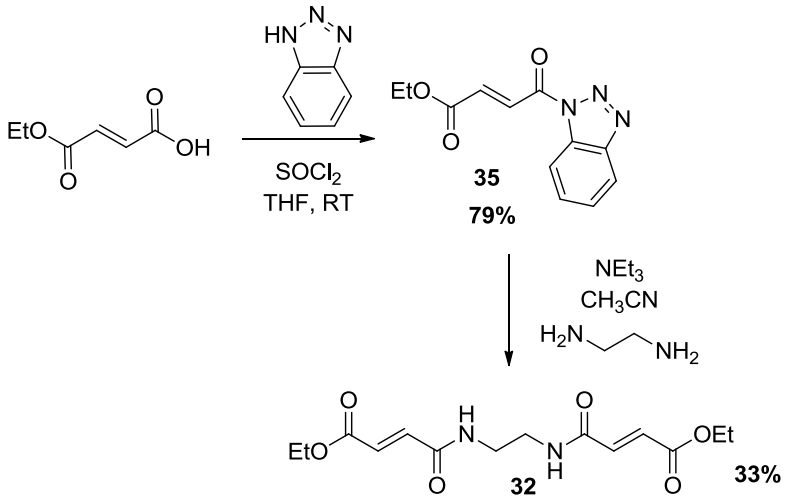

Scheme 2.10: Benzotriazole synthetic route to diamide thread precursor **32**.

Saponification of the ester groups of the diamide thread precursor **33** was performed in quantitative yield using sodium hydroxide in methanol (Scheme **2.11**). The resulting diacid **36** was used in several coupling reactions with 2,2-diphenylethylamine.

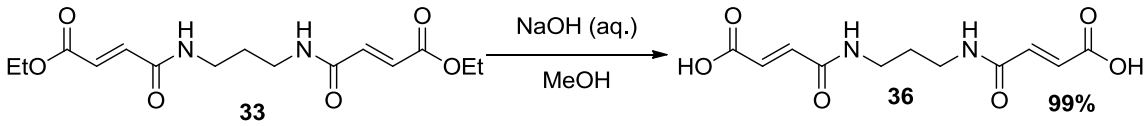

Scheme 2.11: Saponification of the diamide thread precursor **33**.

Amide coupling reactions of **36** with EDC or DCC as the coupling reagent did not form the desired product and the starting material was recovered. The major reason for this result may be the lack of solubility in organic media of the diacid **36**. Therefore an activation of the diacid as the acid chloride intermediate followed by reaction with 2,2-diphenylethylamine was tested. Unfortunately, all attempted approaches were unsuccessful and resulted in recovery or decomposition of the starting material.

Due to the insolubility and unreactivity of the diacid **36**, an alternative approach to the double fumaric thread **21** was investigated.

The direct synthesis of an amide starting from an ester and an amine is well known. This type of amide coupling is normally catalysed by $Zr(O^tBu)_4$ with 1-hydroxy-7-azabenzotriazole (HOAt) and can be very potent, as described by Porco (Scheme 2.12).[75]

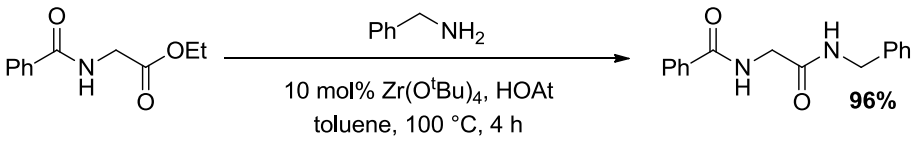

Scheme 2.12: Zr-mediated amide coupling.

These reaction conditions were used to synthesise the known fumaric thread **6**; which was isolated in 60% yield (Scheme 2.13).

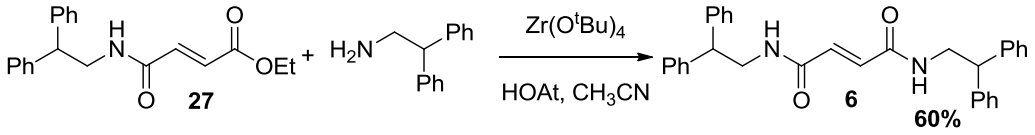

Scheme 2.13: Zr-mediated amide coupling to synthesise thread **6**.

Unfortunately, under analogous conditions conversion of the ester **33** to the amide **37** was not observed (Scheme 2.14). The double amide thread **33** was not soluble in any solvent previously described for this reaction. The thread **33** is readily soluble in methanol, however methanol is not a suitable solvent for this reaction.

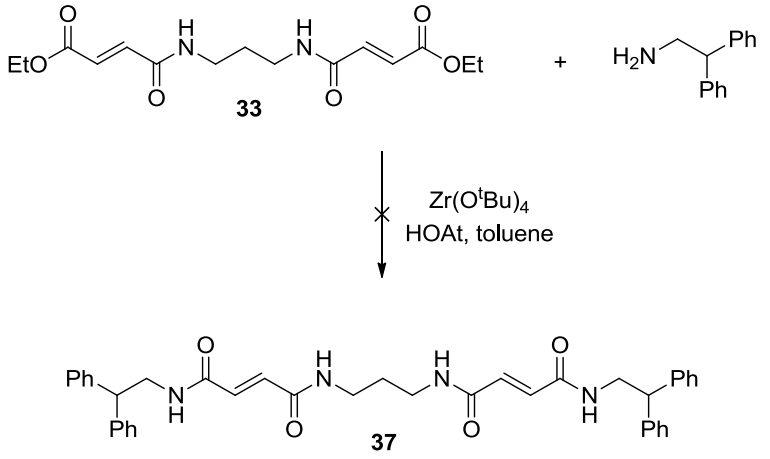

Scheme 2.14: Attempted Zr-mediated amide coupling.

In view of these disappointing results, an alternative synthetic route was investigated (Scheme 2.15). The reaction of the ester **22** with ethylenediamine was carried out in different solvents using various Lewis acids. However in no instance was the desired product obtained. A possible explanation for this lack of

reactivity could be binding of ethylenediamine to Zr, effectively poisoning the catalyst.

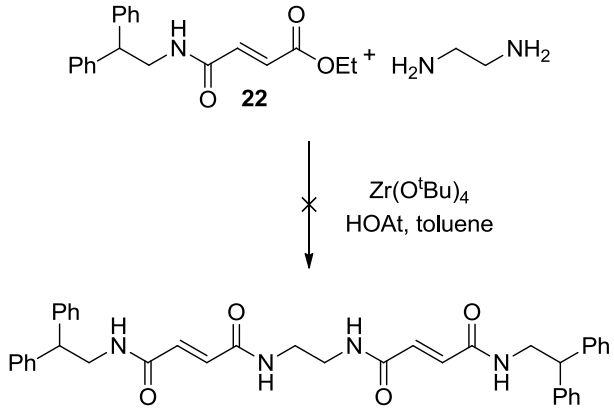

Scheme 2.15: Attempted Zr-mediated amide coupling using ethylenediamine and ester **22**.

As alternatives to $Zr(O^tBu)_4$, aluminium chloride and zirconium chloride were used in stoichiometric quantities. These catalysts did not show any reactivity either.

It is possible that the aluminium chloride and zirconium chloride are not strong enough to promote this reaction. Unfortunately, $Zr(O^tBu)_4$ seems to be very powerful and produces numerous products. MALDI analysis did not show the desired mass peaks of either single or double coupling products.

2.2.3 Synthetic route C towards thread 21

Route C does not involve the use of diamines as spacer groups (Scheme 2.16). The key intermediate is the amide **38** bearing a functional group suitable for dimerisation to afford the desired thread **21**, e.g. via Grubbs-metathesis, or ether

or anhydride formation. The amide **38** could be formed by reaction between the fumaric acid **23** and an amine with an appropriate functional group.

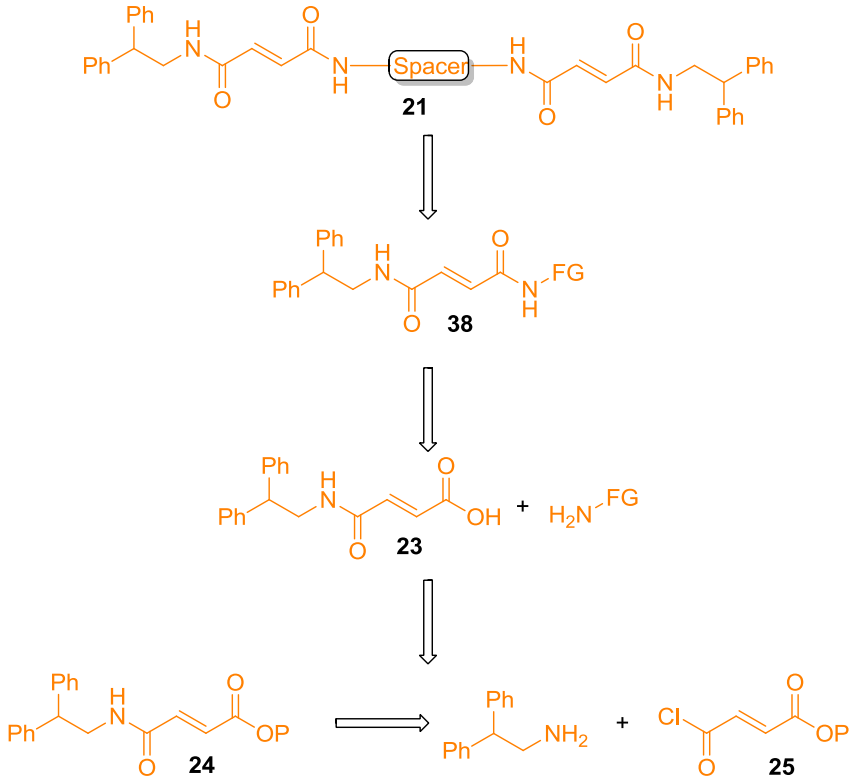

Scheme 2.16: Retrosynthetic analysis of route C towards the synthesis of the thread **21**.

As previously discussed, several attempts to couple the thread precursor **23** with diamines proved unsuccessful. However, a mono reacted amide coupling mediated by EDC was detected (see Scheme 2.6). Therefore, EDC as coupling agent was tested for the coupling of acid **23** and allylamine (Scheme 2.17).

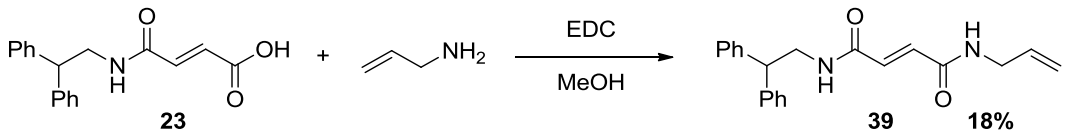

Scheme 2.17: EDC mediated amide coupling between the thread precursor **23** with allylamine.

The desired product was observed however its purity and yield were low. For this reason several attempts to optimise this reaction were carried out (Table 2.2).

Table 2.2: Different coupling reaction conditions studied for the thread precursor **23** with allylamine.

Entry	Reagent	Additive	Solvent	Time	Temp.	Result
1	DCC	-	THF	48 h	RT	7%
2	EDC	-	MeOH	18 h	RT	18%
3	NMM/IBCF	-	THF	30 min	-15 °C	3%

However, the EDC mediated coupling reaction gave the best results. Since the thread precursor **39** was synthesised in only 18% yield and the product was not completely pure, this approach was not investigated any further. Nevertheless, a possible reaction could be dimerisation by Grubbs-metathesis. The Grubbs-metathesis should lead to an *E / Z* mixture, which might be difficult to purify.

A $Zr(O^tBu)_4$ mediated coupling reaction was also tested (Scheme 2.18). However, only the starting ester **27** was recovered. This might be due to reaction or coordination of allylamine with to the Zr. Therefore, no other Lewis acid was investigated.

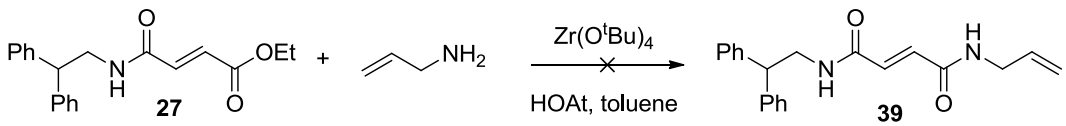

Scheme 2.18: Attempted Zr-mediated amide coupling.

The desired thread **21** has a diphenylethane motif as the secondary amide stopper, however this particular stopper group did not prove easily amenable for the proposed synthesis of the thread **21** (Sections 2.2.1 to 2.2.3). Therefore, an alternative thread system with similar templating-effect was investigated.

2.3 Synthesis of azo rotaxanes

In July 2010, Berná *et al.*[76] reported an azodicarboxamide thread system (Scheme **2.19**) with a similar templating-effect to the fumaric threads described by Leigh and co-workers (see Section 1.2.2).

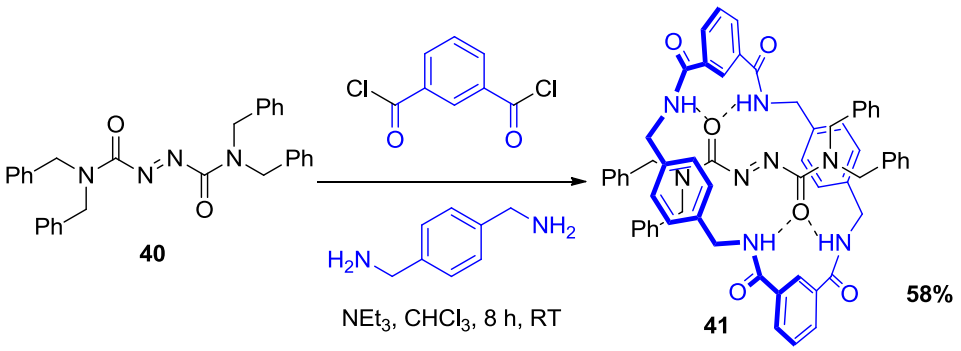

Scheme 2.19: Synthesis of the azodicarboxamide [2]rotaxane **41** by Berná.[76]

To gain a fuller understanding of this new thread system the previously reported thread **40**, as well as its building blocks, and the [2]rotaxane **41** were synthesised. The yields obtained were comparable to those reported and were easily reproducible (Scheme 2.20).

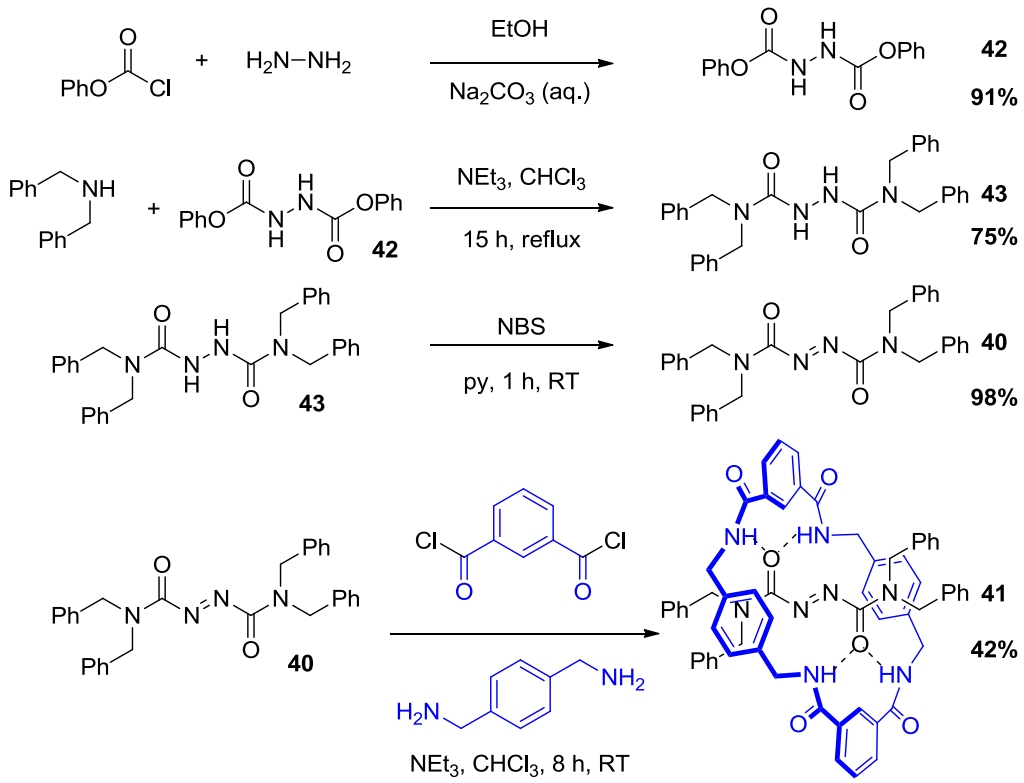

Scheme 2.20: Synthesis of the known azodicarboxamide [2]rotaxane **41**.

In the first step, phenylchloroformate was reacted with hydrazine to form the hydrazophenylcarbamate **42** in 91% yield. Phenylcarbamates are not very reactive, however they can be activated with heat and the addition of a base (e.g. triethylamine).[77] The phenylcarbamate **42** reacted with dibenzylamine under basic conditions in refluxing $CHCl_3$ to form the hydrazoamide **43**. Oxidation with *N*-bromosuccinimide (NBS) afforded the azo thread **40**. In a clipping process the azo [2]rotaxane **41** was formed using *p*-xylylenediamine and isophthaloyl dichloride. The yield was significantly lower than that reported by Leigh and co-workers for their [2]rotaxane, which suggests that the templating station is not as potent as the fumaric one. Despite the lower yield for the clipping process, the

efficient synthesis of the azo [2]rotaxane **41** might to enable a new route towards the synthesis of the desired [3]rotaxane.

Following an analogous pathway to that described for synthetic route A in Section 2.2.1, the azo thread **46** could be obtained via oxidation of the hydrazo thread **45** using NBS (Scheme 2.21). The desired hydrazo thread **45** could be formed by reaction of the hydrazophenylester **44** with various diamines. The hydrazophenylester **44** can be generated from the reaction between the diphenylester **42** and dibenzylamine.

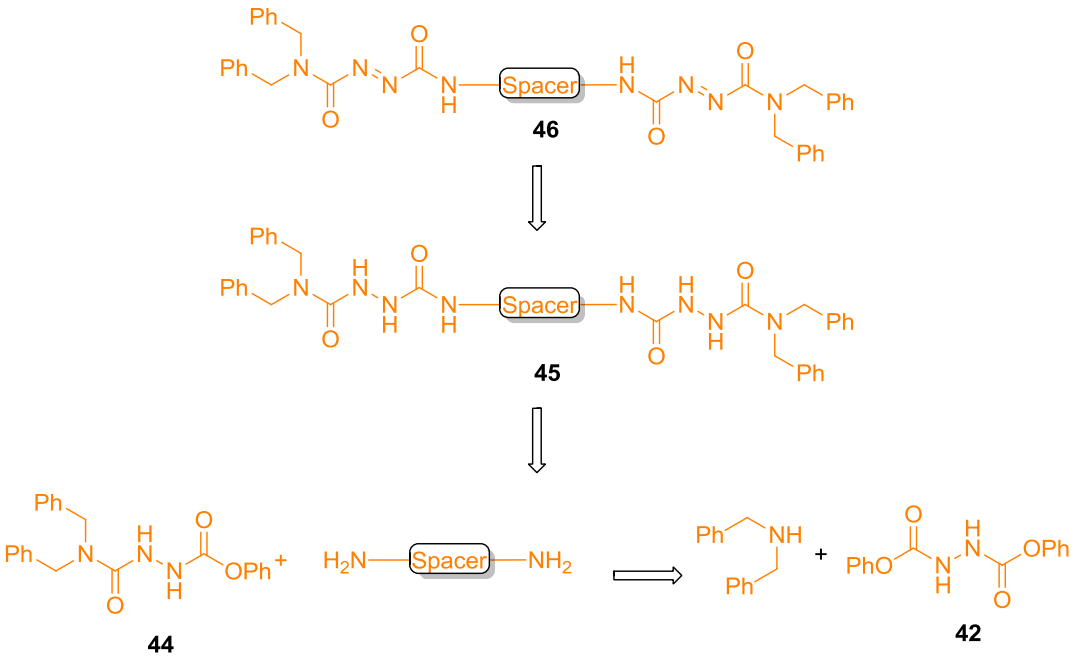

Scheme 2.21: Retrosynthesis of azo thread **46**.

Berná *et al*. described the synthesis of the building block **44** in 74% yield, which was used to form a two station [2]rotaxane with the ability to shuttle its macrocycle.

This building block was synthesised in 81% yield and purified via recrystallisation instead of by column chromatography as Berná described.

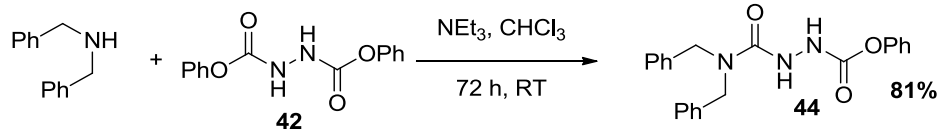

Scheme 2.22: Synthesis of the hydrazophenylester **44**.

By conducting the reaction at room temperature and decreasing the number of equivalents of dibenzylamine used, the formation of the mono-reacted hydrazophenylester **44** is favoured over the di-reacted azo dicarboxamide **43**.

2.3.1 Synthesis of azo rotaxanes with a three carbon spacer unit

The initial studies on the double fumaric thread system indicated that the use of 1,3-diaminopropane provided the highest yields compared to other diamines (see Section 2.2.2). Therefore, hydrazophenylester **44** was coupled with 1,3-diaminopropane in refluxing chloroform using NEt_3 as base (Scheme 2.23). The resulting reaction mixture was challenging to purify. Column chromatography resulted in crystallisation of the new hydrazo thread **47** on the column and only 38% of the product was isolated. An attempt to recrystallise the crude hydrazo thread **47** proved unsuccessful. Therefore, the moderate yield of 38% after chromatography was deemed acceptable.

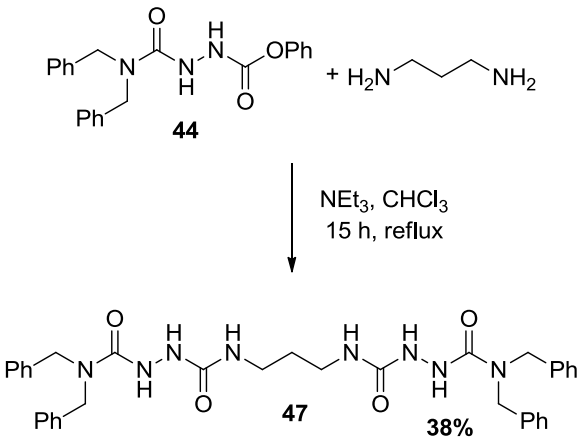

Scheme 2.23: Synthesis of the hydrazo thread **47**.

The hydrazo thread was then oxidised to the corresponding azo thread **48** using NBS (Scheme 2.24).

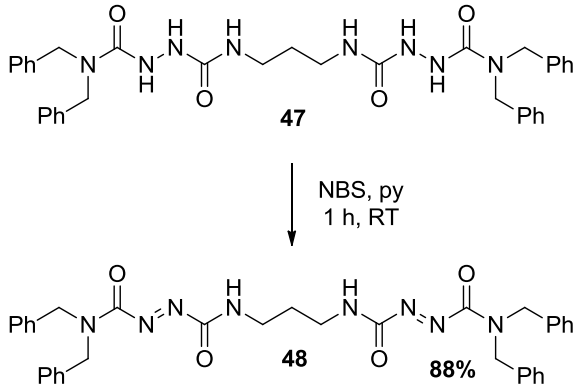

Scheme 2.24: Oxidation of the hydrazo thread **47** to the corresponding azo thread **48**.

It is noteworthy that in the process of changing the double fumaric thread (described in Section 2.2) to the azo thread, three important modifications to the synthetic route and to the overall thread structure have been introduced:

- the templating station has been altered from fumaric to azo-dicarboxylate;

- the activated species to couple the station with the spacer unit has been changed from an activated acid to a phenylester;
- the amines that generate the stopper groups have been modified from primary amines to secondary amines.

The azo thread **48** was then used in a rotaxane formation reaction via the clipping method using *p*-xylylenediamine and isophthaloyl dichloride.

MALDI analysis of the crude sample suggested the formation of a [2]rotaxane with a mass of 1192 Da and a [3]rotaxane with a mass of 1726 Da (Figure 2.6).

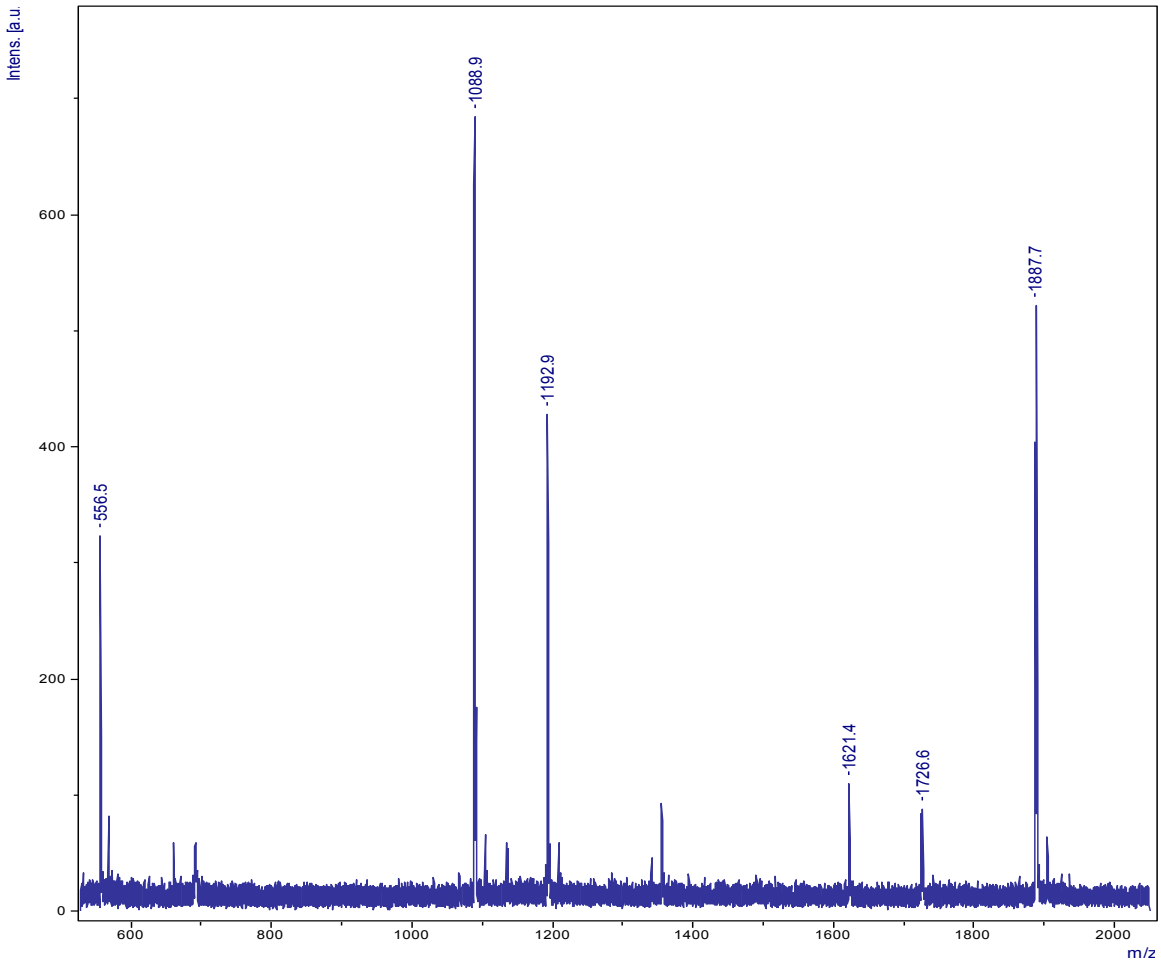

Figure 2.6: MALDI spectrum of rotaxane reaction using azo thread **48**.

Both of the mass peaks suggested that complete reduction of the azo stations had occured during the clipping process.

When attempting to purify the crude sample the major product of this reaction was found to be the unwanted catenane described by Leigh and co-workers,[78] accompanied by three different rotaxanes, the [2]rotaxanes **49** and **50** and the [3]rotaxane **51** (Scheme 2.25).

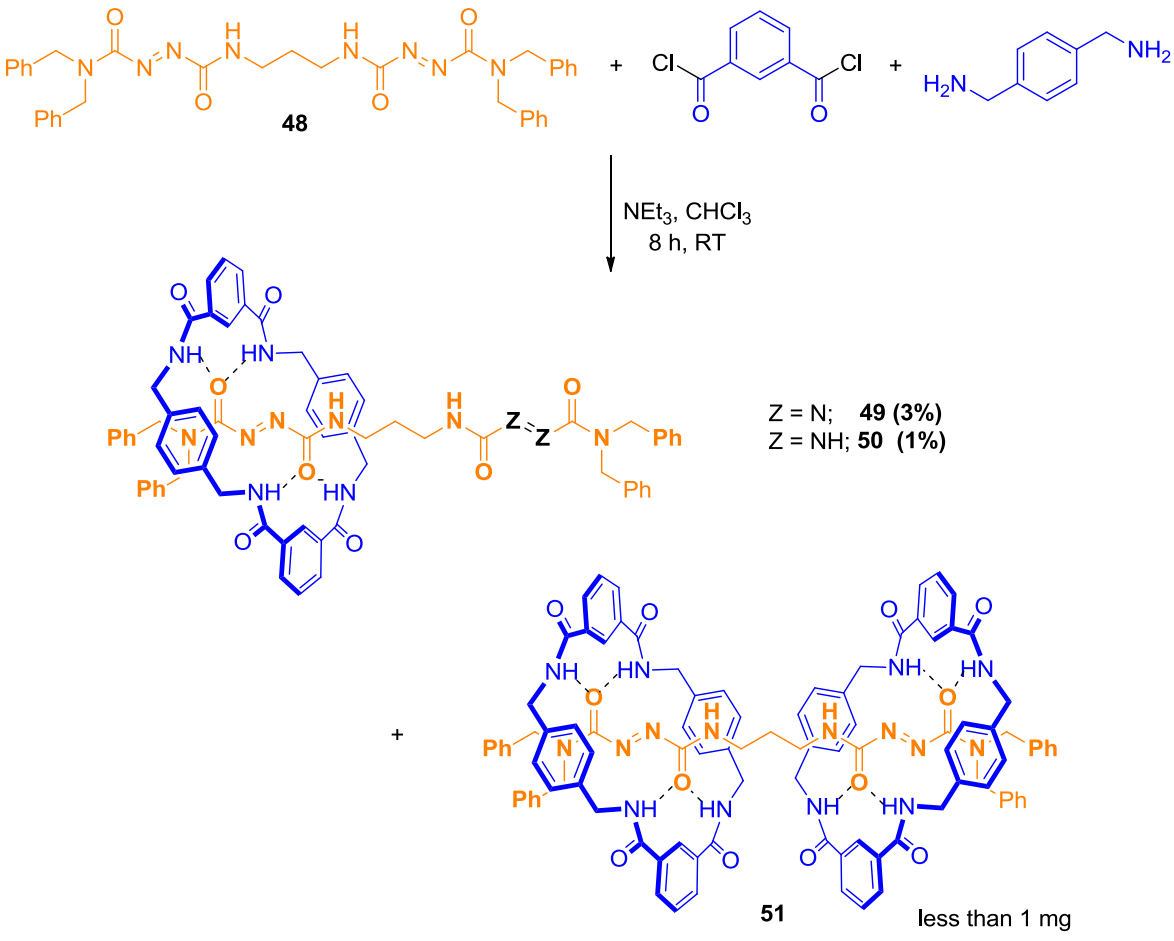

Scheme 2.25: Synthesis of three different azo rotaxanes with a three carbon spacer unit.

High Pressure Liquid Chromatography (HPLC) proved to be very useful for the identification and isolation of the diazo [2]rotaxane **50** and the partially reduced [2]rotaxane **49** (Figure 2.7).

A gradient method using a ramp from 100% water to 100% methanol over a period of 1 hour was used on a HPLC reverse phase column at a flow rate of 1 mL/min. This initial chromatogram helped to determine the ratio between the [2]- and [3]rotaxanes in the crude mixture. The presence of [2]rotaxanes was in an excess of 10:1 with respect to the desired [3]rotaxane. At this stage it was not obvious that two different [2]rotaxanes were formed.

There are several possible explanations for this product distribution. Assuming that the [2]rotaxane is formed first, the macrocycle could shuttle rapidly between the two stations and diminish the formation of the [3]rotaxane **51**. Another possibility is that the two macrocycles are too close together such that the first formed macrocycle blocks the second one from assembling at the other station.

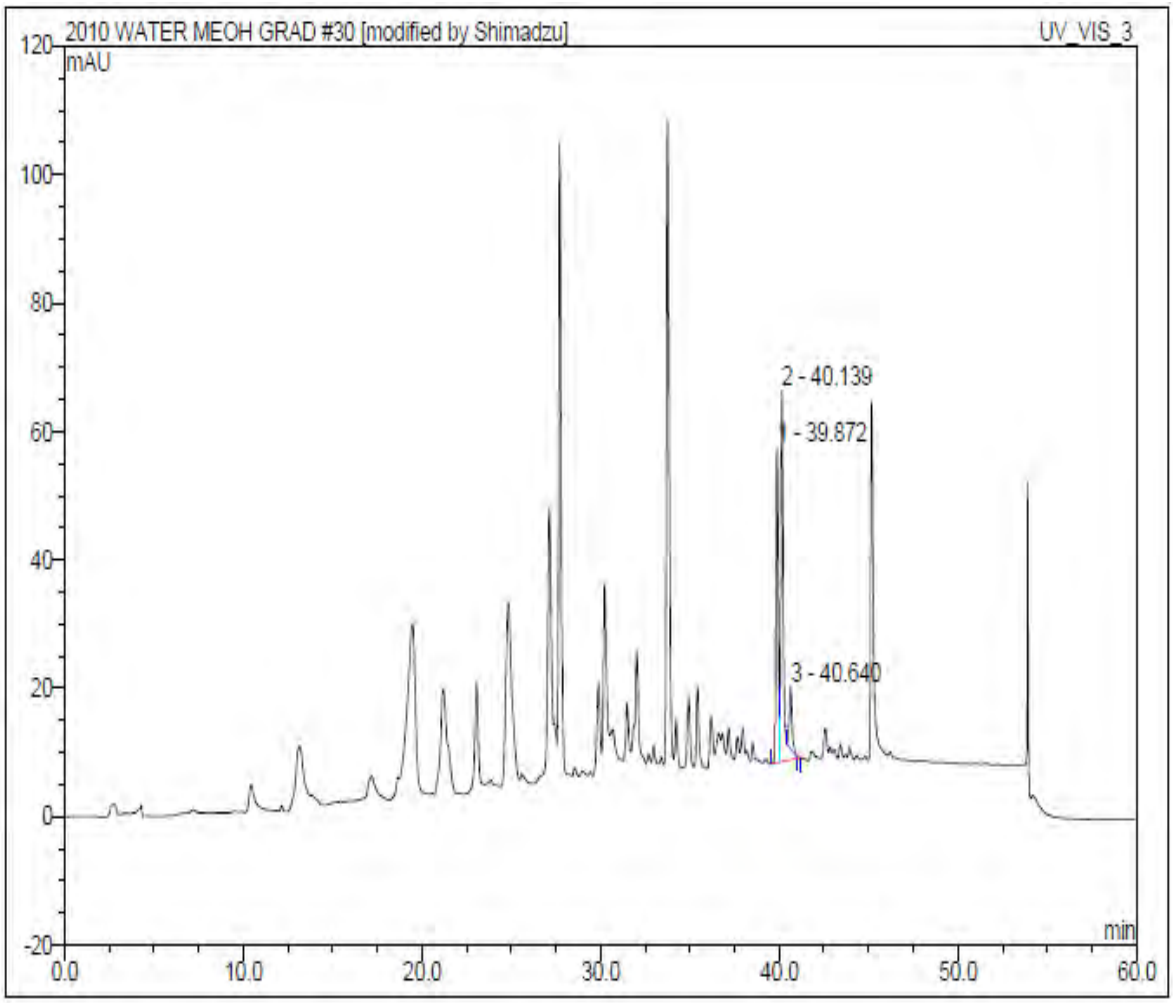

No.	Ret.Time min	Peak Name	Height mAU	Area mAU*min	Rel.Area %	Amount	Type
1	39.87	n.a.	49.214	7.361	38.41	n.a.	BM
2	40.14	n.a.	57.802	10.063	52.50	n.a.	MB
3	40.64	n.a.	9.704	1.742	9.09	n.a.	Rd
Total:			116.720	19.167	100.00	0.000	

Figure 2.7: Analytical HPLC chromatogram of the rotaxane reaction using the azo thread **48**. The first peak (39.87 min) corresponds to the reduced [2]rotaxane **49**, the peak at 40.14 min corresponds to the diazo [2]rotaxane **50** and the third highlighted peak at 40.64 min corresponds to the [3]rotaxane **51**.

2.3.2 Synthesis of azo rotaxanes with a four carbon spacer unit

In order to further investigate these hypotheses, an azo thread with a four carbon spacer unit was synthesised. Initially, the hydrazophenylester **44** was coupled with 1,4-diaminobutane in refluxing chloroform using NEt_3 as base (Scheme 2.26).

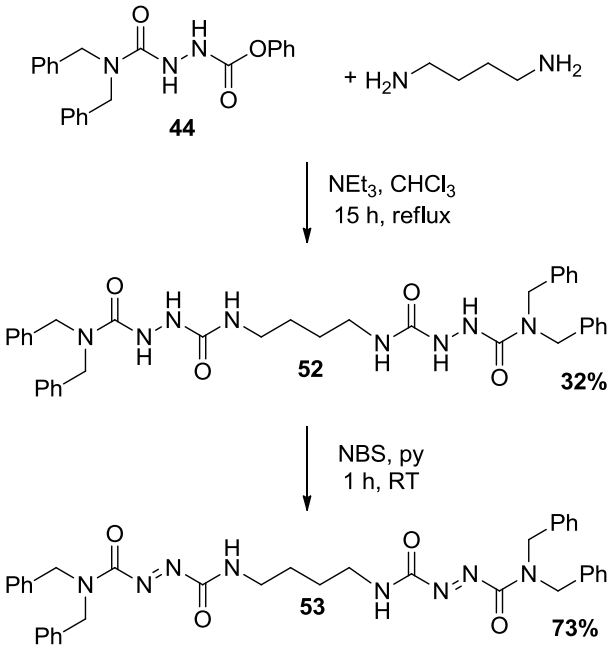

Scheme 2.26: Synthesis of the azo thread **53**.

The newly synthesised hydrazo thread **52** presented similar purification issues to those observed for the hydrazo thread **47**. Therefore, the thread **52** could only be purified via column chromatography in 32% yield. Oxidation of **52** using NBS afforded the azo thread **53** in 73% yield.

The azo thread **53** was subsequently reacted under the previously described clipping conditions and analysed via HPLC and MALDI. The HPLC chromatogram showed an increased in the formation of the [3]rotaxane, with a ratio of 6:1 between the [2]- and [3]rotaxanes.

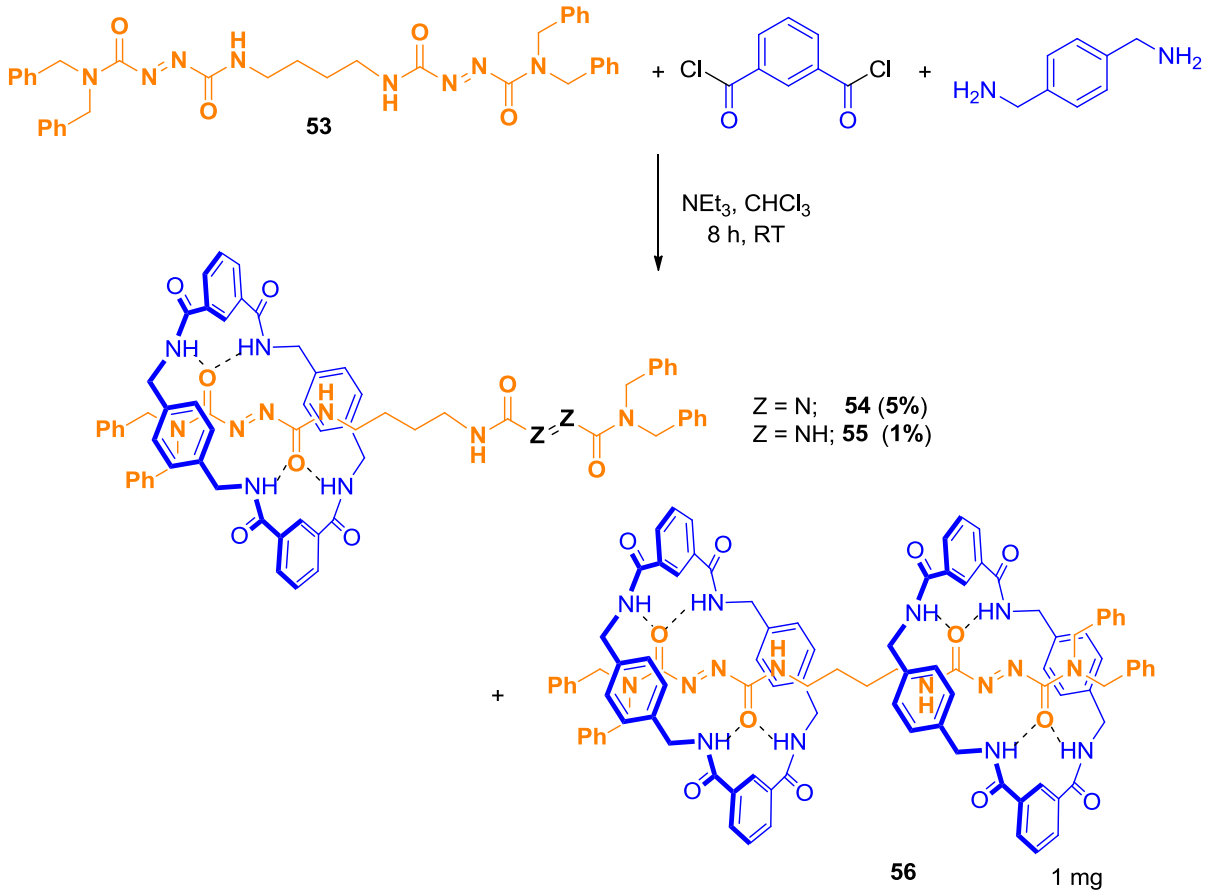

Scheme 2.27: Synthesis of three different azo rotaxanes with a four carbon spacer unit

However, only the two different [2]rotaxanes could be isolated using HPLC. When trying to isolate these [2]rotaxanes via flash column chromatography an interesting phenomenon was observed. The [2]rotaxane **54** and the free macrocycle co-eluted with nearly a perfect 1:1 ratio. Consequently, the ^{1}H NMR spectrum suggested the isolation of the [3]rotaxane **56**, which contradicted the results observed by ES+ and MALDI mass spectrometries.

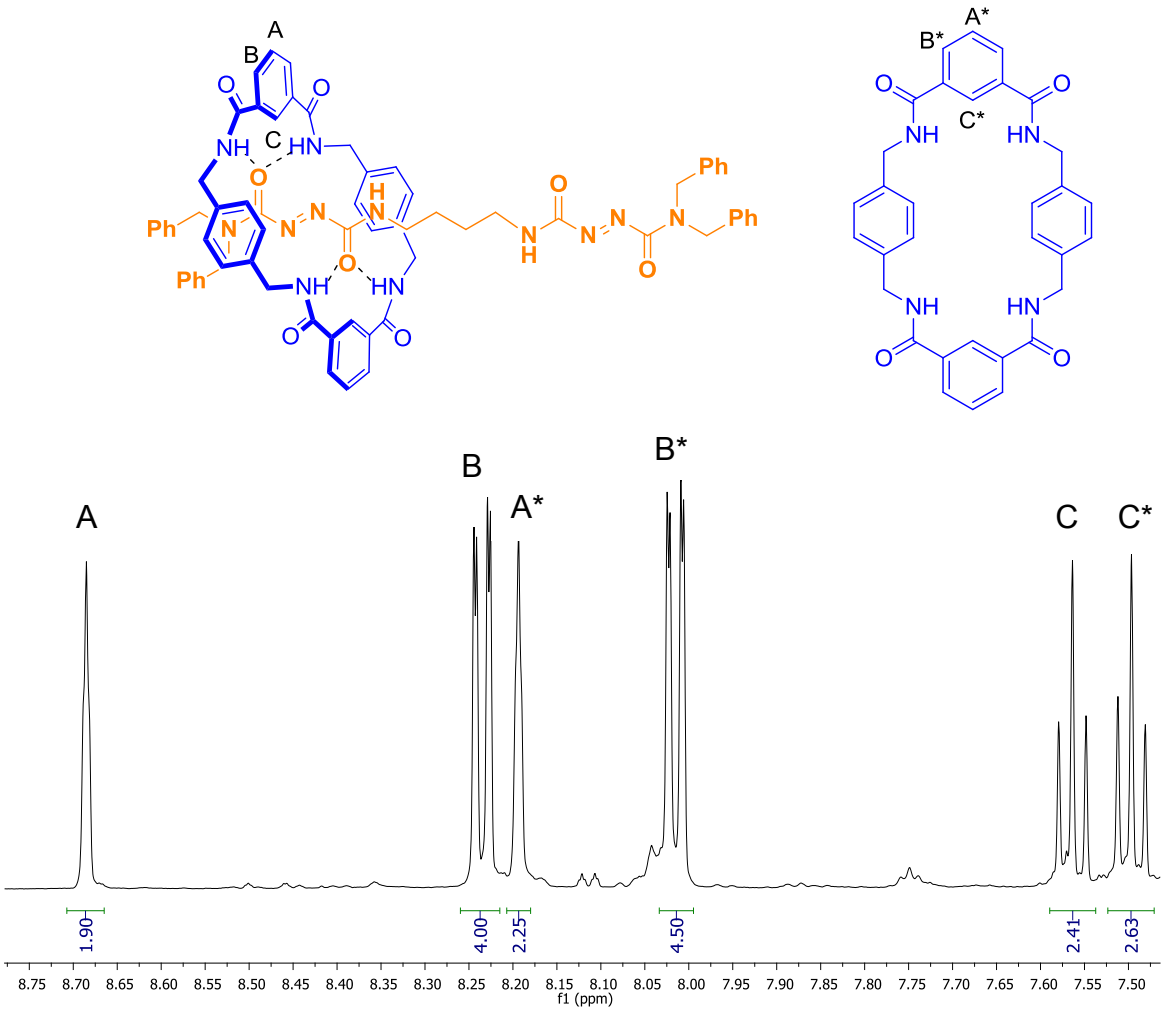

Figure 2.8: ^{1}H NMR spectrum of [2]rotaxane **54** and free macrocycle.

Figure 2.8 shows the aromatic region of the ^{1}H NMR spectrum of the purified material. A doubling of the signals of the distinctive A, B and C protons is observed. The protons with a star correspond to the free macrocycle and the ones without, to the [2]rotaxane **54**. The integration is nearly 1:1, which suggested the isolation of the desired [3]rotaxane. However, the splitting of the signals for the A, B and C protons into two pair of sets contradicts the existence of the [3]rotaxane. In order to elucidate whether some sort of uncommon conformer issue was

observed, saturation transfer experiments (GOSY) and variable temperature NMR studies (Figure 2.9) were performed.

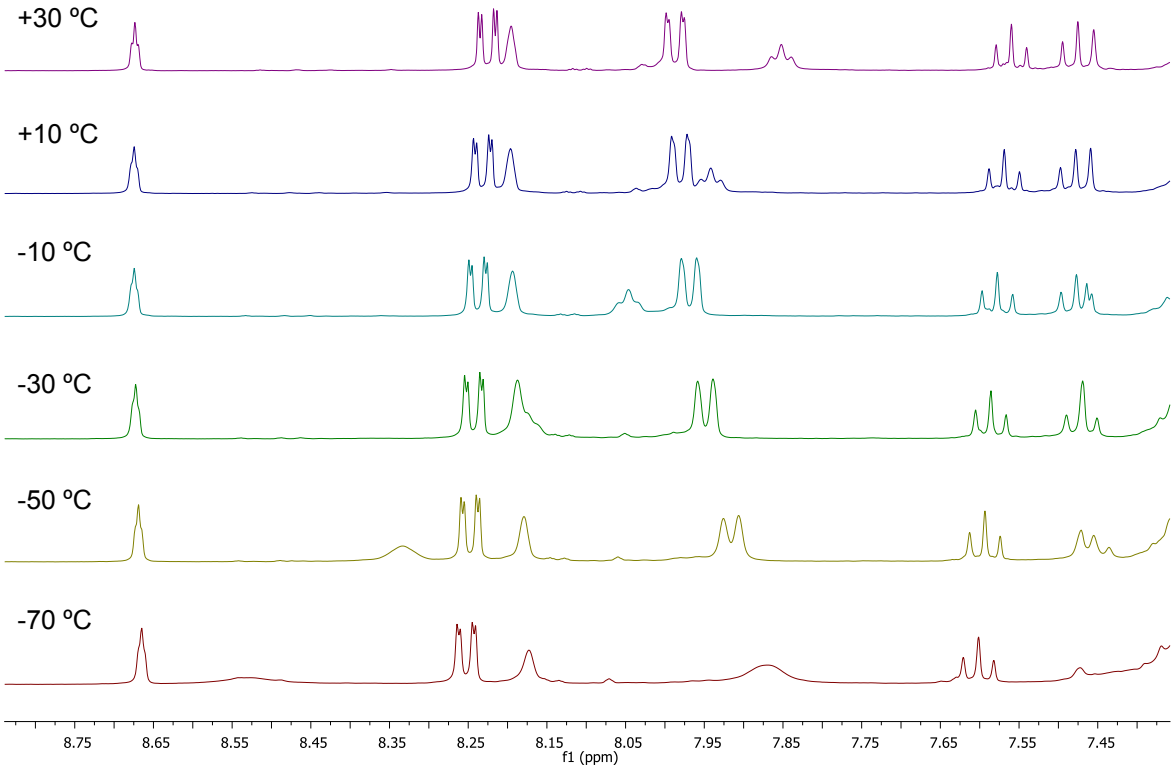

Figure 2.9: VT-NMR spectra of the 1:1 mixture of [2]rotaxane **54** and free macrocycle.

At lower temperature only the signals of the [2]rotaxane **54** are sharp and definite, while the signals of the free macrocycle are broad. The two sets of signals did not convert into one set either, which strongly implies the existence of two different compounds.

The existence of the two species was further proven by injecting the NMR sample into a HPLC column to separate the two compounds. The ^{1}H NMR spectra of the

HPLC purified [2]rotaxane **54** showed the expected A, B and C protons and the lack of the macrocyclic A*, B* and C* protons.

2.3.3 Synthesis of azo rotaxanes with a five carbon spacer unit

Since a significant increase in the formation of [3]rotaxane was observed when increasing the spacer length (from three to four carbons), a five-carbon linker was investigated next. The hydrazophenylester **44** was coupled with 1,5-pentanediamine in refluxing chloroform using NEt_3 as base (Scheme 2.28). The hydrazo thread **57** was isolated in moderate 29% yield as it presented the same behaviour observed for threads **47** and **52**. The hydrazo thread **57** was oxidised to the azo thread **58** in 88% yield.

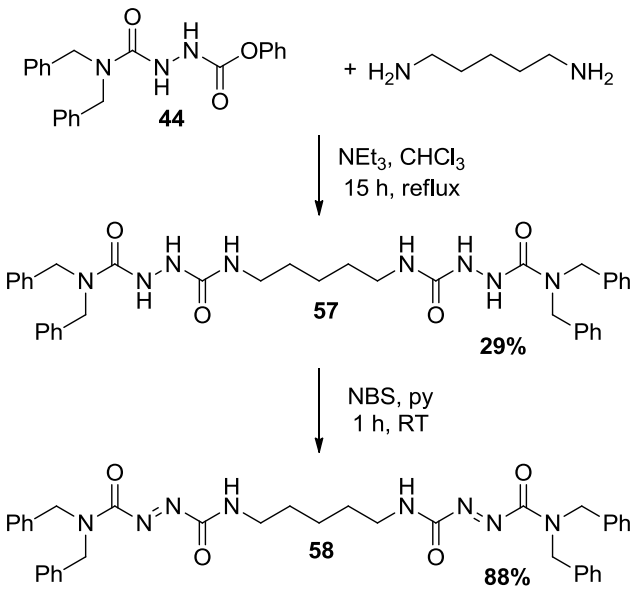

Scheme 2.28: Synthesis of the azo thread **58**.

The azo thread **58** was used to synthesise the desired [3]rotaxane **61**, although in a very low yield (3%). Unsurprisingly, the azo [2]rotaxane **59** and the hydrazo [2]rotaxane **60** were also observed and these were isolated.

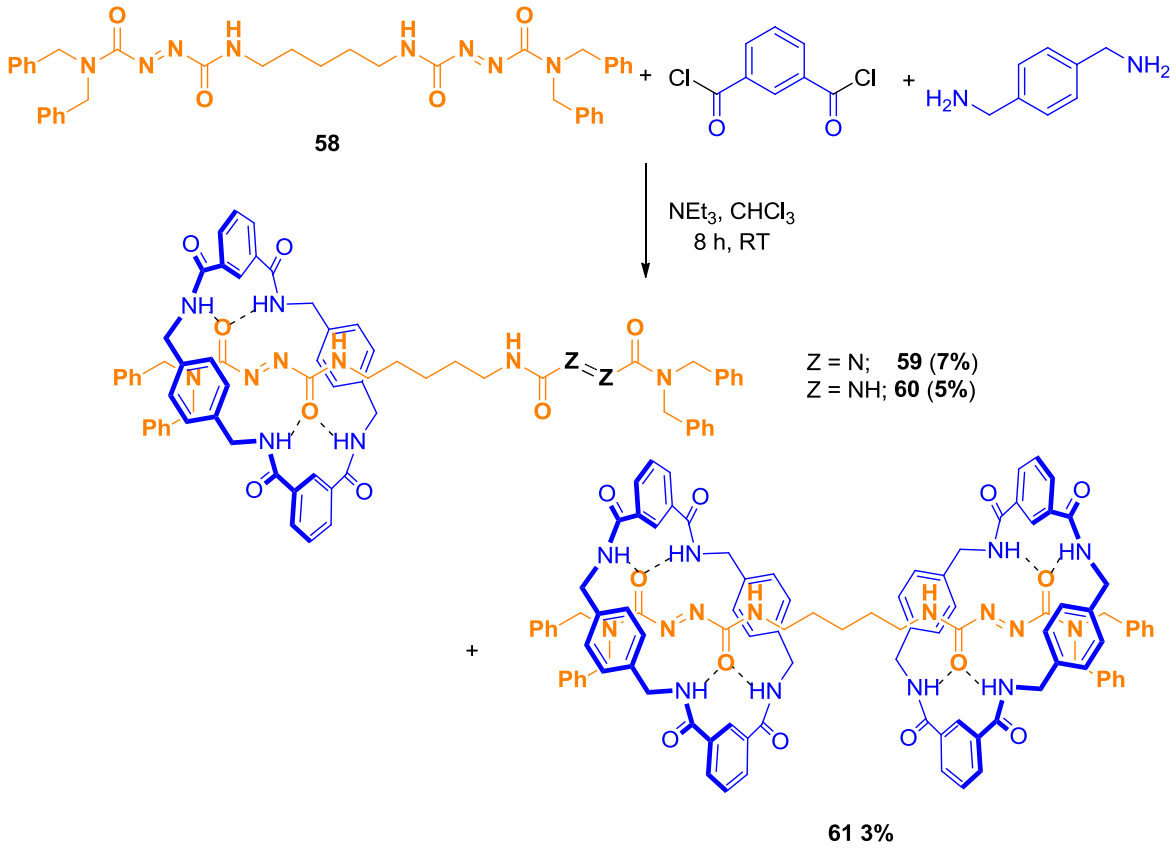

Scheme 2.29: Synthesis of three different azo rotaxanes with a five carbon spacer unit.

Isolation and characterisation of the desired [3]rotaxane **61** was realised via an isocratic HPLC method using a mixture of methanol and water (75 : 25). Significant quantities of the azo **59** and hydrazo **60** [2]rotaxanes were also isolated and fully characterised. Figure 2.10 show the resulting HPLC chromatogram.

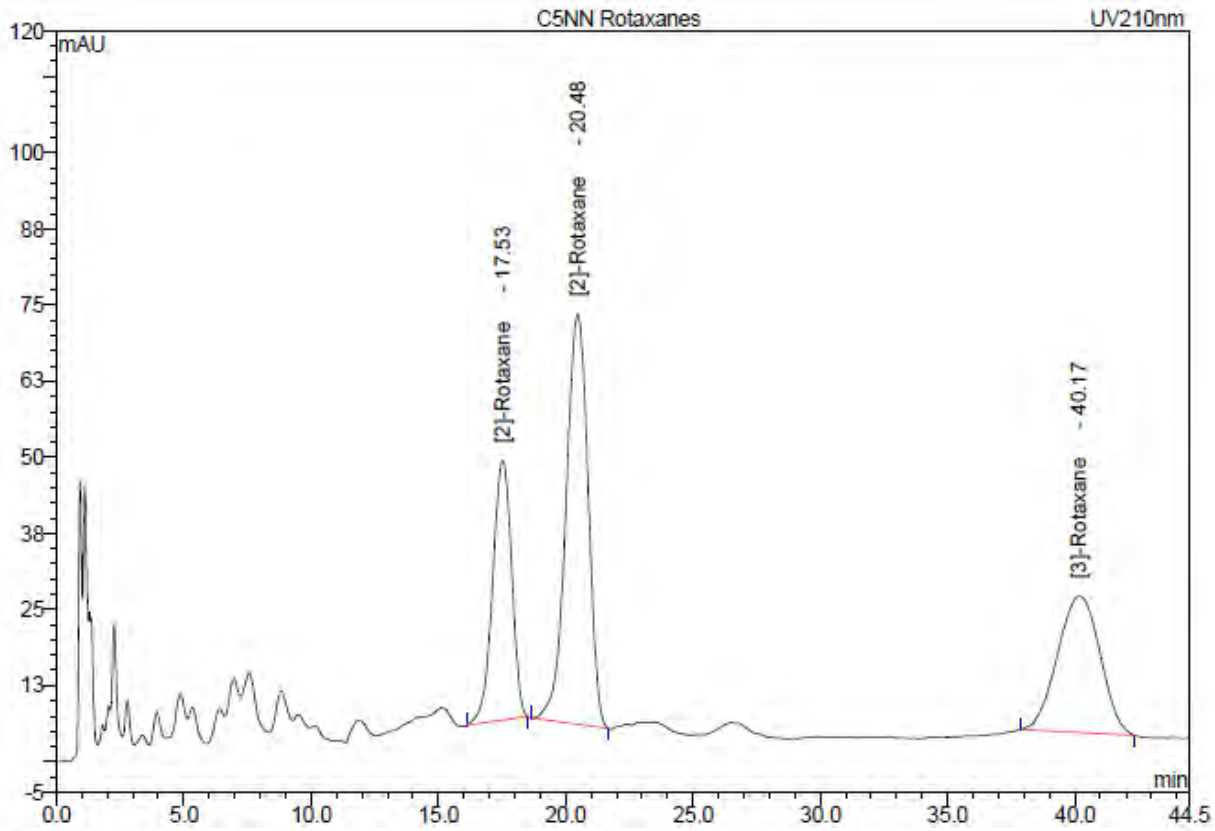

No.	Ret.Time min	Peak Name	Height mAU	Area mAU*min	Rel.Area %	Amount	Type
1	17.53	[2]-Rotaxane	42.614	36.774	24.87	n.a.	BMB*^
2	20.48	[2]-Rotaxane	67.288	67.659	45.76	n.a.	BMB*^
3	40.17	[3]-Rotaxane	22.389	43.408	29.36	n.a.	BMB*^
Total:			132.291	147.840	100.00	0.000	

Figure 2.10: Analytical HPLC chromatogram of the rotaxane reaction using the azo thread **58**. Hydrazo [2]rotaxane **60** at 17.53 min, azo [2]rotaxane **59** at 20.48 min and [3]rotaxane **61** at 40.17 min.

Attempts to increase the yield of the desired [3]rotaxane **61** were unsuccessful. Neither slower addition nor changing the monomer concentration led to an increase in the formation of the [3]rotaxane **61**.

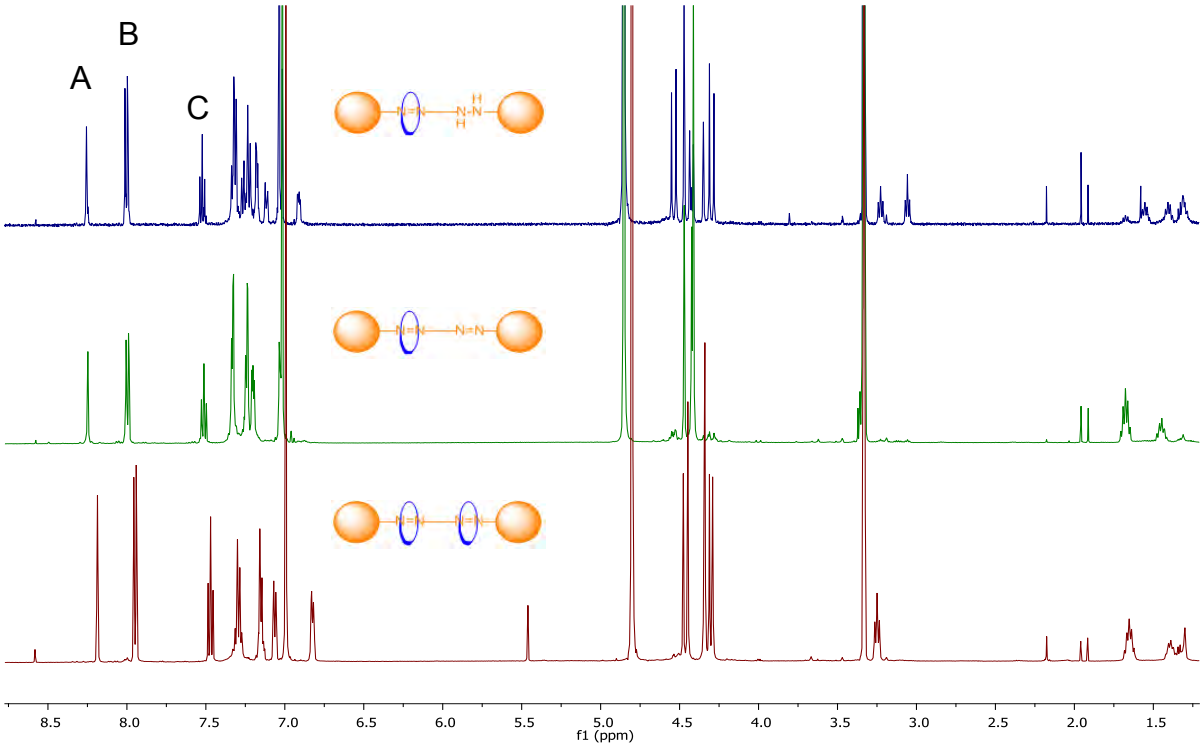

Figure 2.11: ^{1}H NMR spectra of the three different azo rotaxanes with a five carbon spacer unit. The hydrazo [2]rotaxane **60** in blue, the azo [2]rotaxane **59** in green and the azo [3]rotaxane **61** in red.

Figure 2.11 shows the ^{1}H NMR spectra of the three different azo rotaxanes with a five carbon spacer unit. In the aromatic region, the A, B and C protons were clearly identified. The aromatic signals of the stopper groups are less defined for the azo and hydrazo [2]rotaxanes. The benzylic region is quite complex and it is expanded in Figure 2.12. The benzylic protons belong to the two benzylic groups of the stoppers and the four benzylic units of the macrocycle.

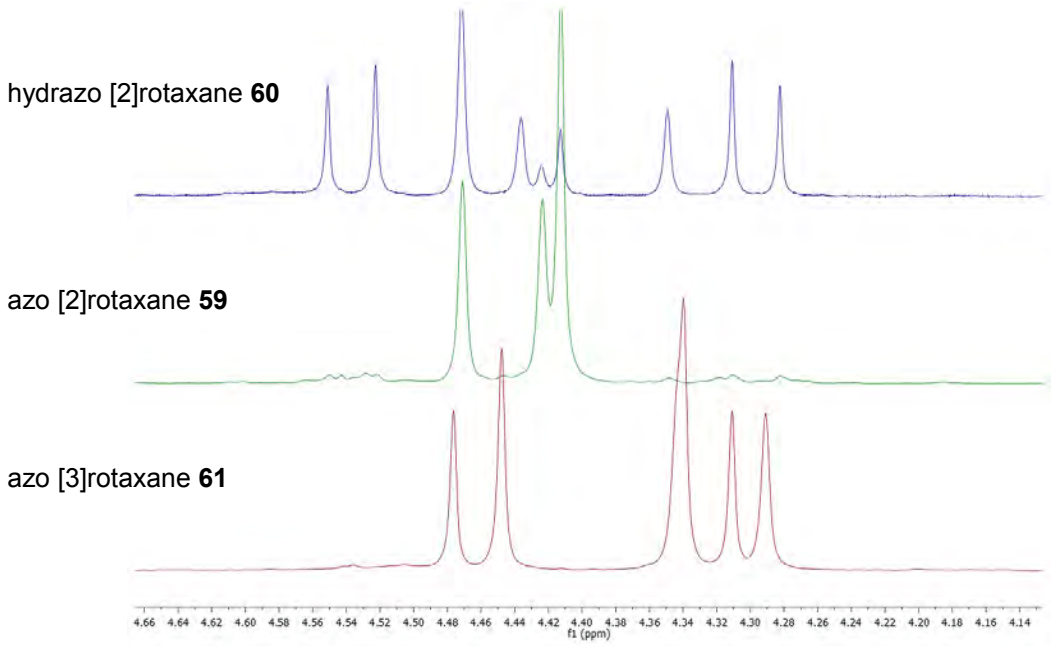

Figure 2.12: Benzylic region of the ^{1}H NMR spectra of the three azo rotaxanes with a five carbon spacer unit. The hydrazo [2]rotaxane **60** in blue, the azo [2]rotaxane **59** in green and the azo [3]rotaxane **61** in red.

The ^{1}H NMR spectrum for the partially reduced hydrazo [2]rotaxane **60** (shown in blue) is rather complex, since the macrocycle is mainly located over the azo station and therefore the [2]rotaxane **60** is unsymmetrical. Consequently, separate benzylic signals are observed for the stoppers on the azo station, hydrazo station and the macrocycle. The aliphatic signals of the [2]rotaxane **60** are also split indicating that the shuttling is stopped. The ^{1}H NMR spectrum of the azo [2]rotaxane **59** (shown in green) presents just three signals in the benzylic region. This is due to the shuttling process between the two stations. Since both stations are identical, a simpler ^{1}H NMR spectrum is observed. The [3]rotaxane **61** (^{1}H NMR spectrum shown in red) has two fully occupied stations and cannot shuttle, therefore five signals are detected. These observations are in agreement with those recently reported by Berná and co-workers.[79]

Berná has reported that only the azo stations and not their reduced counter parts are able to form a rotaxane in good yield.[76] Since a 12% yield of unwanted [2]rotaxanes was obtained and given that the oxidised [2]rotaxane **59** might form the desired [3]rotaxane **61**, it was investigated whether the reduced [2]rotaxane **60** could be re-oxidised to the [2]rotaxane **59**. After the HPLC purification, the reduced hydrazo [2]rotaxane **60** could not be completely purified. Therefore, the obtained 4:1 (reduced : oxidised) mixture was oxidised to completion using NBS (Scheme 2.30).

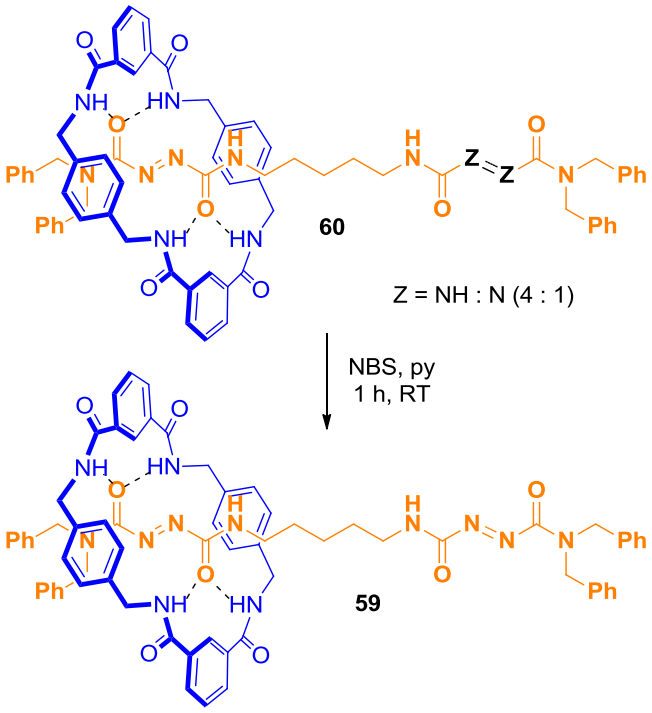

Scheme 2.30: Oxidation of the [2]rotaxane **60**.

A second clipping reaction was then performed on the azo [2]rotaxane **59** and the [3]rotaxane **61** was successfully isolated in 22% yield (Scheme 2.31). Not surprisingly, spontaneous reduction of one of the azo stations on the [2]rotaxane

59 to yield **60** was also observed. This is the main drawback of this approach as only 13% combined yield of the starting and reduced [2]rotaxanes could be obtained.

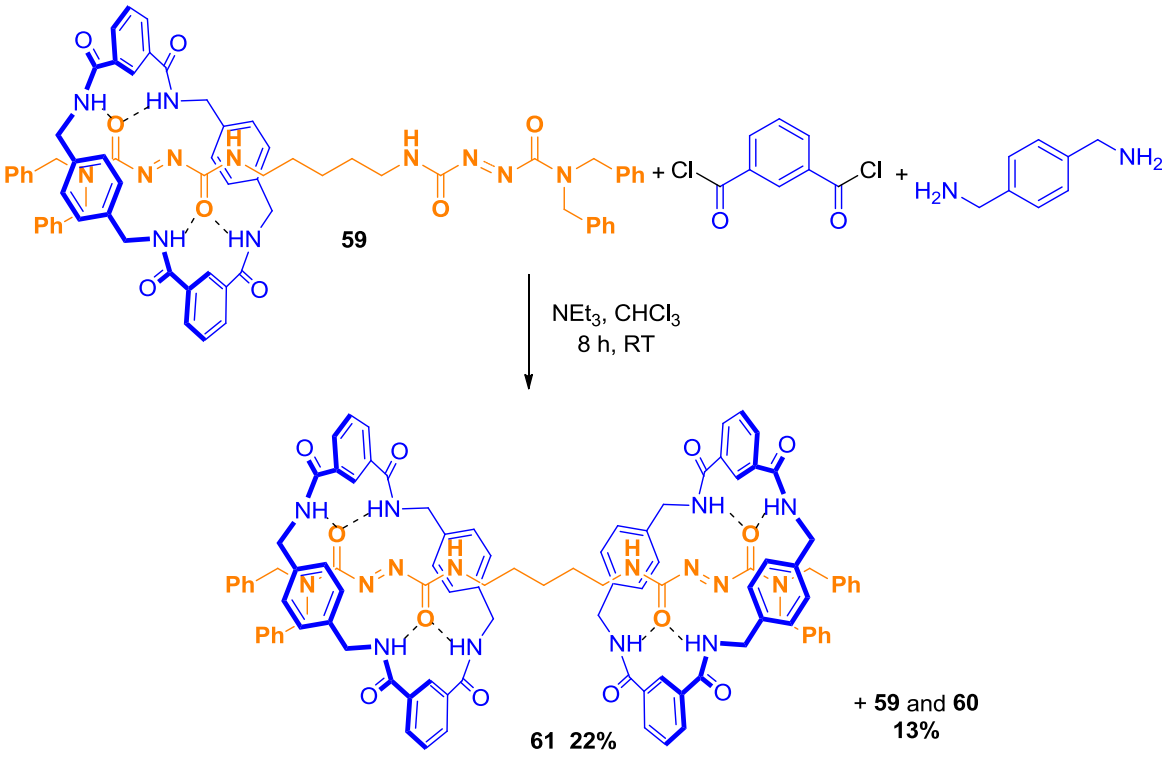

Scheme 2.31: Clipping reaction starting from [2]rotaxane **59**.

Colourless crystals suitable for X-ray diffraction were obtained by slow evaporation of a dichloromethane : methanol (1:1) solution of [3]rotaxane **61**. The X-ray crystal structure confirms the formation of a [3]rotaxane as shown in Figure 2.13, where the macrocycles are highlighted in blue and the thread in orange.

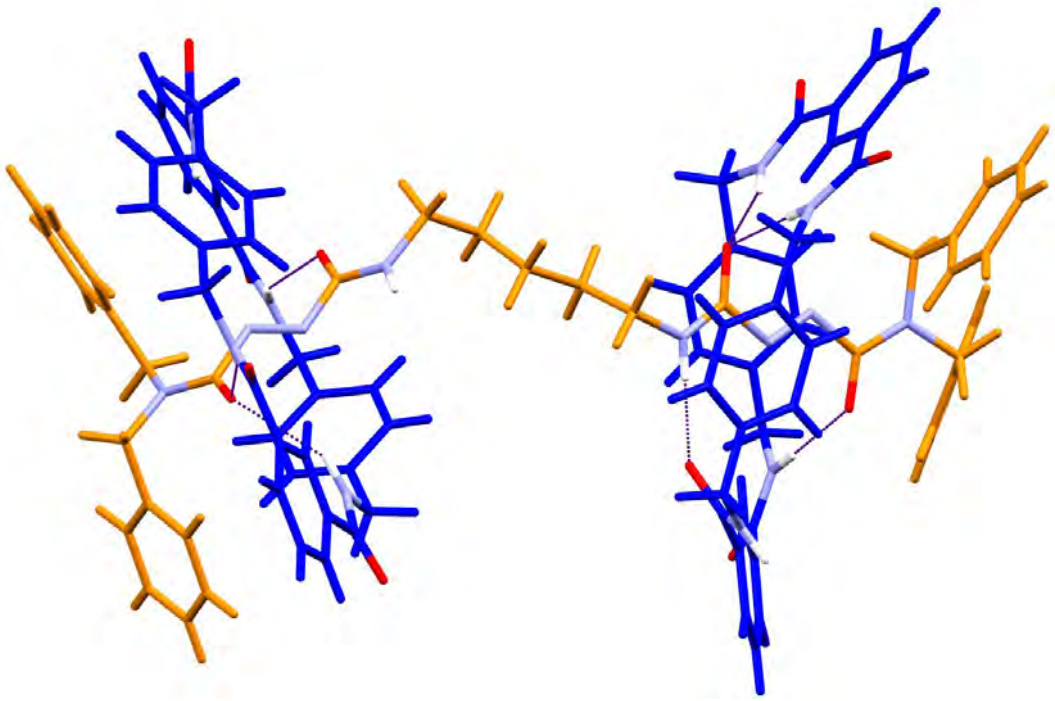

Figure 2.13: Crytal structure of [3]rotaxane **61**. Solvent molecules have been omitted for clarity.

The macrocycles have a twisted boat-like structure. As previously discussed (see Section 1.2.2), this conformation suggests that the critical cyclic *syn syn* intermediate around the thread is not effectively formed, which is also represented in the low yield obtained. The macrocycles are twisted with respect to one another by 38° and they are located at 11.6 Å from each other. Hydrogen bonds (shown in purple) are observed between the thread and the macrocycles. The bond length distance between donor and acceptor ranges from 2.834(10) to 3.279(9) Å. The macrocycle on the right is twisted and one carbonyl group can hydrogen bond to one NH group of the spacer unit on the thread.

2.3.4 Spontaneous reduction of azo systems

In order to further investigate the spontaneous reduction observed on the azo rotaxanes, a series of experiments were undertaken on the simple azo thread **40**. This thread system can be readily synthesised in large quantities in three steps, providing access to a simple model system on which the spontaneous reduction reaction can be studied.

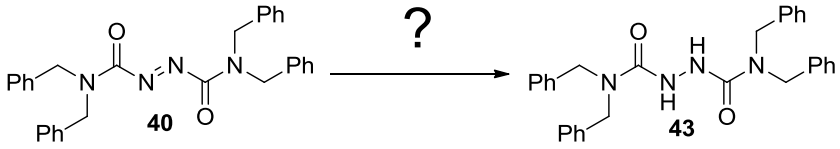

Scheme 2.32: Benchmark reaction for the spontaneous reduction.

Several reagents to reduce the azo thread **40** to its hydrazo analogue **43** (Scheme **2.32**) were tested and these are shown in Table 2.3.

Table 2.3: Reaction conditions studied for the reduction of the azo compound **40**.

Entry	Reagent	Amount	Time	Conversion
1	NEt_3	48 eq.	8 h	18%
2	HCl	48 eq.	8 h	1%
3	NEt_3 / HCl	48 eq.	8 h	2%
4	DMAP	500 eq.	6 d	-
5	NEt_3	500 eq.	6 d	quant.

When 48 equivalents of NEt_3 were used over a period of eight hours, the same conditions used in the clipping process, a conversion of 18% from the azo to the

hydrazo compound was observed. On the other hand, if HCl was used a conversion of only 1% was detected, although this may be due to a different reaction pathway. A mixture of NEt_3 and HCl yielded 2% conversion. This result suggests that the rates of reduction for NEt_3 and HCl are different since a higher yield was observed when the combination of both reagents was used. 500 equivalents of NEt_3 led to full conversion of the azo compound **40** to the reduced hydrazo analogue after six days at RT. DMAP did not give any conversion.

These reactions were monitored by ^1H NMR spectroscopy and the percentage of conversion was calculated according to the integration of the different peaks (Figure 2.14). The benzylic region is significantly different in the azo and hydrazo compounds.

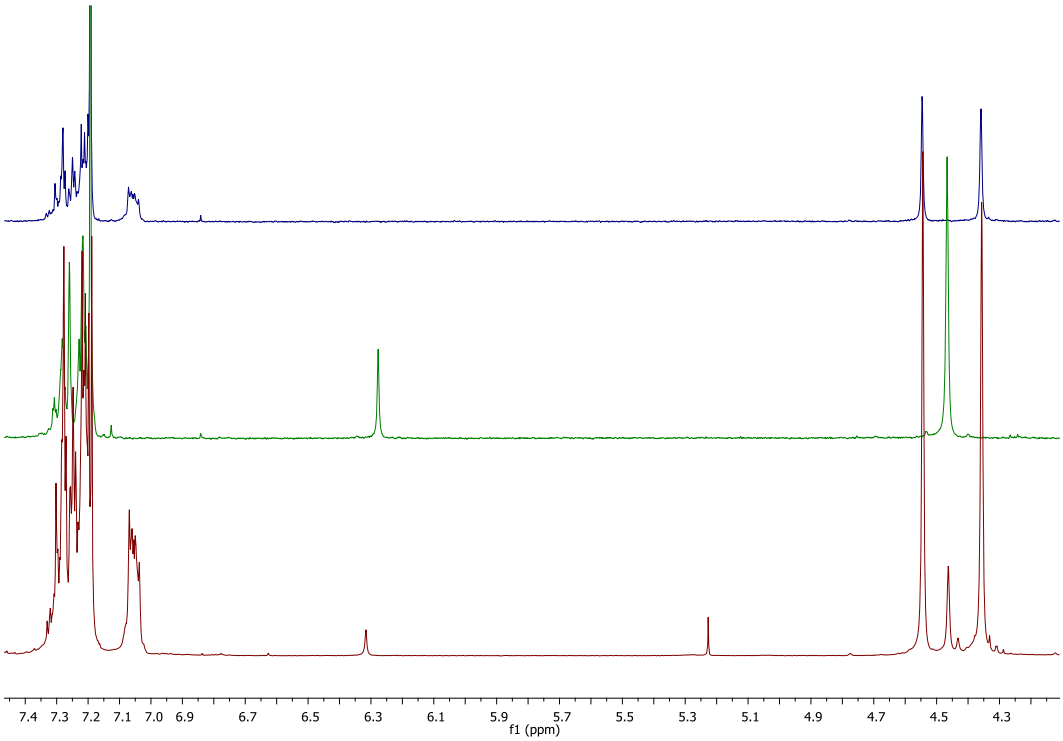

Figure 2.14: ^1H NMR spectra from the azo thread **40** (in blue), the hydrazo thread **43** (in green) and the reaction mixture of the azo thread **40** and 48 eq. of NEt_3 (in red).

The ^{1}H NMR spectrum shown in blue corresponds to the azo thread **40** and presents two benzylic signals, since **40** is conformationally locked due to amide rotamer restriction. However, in the hydrazo thread **43** (^{1}H NMR spectrum shown in green) these benzylic protons coalesced at RT and a singlet is observed. In the spectrum shown in red, which corresponds to the reaction mixture of the azo compound **40** with 48 equivalents of NEt_3, a new peak at 4.46 ppm corresponding to the hydrazo compound is observed.

As mentioned above, there are several possible mechanisms for this spontaneous reduction process. However, to date, it has not been possible to clearly elucidate it. The most feasible reaction pathway is depicted in Scheme 2.33.

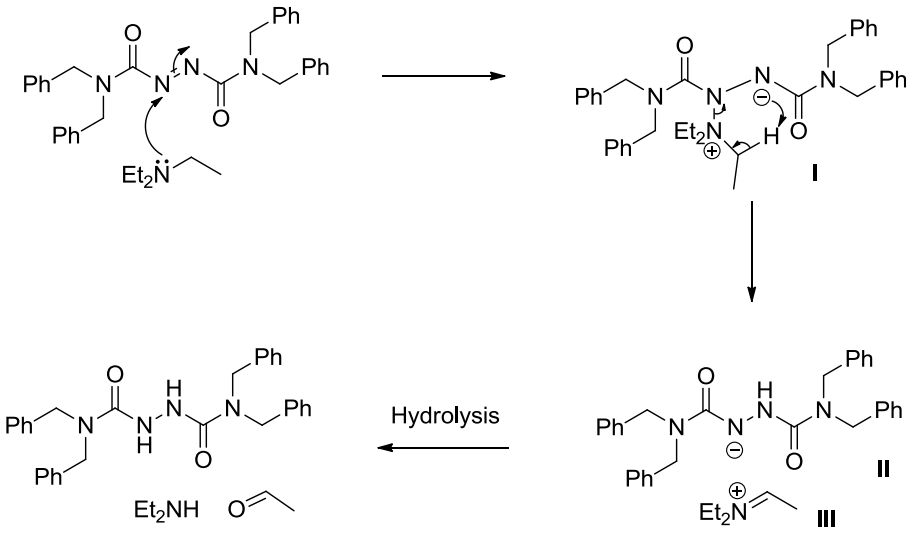

Scheme 2.33: Proposed mechanism for the formation of the hydrazo compound **43**.

In the first step, NEt_3 might add to the azo compound in the same way that PPh_3 does in a Mitsunobu reaction, and the zwitterionic intermediate **I** might be formed. An α-hydrogen abstraction, via a five-membered ring transition state, followed by

elimination might lead to the negatively charged hydrazo species **II** and the positively charged iminium intermediate **III**. Hydrolysis might yield the hydrazo compound **43**, diethylamine and acetaldehyde. This proposed mechanism could be considered as an addition / elimination / hydrolysis sequence. However, the term reduction seems appropriate in order to compare the azo and hydrazo compounds.

2.4 Synthesis of fumaric rotaxanes

An alternative approach intending to overcome the spontaneous reduction, the low yield for the formation of the desired [3]rotaxanes, and the fact that the two macrocycles are quite separated from each other, was explored. The idea that a change of the stopper group could lead to a double fumaric thread was explored.

2.4.1 Synthesis of a fumaric [2]rotaxane with dibenzylamide stopper groups

As a starting point, the successful dibenzyl motif used on the azo rotaxanes was chosen as the stopper group for the new fumaric threads. The thread **62** was synthesised in order to test the effect of using dibenzylamine as a stopper group in the formation of a simple thread (Scheme 2.34).

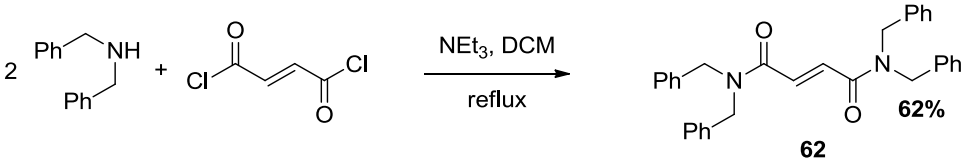

Scheme 2.34: Synthesis of the fumaric thread **62**.

The thread **62** was then reacted under the previously used clipping reaction conditions for rotaxane formation and the [2]rotaxane **63** could be purified via column chromatography and was isolated in 84% yield (Scheme 2.35).

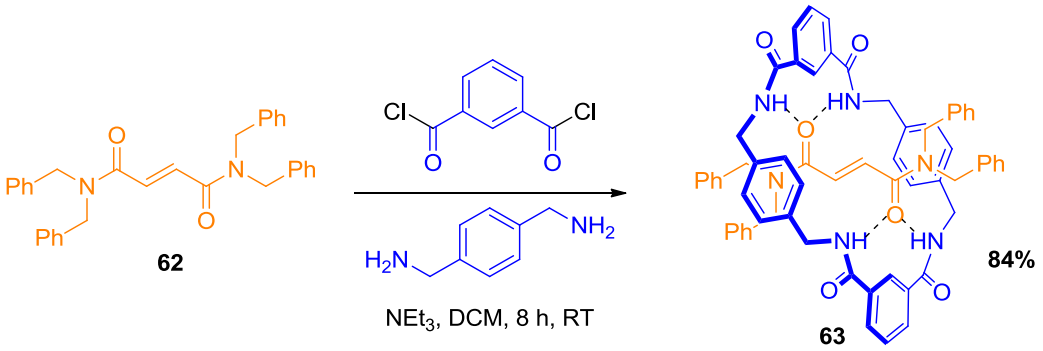

Scheme 2.35: Synthesis of the [2]rotaxane **63**.

In the aromatic region of the [2]rotaxane **63** the A, B, C and D protons of the macrocycle were clearly identified.

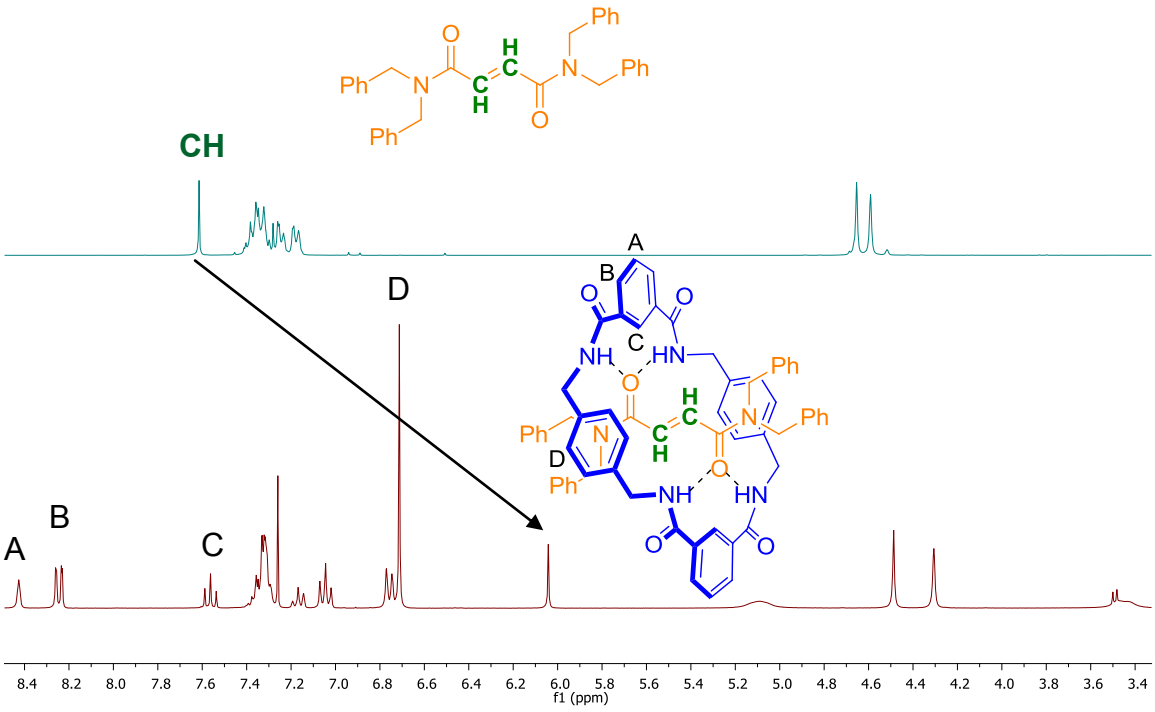

Figure 2.15: 1H NMR of thread **62** (in blue) and [2]rotaxane **63** (in red).

The olefinic protons (highlighted in green) of the thread **62** shifted upfield (from 7.61 to 6.04 ppm) upon formation of the [2]rotaxane **63**. This shielding effect is well documented and observed in several supramolecular systems, e.g. the fumaramides reported by Leigh *et al.*.[80] This shielding effect of the olefinic protons was observed in all of the following fumaramide based rotaxanes synthesised.

Colourless crystals suitable for X-ray diffraction were obtained by slow evaporation of a chloroform : methanol (10 : 1) solution of [2]rotaxane **63**.

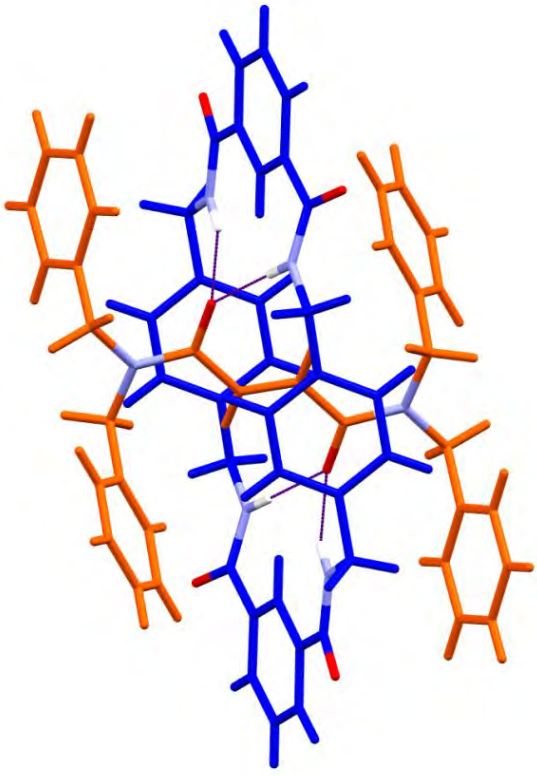

Figure 2.16: Crystal structure of [2]rotaxane **63**. Solvent molecules have been omitted for clarity.

The crystal structure confirms the formation of the desired fumaric [2]rotaxane with hydrogen bonds between the two O-atoms of the station and the NH of the

macrocycle being observed (Figure 2.16). The bond length distance between donor and acceptor ranges from 2.9772(18) to 3.2685(19) Å. The macrocycle is quite packed in between the two stopper groups, leaving little space between them. For this reason, the high yield formation of [2]rotaxane **63** is quite surprising. On the other hand, the macrocycle has a chair-like structure indicating that the cyclic *syn syn* intermediate around the thread is effectively formed, which results in a good yield. The centre of the molecule is located on an inversion centre such that only half of the [2]rotaxane is crystallographically unique with a symmetry relation of -x,-y,-z. In contrast with the twisting observed for the macrocycles of the [3]rotaxane **61**, the tetraamide macrocycle of this [2]rotaxane is at a near right angle with the thread.

2.4.2 Synthesis of a fumaric [3]rotaxane with a two carbon spacer unit

Encouraged by these promising results, a new synthetic route based on that described in Section 2.2.1 (route A) was investigated. Treatment of the acid chloride **26** with dibenzylamine gave the ester **64** in 86% yield. The ester **64** was then hydrolysed to afford the fumaric thread precursor **65** in essentially quantitative yield (99%). As discussed in Section 2.2, the acid chloride **26** is commercially available, however it was synthesised in quantitative yield in one step from mono-ethyl fumarate using thionyl chloride under reflux conditions.

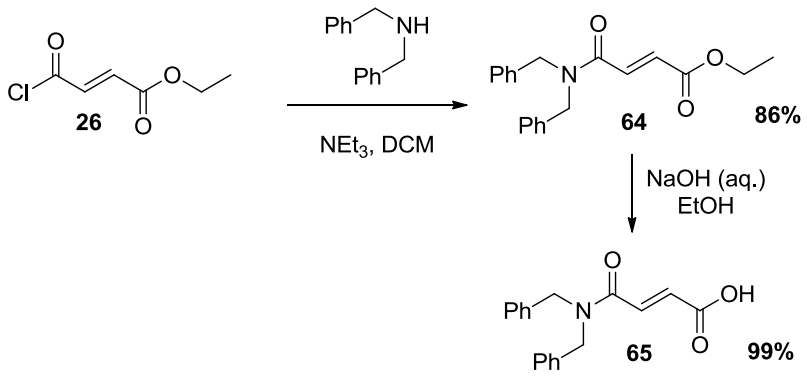

Scheme 2.36: Synthesis of the thread precursor **65**.

The thread precursor **65** was transformed into the corresponding acid chloride using thionyl chloride under reflux conditions. Treatment of the acid chloride with ethylenediamine gave the desired double fumaric thread **66** in 66% yield (Scheme **2.37**). This positive result emphasises that the previously chosen amide stopper group (Section 2.2) was not optimal to create the desired double fumaric thread.

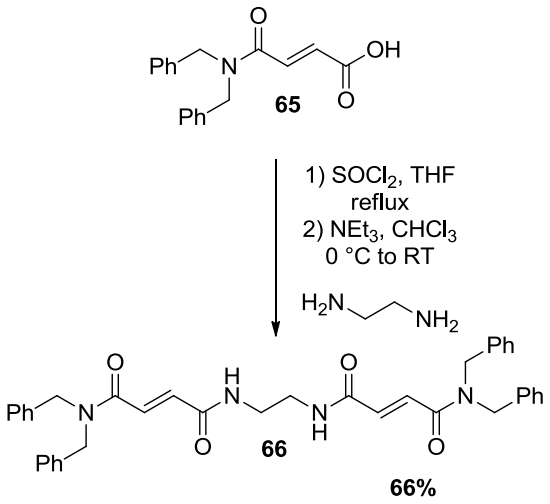

Scheme 2.37: Synthesis of the thread **66**.

The newly synthesised double fumaric thread **66** was able to form the desired [3]rotaxane **67** in 8% yield (Scheme 2.38). This [3]rotaxane is very insoluble in any

organic solvent other than methanol and had to be isolated via HPLC using a mixture of methanol and water (75 : 25). The corresponding [2]rotaxane was also detected, however it could not be isolated. Many different purification techniques such as column chromatography, recrystallisation or different HPLC methods were attempted, however these did not lead to bigger amounts of pure product.

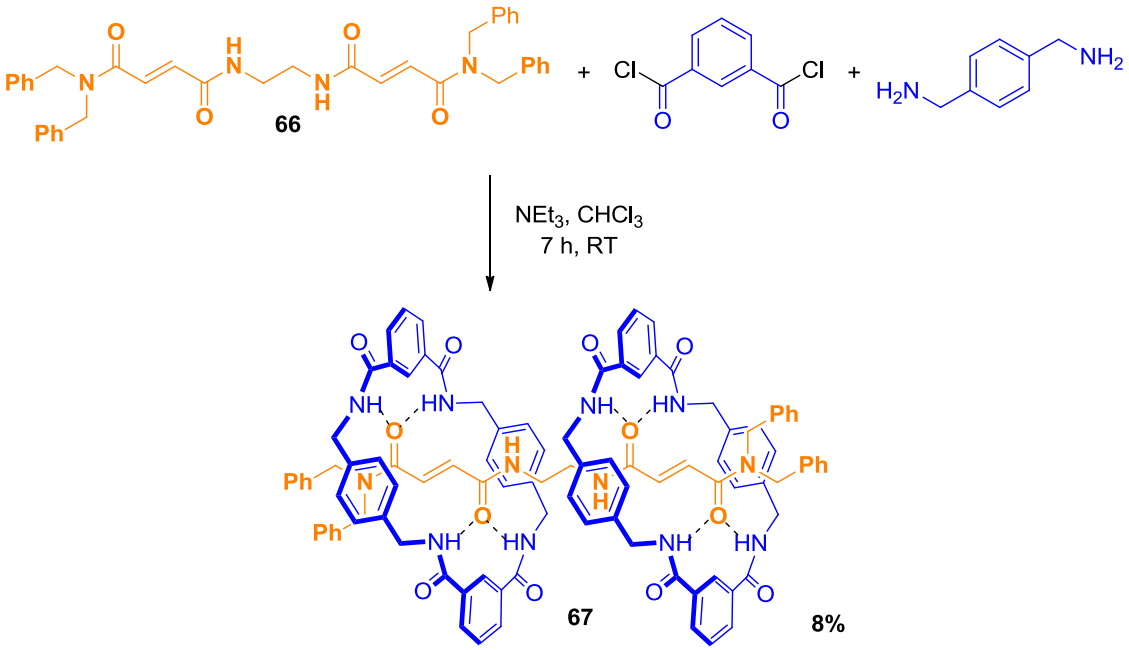

Scheme 2.38: Clipping reaction to form the [3]rotaxane **67**.

Thus, by changing the templating station from azo dicarboxamide to fumaramide and shortening the spacer unit from five to two carbons, the yield of the [3]rotaxane was significantly increased from 3 to 8%.

2.4.3 Synthesis of a fumaric [3]rotaxane with a three carbon spacer unit

In order to investigate whether a longer spacer group would promote a higher yield, 1,3-diaminopropane was tested as spacer group. The thread precursor **65** was transformed into the corresponding acid chloride. Treatment of the acid chloride with 1,3-diaminopropane gave the desired double fumaric thread **68** in 42% yield (Scheme 2.39).

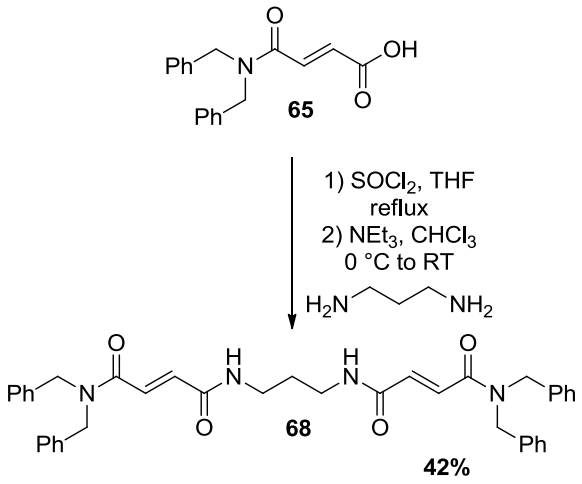

Scheme 2.39: Synthesis of double fumaric thread **68**.

The newly synthesised double fumaric thread **68** was able to form the desired [3]rotaxane **69** in 17% yield (Scheme 2.40). The purification of this [3]rotaxane was challenging, as it presents poor solubility in organic solvents. Column chromatography gave a mixture of [3]rotaxane and catenane. Recrystallisation was also unsuccessful. However, the [3]rotaxane **69** could be purified and isolated via HPLC. The corresponding [2]rotaxane was also formed as a minor product.

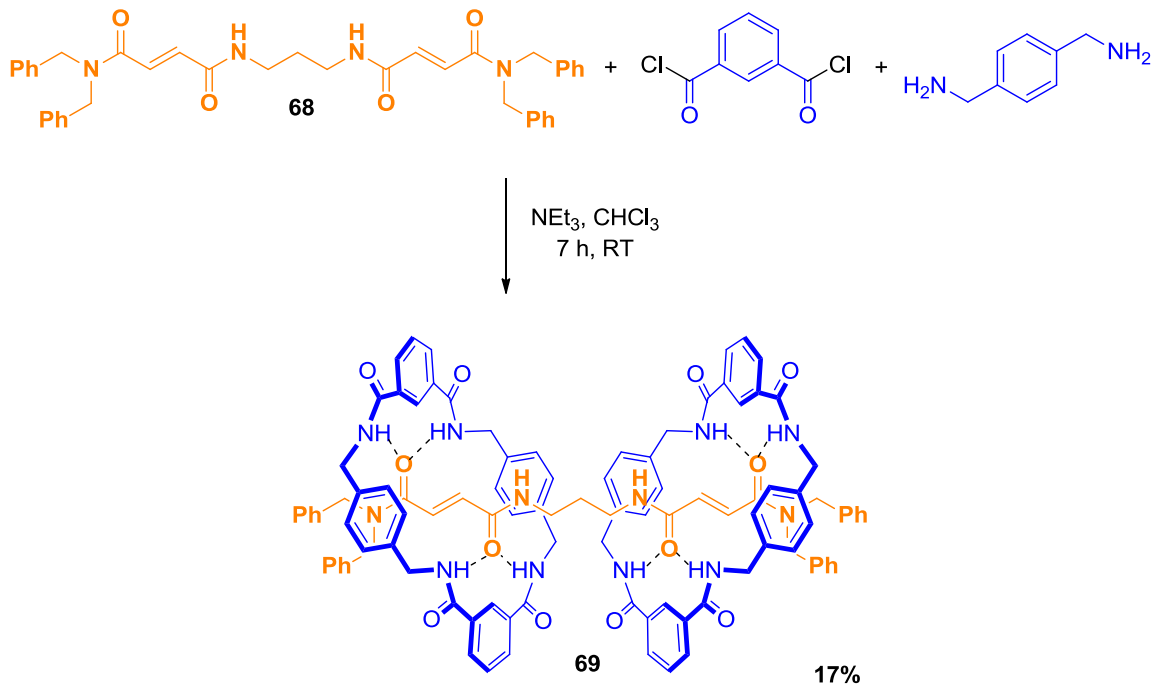

Scheme 2.40: Clipping reaction to from the [3]rotaxane **69**.

Colourless crystals suitable for X-ray diffraction were obtained by slow evaporation of a dichloromethane : ethanol (1:1) solution of [3]rotaxane **69**. The crystal structure confirms the formation of a [3]rotaxane (Figure 2.17). Hydrogen bonds between the thread and the macrocycles are observed, the bond length distance between donor and acceptor being in a range from 2.670(9) to 3.398(5) Å. The macrocycles are in a half chair / twisted boat conformation indicating a semi-efficient cyclic *syn syn* intermediate around the thread, which leads to a moderate yield. The macrocycles are twisted with respect to one another by 30° and they are located at 9.2 Å from each other. A cross coupling linking event between both macrocycles seems now more likely to occur, since the two macrocycles are closer to each other and the angle between them has been

reduced. However, the conformation in the solid state might be different from that in solution.

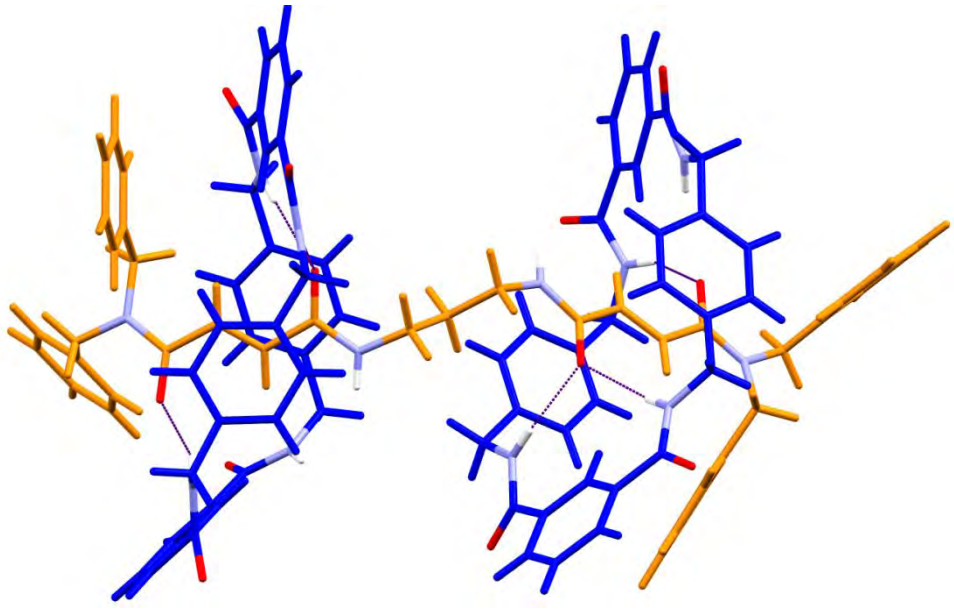

Figure 2.17: Crystal structure of [3]rotaxane **69**. Solvent molecules have been omitted for clarity.

Therefore, by increasing the length of the spacer group in the double fumaric thread the yield for the formation of the [3]rotaxane has increased considerably (from 8% to 17%). Consequently, a three carbon spacer unit seems a good compromise between an acceptable yield for the desired [3]rotaxane and the distance between the two macrocycles.

2.4.4 Synthesis of a fumaric [3]rotaxane with a three carbon spacer unit and a phenylbenzyl amide stopper

In 2008, Leigh and co-workers[81] reported a secondary amide stopper group using phenylbenzylamine. This stopper group was also investigated in this study in order to assess the effect of different stopper groups upon rotaxane formation. The yield for the formation of the ester **70** was improved using the previously described acid chloride protocol. The saponification step was carried out by using the same conditions described by Leigh et *al.* to yield the desired acid precursor **71** in 68% yield (Scheme 2.41).

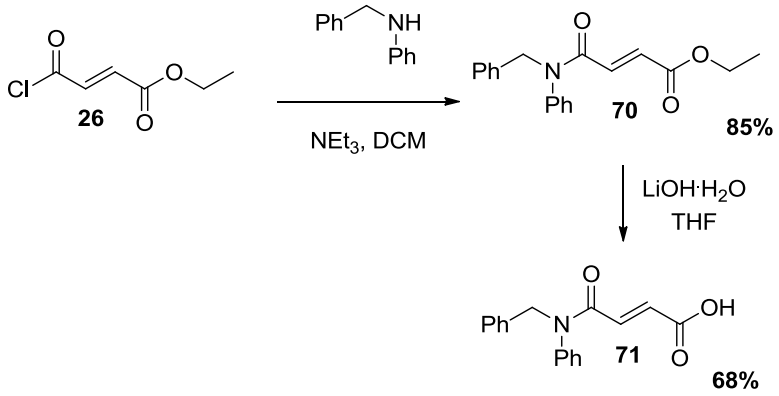

Scheme 2.41: Synthesis of the carboxylic acid **71**.

The carboxylic acid **71** was transformed into the corresponding acid chloride using thionyl chloride. Treatment of the resulting acid chloride with 1,3-diaminopropane gave the desired double fumaric thread **72** in an acceptable 84% yield (Scheme **2.42**).

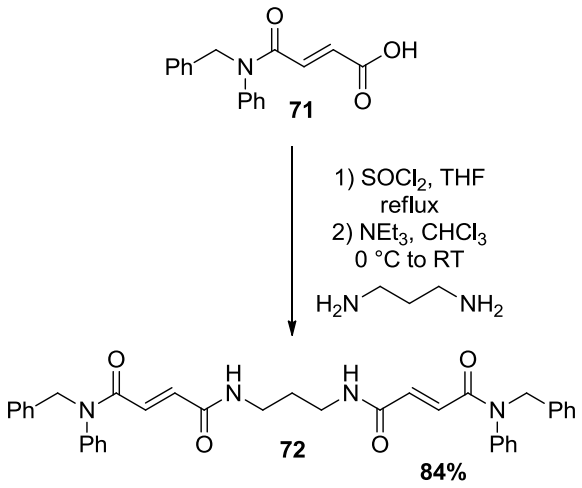

Scheme 2.42: Synthesis of the fumaric thread **72**.

This new double fumaric thread **72** was able to form the desired [3]rotaxane **73** in a notable 40% yield (Scheme 2.43). The [3]rotaxane **73** could be purified by column chromatography and this might be a reason for the higher yield compared to its predecessors that needed to be purified by HPLC methods. The corresponding [2]rotaxane **74** was also observed and isolated (5% yield).

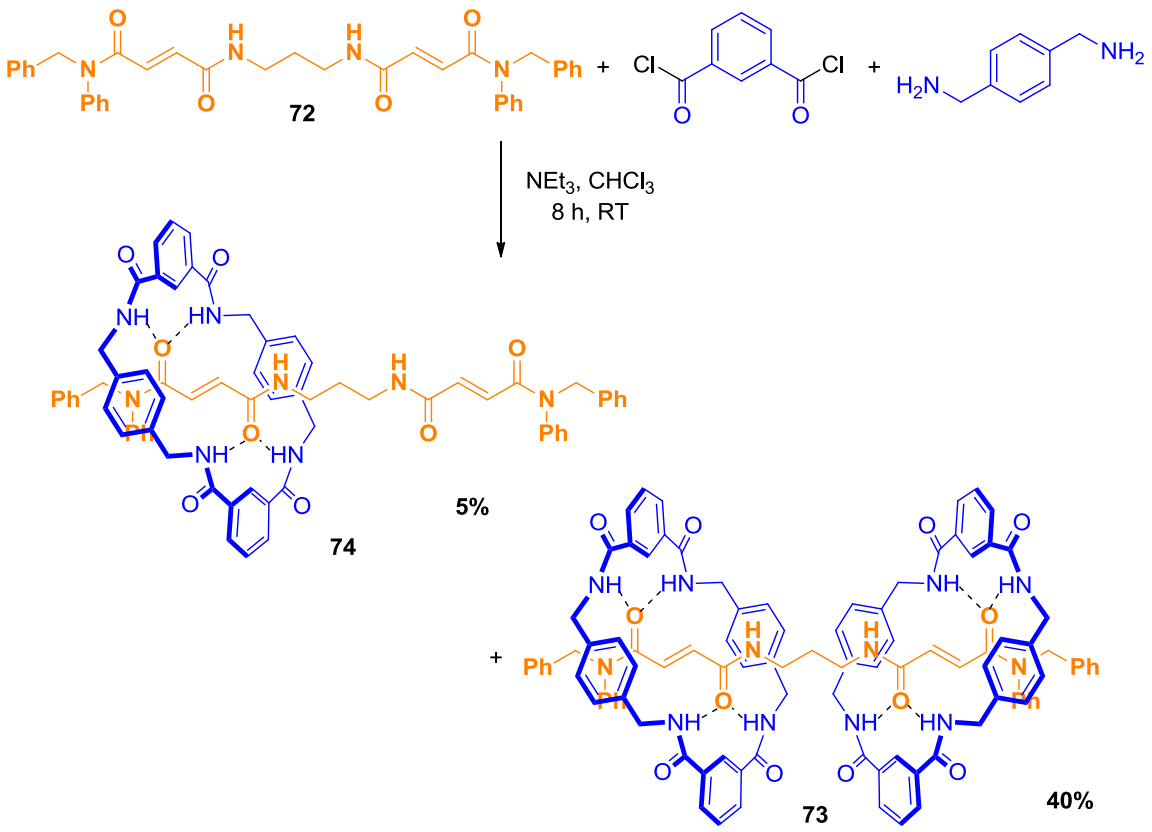

Scheme 2.43: Synthesis of [3]rotaxane **73**.

Colourless crystals suitable for X-ray diffraction were obtained by slow evaporation of a dichloromethane : ethanol (1:1) solution of pure [3]rotaxane **73**. The crystal structure confirms the formation of a [3]rotaxane (Figure 2.18).

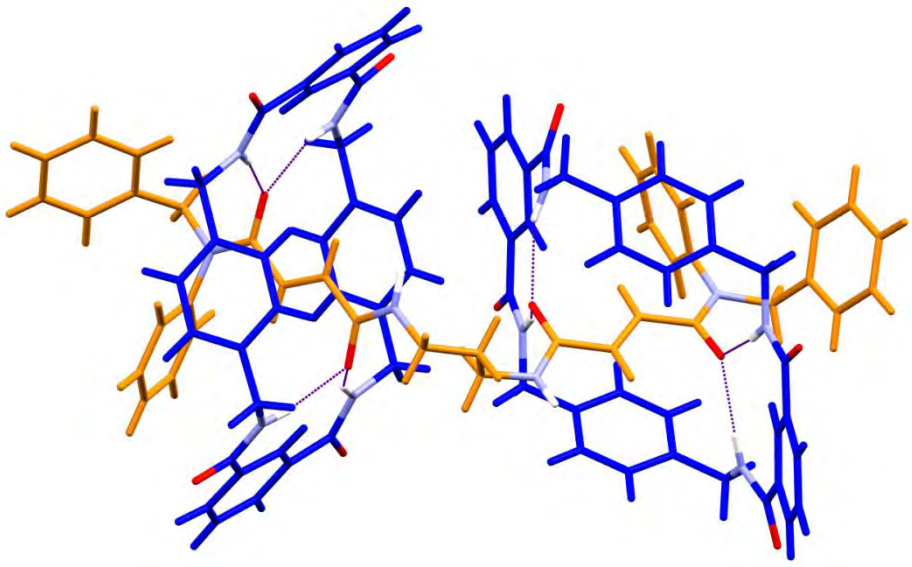

Figure 2.18: Crystal structure of [3]rotaxane **73**. Solvent molecules have been omitted for clarity.

The two macrocycles are twisted with respect to one another by 73º, which is a greater twist compared to that observed for the [3]rotaxane **61** (30º). However, the distance between both macrocycles remains 9.2 Å. The macrocycles are in a perfect chair conformation, which indicates that the cyclic *syn syn* intermediate around the thread is formed effectively and this is represented by the higher yield. Hydrogen bonds are observed between the thread and the macrocycles, with bond length distances between donor and acceptor ranging from 2.711(4) to 3.127(3) Å.

2.5 Further reactions towards a molecular cage

The next step to obtain the desired box is to link the two macrocycles together. Initially, allylation or propargylation of the N-atoms of the macrocycles were investigated for the [2]rotaxane **63**. However, these reactions proved ineffective.

This might result from the direction in which the amide protons of the macrocycle point towards the carbonyl groups of the templating stations, due to the attractive hydrogen bonding interaction. The high rigidity of the tetraamide macrocycle can also limit the reactivity of the amide protons. In contrast, the methylation reaction of [2]rotaxane **63** was successful, as confirmed by MALDI spectrometry. This could be due to the smaller size of the methyl groups that might have enough space to fit in between the macrocycle and the thread.

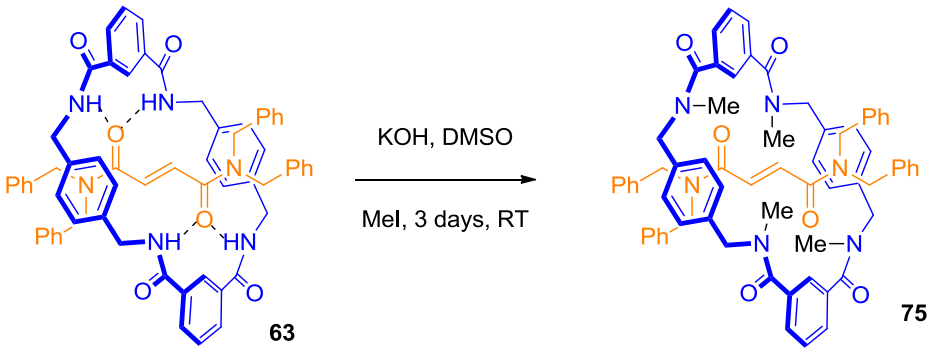

Scheme 2.44: Methylation of [2]rotaxane **63**.

The reactivity of the nitrogen atoms of the amide macrocycle could be enhanced by reduction of the amides to amines. This would create a more flexible macrocycle and lead to more reactive N-atoms. This new strategy was therefore investigated.

2.5.1 Reduction of the tetraamide macrocycles

In 2001, Takata *et al.* demonstrated the possibility to methylate and reduce the same tetraamide macrocycle used in this study (Scheme 2.45).[82]

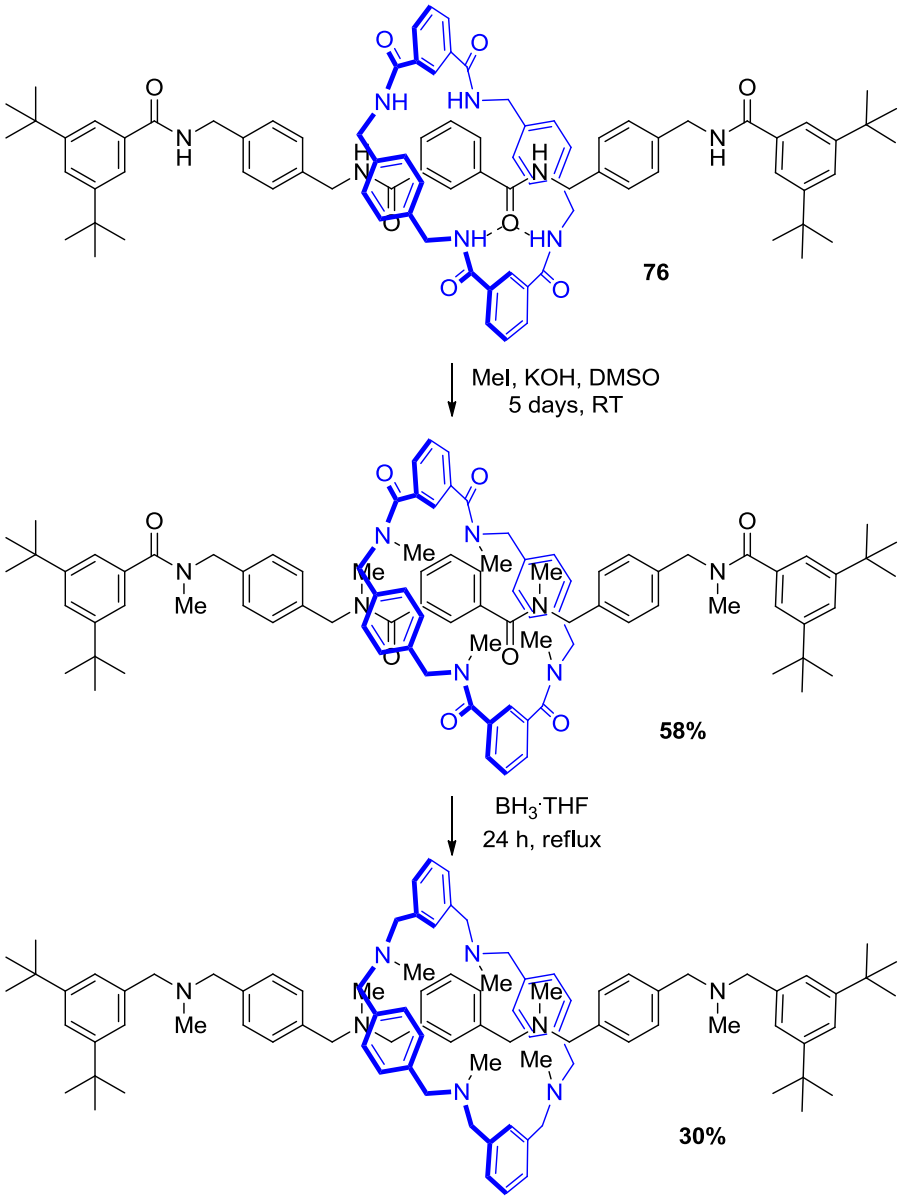

Scheme 2.45: Methylation and reduction of [2]rotaxane **76**.[82]

The methylation of all eight amides in the [2]rotaxane **76** was achieved in 58% yield by using potassium hydroxide as the base and iodomethane as methylating agent. Reduction of the resulting tertiary amides to the corresponding tertiary amines by employing 200 equivalents of borane in THF was performed in a 30% yield.[82] This low yield indicates that the reduction of multiple amides is not trivial.

Takata proposed that a reduction followed by an alkylation of the resulting secondary amines would also be possible. Reduction of the secondary amide [2]rotaxane **76** using borane in THF to its corresponding secondary amine [2]rotaxane was performed in 24% yield.[83] Full characterisation of this secondary amine [2]rotaxane was not achieved. However, the resulting ^{1}H NMR spectrum was partially assigned and a mass spectrometric analysis was performed.

The reduction of the azo [2]rotaxane **41** using 200 equivalents of borane in refluxing THF provided the hydrazo [2]rotaxane **77** in 35% yield, indicating the high sensitivity of the azo station in the presence of reducing agents (Scheme 2.46).

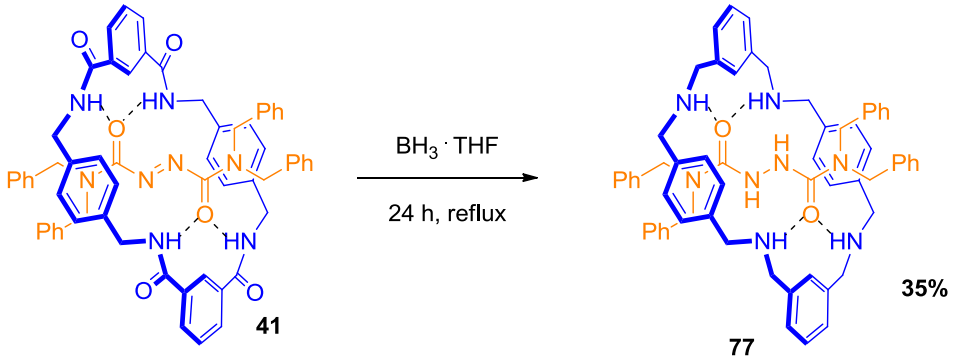

Scheme 2.46: Reduction of the azo [2]rotaxane **41**.

Full reduction of the macrocycle of the fumaric [2]rotaxane **63** was not observed when using borane in refluxing THF, however the borane DMS complex as reducing agent provided the desired [2]rotaxane **78** after column chromatography. The characterisation of this reduced [2]rotaxane **78** proved to be quite challenging. The ^{1}H NMR spectrum was inconclusive questioning the formation of this new rotaxane. However, a high resolution mass spectrum could be obtained indicating the formation of the [2]rotaxane **78**.

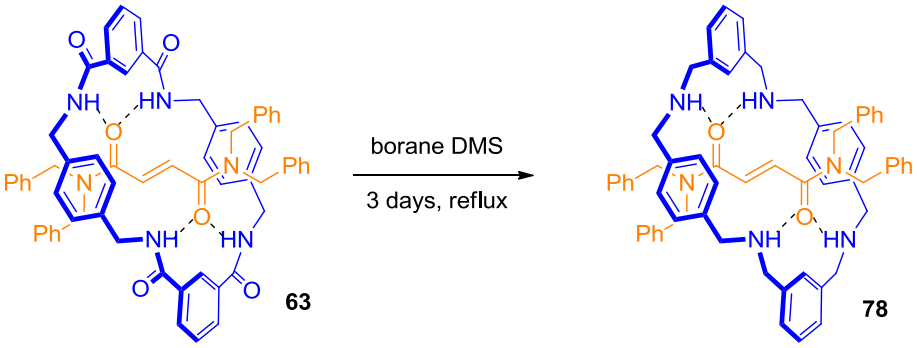

Scheme 2.47: Reduction of the fumaric [2]rotaxane **63**.

Alternative reducing agents listed in Table 2.4 were also investigated. However, the borane DMS complex in refluxing DCM provided the best results for the reduction of the tetraamide macrocycle.

Table 2.4: Reduction conditions tested.

Entry	Reagent	Solvent	Time	Temp.	Result
1	LiAlH	THF	17 h	70 °C	full reduction
2	$NaBH_4$	MeOH	17 h	70 °C	-
3	Superhydride	THF	48 h	70 °C	reduction of 1 CO
4	Borane in THF	THF	4 days	70 °C	full reduction
5	Borane DMS	DCM	3 days	50 °C	full reduction
6	9-BBN	THF	4 days	70 °C	-
7	1) Lawesson's Reagent	toluene	12 h	100 °C	-
	2) $NaBH_4$	MeOH	3 h	0 °C - RT	

Since the hydrazo [2]rotaxane **77** could be isolated, the reduction of the azo [3]rotaxane **61** was attempted by employing the borane DMS complex in refluxing

DCM, which are the same conditions used for the fumaric [2]rotaxane (Scheme **2.48**).

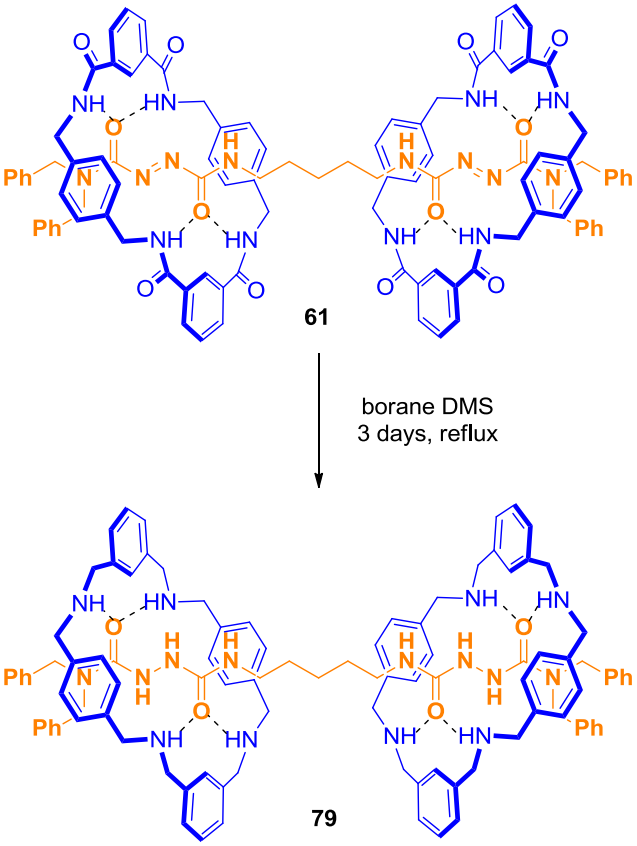

Scheme 2.48: Reduction of the [3]rotaxane **61** using borane DMS.

The outcome of this reaction was analysed via MALDI spectrometry and two main peaks were observed (Figure 2.19). The peak at 1619 Da corresponds to the desired hydrazo [3]rotaxane **79**. However, the major peak at 1142 Da is assigned to the presence of a hydrazo [2]rotaxane. Unfortunately, isolation of the [3]rotaxane **79** could not be achieved due to the small amount of material available and its difficult purification.

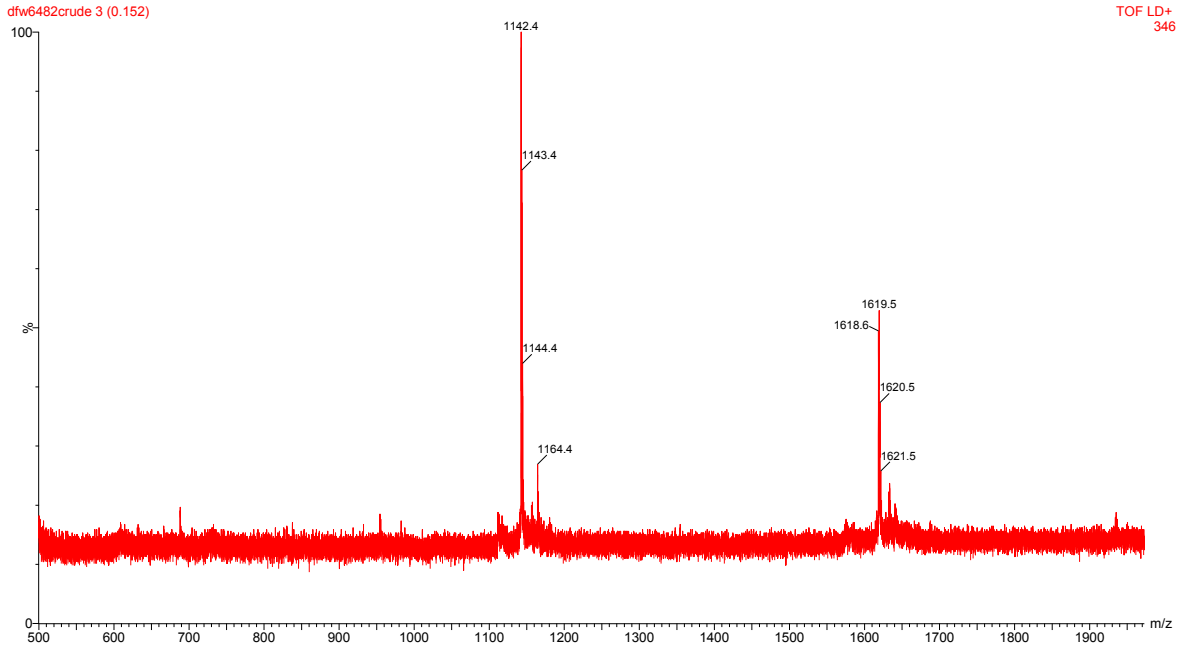

Figure 2.19: MALDI spectra of the crude mixture after reduction of **61**.

Since the fumaric [3]rotaxane **69** is easier to synthesise, it was then tested under the same reduction reaction conditions. The resulting reaction mixture was also analysed via MALDI spectrometry. A complex MALDI spectrum was obtained, where a mixture of reduced [2]rotaxanes, free reduced macrocycle, reduced thread and several [3]rotaxanes were detected (Figure 2.20). The major peaks at 1097 and 1573 Da correspond to the [2]- and [3]rotaxanes with fully reduced macrocycles, respectively. In each product distribution, the mass peaks with higher molecular weight correspond to partially reduced macrocycles and the mass peaks with lower molecular weight involve a reduction of carbonyl groups on the thread. These reduced rotaxanes can undergo a deslipping event, which explains the presence of reduced [2]rotaxanes. Although secondary amines are still competent hydrogen bond donors, the increased conformational freedom in the reduced tetraamine macrocycle clearly facilitates the deslipping process. The

reduction of the stations, i.e. removal of the supramolecular glue, also promotes the deslipping event.

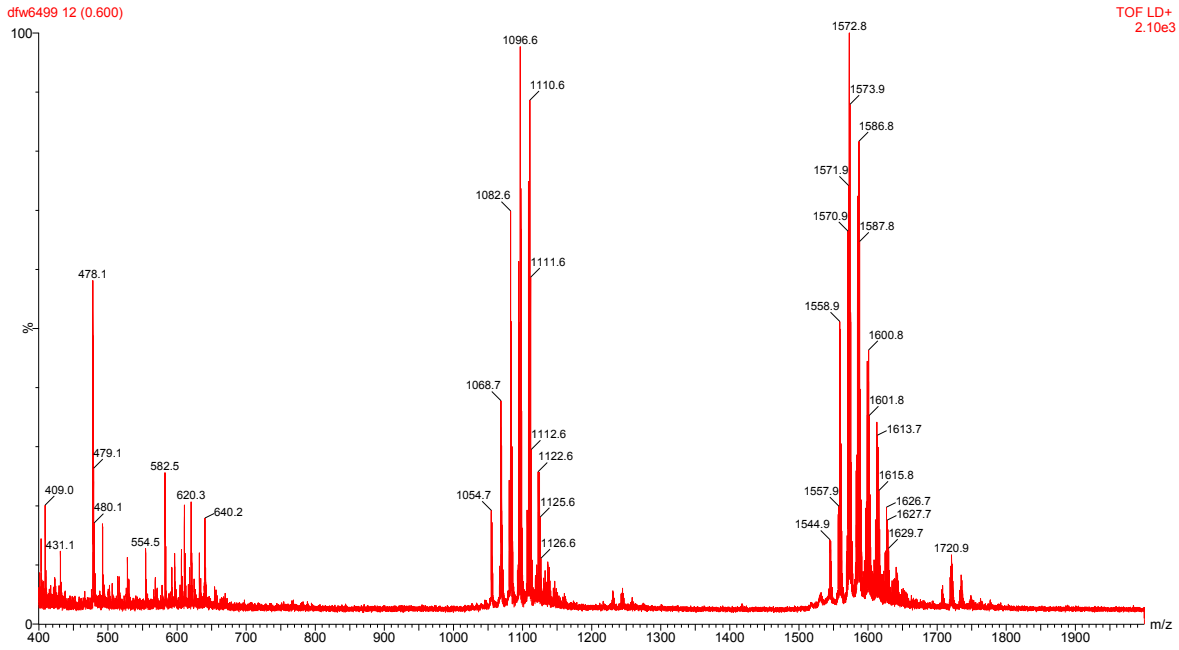

Figure 2.20: MALDI spectra after reduction of [3]rotaxane **69**.

In 2009, Smith and co-workers discussed the effect of the dibenzyl stopper groups on the solvent dependent stability of some squaraine rotaxanes bearing a tetraamide macrocycle (Figure 2.21).[84] In non-polar solvents, the squaraine [2]rotaxane **80** is stable due to strong hydrogen bonds between the macrocycle and the station. In polar aprotic solvents, such as DMSO, an unthreading event occurs, such that within 40 days at RT in DMSO, half of the squaraine is dethreaded. Smith suggested that the two phenyl groups acting as stoppers can interact via π–π stacking to form a more compact structure, enabling the deslipping process.

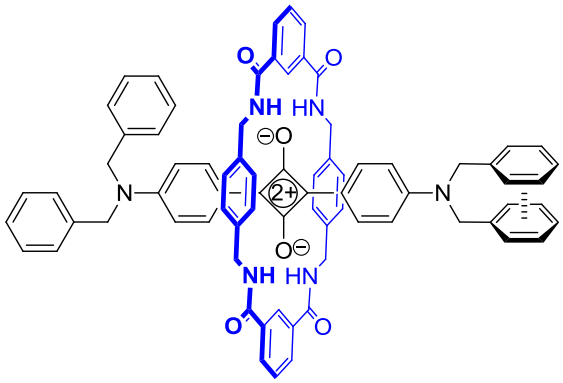

Figure 2.21: Squaraine [2]rotaxane **80**.

The stopper group used by Smith is the same dibenzyl motif used in the fumaric and azo rotaxanes reported above, and the deslipping process occurs in the squaraine system with the more rigid tetraamide macrocycle. In addition, the squaraine rotaxane hydrogen bonding interactions are stronger when compared to those observed for the fumaric or azo rotaxanes.

For these reasons, the reduction of the [3]rotaxane **73** was tested. This [3]rotaxane is formed with two phenylbenzyl stopper groups which will disable the π–π stacking interaction. However, the reaction outcome was analogous to that obtained for the dibenzyl [3]rotaxane **69**. Therefore, it seems that this stopper group is not bulky enough to prevent the deslipping of the tetraamine macrocycle.

2.5.2 Attempts to use alternative stopper groups

In order to overcome this deslipping issue, different sized stopper groups were investigated. A diphenyl amide motif was explored first, since this group appears somewhat inflexible and might prevent the ring deslipping. The fumaric thread **83**

was synthesised (Scheme 2.49) following an analogous protocol to that previously reported (see Section 2.4). Interestingly, the ester **81** and the acid **82** showed rota conformers in the ^{13}C NMR resulting in broad signals and this was confirmed via VT-NMR studies.

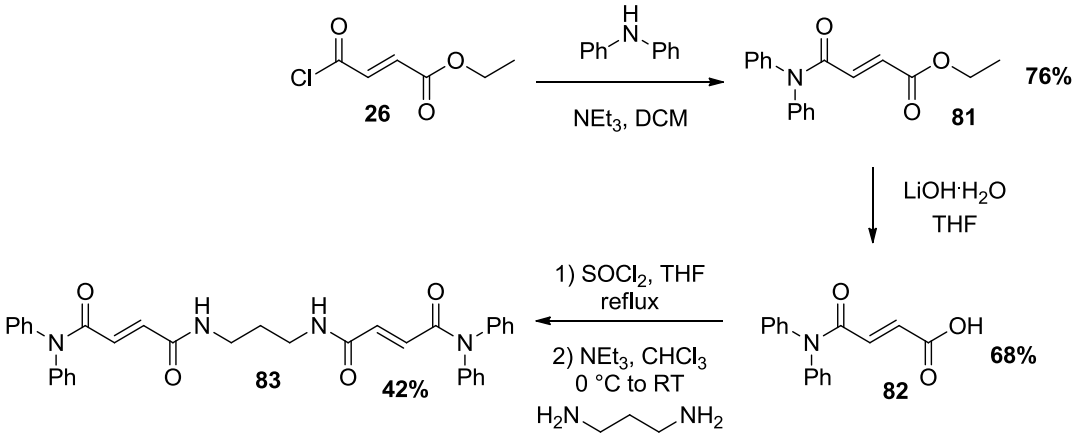

Scheme 2.49: Synthesis of the double fumaric thread **83**.

The newly synthesised double fumaric thread **83** was able to form the desired [3]rotaxane **84** in 8% yield and the corresponding [2]rotaxane **85** in 6% yield (Scheme 2.50). These striking low yields may be due to the poor solubility of these rotaxanes and therefore the need to isolate them via HPLC using a mixture of methanol and water (80 : 20).

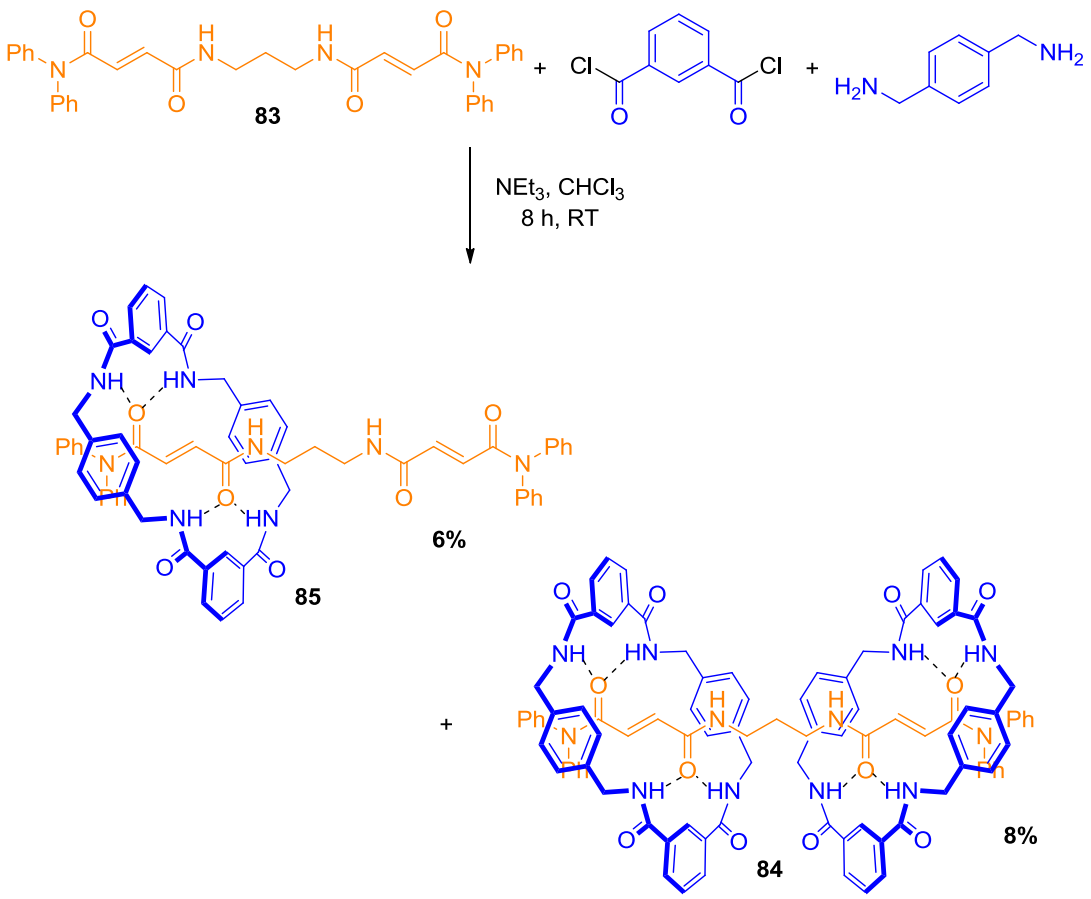

Scheme 2.50: Synthesis of the [3]rotaxane **84**.

The reduction of the [3]rotaxane **84** using the borane DMS complex in refluxing DCM resulted in a similar product distribution to that observed in the reduction of [3]rotaxane **69**, as seen by MALDI spectrometry. However, the formation of the corresponding [2]rotaxanes via deslipping was significantly increased. This deslipping process seems to occur easily, as mass peaks corresponding to three remaining carbonyl groups on the macrocycle were also observed. This can be due to the smaller size of this diphenyl stopper group.

For this reason, dibromodiphenylamine as building block for the stopper group was investigated. Dibromodiphenylamine reacts with ethyl fumaroyl chloride in 33% yield to afford the ester **86**. This ester was then hydrolysed to the corresponding carboxylic acid **87**. This acid was then reacted with thionyl chloride in refluxing THF to form the corresponding acid chloride, which was reacted with 1,3-diaminopropane in 19% yield over the two steps (Scheme 2.51). This novel fumaric thread **88** was able to form the corresponding [2]- and [3]rotaxanes. However, purification of these was not possible. Several HPLC methods only yielded a mixture of the two different rotaxanes.

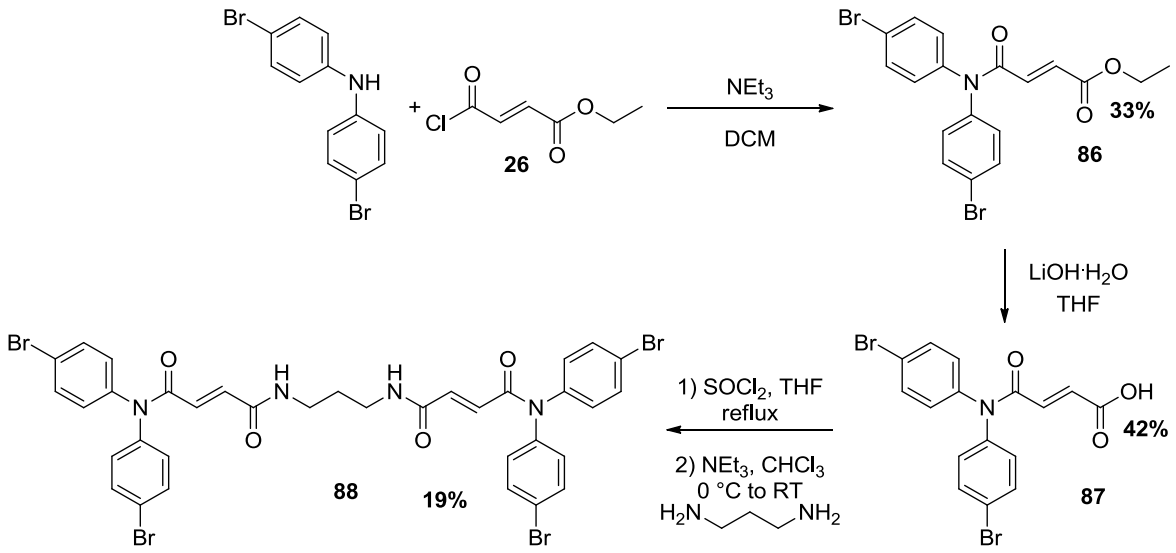

Scheme 2.51: Synthesis of the double fumaric thread **88**.

The reduction of the mixture of these two rotaxanes was not investigated, since that would result in a product distribution of various [2]- and [3]rotaxanes, which would not indicate whether a deslipping event is occurring.

The hypothesis of increasing the stopper group size without significantly modifying the developed synthetic route was further explored with an anthracene benzyl motif as stopper group. Since anthrabenzylamine is not commercially available, it was synthesised via condensation of 9-anthraldehyde and benzylamine (Scheme **2.52**).

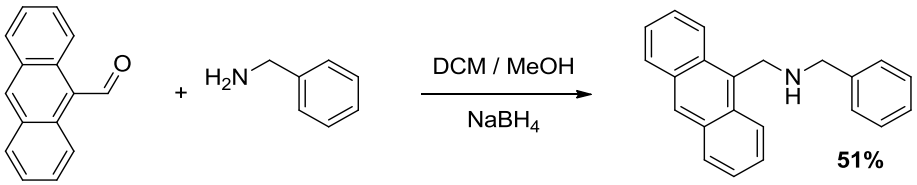

Scheme 2.52: Synthesis of anthrabenzylamine.

The reaction between anthrabenzylamine and ethyl fumaroyl chloride did not form the desired ester. Instead, the addition of ethyl fumaroyl chloride followed by an intramolecular Diels-Alder reaction to form the pentacyclic product **89** had occurred (Scheme 2.53).

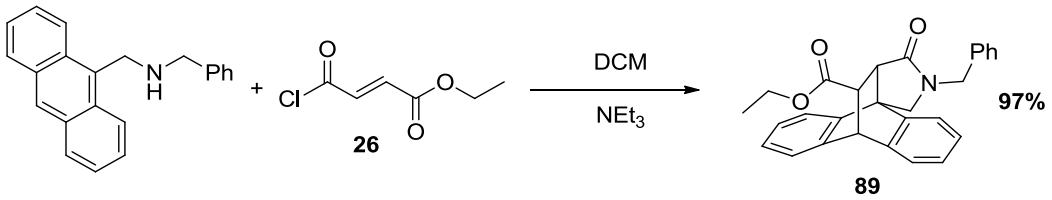

Scheme 2.53: Synthesis of the Diels-Alder adduct **89**.

The groups of Ciganek and Hahn have reported an intramolecular Diels-Alder reaction at high temperature which forms an analogous pentacyclic product under reflux conditions.[85,86] In contrast to the observations of Ciganek and Hahn, the reaction described in Scheme 2.53 was performed at RT, suggesting that the ester

group on the dienophile lowers the lowest molecular orbital to promote this very mild intramolecular Diels-Alder reaction.

Colourless crystals suitable for X-ray diffraction were obtained by slow evaporation of a DCM solution of compound **89**. The crystal structure confirms the formation of the pentacyclic structure with the expected *anti* geometry for the bridged six membered ring, arising from the *E* double bond of the ethyl fumaroyl chloride (Figure 2.22). Several attempts to perform a cycloreversion were unsuccessful; therefore alternative stopper groups were investigated.

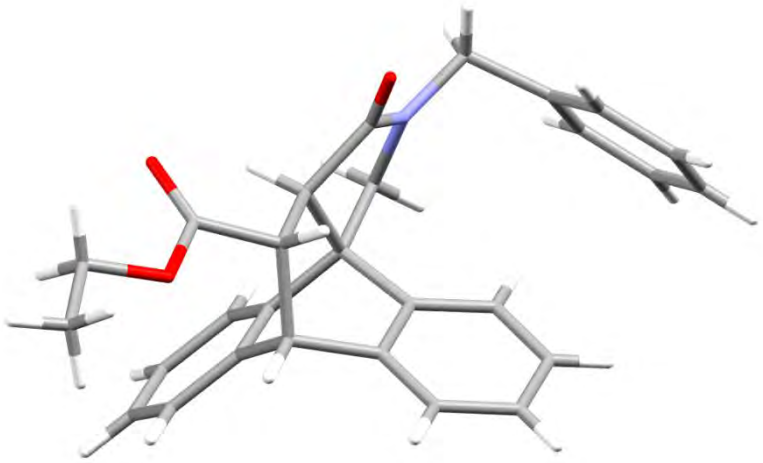

Figure 2.22: Crystal structure of the Diels-Alder adduct **89**.

Trityl groups are significantly larger and have been effectively used as stopper groups in rotaxane synthesis.[87] Therefore, the possibility to use a trityl motif as stopper group to synthesise a new double fumaric thread was investigated and a secondary amine (tritylphenyl amine) was the first choice. Tritylphenyl amine is not commercially available and was synthesised via reaction of trityl chloride with aniline following a literature procedure.[88]

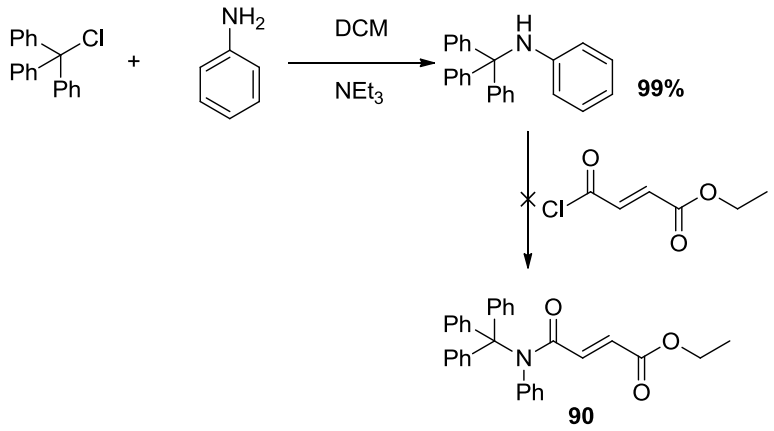

Scheme 2.54: Attempted synthesis of amide ester **90**.

The reaction of tritylphenyl amine with ethyl fumaroyl chloride did not produce the desired ester (Scheme 2.54). Mass spectrometry analysis suggested that the trityl group had been lost instead. This result can be attributed to the fact that trityls are known to be reasonable good leaving groups.[89]

As a result of this, the trityl motif as stopper group was investigated as a primary amine instead. Tritylamine is commercially available, however it was synthesised in a simple one pot reaction using trityl chloride and aqueous ammonia (Scheme **2.55**).[90]

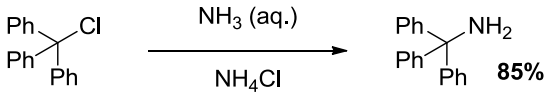

Scheme 2.55: Synthesis of tritylamine.

Tritylamine was reacted with ethyl fumaroyl chloride to give the ester **91** in 78% yield. This ester was then hydrolysed to the corresponding carboxylic acid **92** in 81% yield (Scheme 2.56).

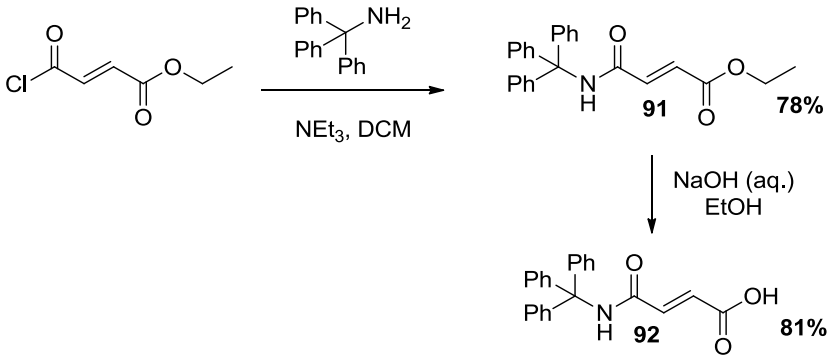

Scheme 2.56: Synthesis of the carboxylic acid **92**.

This acid **92** was then treated with thionyl chloride in refluxing THF to form the corresponding acid chloride, which was coupled with 1,3-diaminopropane in 20% yield over the two steps (Scheme 2.57).

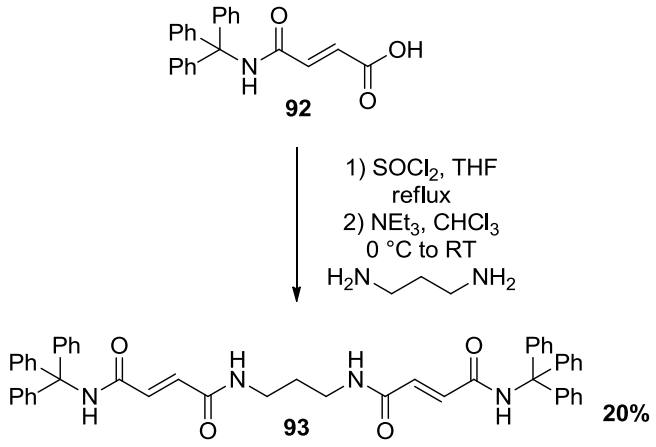

Scheme 2.57: Synthesis of the double fumaric thread **93**.

This novel fumaric thread **93** was able to form the expected [2]- and [3]rotaxanes. However, the formation of the [2]rotaxane was considerably favoured over the desired [3]rotaxane and only the [2]rotaxane **94** could be isolated in sufficient amount to be fully characterised (Scheme 2.58). This might be due to the close proximity of the very bulky trityl stopper groups to the templating stations.

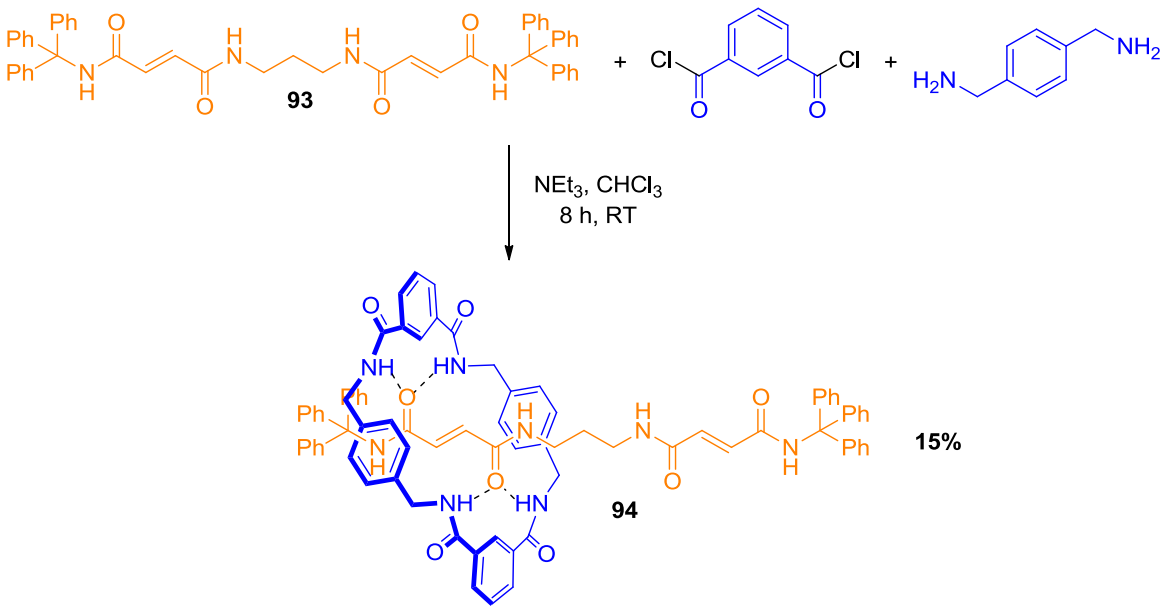

Scheme 2.58: Synthesis of the [2]rotaxane **94**.

Consequently, the distance between the bulky stopper and the templating station needed to be increased without significantly changing the established synthetic route. For this reason, 4-tritylaniline was chosen as a new stopper group. 4-Tritylaniline was reacted with ethyl fumaroyl chloride in 59% yield to afford the ester **95** (Scheme 2.59).

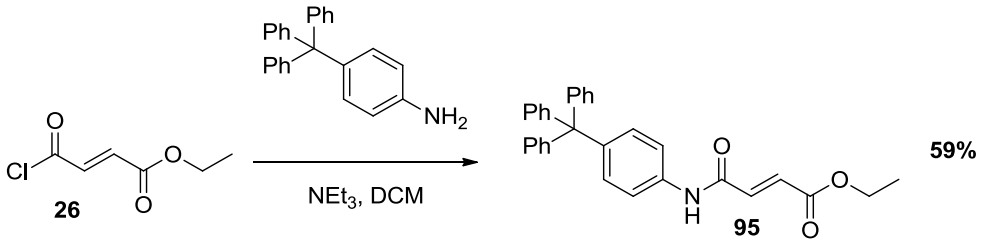

Scheme 2.59: Synthesis of the amide ester **95**.

This ester was hydrolysed under standard conditions to give the corresponding carboxylic acid **96**. This acid was reacted with thionyl chloride in refluxing THF to

form the corresponding acid chloride, which was further reacted with 1,3-diaminopropane in 23% yield over the two steps (Scheme 2.60).

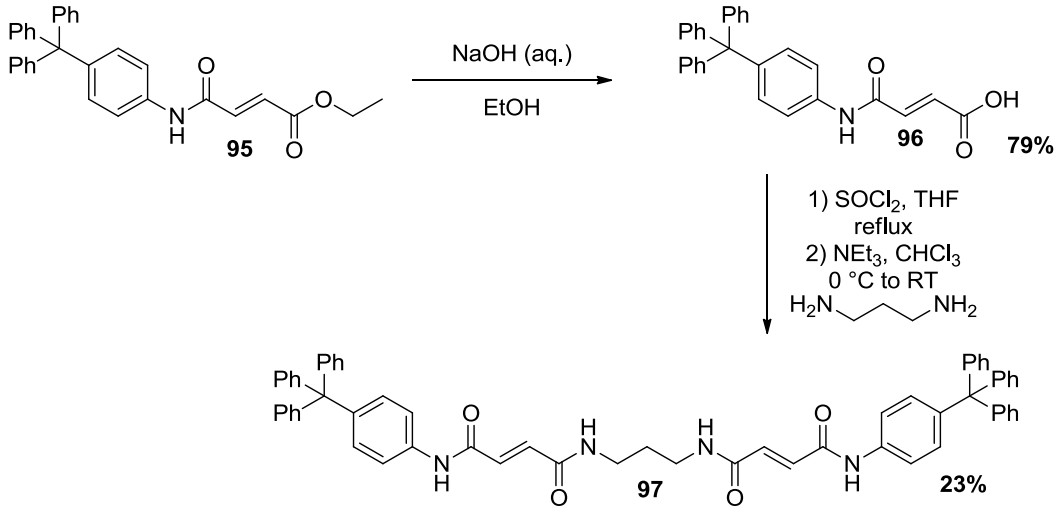

Scheme 2.60: Synthesis of the double fumaric thread **97**.

The newly synthesised fumaric thread **97** presents poor solubility in organic solvents and consequently did not yield in sufficient amount the desired [3]rotaxane during the clipping process. The unwanted catenane was the main product and no rotaxane could be isolated. This unfavoured rotaxane formation can be attributed to the poor solubility of the thread that holds the templating stations which remains in the solid state, while the monomers required for the macrocycle, catenane and rotaxane formation are in solution.

In this Section several attempts to synthesise a [3]rotaxane with bulky stoppers were investigated. To date, a [3]rotaxane that might allow an overall reduction without deslipping of the tetraamine macrocycle could not be synthesised or isolated. Nevertheless, the examples shown and discussed above have given a better understanding of the complexity of these particular systems, where size,

solubility and accessible synthetic routes need to be considered on the molecular design of novel [3]rotaxanes.

2.6 Pseudorotaxanes

A different strategy towards the synthesis of a novel molecular box was also explored. This strategy would avoid the reduction step required to link the two macrocycles. Therefore, starting from the two already reduced macrocycles, these can be located next to each other by the formation of a supramolecular complex, e.g. a pseudorotaxane, followed by a cross linking event.

Pseudorotaxanes are very common synthetic tools used in supramolecular chemistry.[91] A pseudorotaxane is a host-guest assembly formed of an unstoppered threading compound and a cyclic species.[92] This host-guest complex is a non interlocked system that can become a rotaxane via a stoppering event. As previously discussed, the digit in brackets indicates the number of components. For example, one macrocycle and one thread will build a [2]pseudorotaxane.

In 1991, Stoddart and co-workers reported the directed self-assembly of the [2]pseudorotaxane **98** (Figure 2.23).[93]

The [2]pseudorotaxane **98** was formed by mixing equimolar amounts of the tetracationic cyclophane, shown in blue, and the linear polyether, shown in black, in MeCN. The host-guest complex is stabilised via π-π stacking interactions between the electron-rich hydroquinone ring on the thread and the

electron-deficient bipyridinium units of the macrocycle. The pseudorotaxane is also stabilised via electrostatic edge to face interactions involving the *p*-phenylene units in the cyclophane.[94] This synthetic approach has allowed the isolation of other [2]pseudorotaxanes and a novel [3]pseudorotaxane.[95] These pseudorotaxanes were characterised via X-ray crystallographic analysis.

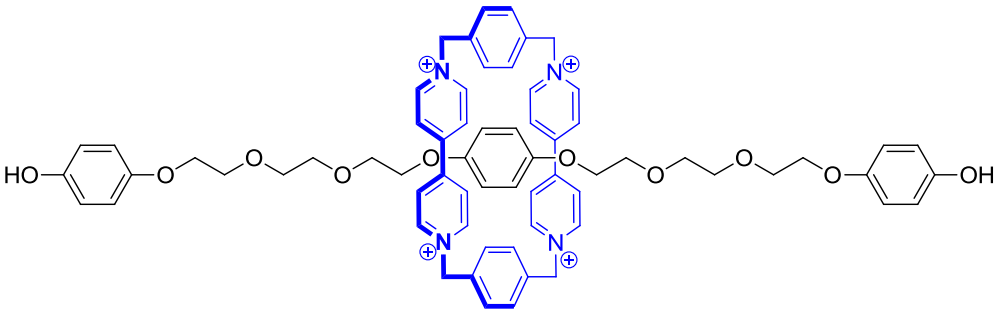

Figure 2.23: Pseudorotaxane **98** formed in MeCN.

Since pseudorotaxanes are non interlocked structures, the linear and cyclic compounds are in equilibrium and therefore, a binding constant for the host-guest complex can be determined by spectroscopic techniques, such as NMR spectroscopy[96] and UV/Vis spectroscopy,[97] or by cyclovoltametry.[98,99]

There are some examples involving hydrogen bonding pseudorotaxanes. In 2007, Chiu and co-workers reported an urea-based [2]pseudorotaxane (Scheme **2.61**).[100] The preformed amide polyether macrocycle **99** is capable of recognising the urea thread **100** in solution to build the [2]pseudorotaxane **101**. This [2]pseudorotaxane is stabilised via hydrogen bonding interactions between the amide protons of the macrocycle and the urea carbonyl group of the thread, as

well as by hydrogen bonding interactions between the urea amide protons of the thread and the ethylene glycol oxygen atoms of the macrocycle.[101]

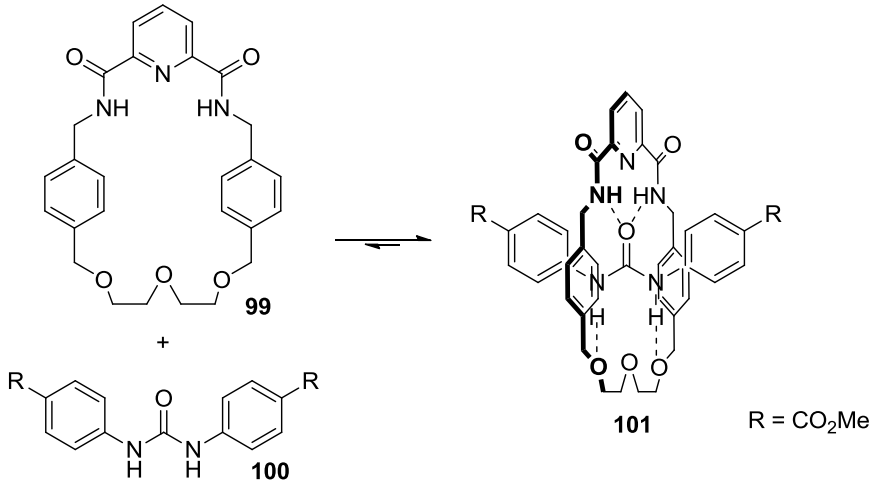

Scheme 2.61: Formation of [2]pseudorotaxane **101**.

The binding constant of this host-guest complex was determined by ^{1}H NMR dilution experiments in $CDCl_3$ and is equal to 180 M^{-1}. When two equivalents of tetrabutylammonium acetate were added to a solution of the [2]pseudorotaxane **101**, this dissociated into its components, as seen in the ^{1}H NMR spectrum where the free macrocycle and a new complex between the urea thread **100** and the acetate anion were observed.[100]

In 2010, Jiang *et. al* found that when employing a pyridine N-oxide derivative in place of the urea thread, the magnitude of the complex binding constant was increased 1000 fold.[102]

More recently, Schalley and co-workers reported several pseudorotaxanes with the amide macrocycle **99** and some amide threads bearing 1,6-dicarbonyl

groups.[103] Several substituents on the thread were tested and the binding constants compared. These binding constants were obtained via NMR titrations, isothermal titration calorimetry (ITC) and density functional theory (DFT) calculations.

To date, a pseudorotaxane involving amine macrocycles or fumaric based threads has not yet been reported. The formation of such pseudorotaxane could be monitored via ^{1}H NMR spectroscopy. In Section 2.4, the chemical shift observed for the olefinic protons upon formation of the supramolecular complex has been discussed. A comparable effect is also expected in an amine macrocycle.

The macrocycle **102** was synthesised over two steps using a modified literature procedure (Scheme 2.62).[104] The 30% yield over the two steps could not be improved when changing different reaction parameters, such as temperature, rate of addition, solvent or reaction time.

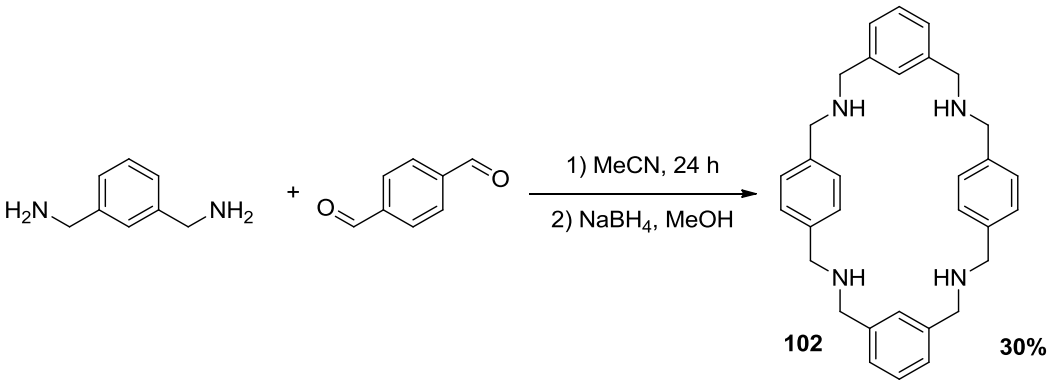

Scheme 2.62: Synthesis of the macrocycle **102**.

The double fumaric unstoppered thread **33** was synthesised in 89% yield over two steps (see Section 2.2.2). A shift of the olefinic protons (highlighted in green),

upon addition of the macrocycle, would indicate the formation of a pseudorotaxane. By adding one equivalent of macrocycle, the [2]pseudorotaxane **103** would be formed. A second equivalent should form the [3]pseudorotaxane **104** (Scheme 2.63). Since both stations are identical, the first equivalent of the macrocycle can shuttle between the two stations and this might prevent the formation of the [3]pseudorotaxane **104**.

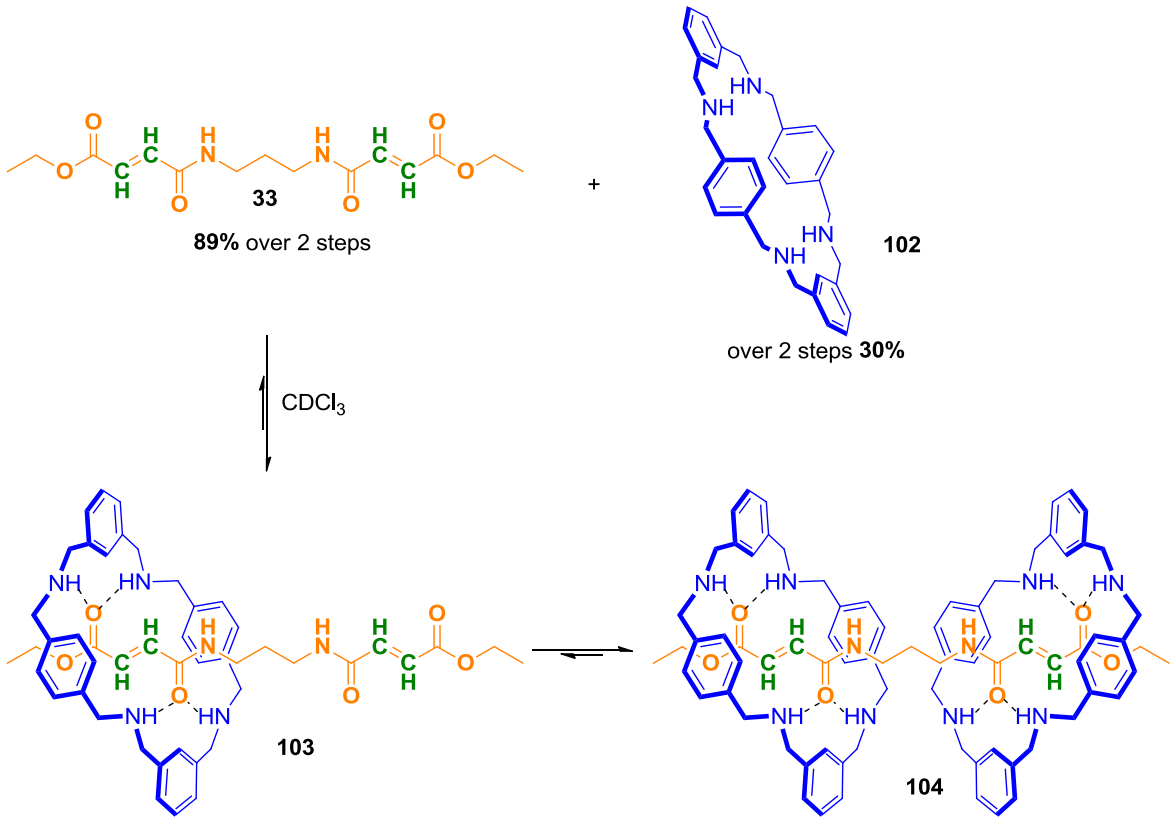

Scheme 2.63: Proposed equilibrium upon addition of one and two equivalents of macrocycle **102** in the presence of one equivalent of the double fumaric thread **33**.

An initial ^{1}H NMR experiment involving the addition of first one equivalent and then a second equivalent of macrocycle **102** showed a shift of around 0.05 ppm of the double bond protons, indicating the formation of the [2]pseudorotaxane **103** and

the [3]pseudorotaxane **104** (Figure 2.24). This small change between the addition of one and two equivalents of the macrocycle might indicate that both macrocycles are located over the two fumaric stations. No shift was detected when using the stoppered thread **72**, which indicates that the macrocycles are located over the stations on the pseudorotaxanes.

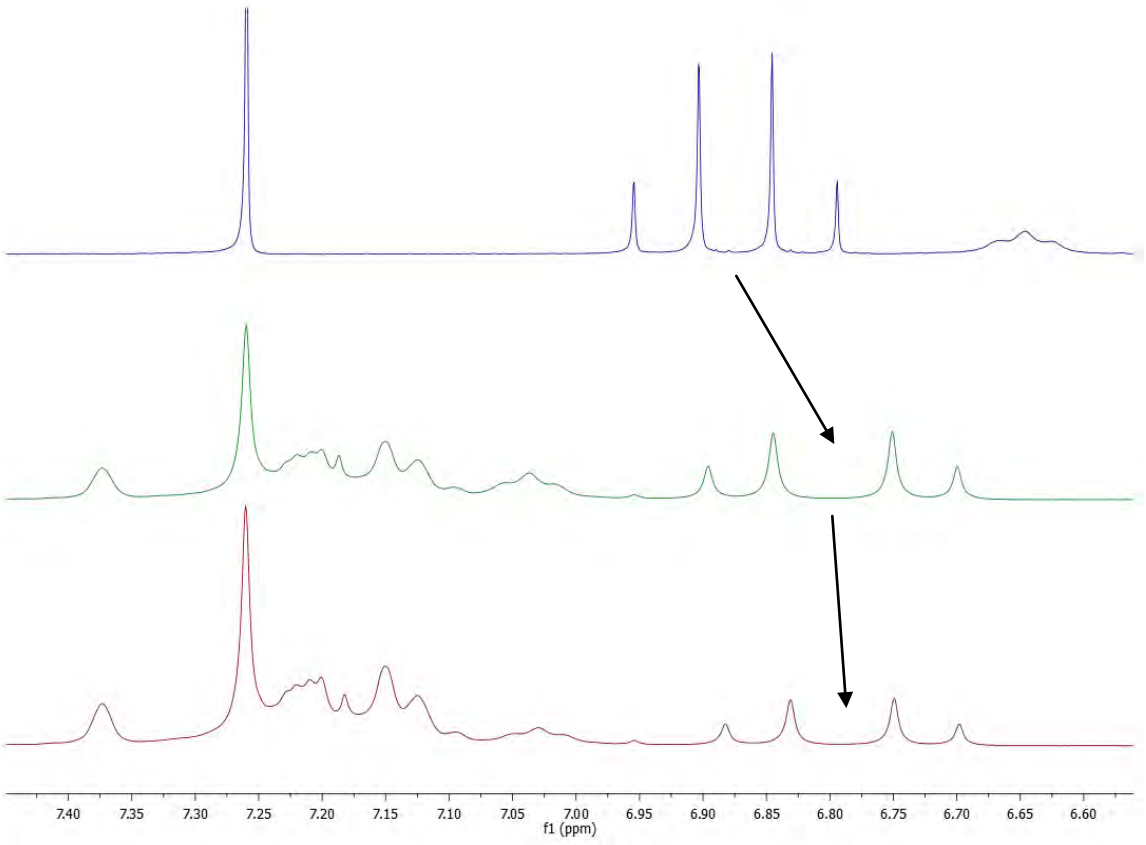

Figure 2.24: ^{1}H NMR spectra of thread **33** (in blue), thread **33** and 1 eq. of macrocycle **102** (in green) and thread **33** and 2 eq. of macrocycle **102** (in red).

In order to be able to calculate a binding constant for this complex, a ^{1}H NMR titration experiment was performed and the resulting ^{1}H NMR spectra are shown in Figure 2.25. To a solution of thread **33** (0.03 M) was added a solution of thread **33** (0.03 M) and macrocycle **102** (0.06 M) in increments of 0.1 equivalents based on

the macrocycle. The resulting ^{1}H NMR spectra show a less dramatic shift (0.02 ppm) than that observed for the initial ^{1}H NMR spectra (0.05 ppm). A possible explanation for this result could be the instrumental error as the two sets of spectra were recorded in different instruments, and this error can be significant when dealing with small shifts. Consequently, ^{1}H NMR spectroscopy does not seem suitable for the determination of the binding constant for the formation of pseudorotaxanes **103** and **104**. Unfortunately, UV/Vis spectroscopy did not prove useful either, as it did not show any differences in the absorption between macrocycle **102**, thread **33** and the formed pseudorotaxanes **103** and **104**.

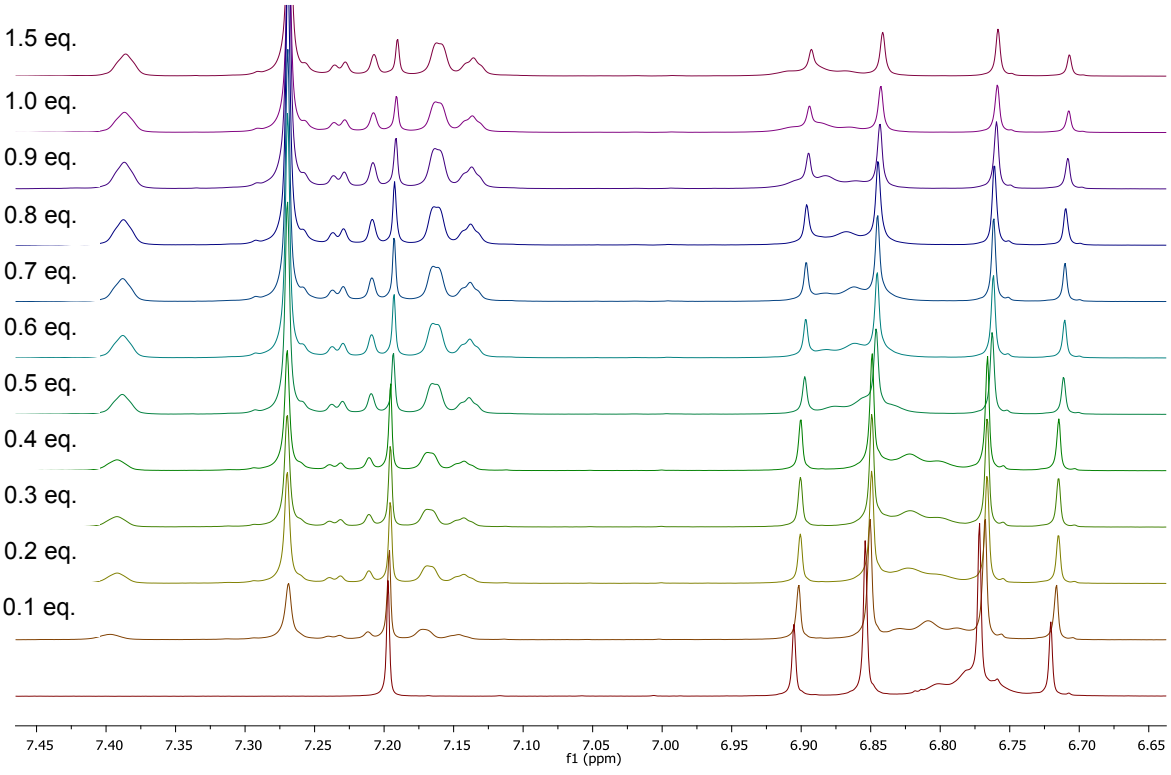

Figure 2.25: ^{1}H NMR spectra of the titration experiments with 0.1 equivalent effective increments of macrocycle **102**.

MALDI spectrometry analysis did not allow the detection of the anticipated [2]- and [3]pseudorotaxanes either. Therefore, a softer ionisation method, such as electrospray (ES), was investigated. Acetonitrile, a non competitive solvent, was chosen as mobile phase so as to not interfere with the formed pseudorotaxanes. The red ES+ spectrum in Figure 2.26 was obtained when injecting a $CDCl_3$ pseudorotaxane solution with a macrocycle to thread ratio of 2 to 1. The spectrum shows the free macrocycle **102** (477 Da) and the [2]pseudorotaxane **103** (803 Da). The spectrum in green is a result of the initial injection of macrocycle, followed by injection of the thread compound. Peaks at 349 Da and 675 Da correspond to the thread **33** and the peak at 477 Da corresponds to the free macrocycle **102**. This strongly implies that the formation of the [2]pseudorotaxane is not promoted during the ES process.

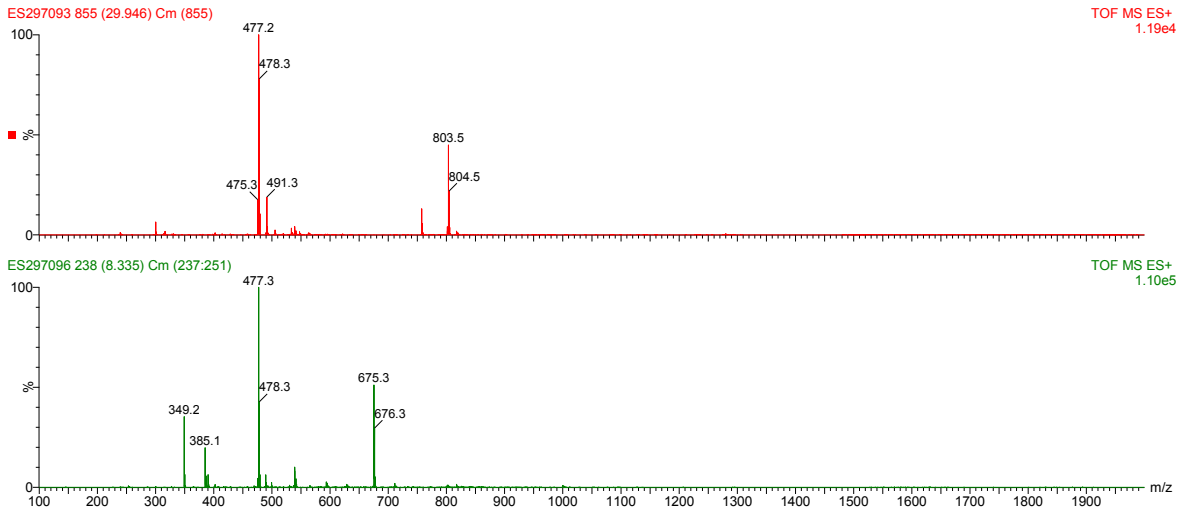

Figure 2.26: ES+ spectra for the pseudorotaxane formation (in red) and the macrocycle and thread components separately injected (in green).

The region where the anticipated [3]pseudorotaxane **104** is expected is expanded in Figure 2.27, where the experimental spectrum is shown in red and the

calculated spectrum is shown in green. The peaks at around 1279 Da confirm the formation of the [3]pseudorotaxane, however the signal intensity for this peak is quite small.

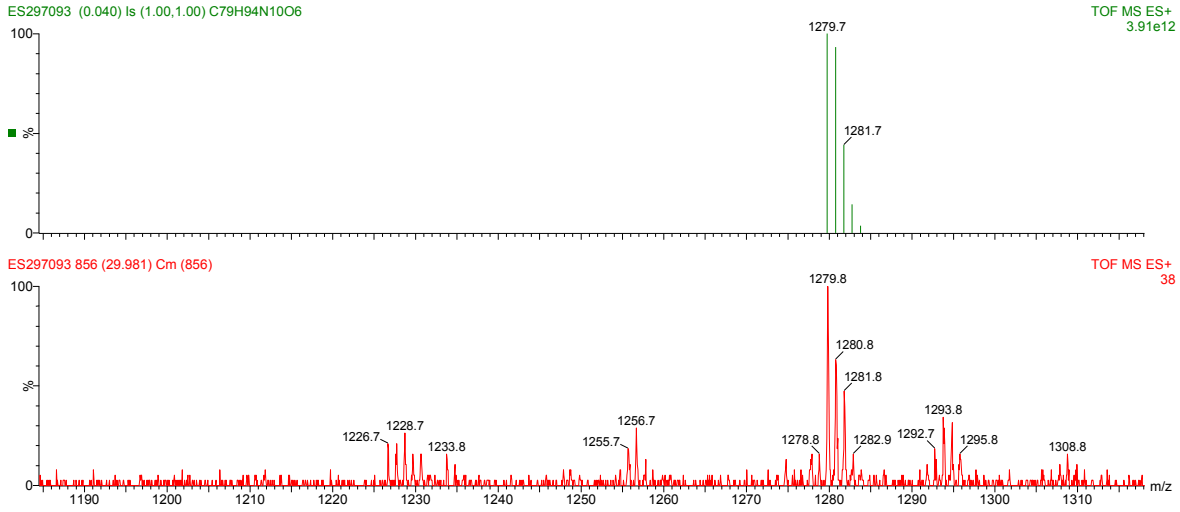

Figure 2.27: ES+ spectra of the calculated [3]pseudorotaxane **104** (in green) and the experimental [3]pseudorotaxane **104** (in red).

A possible explanation for this behaviour could be that there is some difficulty to ionize the [3]pseudorotaxane **104**, compared to the other species, such as the macrocycle, and therefore the state of population of the individual species cannot be exactly determined.

The next step towards the formation of the desired molecular box is a linking event of the two macrocycles in the [3]pseudorotaxane **104**. *Cis*-1,4-dichloro-2-butene, *trans*-1,4-dichloro-2-butene and α,α'-dibromo-*p*-xylene were tested as possible linkers. However, only α,α'-dibromo-*p*-xylene was able to form several linkages between the two macrocycles to yield the desired molecular box as depicted in

Scheme 2.64, where a box created by computational calculations is shown in grey and a symbolic cartoon representation is shown in blue and black.

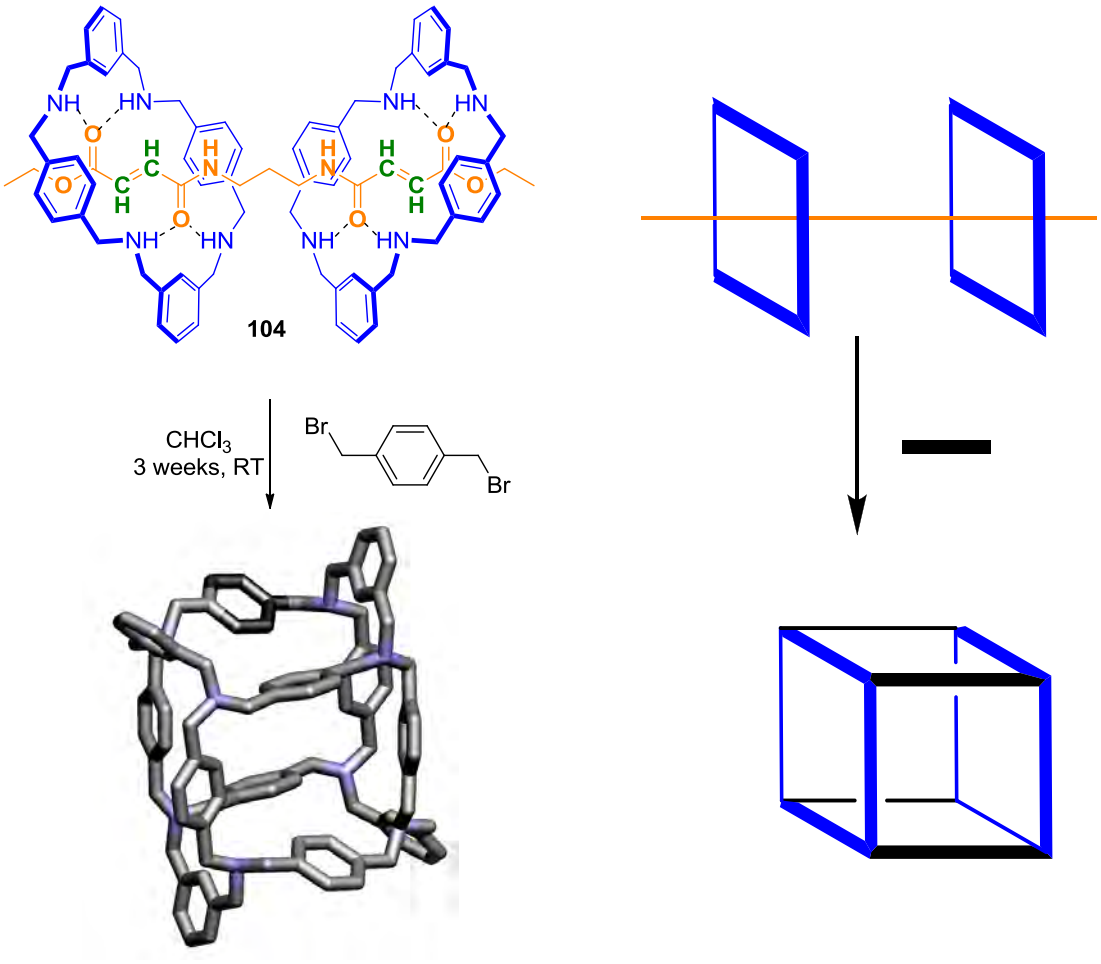

Scheme 2.64: Box formation through [3]pseudorotaxane **104**.

The linking reaction between [3]pseudorotaxane **104** and α,α'-dibromo-*p*-xylene was monitored via MALDI spectrometry (Figure 2.28). After one week, new peaks in the MALDI spectrum were detected. The peak at 1057 Da corresponds to the two macrocycles with one linker, the peak at 1159 Da to the two macrocycles connected by two linkers, the peak at 1261 Da where three linkers are present and the peak at 1363 Da to the molecular box. Within three weeks the desired

molecular box was formed. Unfortunately, the purification and full characterization of the box **105** is not trivial. Even when the MALDI spectrum suggested the complete formation of the box, singly linked, doubly linked and triply linked intermediates, as well as starting linker were still present. Several purification techniques including recrystallisation, HPLC and column chromatography were explored. However, these were not successful. The final NMR spectra showed the expected signals and some impurities.

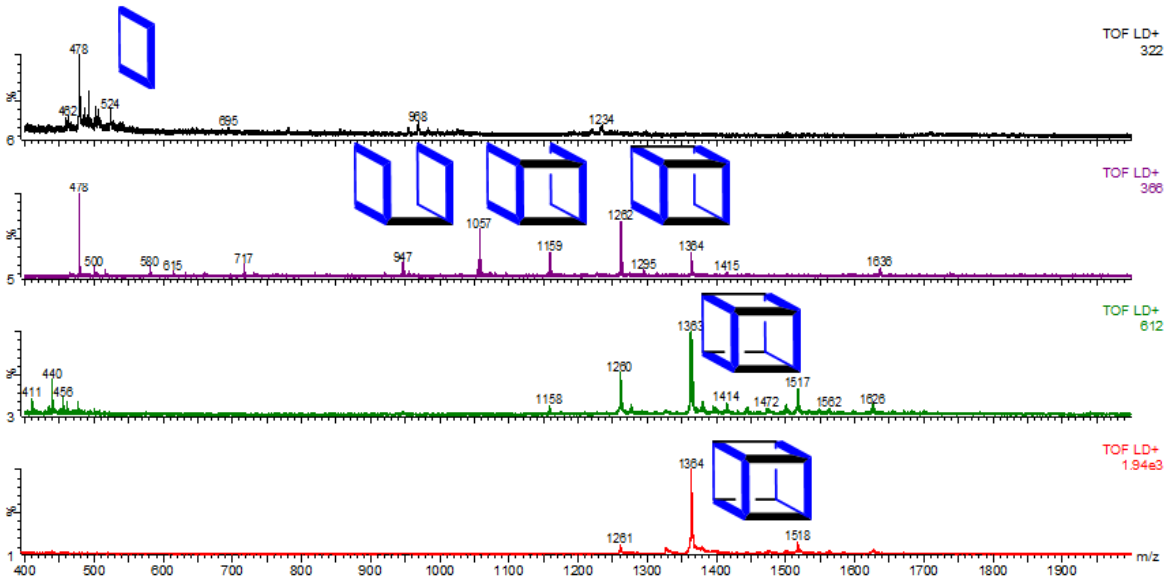

Figure 2.28: MALDI spectra for the formation of the molecular box **105** after 1 day (in black), after 1 week (in purple), after 2 weeks (in green) and after 3 weeks (in red).

Increasing the number of equivalents of the linker resulted in faster reaction times. However, the purification remained challenging. When adding a base, such as NaOH or $NaHCO_3$, hydrolysis of the double fumaric thread and formation of the box **105** occurred. However, the purification process was of the same difficulty.

Addition of NEt_3 as a base resulted in the quenching of the reaction and formation of the expected products did not occur.

In order to ensure that the thread and the [3]pseudorotaxane **104** have a significant effect on the formation of the molecular box, studies involving just the macrocycle **102** and the linker were also performed. The box **105** is also formed without the thread and results in a similar product distribution. However, the reaction proceeds over a longer period of time (6 weeks). In fact, related cages have been previously synthesised by Murakami, where two tetraamine macrocycles were linked by employing methyl 4-(chloroformyl)benzoate. Similar purification issues were also observed on these systems.[105,106]

A stoppering approach to capture the [3]pseudorotaxane **104** to form a [3]rotaxane was also investigated, in order to increase the variety of the linkers used and to demonstrate the generality of this synthetic method. An unstoppered thread can associate with a macrocycle to form a pseudorotaxane. This pseudorotaxane can then be captured irreversibly via a stoppering event to form a rotaxane. However, when the unstoppered thread reacts directly with the capping reagent, then a thread, which does not contain the macrocycle, is formed (Scheme 2.65).

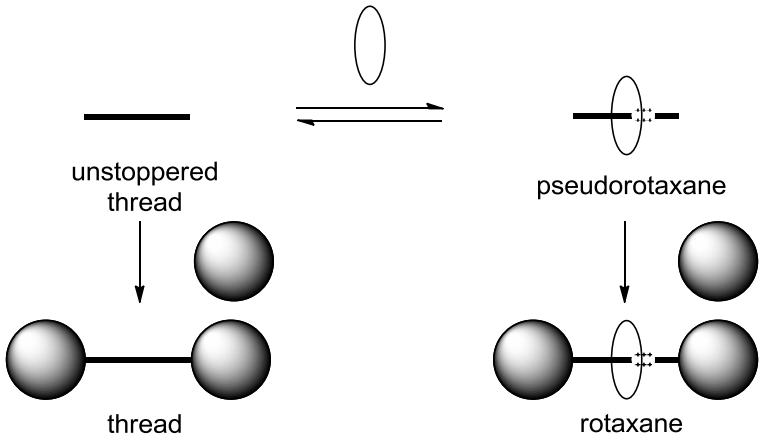

Scheme 2.65: Equilibria between thread, pseudorotaxane and rotaxane.

To maximise the amount of rotaxane formed via this method, the central equilibrium has to be manipulated to increase the population of the pseudorotaxane. This could be achieved either by a strong recognition between macrocycle and thread as shown by Stoddart (*vide supra*) or by modifying the reaction temperature. Lowering the temperature increases the formation of pseudorotaxane. However, it also decreases the efficiency of the capping reaction.

Douglas *et al.* have recently discussed the possibility of synthesising rotaxanes via capturing pseudorotaxanes at low temperature (Scheme 2.66).[107,108]

The amide macrocycle **106** (the same used by Chiu in 2007) and the amide thread **107** afforded the pseudorotaxane **108** and by addition of PPh_3 at low temperature the rotaxane **109** was formed. The reaction of azides with phosphines is very rapid[109] and can therefore be used for this kind of stoppering reaction at low temperature.

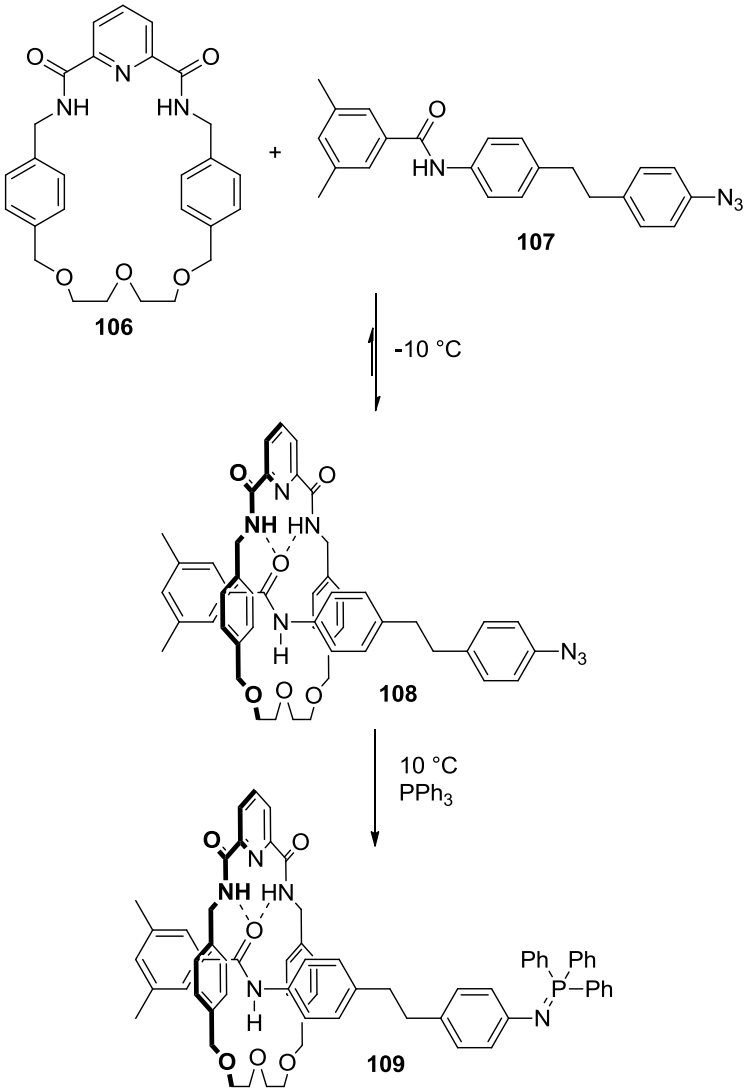

Scheme 2.66: Formation of the [2]pseudorotaxane **108** and its transformation into the [2]rotaxane **109**.

Terminal alkynes and organic azides can undergo a 1,3-dipolar cycloaddition and this was initially studied by Huisgen.[110] Its Cu(I)-catalysed version has been recently renamed as the “click” reaction.[111,112] The CuAAC or click reaction can produce under mild reaction conditions 1,4-substituted-1,2,3-triazoles in excellent yields.[111] In 2011, Schalley *et al.* reported the synthesis of the [2]rotaxane **110** using this methodology (Figure 2.29). A novel dipropargyl diketopiperazine is used

as a template for a tetraamide macrocycle. The stopper groups were attached to the thread through click chemistry.[113]

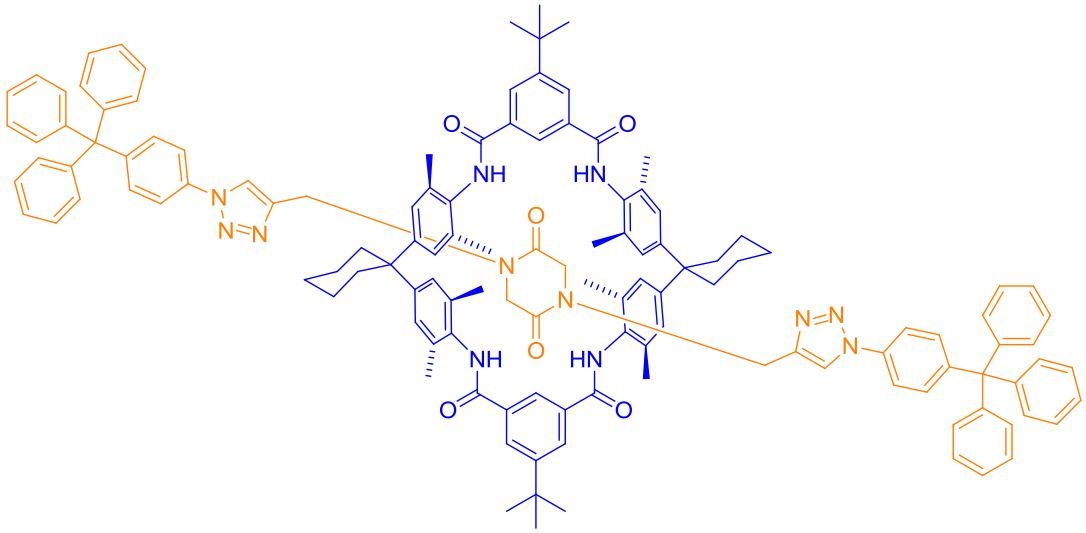

Figure 2.29: The diketopiperazines [2]rotaxane **110**.

Stoppering the double fumaric thread via click chemistry was chosen as a method to capture the [3]pseudorotaxane. Transformation of the diester **33** to the corresponding diacid **36** was described in Section 2.2.2. The resulting diacid presents poor solubility in any organic solvent, therefore only the transformation from the diacid **36** to the dipropargylester **111** was successful (Scheme 2.67).

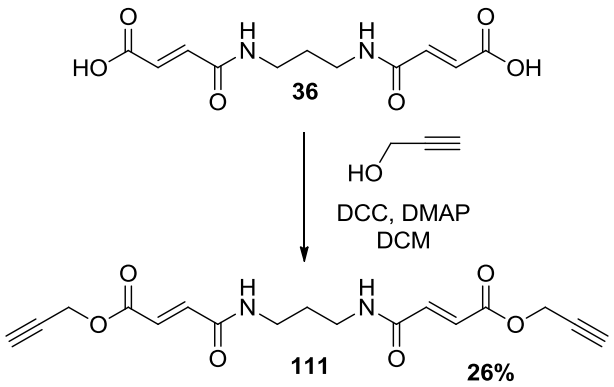

Scheme 2.67: Synthesis of the dipropargylester **111**.

Since the dipropargylester **111** presents poor solubility in chloroform, DMSO was used as solvent for the rotaxane formation reaction. However, a chemical shift of the proton signals in the ^{1}H NMR spectrum was not observed and consequently the formation of the expected pseudorotaxane could not be confirmed. The attempted click reaction (Scheme 2.68) was unsuccessful with a complex mixture being observed. This could be due to either the poor solubility of the thread, the Cu catalyst or the macrocycle itself.

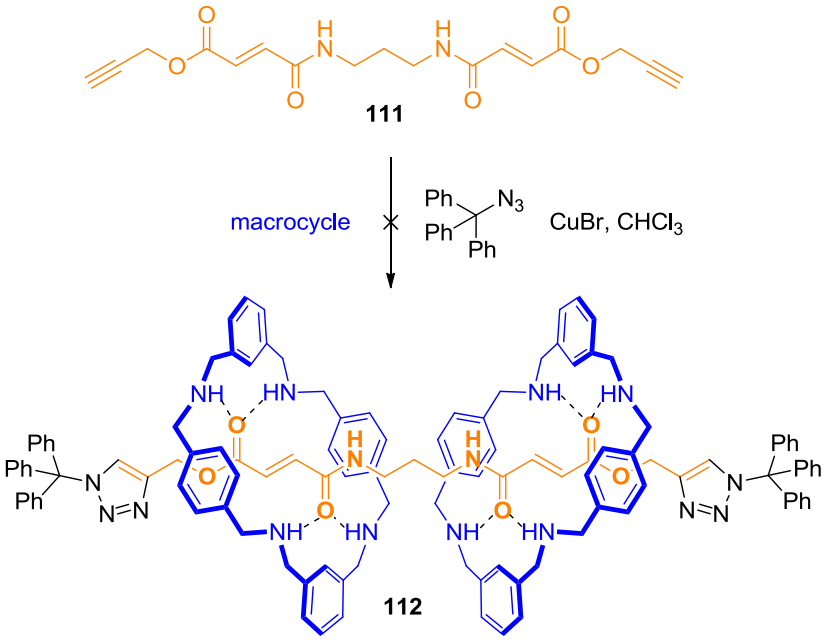

Scheme 2.68: Attempted click reaction.

A methyl group on the diamine was introduced to increase the solubility of the double fumaric thread. The ester **113** was synthesised in 72% yield and was hydrolysed in nearly quantitative yield (99%) (Scheme 2.69).

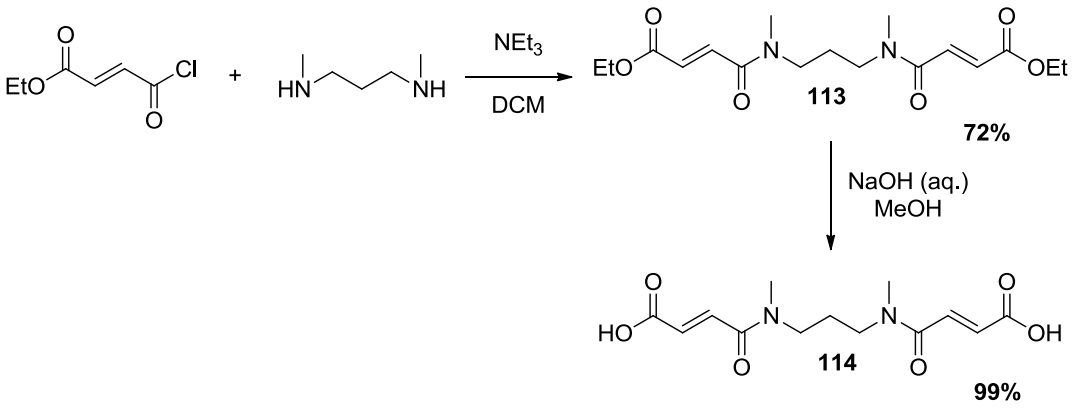

Scheme 2.69: Synthesis of the diacid **114**.

The diacid **114** showed better solubility than the diacid **36**. However, when converting it to the corresponding dipropargylester **115**, only an 18% yield of this product was obtained (Scheme 2.70).

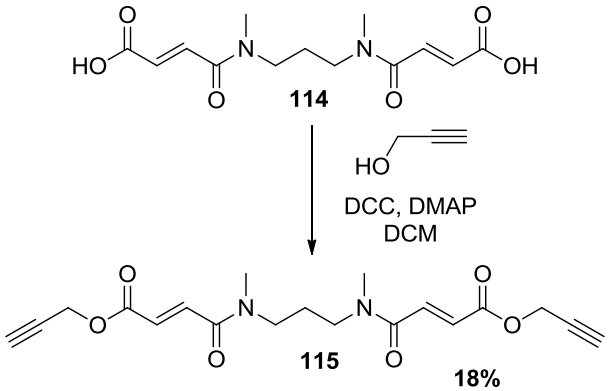

Scheme 2.70: Synthesis of the dipropargylester **115**.

The dipropargylester **115** is soluble in deuterated chloroform and this allows the monitoring of the reaction for the formation of the [3]pseudorotaxane and the click reaction to capture it. However, when testing different catalysts for the click reaction, the formation of the [3]rotaxane **116** could not be detected with a complex mixture being observed (Scheme 2.71).

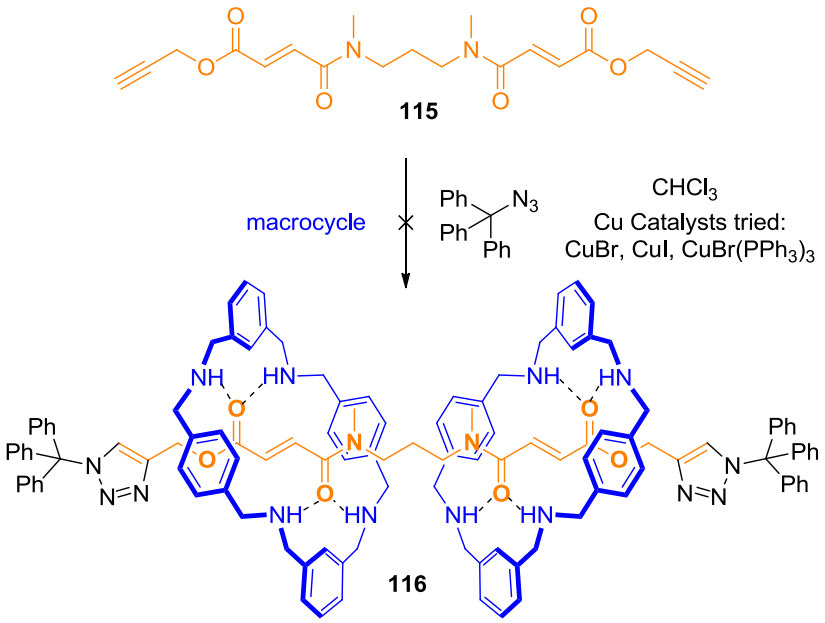

Scheme 2.71: Attempted click reaction.

The ES+ spectrum of the free macrocycle was analysed again and a Cu(I) adduct was detected. The Cu(I) can be picked up by the macrocycle from the residue of the injection tube. The binding of the tetraamine macrocycle to the fumaric station is not particularly strong. In contrast, the binding of the macrocycle to a metal such as Cu(I), which is the catalyst for the click reaction, seems to be considerable.

The synthesis of half stoppered thread systems was also investigated. In Section 2.2.3 a double fumaric thread via dimerisation was investigated. However, the yields of the required precursors were low and this route was therefore abandoned. When switching to the azo derivative and using a dibenzyl stopper group a high yield for the corresponding hydrazo precursor **117** was achieved. The half hydrazo thread was oxidised to the corresponding half azo thread **118** using NBS (Scheme 2.72).

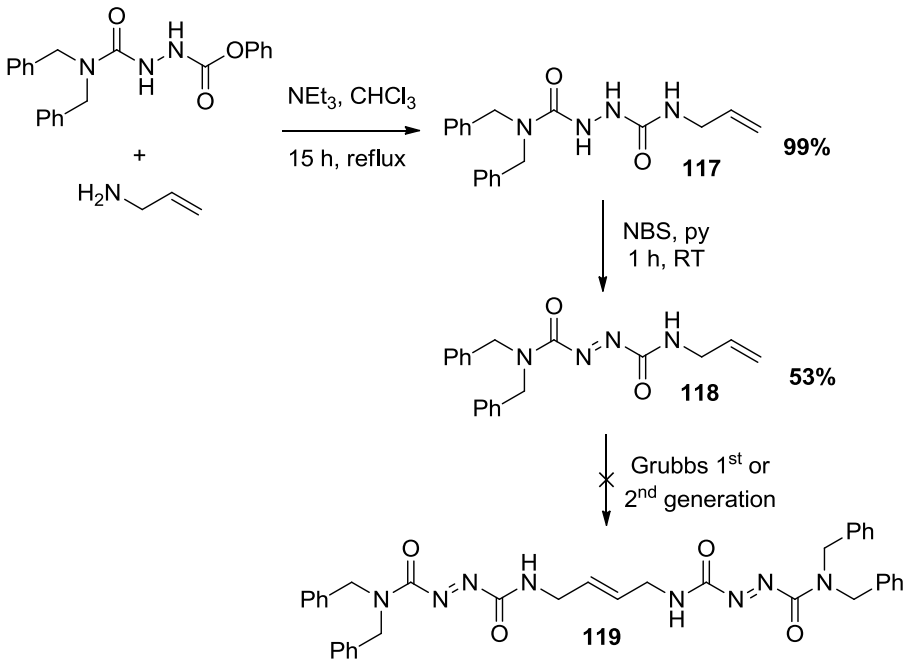

Scheme 2.72: Synthesis of the half azo thread **118** and attempted synthesis of the double azo thread **119**.

In order to confirm that the desired double azo thread can be formed in the absence of the macrocycle a Grubbs metathesis reaction was investigated. Unfortunately, this reaction did not form the desired double azo thread **119**. The resulting reaction mixture did not show any starting material either. A deallylation reaction as described by Alcaide *et al.*[114] would explain the absence of the starting material and the double azo thread **119**. The same result was observed when using the hydrazo derivative **117** in the Grubbs metathesis reaction.

In summary, a method to form pseudorotaxanes was developed and these pseudorotaxanes are able to form molecular cages. However, to date an effective stoppering event could not be found and this has to be further investigated.

Chapter 3: Conclusions and Future Work

Three main synthetic routes towards the formation of double fumaric threads were identified and investigated. However, these were unsuccessful. On the other hand, azo-dicarboxylate threads were formed when the stopper groups were changed from a primary amine to a secondary one. These new threads allowed the synthesis of several novel [2]- and [3]rotaxanes. Nevertheless, a spontaneous reduction during the clipping processes affected the formation of the desired [3]rotaxanes, and this reduction was studied in detail and a mechanism proposed.

It was possible to synthesise double fumaric threads when using the secondary amine stopper groups used in the azo-dicarboxylate systems. These new threads were able to form the desired [3]rotaxanes in dramatically increased yields. As a result an effective route for the high yielding synthesis of [3]rotaxanes with fumaramide stations was explored. The change from primary to secondary amines on the stopper groups seems to be key for the high yielding synthesis of rotaxanes. In comparison, the fumaramide station seems to be more effective than the azo dicarboxamide station to facilitate the rotaxane formation.

In order to be able to link the two macrocycles and access the molecular cage, direct alkylations on the tetraamide macrocycles were investigated. However, these were unsuccessful. Consequently, a reduction of the amide carbonyl groups on the macrocycle was investigated, as this would create more conformational freedom of the *N*-atoms on the macrocycle for the anticipated alkylations.

However, these reductions prove to be very challenging and deslipping of the reduced and partially reduced macrocycles was observed.

Fumaric threads with larger stopper groups were synthesised with regard to overcome the deslipping issues. These new fumaric threads presented solubility and purification issues, which prevented the isolation of any [3]rotaxane. Therefore, the full reduction of all the amide carbonyls on the macrocycles and the isolation of the desired fully reduced rotaxane could not be realised. Different stopper groups could be further investigated on this fumaric system. These stopper groups will need to be larger and will require solubilising agents, such as glycol chains, to overcome the solubility issues.

A different approach to obtain a novel molecular cage was also explored. This strategy involved the formation of pseudorotaxanes with a tetraamine macrocycle. A novel [3]pseudorotaxane was synthesised and detected via ^{1}H NMR spectroscopy and mass spectrometry. However, the binding constant between the unstoppered thread and the tetraamine macrocyle could not be determined since the chemical shift observed in the ^{1}H NMR was quite small.

When coupling the newly synthesised [3]pseudorotaxane with an appropriate linker, the desired molecular box was formed and could be detected via MALDI spectrometry. However, purification of this novel molecular box proved to be very challenging and a completely pure cage could not be isolated. Studies where the molecular box is formed in the absence of thread were also explored. However, these required longer reaction times.

Attempts to perform a stoppering event to capture the pseudorotaxane were unsuccessful and have to be further investigated. One possibility could be the formation of a metal complex, where one of the ligands can be replaced by a pre-formed pseudorotaxane (Figure 3.1).

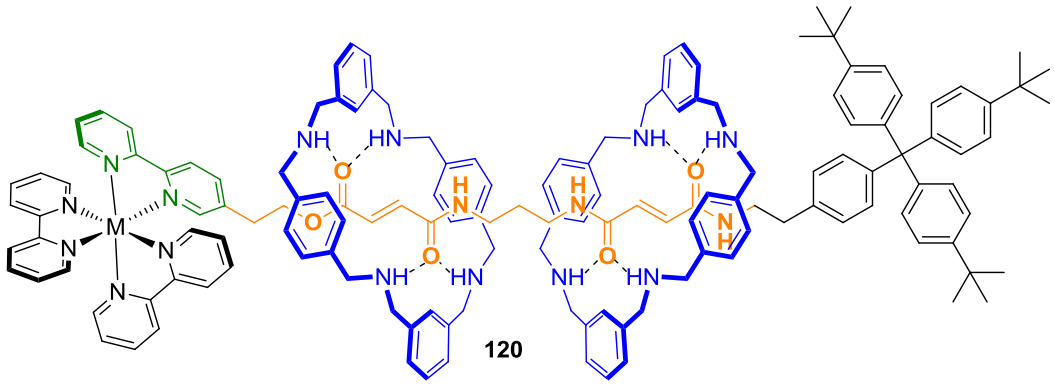

Figure 3.1: Proposed [3]rotaxane **120** bearing a metal complex as stopper group.

Another possibility could be the capture of an anticipated pseudorotaxane via a low temperature stoppering event. Such a stoppering event could be a glycosylation reaction between a primary alcohol and a sugar moiety (Figure 3.2). Kahne *et al.* have showed that this kind of reaction can be performed in good yields at low temperature via sulfoxide activation using Tf_2O.[115] A highly reactive glycosyl donor could be generated which should react rapidly with the terminal alcohols of the preformed pseudorotaxane **121**.

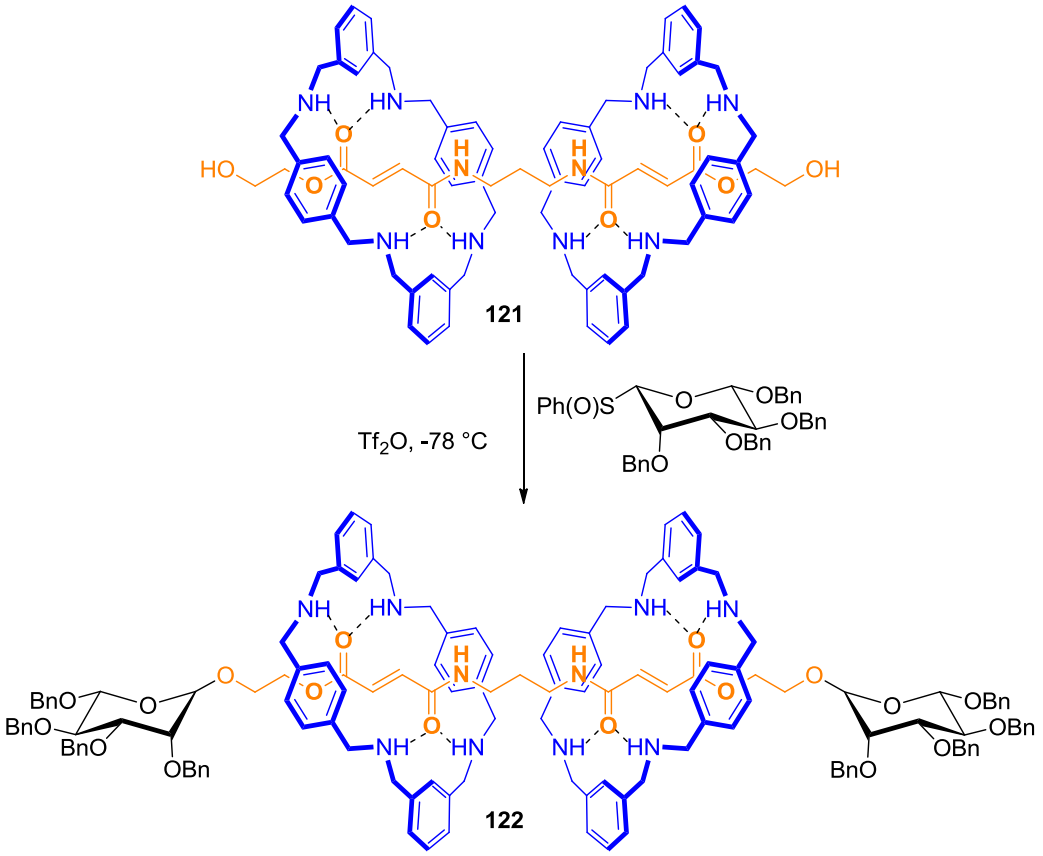

Figure 3.2: Proposed synthesis of the [3]rotaxane **122** with sugar stopper groups.

A rotaxane with a sugar stopper has been previously synthesised by Leigh.[116] It was demonstrated, that this sugar stopper group can be easily cleaved. The benefit of these stopper groups is that they are unreactive under various reaction conditions, which would allow an effective cross linking event of the two macrocycles. Once the desired molecular box has been formed, the sugar protecting group could be easily removed.

Chapter 4: Experimental

4.1 Materials and methods

Reactions were carried out under dry N_2 using dry glassware. Tetrahydrofuran (THF) was distilled from sodium/benzophenone. Dichloromethane, diethyl ether, methanol and toluene were collected from the Pure Solv-MD Solvent Purification System. All other reagents and solvents were used as received from commercial suppliers unless otherwise indicated. Liquid volumes less than 1 mL were measured and dispensed with Hamilton gastight syringes. Reaction temperatures refer to the temperature measured in an external bath. NMR data were recorded either on a Bruker AV300, AVIII300, AV400, AVIII400 or DRX500 spectrometers in the deuterated solvents indicated and the spectra were calibrated on residual solvent peaks. Chemical shifts (δ) are quoted in ppm and *J* values are quoted in Hz. In reporting spectral data, the following abbreviations were used: s (singlet), d (doublet), t (triplet), q (quartet), dd (doublet of doublets), dt (doublet of triplets), tt (triplet of triplets), m (multiplet), br (broad). In the case of ambiguous assignments, 2-dimensional homonuclear (^{1}H - ^{1}H) and heteronuclear (^{1}H - ^{13}C) NMR experiments were used. All NMR spectra were processed using MestReNova.[117] NH and OH protons were not reported when these were not observed. Progress of reactions was monitored by thin layer chromatography (TLC) using Merck Silica Gel 60 F_{254} aluminium or plastic backed plates that were visualized with UV light, *p*-anisaldehyde or potassium permanganate. Flash

column chromatography was carried out using Davisil 60 Å Silica Gel in the solvent systems indicated. Melting points were recorded using a Gallenkamp melting point apparatus and are uncorrected. Infrared spectra were recorded on a Perkin Elmer Spectrum 100 FTIR spectrometer as neat films, wavelengths (ν) are quoted in cm^{-1}. Mass spectra were acquired on a Waters Micromass LCT TOF spectrometer using electrospray ionisation (ESI). Electron impact (EI) spectra were recorded on a Waters Micromass Zabspec/Magnetic sector mass spectrometer. Matrix-Assisted Laser Desorption Ionization (MALDI) spectra were either recorded on a Bruker Bi-flex MALDI Time of Flight mass spectrometer or a Waters Micromass MALDI mirco MX mass spectrometer. X-ray diffraction data was collected either at the National Crystallography Service at the University of Southampton in a Rigaku FR-E Ultra High Flux diffractometer or at the University of Birmingham in a Bruker Smart 6000 CCD diffractometer. COLLECT was used for data collection and DENZO to refine the data. SADABS was used to correct the experimental absorption. SIR92 was used as method to solve the resulting crystal structures, and their refinements were performed by a full-matrix least-squares procedure on F^2 in SHELXL-97. Via anisotropic displacement parameters all non-hydrogen atoms were refined. The hydrogen atoms were fixed as riding models. Mercury 3.0[72] was used to process .cif files of crystal structures solved by Dr. Louise Male from the University of Birmingham or Dr. Mateusz Pitak from the National Crystallography Service at the University of Southampton. HPLC was carried out on a DIONEX summit P580 quaternary low pressure gradient pump with a built-in vacuum degasser using a Summit UVD 170s UV/Vis multi-channel

detector. Solvents were used as HPLC grade. Chromeleon software was used to visualise and process the obtained chromatograms. Analytical separations used a flow rate of 1 mL/min, and semi-preparative used a flow rate of 3 mL/min and preparative used a flow rate of 20 mL/min.

4.2 Experimental for Section 2.2

(*E*)-ethyl-4-((2,2-diphenylethyl)amino)-4-oxobut-2-enoate (27)[118]

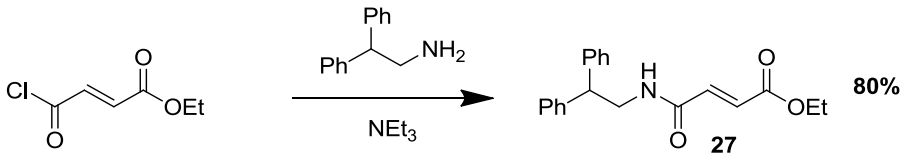

Ethyl fumaroyl chloride (162 mg, 1.0 mmol, 1.0 eq.) was dissolved in dry DCM (10 mL) at RT. A solution of 2,2-diphenylethylamine (197 mg, 1.0 mmol, 1.0 eq.) and NEt_3 (2 mL, 14 mmol, 14 eq.) in dry DCM (10 mL) was added using a syringe pump over a period of 2 h. The reaction was stirred overnight and the solvent was removed *in vacuo*. The crude product was purified by column chromatography with EtOAc / pet (1 / 1) as eluent to afford (*E*)-ethyl-4-((2,2-diphenylethyl)amino)-4-oxobut-2-enoate (**27**) as a white solid (258 mg, 80%). m.p. 110 - 113 °C [lit. 112 - 113 °C][118]; FTIR (film) ν_{max} 3281, 3082, 2981, 2931, 1722, 1652, 1557, 1273, 1035, 695; ^{1}H NMR (300 MHz, $CDCl_3$) δ 7.41 – 7.17 (m, 10H, Ar, C*H*), 6.87 – 6.69 (m, 2H, C*H*), 6.28 (br s, 1H, N*H*), 4.34 – 4.11 (m, 3H, C*H*C*H*$_2$), 3.99 (q, *J* = 7.1 Hz, 2H, C*H*$_2$), 1.30 (t, *J* = 7.1 Hz, 3H, C*H*$_3$); ^{13}C NMR (100 MHz, $CDCl_3$) δ 165.6 (*C*OO), 163.7 (*C*ON), 141.6 (Ar, *C*), 136.2 (*C*H), 130.4 (*C*H), 128.8 (Ar, *C*H), 128.0

(Ar, *C*H), 127.0 (Ar, *C*H), 61.2 (*C*H_2), 50.4 (*C*H), 44.2 (*C*H_2), 14.2 (*C*H_3); HRMS (ES+) calculated for $C_{20}H_{21}NO_3Na$ $[M+Na]^+$ 346.1419, found 346.1418.

Data were in agreement with those previously reported.[118]

N^1,N^6-bis(2,2-diphenylethyl)fumaramide (6)[80]

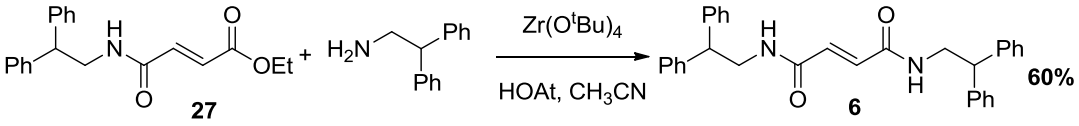

HOAt (1.5 mg, 0.01 mmol, 0.05 eq.) followed by Zr(O*t*Bu)$_4$ (4 mL, 0.01 mmol, 0.05 eq.) was added to a solution of (*E*)-ethyl-4-((2,2-diphenylethyl)amino)-4-oxobut-2-enoate (**27**) (69 mg, 0.18 mmol, 1 eq.) and 2,2-diphenylethylamine (39 mg, 0.2 mmol, 1.1 eq.) in acetonitrile (0.8 mL). The reaction mixture was heated to reflux for 3 h and quenched by addition of MeOH (2 mL) and DCM (2 mL). The solvent was removed *in vacuo* and the crude product was purified by column chromatography with EtOAc / pet (1 / 1) as eluent to afford the titled product as a white solid (51 mg, 60%). m.p. 213 - 214 °C; FTIR (film) ν_{max} 3264, 3081, 2924, 1631, 1552, 1493, 1330, 1196, 990, 745, 694; ^{1}H-NMR (300 MHz, MeOD / $CDCl_3$) δ 8.20 (br s, 2 H, N*H*), 7.30-7.20 (m, 20 H, Ar, C*H*), 6.70 (s, 2 H, C*H*CO), 4.28 (t, *J* = 7.7 Hz, 2 H, C*H*), 3.93 (d, *J* = 7.7 Hz, 4 H, CH_2); ^{13}C-NMR (100 MHz, MeOD / $CDCl_3$) δ 166.1 (*C*ON), 142.8 (Ar, *C*), 133.5 (*C*H), 129.5 (Ar, *C*H), 129.0 (Ar, *C*H), 127.6 (Ar, *C*H), 51.0 (*C*H), 45.1 (*C*H_2); HRMS (ES) calculated for $C_{32}H_{30}N_2O_2Na$ $[M+Na]^+$ 497.2205, found 497.2207.

Data were in agreement with those previously reported.[80]

(*E*)-4-((2,2-diphenylethyl)amino)-4-oxobut-2-enoic acid (23)[118]

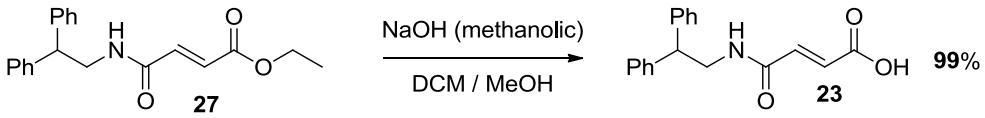

(*E*)-ethyl-4-((2,2-diphenylethyl)amino)-4-oxobut-2-enoate (**27**) (211 mg, 0.66 mmol, 1.0 eq.) was dissolved in 10 mL DCM / MeOH (9 / 1). 2 M NaOH methanol solution (1 mL) was then added. The reaction was stirred for 38 h at RT and monitored by TLC. The reaction mixture was acidified with 1 M HCl (2 mL), extracted with DCM (3 x 20 mL) and washed with brine (20 mL). The organic layers were combined, dried over $MgSO_4$ and concentrated under reduced pressure to afford (*E*)-4-((2,2-diphenylethyl)amino)-4-oxobut-2-enoic acid (**23**) (195 mg, 99%) as a white solid. m.p. >270 °C (decomp) [lit. >270 °C (decomp)][118]; ^{1}H NMR (300 MHz, d_6-DMSO) δ 8.09 (s, 1H, N*H*), 7.41 – 7.09 (m, 10H, Ar, C*H*), 6.41 (d, *J* = 15.4 Hz, 1H, C*H*), 6.23 (d, *J* = 15.4 Hz, 1H, C*H*), 4.26 – 4.21 (m, 1H, C*H*), 3.78 – 3.66 (m, 2H, CH_2); ^{13}C NMR (100 MHz, MeOD / $CDCl_3$) δ 174.3 (*C*OO), 172.0 (*C*ON), 143.4 (Ar, *C*), 137.8 (*C*H), 131.6 (*C*H), 129.8 (Ar, *C*H), 129.0 (Ar, *C*H), 127.9 (Ar, *C*H), 51.7 (*C*H), 40.4 (CH_2); HRMS (ES-) calculated for $C_{18}H_{16}NO_3$ $[M-H]^-$ 294.1130, found 294.1132.

Data were in agreement with those previously reported.[118]

N-(4-aminophenyl)-*N*-(2,2-diphenylethyl)fumaramide (28)

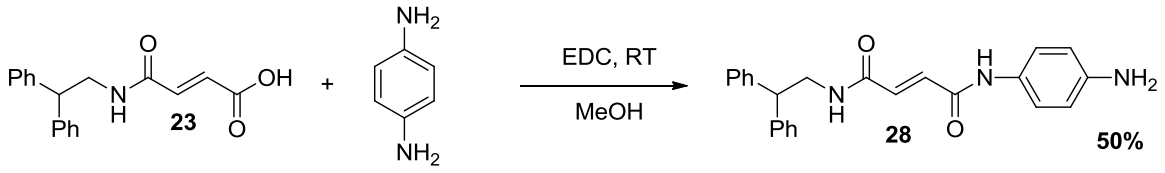

(*E*)-4-((2,2-diphenylethyl)amino)-4-oxobut-2-enoic acid (**23**) (200 mg, 0.67 mmol, 2.0 eq.) followed by EDC (104 mg, 0.67 mmol, 2.0 eq.) was added to a stirred suspension of *p*-phenylamine (35 mg, 0.33 mmol, 1.0 eq.) in methanol (4 mL). The reaction mixture was stirred at RT for 24 h. The reaction mixture was then diluted with water and extracted with DCM (3 x 20 mL). The organic layers were combined, washed with brine, dried over $MgSO_4$ and concentrated under reduced pressure. The crude product was purified by column chromatography with DCM / MeOH (10 / 1) as eluent to afford of *N*-allyl-*N*-(2,2-diphenylethyl)fumaramide (**28**) as a white solid (63 mg, 50%). m.p. 178 °C; FTIR (film) ν_{max} 3313, 2932, 1634, 1515, 1450, 1402, 1221, 1114, 1029, 739, 698; ^{1}H NMR (300 MHz, MeOD / $CDCl_3$) δ 7.37 (d, *J* = 8.9 Hz, 2H, Ar, C*H*), 7.32 – 7.14 (m, 10H, Ar, C*H*), 6.96 (d, *J* = 15.1 Hz, 1H, C*H*), 6.79 (d, *J* = 15.1 Hz, 1H, C*H*), 6.69 (d, *J* = 8.9 Hz, 2H, Ar, C*H*), 4.29 (t, *J* = 8.1 Hz, 1H, C*H*), 3.92 (dd, *J* = 8.1, 4.0 Hz, 2H, NHC*H*$_2$); ^{13}C NMR (100 MHz, MeOD / $CDCl_3$) δ 167.3 (*C*ON), 166.3 (*C*ON), 142.9 (Ar, *C*), 134.2 (*C*H), 133.3 (*C*H), 129.2 (Ar, *C*H), 128.7 (Ar, *C*H), 127.4 (Ar, *C*H), 122.5 (Ar, *C*H), 116.4 (Ar, *C*H), 51.1 (*C*H), 45.1 (*C*H_2); HRMS (EI+) calculated for $C_{24}H_{23}N_3O_2Na$ $[M+Na]^+$ 408.1688, found 408.1677.

(2*E*,2'*E*)-diethyl 4,4'-(ethane-1,2-diylbis(azanediyl))bis(4-oxobut-2-enoate) (32)[119]

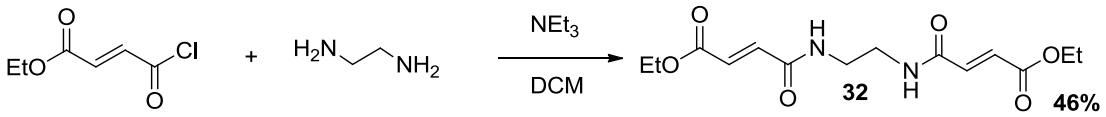

Ethyl fumaroyl chloride (178 mg, 1.1 mmol, 2.2 eq.) was dissolved in dry DCM (19 mL) at RT. A solution of ethylenediamine (30 mg, 0.5 mmol, 1.0 eq.) and NEt_3 (0.7 mL, 5.0 mmol, 10 eq.) in dry DCM (19 mL) was added using a syringe pump over a period of 2 h. The reaction was stirred overnight and the solvent was removed *in vacuo*. The crude product was purified by column chromatography with EtOAc as eluent to afford (2*E*,2'*E*)-diethyl 4,4'-(ethane-1,2-diylbis(azanediyl))bis(4-oxobut-2-enoate) (**32**) as a white solid (72 mg, 46%). m.p. 186 °C [lit. 189 - 190 °C][119]; FTIR (film) ν_{max} 3290, 3072, 1947, 1711, 1634, 1570, 1437, 1293, 1161, 1094, 1032, 756, 701; ^{1}H NMR (300 MHz, MeOD / $CDCl_3$) δ 8.20 (br s, 2H, N*H*), 6.80 (q, *J* = 15.5 Hz, 4H, C*H*), 4.20 (q, *J* = 7.1 Hz, 4H, OCH_2), 3.41 – 3.40 (m, 4H, CH_2NH), 1.27 (t, *J* = 7.1 Hz, 6H, CH_3); ^{13}C NMR (100 MHz, MeOD / $CDCl_3$) δ 166.1 (*C*OO), 165.3 (*C*ON), 136.4 (*C*H), 130.4 (*C*H), 61.5 (O*C*H_2), 39.4 (*C*H_2NH), 14.1 (*C*H_3); HRMS (ES+) calculated for $C_{14}H_{20}N_2O_6Na$ $[M+Na]^+$ 335.1219, found 335.1210.

Data were in agreement with those previously reported.[119]

(2*E*,2'*E*)-diethyl 4,4'-(propane-1,3-diylbis(azanediyl))bis(4-oxobut-2-enoate) (33)

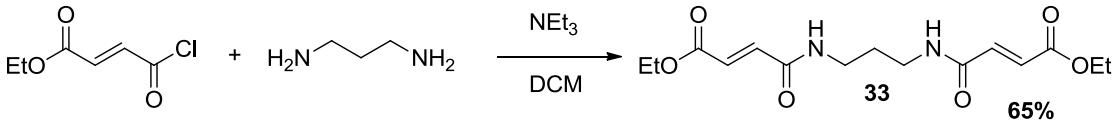

Ethyl fumaroyl chloride (178 mg, 1.1 mmol, 2.2 eq.) was dissolved in dry DCM (19 mL) at RT. A solution of 1,3-diaminopropane (37 mg, 0.5 mmol, 1.0 eq.) and NEt_3 (0.7 mL, 5.0 mmol, 10 eq.) in dry DCM (19 mL) was added using a syringe pump over a period of 2 h. The reaction was stirred overnight and the solvent was removed *in vacuo*. The crude product was purified by column chromatography with EtOAc as eluent to afford (2*E*,2'*E*)-diethyl 4,4'-(propane-1,3-diylbis(azanediyl))bis(4-oxobut-2-enoate) (**33**) as a white solid (110 mg, 65%). m.p. 135 °C; FTIR (film) ν_{max} 3263, 3087, 1716, 1626, 1551, 1473, 1294, 1160, 975, 869, 749, 666; ^{1}H NMR (300 MHz, $CDCl_3$) δ 7.15 – 7.11 (m, 2H, N*H*), 6.96 (d, *J* = 15.4 Hz, 2H, C*H*), 6.79 (d, *J* = 15.4 Hz, 2H, C*H*), 4.23 (q, *J* = 7.1 Hz, 4H, OCH_2), 3.43 – 3.37 (m, 4H, CH_2NH), 1.83 – 1.68 (m, 2H, $CH_2CH_2CH_2$), 1.30 (t, *J* = 7.1 Hz, 6H, CH_3); ^{13}C NMR (100 MHz, $CDCl_3$) δ 165.7 (*C*OO), 164.6 (*C*ON), 136.4 (*C*H), 130.6 (*C*H), 61.4 (O*C*H_2), 36.6 (*C*H_2NH), 29.5 (*C*H_2), 14.3 (*C*H_3); HRMS (ES+) calculated for $C_{15}H_{22}N_2O_6Na$ $[M+Na]^+$ 349.1376, found 349.1372.

(2*E*,2'*E*)-diethyl 4,4'-(butane-1,4-diylbis(azanediyl))bis(4-oxobut-2-enoate) (34)

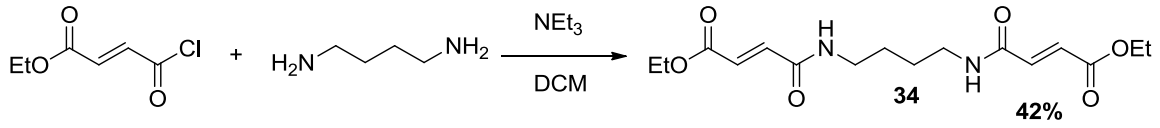

Ethyl fumaroyl chloride (178 mg, 1.1 mmol, 2.2 eq.) was dissolved in dry DCM (19 mL) at RT. A solution of 1,4-diaminobutane (44 mg, 0.5 mmol, 1.0 eq.) and NEt_3 (0.7 mL, 5.0 mmol, 10 eq.) in dry DCM (19 mL) was added using a syringe pump over a period of 2 h. The reaction was stirred overnight and the solvent was removed *in vacuo*. The crude product was purified by column chromatography with EtOAc as eluent to afford (2*E*,2'*E*)-diethyl 4,4'-(butane-1,4-diylbis(azanediyl))bis(4-oxobut-2-enoate) (**34**) as a white solid (72 mg, 42%). m.p. 143 °C; FTIR (film) ν_{max} 3302, 1706, 1619, 1547, 1444, 1174, 1031, 9991, 747, 688; ^{1}H NMR (300 MHz, MeOD) δ 8.12 (br s, 2H, N*H*), 6.89 (d, *J* = 15.5 Hz, 2H, C*H*), 6.72 (d, *J* = 15.5 Hz, 2H, C*H*), 4.20 (q, *J* = 7.1 Hz, 4H, OCH_2), 3.27 – 3.25 (m, 4H, CH_2NH), 1.55 – 1.51 (m, 4H, $CH_2CH_2CH_2CH_2$), 1.27 (t, *J* = 7.1 Hz, 6H, CH_3); ^{13}C NMR (100 MHz, MeOD) δ 166.3 (*C*OO), 164.8 (*C*ON), 136.8 (*C*H), 130.0 (*C*H), 61.5 (O*C*H_2), 39.3 (*C*H_2NH), 26.5 (*C*H_2), 14.1 (*C*H_3); HRMS (ES+) calculated for $C_{16}H_{24}N_2O_6Na$ $[M+Na]^+$ 363.1532, found 363.1529.

(*E*)-ethyl 4-(1H-benzo[d][1,2,3]triazol-1-yl)-4-oxobut-2-enoate (35)

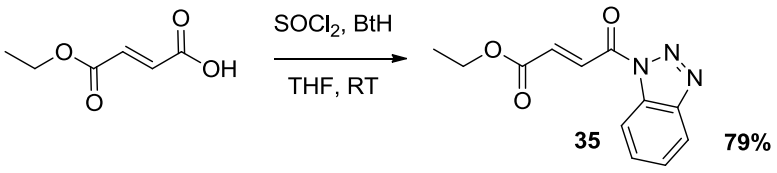

Thionyl chloride (87 μL, 1.2 mmol, 1.2 eq.) was added to a solution of benzotriazole (495 mg, 4.2 mmol, 4.2 eq.) in anhydrous THF (5 mL) at 0 °C, and the reaction mixture was stirred for 20 min at this temperature. Mono-ethyl fumarate (144 mg, 1.0 mmol, 1.0 eq.) was dissolved in dry THF (3 mL) and added dropwise to the reaction mixture at 0 °C. The reaction was stirred for 4 h at this temperature and was allowed to warm to RT overnight. The precipitate was filtered, and the filtrate was concentrated under reduced pressure. The residue was diluted with DCM (25 mL) and washed with a saturated aqueous solution of Na_2CO_3 (3 x 10 mL), brine (10 mL) and dried over $MgSO_4$ to afford (*E*)-ethyl 4-(1H-benzo[d][1,2,3]triazol-1-yl)-4-oxobut-2-enoate (**35**) as a white solid (194 mg, 79%). m.p. 105 °C; FTIR (film) ν_{max} 3419, 3101, 2978, 1707, 1595, 1487, 1448, 1375, 1291, 1162, 1067, 975, 869, 745; ^{1}H NMR (400 MHz, $CDCl_3$) δ 8.45 (d, *J* = 15.7 Hz, 1H, C*H*), 8.37 (d, *J* = 8.3 Hz, 1H Ar, C*H*), 8.18 (d, *J* = 8.3 Hz, 1H Ar, C*H*), 7.74 – 7.70 (m, 1H Ar, C*H*), 7.63 – 7.53 (m, 1H Ar, C*H*), 7.29 (d, *J* = 15.7 Hz, 1H, C*H*), 4.37 (q, *J* = 7.1 Hz, 2H, OCH_2), 1.41 (t, *J* = 7.1 Hz, 3H, CH_3); ^{13}C NMR (100 MHz, $CDCl_3$) δ 164.5 (*C*OO), 162.5 (*C*ON), 146.5 (Ar, *C*), 136.8 (*C*H), 131.3 (*C*H), 131.2 (Ar, *C*), 130.9 (Ar, *C*H), 126.9 (Ar, *C*H), 120.6 (Ar, *C*H), 114.7 (Ar, *C*H), 61.9 (O*C*H_2), 14.3 (*C*H_3); HRMS (EI+) calculated for $C_{12}H_{11}N_3O_3$ $[M]^+$ 245.0800, found 245.0797.

(2*E*,2'*E*)-4,4'-(propane-1,3-diylbis(azanediyl))bis(4-oxobut-2-enoic acid) (36)

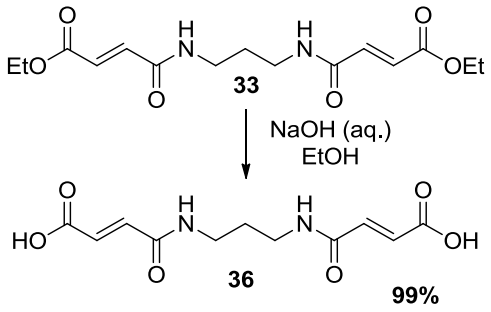

(2*E*,2'*E*)-diethyl 4,4'-(propane-1,3-diylbis(azanediyl))bis(4-oxobut-2-enoate) (**33**) (78 mg, 0.24 mmol, 1.0 eq.) was dissolved in EtOH (10 mL). Then NaOH (20 mg, 0.5 mmol, 1.2 eq.) dissolved in water (0.5 mL) was added dropwise over a period of 5 minutes via syringe. The reaction was stirred for 16 h at RT and monitored by TLC. The reaction mixture was acidified with 1 M HCl (0.5 mL), extracted with DCM (3 x 20 mL) and washed with brine (20 mL). The organic layers were combined, dried over $MgSO_4$ and concentrated under reduced pressure to afford (2*E*,2'*E*)-4,4'-(propane-1,3-diylbis(azanediyl))bis(4-oxobut-2-enoic acid) (**36**) as a yellow solid (64 mg, 99%). m.p. >244 °C (decomp); FTIR (film) ν_{max} 3322, 2926, 1641, 1561, 1411, 1322, 1261, 1188, 1141, 960, 788; ^{1}H NMR (300 MHz, MeOD) δ 9.49 (t, *J* = 5.6 Hz, 2H, N*H*), 7.75 (d, *J* = 15.5 Hz, 2H, C*H*), 7.32 (d, *J* = 15.5 Hz, 2H, C*H*), 4.06 – 3.89 (m, 4H, CH_2NH), 2.52 – 2.34 (m, 2H, $CH_2CH_2CH_2$); ^{13}C NMR (100 MHz, D_2O) δ 173.5 (*C*OO), 167.7 (*C*ON), 136.4 (*C*H), 131.1 (*C*H), 37.1 (*C*H_2NH), 27.7 (*C*H_2); HRMS (ES-) calculated for $C_{11}H_{13}N_2O_6$ $[M-H]^-$ 269.0770, found 269.0774.

N^1-allyl-N^6-(2,2-diphenylethyl)fumaramide (39)

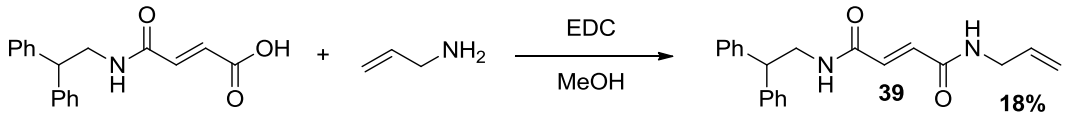

(*E*)-4-((2,2-Diphenylethyl)amino)-4-oxobut-2-enoic acid (**23**) (200 mg, 0.7 mmol, 1.0 eq.) then EDC (104 mg, 0.7 mmol, 1.0 eq.) was added to a stirred suspension of allylamine (38 mg, 0.7 mmol, 1.0 eq.) in methanol (4 mL). The reaction mixture was stirred at RT for 24 h. The reaction mixture was diluted with water and extracted with DCM (3 x 20 mL). The organic layers were combined, washed with brine, dried over $MgSO_4$ and concentrated under reduced pressure. The crude product was purified by column chromatography with EtOAc as eluent to afford N^1-allyl-N^6-(2,2-diphenylethyl)fumaramide (**39**) as a white solid (40 mg, 18%).m.p. 79 °C; FTIR (film) ν_{max} 2987, 2901, 1696, 1644, 1535, 1452, 1407, 1250, 1066, 893, 779; ^{1}H NMR (300 MHz, MeOD / $CDCl_3$) δ 7.32 – 7.11 (m, 10H, Ar, C*H*), 6.71 (d, *J* = 15.2 Hz, 2H, C*H*), 5.85 – 5.72 (m, 1H, C*H*), 5.18 – 5.09 (m, 2H, CH_2), 4.22 (t, *J* = 8.0 Hz, 1H, C*H*), 3.93 – 3.80 (m, 4H, CH_2); ^{13}C NMR (100 MHz, MeOD / $CDCl_3$) δ 165.3 (*C*ON), 165.1 (*C*ON), 142.0 (Ar, *C*), 133.3 (*C*H), 132.6 (*C*H), 128.7 (Ar, *C*H), 128.0 (Ar, *C*H), 126.9 (Ar, *C*H), 116.6 (*C*H_2), 50.4 (*C*H), 44.4 (*C*H_2), 42.2 (*C*H_2); HRMS (ES+) calculated for $C_{21}H_{22}N_2O_2Na$ $[M+Na]^+$ 357.1579, found 357.1567.

4.3 Experimental for Section 2.3

Diphenylhydrazo-1,2-dicarboxylate (42)[76,120]

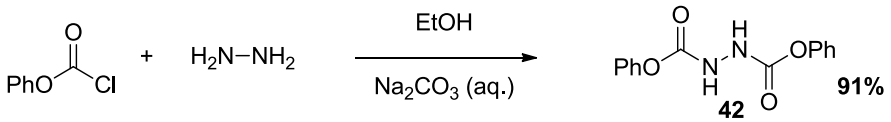

Hydrazine hydrate (4.8 mL, 100.0 mmol, 1.0 eq.) was dissolved in ethanol (50 mL) and cooled to 0°C. Phenyl chloroformate (12.6 mL, 100.0 mmol, 1.0 eq.) was then added followed by the simultaneous addition of phenyl chloroformate (12.6 mL, 100.0 mmol, 1.0 eq.) and Na_2CO_3 (10.2 g, 100.0 mmol, 1.0 eq.) in water (12.5 mL). Once the additions were finished water (15 mL) was added and the reaction mixture stirred for 30 minutes at RT. The resulted precipitate was collected, washed with ice cold water (200 mL) and dried *in vacuo* to afford diphenylhydrazo-1,2-dicarboxylate (**42**) as a white solid (24.77 g, 91%). m.p. 180 °C [lit. 183 - 185 °C][76]; ^{1}H NMR (300 MHz, $CDCl_3$) δ 7.45 - 7.35 (m, 10H, Ar, C*H*); ^{13}C NMR (100 MHz, $CDCl_3$) δ 155.0 (*C*OO), 150.6 (Ar, *C*), 129.6 (Ar, *C*H), 126.1 (Ar, *C*H), 121.5 (Ar, *C*H); HRMS (ES+) calculated for $C_{14}H_{12}N_2O_4Na$ $[M+Na]^+$ 295.0695, found 295.0704.

Data were in agreement with those previously reported.[76,120]

N,*N*,*N*',*N*'-tetrakis(2,2-diphenylethyl)-1,2-hydrazodicarboxamide (43)[76]

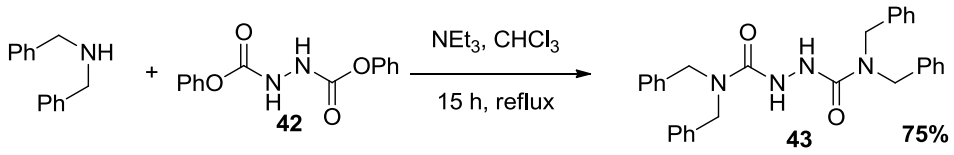

Dibenzylamine (2.0 mL, 10.8 mmol, 2.1 eq.) followed by NEt_3 (1.5 mL, 10.8 mmol, 2.1 eq.) were added to a solution of diphenylhydrazo-1,2-dicarboxylate (**42**) (1.4 g, 5.1 mmol, 1.0 eq.) in $CHCl_3$ (40 mL). The reaction mixture was heated at reflux for 15 h. The reaction mixture was cooled, concentrated under reduced pressure and the crude product purified by column chromatography with $CHCl_3$ / MeOH (97 / 3) as eluent to afford *N*,*N*,*N*',*N*'-tetrakis(2,2-diphenylethyl)-1,2-hydrazodicarboxamide (**43**) as a white solid (1.93 g, 75%). m.p. 173 °C [lit. 173 - 174 °C][76]; ^{1}H NMR (300 MHz, $CDCl_3$) δ 7.45 – 7.24 (m, 20H, Ar, C*H*), 4.55 (br s, 8H, CH_2); ^{13}C NMR (100 MHz, $CDCl_3$) δ 159.5 (*C*ON), 136.9 (Ar, *C*), 128.8 (Ar, *C*H), 127.6 (Ar, *C*H), 127.5 (Ar, *C*H), 50.0 (*C*H_2);LR MS (ES+) 501.5 ([M+Na]$^+$, 100%).

Data were in agreement with those previously reported.[76]

_N_,_N_,_N_',_N_'-tetrakis(2,2-diphenylethyl)-1,2-azodicarboxamide (40)[76]

Pyridine (0.3 mL, 3.7 mmol, 1.1 eq.) and NBS (0.6 g, 3.4 mmol, 1.0 eq.) were added to a solution of _N_,_N_,_N_',_N_'-tetrakis(2,2-diphenylethyl)-1,2-hydrazo dicarboxamide (**43**) (1.6 g, 3.4 mmol, 1.0 eq.) in dry DCM (50 mL). The resulting orange solution was stirred at RT for 1 h. The reaction mixture was diluted with DCM (25 mL) and sequentially washed with water (3 x 50 mL), a saturated aqueous solution of $Na_2S_2O_3$ (50 mL) and a saturated aqueous solution of $NaHCO_3$ (2 x 50 mL). The organic phase was dried over anhydrous $MgSO_4$, concentrated under reduced pressure and purified by column chromatography with $CHCl_3$ / MeOH (98 / 2) as eluent to afford _N_,_N_,_N_',_N_'-tetrakis(2,2-diphenylethyl)-1,2-azodicarboxamide (**40**) as a yellow solid (1.58 g, 98%). m.p. 148 °C [lit. 151 - 153 °C][76]; ^{1}H NMR (300 MHz, $CDCl_3$) δ 7.42 – 7.24 (m, 16H, Ar, C*H*), 7.17 – 7.08 (m, 4H, Ar, C*H*), 4.61 (s, 4H, CH_2), 4.43 (s, 4H, CH_2); ^{13}C NMR (100 MHz, $CDCl_3$) δ 161.9 (*C*ON), 135.5 (Ar, *C*), 135.4 (Ar, *C*), 129.0 (Ar, *C*H), 128.7, (Ar, *C*H) 128.1 (Ar, *C*H), 127.6 (Ar, *C*H), 49.1 (*C*H_2), 48.9 (*C*H_2); HRMS (ES+) calculated for $C_{30}H_{28}N_4O_2Na$ $[M+Na]^+$ 499.2110, found 499.2095.

Data were in agreement with those previously reported.[76]

N,*N*,*N*',*N*'-tetrakis(2,2-diphenylethyl)-1,2-azodicarboxamide [2]rotaxane (41)[76]

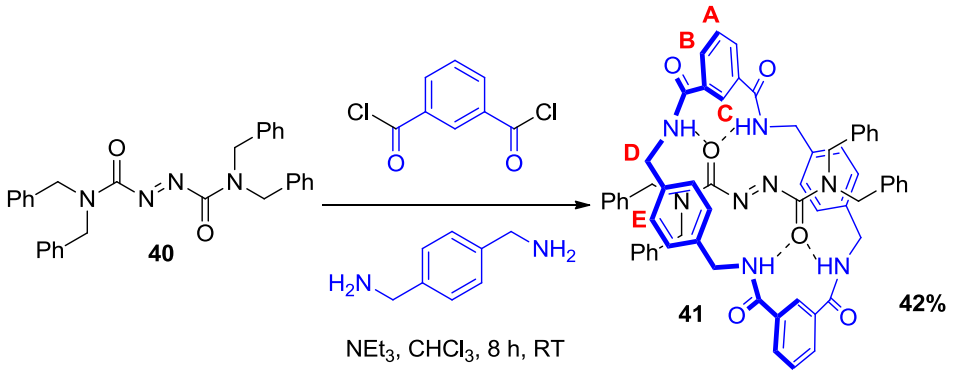

Et_3N (3.4 mL, 24.0 mmol, 24.0 eq.) was added to a stirred solution of *N*,*N*,*N*',*N*'-tetrakis(2,2-diphenylethyl)-1,2-azodicarboxamide (**40**) (476 mg, 1.0 mmol, 1.0 eq.) in anhydrous $CHCl_3$ (400 mL). The solution was stirred vigorously whilst solutions of *p*-xylylene diamine (1.6 g, 12.0 mmol, 12.0 eq.) in anhydrous $CHCl_3$ (63 mL) and isophthaloyl dichloride (2.4 g, 12.0 mmol, 12.0 eq.) in anhydrous $CHCl_3$ (63 mL) were simultaneously added over a period of 4 h using a motor-driven syringe pump. After a further 4 h period the resulting suspension was filtered through a Celite® pad and the solvent removed under reduced pressure. The crude product was purified by column chromatography with $CHCl_3$ / MeOH (96 / 4) as eluent to afford the title product (**41**) as an orange solid (430 mg, 42%). m.p. 198 °C [lit. 198 - 199 °C][76]; ^{1}H NMR (300 MHz, $CDCl_3$) δ 8.11 (dd, *J* = 7.7, 1.5 Hz, 4H, Ar, C*H*, H_B), 8.07 (br s, 2H, Ar, C*H*, H_C), 7.49 – 7.30 (m, 12H, 6 Ar, C*H*, 2 Ar, C*H*, H_A, 4 N*H*), 7.20 – 7.11 (m, 6H, Ar, C*H*), 7.01 – 6.92 (m, 4H, Ar, C*H*), 6.84 – 6.81 (m, 4H, Ar, C*H*), 6.69 (s, 8H, Ar, C*H*, H_E), 5.01 (br s, 4H, CH_2, H_D), 4.60 (s, 4H, CH_2), 4.47 (s, 4H, CH_2), 3.62 (br s, 4H, CH_2, H_D); ^{13}C NMR (100 MHz, $CDCl_3$) δ 165.5 (*C*ON), 158.8 (*C*ON), 137.6 (Ar, *C*), 134.6 (Ar, *C*), 133.7 (Ar, *C*), 133.2 (Ar,

*C*H), 132.2 (Ar, *C*H), 130.3 (Ar, *C*H), 129.3 (Ar, *C*H), 129.1 (Ar, *C*H), 128.7 (Ar, *C*H), 128.5 (Ar, *C*H), 126.9 (Ar, *C*H), 121.9 (Ar, *C*H), 51.1 (*C*H_2), 50.9 (*C*H_2), 43.6 (*C*H_2); HRMS (ES+) calculated for $C_{62}H_{56}N_8O_6Na$ $[M+Na]^+$ 1031.4221, found 1031.4229.

Data were in agreement with those previously reported.[76]

Phenyl *N*,*N*-dibenzylaminocarbonylhydrazinecarboxylate (44)[76]

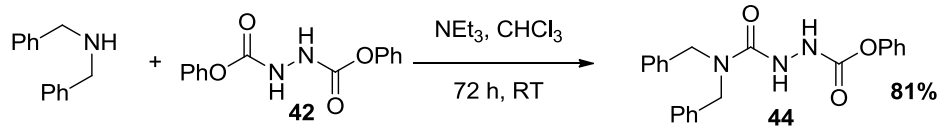

Dibenzylamine (1.8 mL, 9.2 mmol, 1.0 eq.) followed by NEt_3 (1.5 mL, 11.0 mmol, 1.2 eq.) were added to a solution of diphenylhydrazo-1,2-dicarboxylate (**42**) (5.0 g, 18.4 mmol, 2.0 eq.) in $CHCl_3$ (250 mL). The reaction mixture was stirred for 72 h at RT after which the reaction was concentrated under reduced pressure and purified by column chromatography with $CHCl_3$ / MeOH (97 / 3) as eluent to afford phenyl *N*,*N*-dibenzylaminocarbonylhydrazinecarboxylate (**44**) as a white solid (2.78 g, 81%). m.p. 100 °C [lit. 103 - 105 °C][76]; ^{1}H NMR (300 MHz, $CDCl_3$) δ 7.35 - 7.28 (m, 10H, Ar, C*H*), 7.19 - 7.15 (m, 5H, Ar, C*H*), 4.54 (br s, 4 H, CH_2); ^{13}C NMR (100 MHz, $CDCl_3$ / MeOD) δ 158.4 (*C*OO), 155.8 (*C*ON), 151.4 (Ar, *C*), 137.6 (Ar, *C*), 129.5 (Ar, *C*H), 128.3 (Ar, *C*H), 126.4 (Ar, *C*H), 122.4 (Ar, *C*H), 116.0 (Ar, *C*H), 50.0 (*C*H_2); HRMS (ES+) calculated for $C_{22}H_{21}N_3O_3Na$ $[M+Na]^+$ 398.1481, found 398.1470.

Data were in agreement with those previously reported.[76]

N^1,$N^{1'}$-(propane-1,3-diyl)bis(N^2,N^2-dibenzylhydrazine-1,2-dicarboxamide) (47)

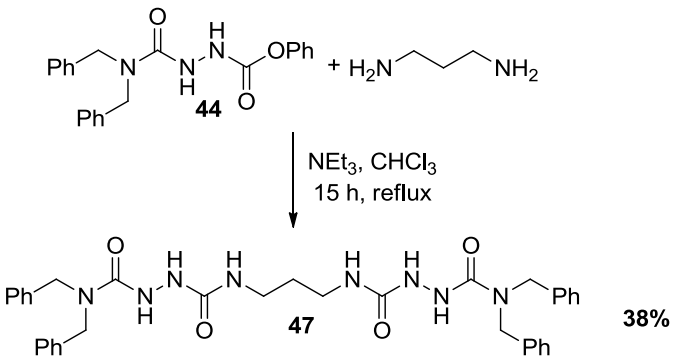

Phenyl *N*,*N*-dibenzylaminocarbonylhydrazinecarboxylate (**44**) (334 mg, 0.9 mmol, 2.0 eq.) and NEt_3 (0.4 mL, 2.9 mmol, 6.4 eq.) were added to a stirred solution of 1,3-diaminopropane (0.04 mL, 0.5 mmol, 1.0 eq.) in $CHCl_3$ (25 mL). The reaction mixture was heated at reflux for 15 h. The reaction mixture was cooled, concentrated under reduced pressure and the crude product purified by column chromatography on silica gel using a DCM / MeOH (95 / 5) mixture as eluent to give the title product as a white solid (108 mg, 38%). m.p. 125 °C; FTIR (film) ν_{max} 3267, 2974, 1638, 1528, 1494, 1242, 1080, 968, 889, 744, 669; ^{1}H NMR (300 MHz, $CDCl_3$) δ 7.43 – 7.25 (m, 20H, Ar, C*H*), 6.43 (s, 2H, N*H*), 5.80 (s, 2H, N*H*), 4.56 (s, 8H, CH_2), 3.44 – 3.42 (m, 4H, CH_2NH), 1.86 – 1.83 (m, 2H, CH_2); ^{13}C NMR (100 MHz, $CDCl_3$) δ 160.3 (*C*ON), 160.0 (*C*ON), 136.9 (Ar, *C*), 128.9 (Ar, *C*H), 127.7 (Ar, *C*H), 127.6 (Ar, *C*H), 50.1 (*C*H_2), 38.8 (*C*H_2NH), 28.7 (*C*H_2); HRMS (ES+) calculated for $C_{35}H_{40}N_8O_4Na$ $[M+Na]^+$ 659.3070, found 659.3066.

(1*E*,1'*E*)-*N*^{1},*N*$^{1'}$-(propane-1,3-diyl)bis(*N*^{2},*N*^{2}-dibenzyldiazene-1,2-dicarboxamide) (48)

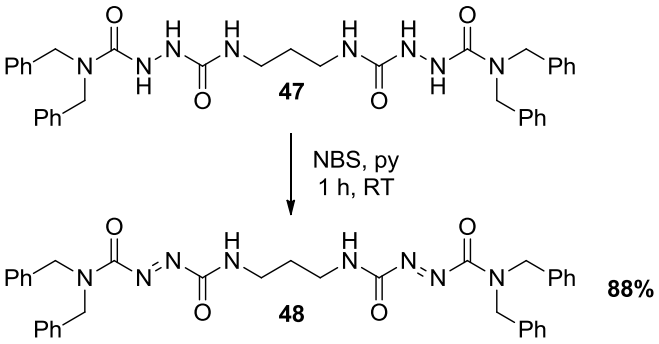

Pyridine (0.2 mL, 2.1 mmol, 2.2 eq.) and NBS (338 mg, 1.9 mmol, 2.0 eq.) were added to a solution of *N*^{1},*N*$^{1'}$-(propane-1,3-diyl)bis(*N*^{2},*N*^{2}-dibenzylhydrazine-1,2-dicarboxamide) (**47**) (607 mg, 1.0 mmol, 1.0 eq.) in dry DCM (30 mL). The resulting solution was stirred for 1 h at RT. The reaction was diluted with DCM (15 mL) and sequentially washed with water (2 x 30 mL), a saturated aqueous solution of $Na_2S_2O_3$ (30 mL) and a saturated aqueous solution of $NaHCO_3$ (2 x 30 mL). The organic phase was dried over anhydrous $MgSO_4$, concentrated under reduced pressure and purified by column chromatography with DCM / MeOH (95 / 5) as eluent to afford the title product (**48**) as a yellow oil (530 mg, 88%). FTIR (film) ν_{max} 3280, 3031, 2938, 1689, 1524, 1495, 1426, 1362, 1217, 1154, 1080, 1028, 749, 696; ^{1}H NMR (300 MHz, $CDCl_3$) δ 7.45 – 7.12 (m, 20H, Ar, C*H*), 4.64 (s, 4H, CH_2), 4.50 (s, 4H, CH_2), 3.53 – 3.47 (m, 4H, CH_2NH), 1.97 – 1.73 (m, 2H, CH_2); ^{13}C NMR (100 MHz, $CDCl_3$) δ 162.2 (*C*ON), 160.4 (*C*ON), 135.4 (Ar, *C*), 129.0 (Ar, *C*H), 128.5 (Ar, *C*H), 128.2 (Ar, *C*H), 127.8 (Ar, *C*H), 49.3 (*C*H_2), 49.2

(CH_2), 37.8 (CH_2NH), 28.9 (CH_2); HRMS (ES+) calculated for $C_{35}H_{36}N_8O_4Na$ $[M+Na]^+$ 655.2757, found 655.2754.

(1*E*,1'*E*)-N^1,$N^{1'}$-(propane-1,3-diyl)bis(N^2,N^2-dibenzyldiazene-1,2-dicarboxamide) [2]rotaxane (49) and (50)

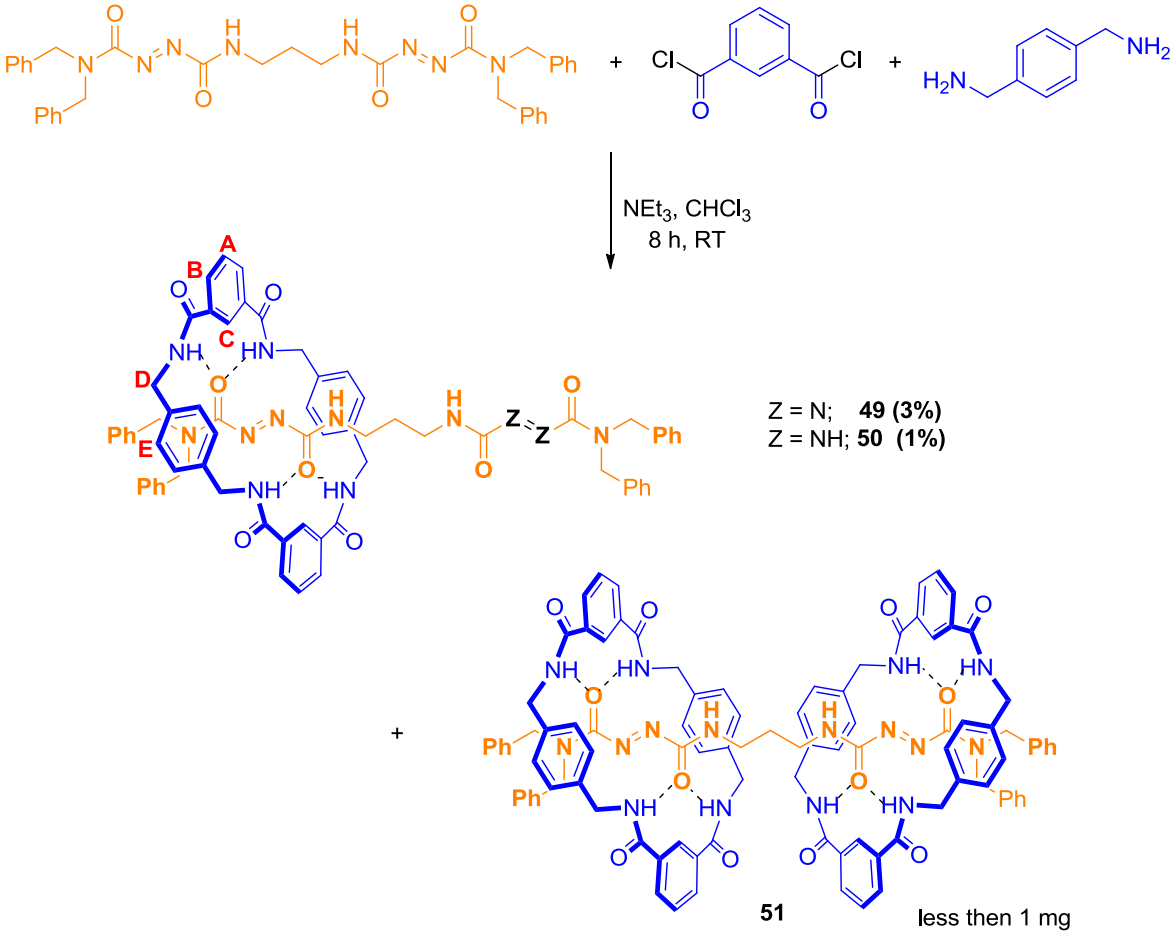

Et_3N (5.0 mL, 35.3 mmol, 48.0 eq.) was added to a stirred solution of (1*E*,1'*E*)-N^1,$N^{1'}$-(propane-1,3-diyl)bis(N^2,N^2-dibenzyldiazene-1,2-dicarboxamide) (**48**) (461 mg, 0.73 mmol, 1.0 eq.) in anhydrous $CHCl_3$ (800 mL). The solution was

stirred vigorously whilst solutions of *p*-xylylene diamine (2.4 g, 17.6 mmol, 24.0 eq.) in anhydrous $CHCl_3$ (126 mL) and isophthaloyl dichloride (3.6 g, 17.6 mmol, 24.0 eq.) in anhydrous $CHCl_3$ (126 mL) were simultaneously added over a period of 4 h using motor-driven syringe pump. After a further 4 h period the resulting suspension was filtered through a Celite® pad and the solvent removed under reduced pressure. The crude product was purified by HPLC to afford the azo [2]rotaxane (**49**) as a white solid (25 mg, 3%), the hydrazo [2]rotaxane (**50**) as a yellow solid (8 mg, 1%) and the azo [3]rotaxane (**51**) as a white solid (0.7 mg). HPLC (t = 0 → 60 min, 75 : 25 MeOH : H_2O): Data for compound **49**: R_t 24.31; m.p. 127 °C; FTIR (film) ν_{max} 3286, 3063, 2926, 1637, 1530, 1453, 1356, 1299, 1080, 965, 818, 729, 697; ^{1}H NMR (300 MHz, MeOD) δ 8.20 (br s, 2H, Ar, C*H*, H_C), 8.13 (s, 4H, N*H*), 7.93 (dd, *J* = 7.8, 1.6 Hz, 4H, Ar, C*H*, H_B), 7.50 – 7.41 (m, 2H, Ar, C*H*, H_A), 7.35 – 7.10 (m, 20H, Ar, C*H*), 6.98 (s, 8H, Ar, C*H*, H_E), 4.57 – 4.27 (m, 16 H, 8 CH_2, H_D, 8 CH_2), 3.75 - 3.68 (m, 4H, CH_2), 2.01 – 1.91 (m, 2H, CH_2); ^{13}C NMR (100 MHz, MeOD) δ 169.6 (*C*ON), 168.8 (*C*ON), 140.2 (Ar, *C*), 138.5 (Ar, *C*), 136.9 (Ar, *C*), 136.4 (Ar, *C*), 135.3 (Ar, *C*), 132.1 (Ar, *C*H), 129.8 (Ar, *C*H), 129.6 (Ar, *C*H), 128.6 (Ar, *C*H), 48.8 (*C*H_2), 44.9 (*C*H_2), 23.9 (*C*H_2); LRMS (ES+) 1187.6 ([M+Na]$^+$, 100%). Data for compound **50**: R_t 21.23; m.p. 132 °C; FTIR (film) ν_{max} 3286, 3063, 2926, 1637, 1530, 1453, 1356, 1299, 1080, 965, 818, 729, 697; ^{1}H NMR (300 MHz, MeOD) δ 8.25 (s, 2H, Ar, C*H*, H_C), 8.19 – 8.15 (m, 2H, N*H*), 7.96 (dd, *J* = 7.8, 1.6 Hz, 4H, Ar, C*H*, H_B), 7.48 (t, *J* = 7.8 Hz, 2H, Ar, C*H*, H_A), 7.35 – 7.10 (m, 16H, Ar, C*H*), 7.07 – 7.04 (m, 2H, Ar, C*H*), 7.01 (s, 8H, Ar, C*H*, H_E), 6.86 – 6.83 (m, 2H, Ar, C*H*), 4.67 – 4.18 (m, 16H, 8 CH_2, H_D, 8 CH_2),

3.35 – 3.32 (m, 4H, CH_2), 1.78 – 1.74 (m, 2H, CH_2); ^{13}C NMR (100 MHz, MeOD) δ 168.6 (*C*ON), 168.3 (*C*ON), 137.7 (Ar, *C*), 136.2 (Ar, *C*), 135.6 (Ar, *C*), 134.6, 131.9 (Ar, *C*H), 131.7 (Ar, *C*H), 130.8 (Ar, *C*H), 130.0 (Ar, *C*H), 129.9 (Ar, *C*H), 129.7 (Ar, *C*H), 129.5 (Ar, *C*H), 129.2 (Ar, *C*H), 128.9 (Ar, *C*H), 128.4 (Ar, *C*H), 128.1 (Ar, *C*H), 125.8 (Ar, *C*H), 44.5 (*C*H_2), 41.4 (*C*H_2), 27.0 (*C*H_2); HRMS (ES+) calculated for $C_{67}H_{66}N_{12}O_8Na$ $[M+Na]^+$ 1189.5024, found 1189,4998. Data for compound **51**: R_t 32.49; m.p. 144 °C; FTIR (film) ν_{max} 3315, 2925, 1616, 1529, 1476, 1454, 1421, 1359, 1304, 1188, 1081, 957, 900, 819, 724, 707, 694; LRMS (ES+) 1720.4 ($[M+Na]^+$, 100%).

N^1,*N*$^{1'}$-(butane-1,4-diyl)bis(*N*^{2},*N*^{2}-dibenzylhydrazine-1,2-dicarboxamide) (52)

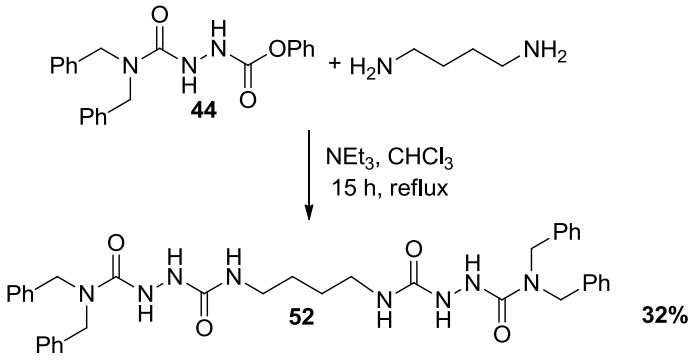

Phenyl *N*,*N*-dibenzylaminocarbonylhydrazinecarboxylate (**44**) (750 mg, 2.0 mmol, 2.0 eq.) and NEt_3 (0.9 mL, 6.4 mmol, 6.4 eq.) were added to a stirred solution of 1,4-diaminobutane (0.1 mL, 1.0 mmol, 1.0 eq.) in $CHCl_3$ (50 mL). The reaction mixture was heated at reflux for 15 h. The reaction mixture was then concentrated under reduced pressure and purified by column chromatography on silica gel

using a DCM / MeOH (96 / 4) mixture as eluent to give the title product as a white solid (210 mg, 32%). m.p. 121 °C; FTIR (film) ν_{max} 3272, 2937, 1673, 1634, 1530, 1495, 1251, 1080, 967, 885, 756, 730, 696; ^{1}H NMR (300 MHz, MeOD / $CDCl_3$) δ 7.44 – 7.03 (m, 20H, Ar, C*H*), 4.48 (s, 8H, CH_2), 3.10 – 3.09 (m, 4H, CH_2NH), 1.42 – 1.41 (m, 4H, CH_2); ^{13}C NMR (75 MHz, MeOD / $CDCl_3$) δ 161.3 (*C*ON), 160.2 (*C*ON), 137.9 (Ar, *C*), 129.4 (Ar, *C*H), 128.3 (Ar, *C*H), 128.1 (Ar, *C*H), 50.4 (*C*H_2), 40.2 (*C*H_2NH), 27.8 (*C*H_2); HRMS (ES+) calculated for $C_{36}H_{42}N_8O_4Na$ $[M+Na]^+$ 673.3227, found 673.3223.

(1*E*,1'*E*)-*N*^{1},*N*$^{1'}$-(butane-1,4-diyl)bis(*N*^{2},*N*^{2}-dibenzyldiazene-1,2-dicarboxamide) (53)

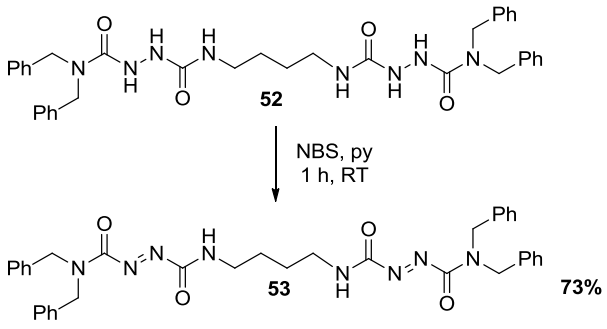

Pyridine (0.1 mL, 1.1 mmol, 2.2 eq.) and NBS (178 mg, 1.0 mmol, 2.0 eq.) were added to a solution of *N*^{1},*N*$^{1'}$-(butane-1,4-diyl)bis(*N*^{2},*N*^{2}-dibenzylhydrazine-1,2-dicarboxamide) (**52**) (330 mg, 0.5 mmol, 1.0 eq.) in dry DCM (10 mL). The resulting solution was stirred for 1 h at RT. The reaction was then diluted with DCM (5 mL) and sequentially washed with water (2 x 10 mL), a saturated aqueous solution of $Na_2S_2O_3$ (10 mL) and a saturated aqueous solution of $NaHCO_3$ (2 x 10

mL). The organic phase was dried over anhydrous $MgSO_4$, concentrated under reduced pressure and purified by column chromatography with DCM / MeOH (95 / 5) as eluent to afford the title product (**53**) as a yellow oil (237 mg, 73%). FTIR (film) ν_{max} 3281, 3031, 2936, 1686, 1524, 1495, 1425, 1361, 1219, 1157, 1081, 1029, 732, 696; ^{1}H NMR (400 MHz, $CDCl_3$) δ 7.42 – 7.10 (m, 20H, Ar, C*H*), 4.63 (s, 4H, CH_2), 4.49 (s, 4H, CH_2), 3.45 – 3.46 (m, 4H, CH_2NH), 1.69 – 1.68 (m, 4H, CH_2); ^{13}C NMR (100 MHz, $CDCl_3$) δ 162.3 (*C*ON), 160.2 (*C*ON), 135.2 (Ar, *C*), 128.9 (Ar, *C*H), 128.4 (Ar, *C*H), 128.2 (Ar, *C*H), 128.1 (Ar, *C*H), 127.8 (Ar, *C*H), 49.2 (*C*H_2), 49.1 (*C*H_2), 40.5 (*C*H_2NH), 26.4 (*C*H_2); HRMS (ES+) calculated for $C_{36}H_{38}N_8O_4Na$ $[M+Na]^+$ 669.2914, found 669.2930.

(1*E*,1'*E*)-N^1,$N^{1'}$-(propane-1,3-diyl)bis(N^2,N^2-dibenzyldiazene-1,2-dicarboxamide) [2]rotaxane (54) and (55)

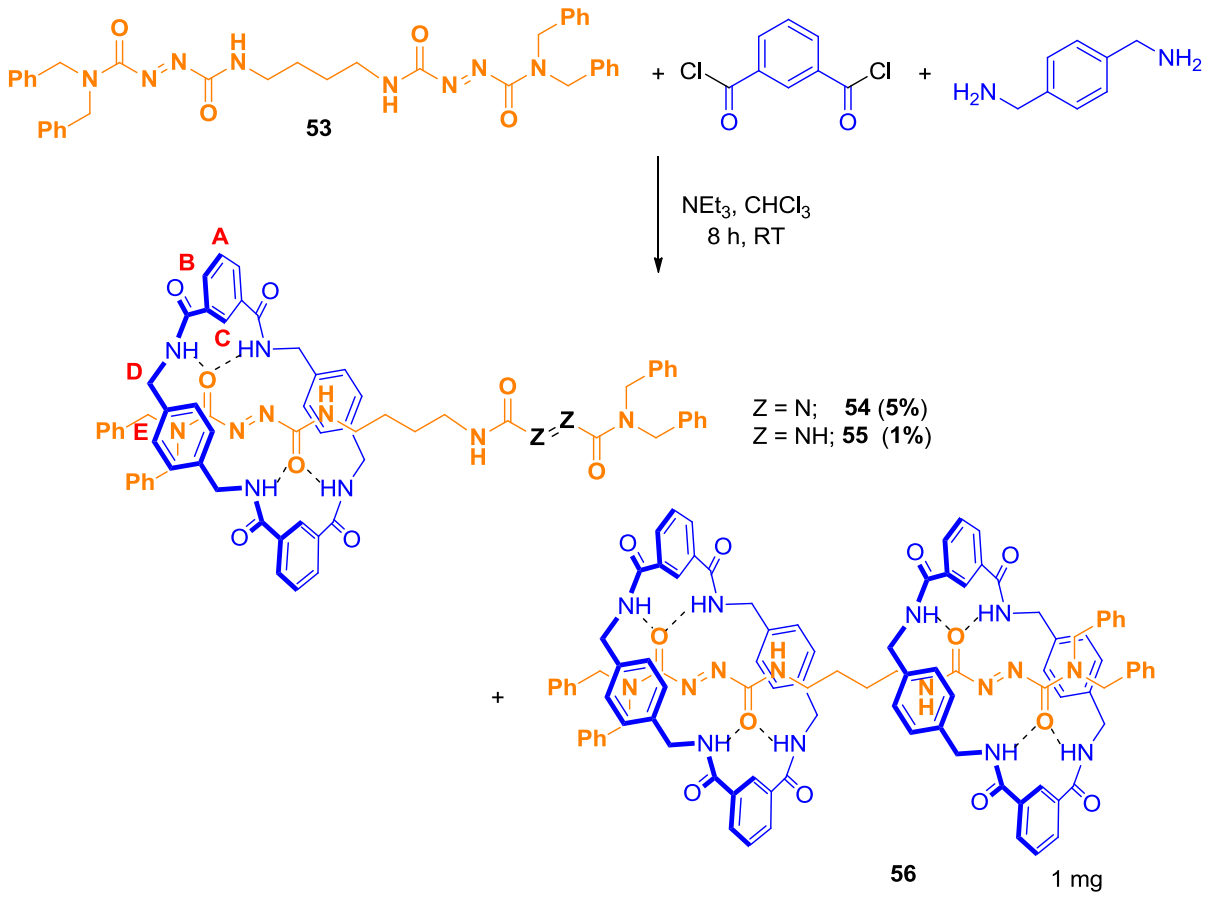

Et_3N (5.0 mL, 35.3 mmol, 48.0 eq.) was added to a stirred solution of (1*E*,1'*E*)-N^1,$N^{1'}$-(butane-1,4-diyl)bis(N^2,N^2-dibenzyldiazene-1,2-dicarboxamide) (**53**) (472 mg, 0.73 mmol, 1.0 eq.) in anhydrous $CHCl_3$ (800 mL). The solution was stirred vigorously whilst solutions of *p*-xylylene diamine (2.4 g, 17.6 mmol, 24.0 eq.) in anhydrous $CHCl_3$ (126 mL) and isophthaloyl dichloride (3.6 g, 17.6 mmol, 24.0 eq.) in anhydrous $CHCl_3$ (126 mL) were simultaneously added over a period of 4 h using a motor-driven syringe pump. After a further 4 h period

the resulting suspension was filtered through a Celite® pad and the solvent removed under reduced pressure. The crude product was purified by HPLC to afford the azo [2]rotaxane (**54**) as a white solid (43 mg, 5%), the hydrazo [2]rotaxane (**55**) as a yellow solid (9 mg, 1%) and the azo [3]rotaxane (**56**) as a white solid (1 mg). HPLC (t = 0 → 60 min, 75 : 25 MeOH : H_2O): Data for compound **54**: R_t 27.30; m.p. 158 °C; FTIR (film) ν_{max} 3307, 3043, 2939, 1693, 1640, 1525, 1453, 1422, 1359, 1273, 1222, 1081, 1029, 759, 726, 694; ^{1}H NMR (500 MHz, MeOD) δ 8.21 (s, 2H, Ar, C*H*, H_C), 7.95 (dd, *J* = 7.8, 1.6 Hz, 4H, Ar, C*H*, H_B), 7.47 (t, *J* = 7.8 Hz, 2H, Ar, C*H*, H_A), 7.31 - 7.29 (m, 6H, Ar, C*H*), 7.21 - 7.19 (m, 6H, Ar, C*H*), 7.15 - 7.14 (m, 4H, Ar, C*H*), 7.00 – 6.94 (m, 12H, 4 Ar, C*H*, 8 Ar, C*H*, H_E), 4.41 (s, 4H, CH_2), 4.38 (s, 8H, CH_2, H_D), 4.33 (s, 4H, CH_2), 3.42 - 3.39 (m, 4H, CH_2), 1.74 - 1.71 (m, 4H, CH_2); ^{13}C NMR (100 MHz, MeOD) δ 168.6 (*C*ON), 160.4 (*C*ON), 137.7 (Ar, *C*), 136.2 (Ar, *C*), 135.6 (Ar, *C*), 134.7 (Ar, *C*H), 134.6 (Ar, *C*), 131.7 (Ar, *C*H), 130.0 (Ar, *C*H), 129.7 (Ar, *C*H), 129.5 (Ar, *C*H), 129.2 (Ar, *C*H), 129.1 (Ar, *C*H), 128.9 (Ar, *C*H), 128.4 (Ar, *C*H), 128.1 (Ar, *C*H), 44.5 (*C*H_2), 41.4 (*C*H_2), 27.0 (*C*H_2); HRMS (ES+) calculated for $C_{68}H_{66}N_{12}O_8Na$ $[M+Na]^+$ 1201.5024, found 1201.5077. Data for compound **55**: R_t 23.78; m.p. 146 °C; FTIR (film) ν_{max} 3299, 1639, 1525, 1359, 1262, 1082, 697; ^{1}H NMR (300 MHz, MeOD) δ 8.26 (s, 2H, Ar, C*H*, H_C), 7.99 (dd, *J* = 7.7, 1.7 Hz, 4H, Ar, C*H*, H_B), 7.51 (t, *J* = 7.7 Hz, 2H, Ar, C*H*, H_A), 7.35 – 7.12 (m, 16H, Ar, C*H*), 7.10 – 7.06 (m, 2H, Ar, C*H*), 7.00 (s, 8H, Ar, C*H*, H_E), 6.92 – 6.85 (m, 2H, Ar, C*H*), 4.58 - 4.53 (m, 4H, CH_2), 4.44 - 4.41 (m, 6H, CH_2, H_D), 4.32 – 4.23 (m, 6H, 2 CH_2, H_D, 4 CH_2), 3.43 – 3.38 (m, 2H, CH_2), 3.21 - 3,16 (m, 2H, CH_2), 1.73 – 1.61 (m, 2H, CH_2), 1.56 - 1.48

(m, 2H, C*H*$_2$); ^{13}C NMR (100 MHz, MeOD) δ 168.5 (*C*ON), 138.4 (Ar, *C*), 135.2 (Ar, *C*), 132.2 (Ar, *C*H), 130.3 (Ar, *C*H), 130.1 (Ar, *C*H), 129.8 (Ar, *C*H), 129.7 (Ar, *C*H), 128.6 (Ar, *C*H), 128.3 (Ar, *C*H), 126.1 (Ar, *C*H), 50.5 (*C*H$_2$), 44.9 (*C*H$_2$), 29.1 (*C*H$_2$); HRMS (ES+) calculated for $C_{68}H_{68}N_{12}O_8Na$ $[M+Na]^+$ 1203.5181, found 1203.5150. Data for compound **56**: m.p. 108 °C; FTIR (film) ν_{max} 3310, 2926, 1645, 1530, 1421, 1359, 1297, 1267, 1082, 1021, 820, 700; LRMS (ES+) 1735.7 ($[M+Na]^+$, 100%).

N^1,*N*$^{1'}$-(pentane-1,5-diyl)bis(*N*^{2},*N*^{2}-dibenzylhydrazine-1,2-dicarboxamide) (57)

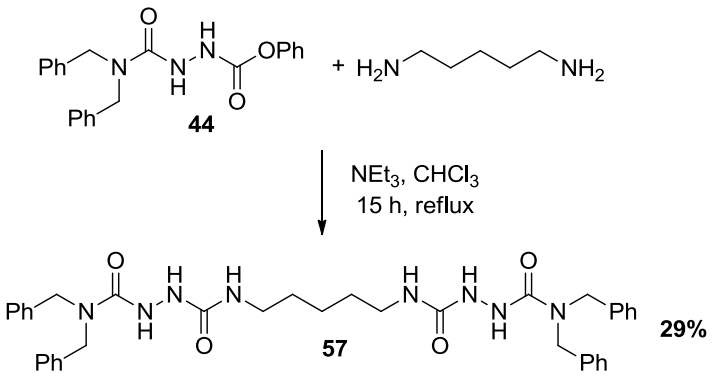

Phenyl *N*,*N*-dibenzylaminocarbonylhydrazinecarboxylate (**44**) (334 mg, 0.9 mmol, 2.0 eq.) and NEt_3 (0.4 mL, 2.9 mmol, 6.4 eq.) were added to a stirred solution of cadaverine (0.05 mL, 0.45 mmol, 1.0 eq.) in $CHCl_3$ (25 mL). The reaction mixture was heated at reflux for 15 h. The reaction mixture was cooled, concentrated under reduced pressure and the crude product purified by column chromatography on silica gel using a DCM / MeOH (98 / 2) mixture as eluent to give the title product as a yellow oil (87 mg, 29%). FTIR (film) ν_{max} 3267, 2929, 1632, 1535,

1495, 1453, 1407, 1240, 1081, 1029, 970, 888, 733, 697; ^{1}H NMR (300 MHz, $CDCl_3$) δ 7.30 – 7.17 (m, 20H, Ar, C*H*), 4.44 (s, 8H, CH_2), 3.05 – 3.03 (m, 4H, CH_2NH), 1.25 – 1.12 (m, 6H, CH_2CH_2CH_2); ^{13}C NMR (100 MHz, $CDCl_3$) δ 160.1 (*C*ON), 159.6 (*C*ON), 137.0 (Ar, *C*), 128.8 (Ar, *C*H), 127.5 (Ar, *C*H), 50.0 (*C*H_2), 39.4 (*C*H_2), 28.9 (*C*H_2), 23.1 (*C*H_2); HRMS (ES+) calculated for $C_{37}H_{44}N_8O_4Na$ $[M+Na]^+$ 687.3383, found 687.3364.

(1*E*,1'*E*)-N^1,$N^{1'}$-(pentane-1,5-diyl)bis(N^2,N^2-dibenzyldiazene-1,2-dicarboxamide) (58)

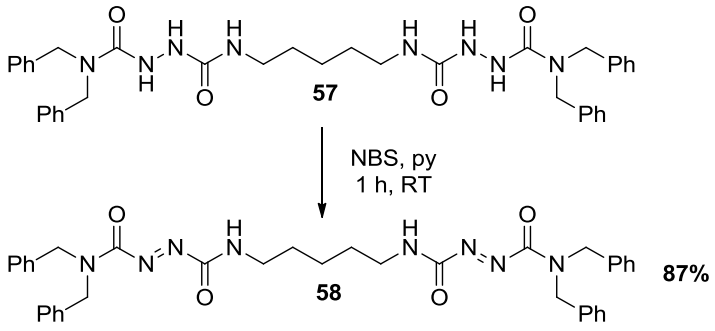

Pyridine (26 μL, 0.3 mmol, 2.2 eq.) and NBS (54 mg, 0.3 mmol, 2.0 eq.) were added to a solution of N^1,$N^{1'}$-(pentane-1,5-diyl)bis(N^2,N^2-dibenzylhydrazine-1,2-dicarboxamide) (**57**) (101 mg, 0.15 mmol, 1.0 eq.) in dry DCM (2 mL). The resulting solution was stirred for 1 h at RT. It was then diluted with DCM (1 mL) and sequentially washed with water (2 x 3 mL), a saturated aqueous solution of $Na_2S_2O_3$ (3 mL) and saturated aqueous solution of $NaHCO_3$ (2 x 3 mL). The organic phase was dried over anhydrous $MgSO_4$, concentrated under reduced pressure and purified by column chromatography with DCM / MeOH (98 / 2) as

eluent to give the title product (**58**) as a yellow oil (86 mg, 87%). FTIR (film) ν_{max} 3281, 3031, 2936, 1686, 1524, 1495, 1425, 1361, 1219, 1157, 1081, 1029, 732, 696; ^{1}H NMR (300 MHz, $CDCl_3$) δ 7.45 – 7.04 (m, 20H, Ar, C*H*), 4.64 (s, 4H, CH_2), 4.49 (s, 4H, CH_2), 3.46 – 3.40 (m, 4H, CH_2NH), 1.73 – 1.63 (m, 4H, CH_2CH$_2$CH_2), 1.53 – 1.39 (m, 2H, CH$_2$CH_2CH$_2$); ^{13}C NMR (100 MHz, $CDCl_3$) δ 162.5 (*C*ON), 160.0 (*C*ON), 135.4 (Ar, *C*), 129.0 (Ar, *C*H), 128.6 (Ar, *C*H), 128.3 (Ar, *C*H), 128.2 (Ar, *C*H), 127.8 (Ar, *C*H), 49.2 (*C*H$_2$), 49.1 (*C*H$_2$), 40.9 (*C*H$_2$NH), 28.9 (*C*H$_2$), 24.0 (*C*H$_2$); HRMS (ES+) calculated for $C_{37}H_{40}N_8O_4Na$ $[M+Na]^+$ 683.3070, found 683.3078.

(1*E*,1'*E*)-N^1,$N^{1'}$-(pentane-1,5-diyl)bis(N^2,N^2-dibenzyldiazene-1,2-dicarboxamide) [2]rotaxanes (59) and (60) and [3]rotaxane (61)

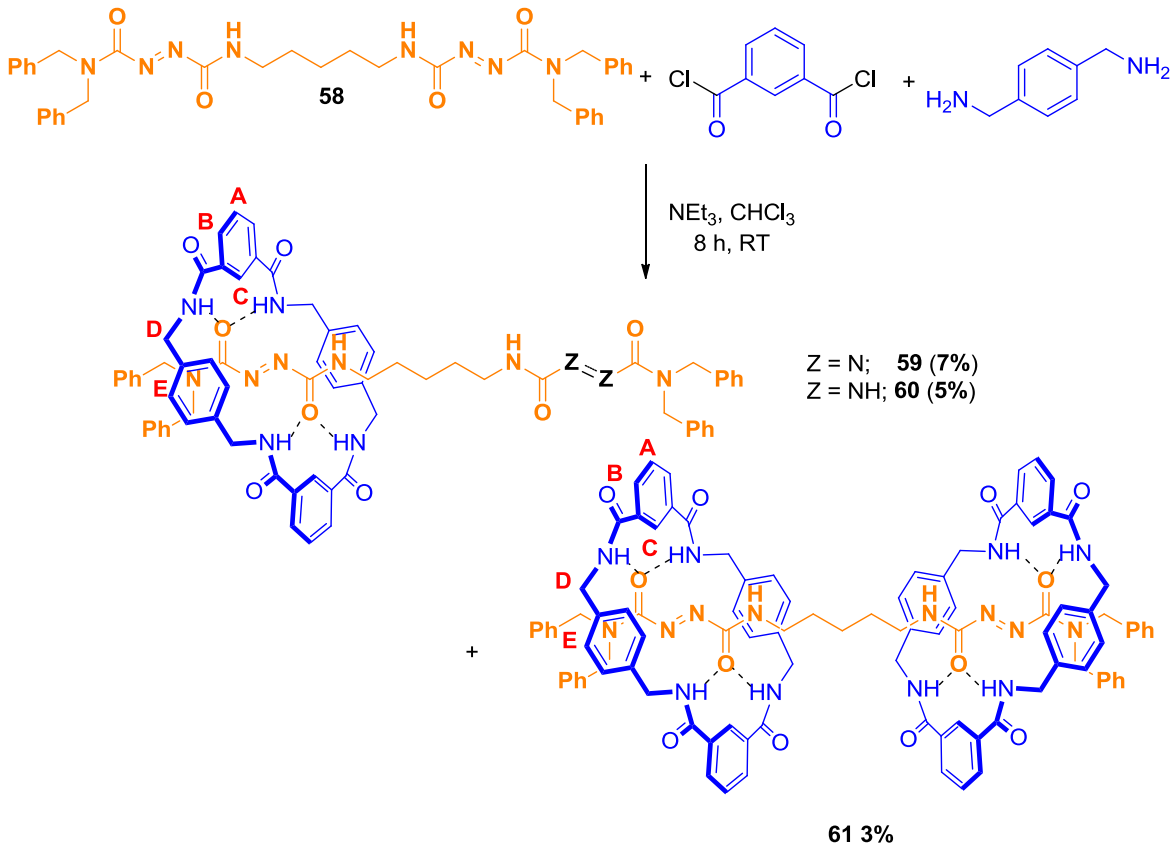

Et_3N (5.0 mL, 35.3 mmol, 48.0 eq.) was added to a stirred solution of (1*E*,1'*E*)-N^1,$N^{1'}$-(pentane-1,5-diyl)bis(N^2,N^2-dibenzyldiazene-1,2-dicarboxamide) (**58**) (482 mg, 0.73 mmol, 1.0 eq.) in anhydrous $CHCl_3$ (800 mL). The solution was stirred vigorously whilst solutions of *p*-xylylene diamine (2.4 g, 17.6 mmol, 24.0 eq.) in anhydrous $CHCl_3$ (126 mL) and isophthaloyl dichloride (3.6 g, 17.6 mmol, 24.0 eq.) in anhydrous $CHCl_3$ (126 mL) were simultaneously added over a period of 4 h using a motor-driven syringe pump. After a further 4 h period the resulting suspension was filtered through a Celite® pad and the solvent

removed under reduced pressure. The crude product was purified by HPLC to afford the azo [2]rotaxane (**59**) as a white solid (58 mg, 7%), the hydrazo [2]rotaxane (**60**) as a yellow solid (44 mg, 5%) and the azo [3]rotaxane (**61**) as a white solid (34 mg, 3%). HPLC (t = 0 → 60 min, 75 : 25 MeOH : H_2O): Data for compound **59**: R_t 20.47; m.p. 135 °C; FTIR (film) ν_{max} 3286, 3063, 2926, 1637, 1530, 1453, 1356, 1299, 1080, 965, 818, 729, 697; ^{1}H NMR (400 MHz, MeOD) δ 8.22 (br s, 2H, Ar, C*H*, H_C), 7.98 - 7.96 (m, 4H, Ar, C*H*, H_B), 7.49 (t, *J* = 7.8 Hz, 2H, Ar, C*H*, H_A), 7.31 - 7.29 (m, 6H, Ar, C*H*), 7.23 - 7.21 (m, 6H, Ar, C*H*), 7.18 - 7.17 (m, 4H, Ar, C*H*), 7.01 - 7.00 (m, 4H, Ar, C*H*), 6.99 (s, 8H, Ar, C*H*, H_E), 4.45 - 4.39 (m, 4H, CH_2), 4.40 - 4.39 (m, 12H, 8 CH_2, H_D, 4 CH_2), 3.35 - 3.31 (m, 4H, CH_2), 1.67 - 1.64 (m, 4H, CH_2), 1.44 - 1.41 (m, 2H, CH_2); ^{13}C NMR (100 MHz, MeOD) δ 168.5 (*C*ON), 162.4 (*C*ON), 161.6 (*C*ONH), 138.5 (Ar, *C*), 136.9 (Ar, *C*), 136.4 (Ar, *C*), 135.2 (Ar, *C*), 132.2 (Ar, *C*H), 130.1 (Ar, *C*H), 129.9 (Ar, *C*H), 129.8 (Ar, *C*H), 129.7 (Ar, *C*H), 129.2 (Ar, *C*H), 129.1 (Ar, *C*H), 128.6 (Ar, *C*H), 126.1 (Ar, *C*H), 51.0 (*C*H_2), 50.8 (*C*H_2), 44.8 (*C*H_2), 41.9 (*C*H_2), 29.6 (*C*H_2), 25.2 (*C*H_2); HRMS (ES+) calculated for $C_{69}H_{68}N_{12}O_8Na$ $[M+Na]^+$ 1215.5181, found 1215.5200. Data for compound **60**: R_t 17.52; m.p. 142 °C; FTIR (film) ν_{max} 3286, 3063, 2926, 1637, 1530, 1453, 1356, 1299, 1080, 965, 818, 729, 697; ^{1}H NMR (400 MHz, MeOD) δ 8.23 (br s, 2H, Ar, C*H*, H_C), 7.99 - 7.97 (m, 4H, Ar, C*H*, H_B), 7.50 (t, *J* = 7.8 Hz, 2H, Ar, C*H*, H_A), 7.32 - 7.29 (m, 8H, Ar, C*H*), 7.22 - 7.15 (m, 8H, Ar, C*H*), 7.11 - 7.09 (m, 2H, Ar, C*H*), 7.01 (s, 8H, Ar, C*H*, H_E), 6.90 - 6.88 (m, 2H, Ar, C*H*), 4.53 - 4.26 (m, 16H, 8 CH_2, H_D, 8 CH_2), 3.22 - 3.19 (m, 2H, CH_2), 3.05 - 3.02 (m, 2H, CH_2), 1.55 - 1.52 (m, 2H, CH_2), 1.40 - 1.37 (m, 2H, CH_2), 1.31 - 1.29 (m, 2H, CH_2); ^{13}C

NMR (100 MHz, MeOD) δ 168.5 (*C*ON), 161.9 (*C*ONH), 160.9 (*C*ON), 160.6 (*C*ONH), 160.5 (*C*ONH), 138.5 (Ar, *C*), 136.9 (Ar, *C*), 136.2 (Ar, *C*), 135.2 (Ar, *C*), 132.2 (Ar, *C*H), 130.2 (Ar, *C*H), 130.1 (Ar, *C*H), 129.8 (Ar, *C*H), 129.7 (Ar, *C*H), 129.3 (Ar, *C*H), 129.2 (Ar, *C*H), 129.1 (Ar, *C*H), 129.0 (Ar, *C*H), 128.6 (Ar, *C*H), 128.4 (Ar, *C*H), 126.2 (Ar, *C*H), 51.3 (*C*H_2), 51.1 (*C*H_2), 50.5 (*C*H_2), 44.8 (*C*H_2), 42.4 (*C*H_2), 40.4 (*C*H_2), 30.8 (*C*H_2), 29.5 (*C*H_2), 25.1 (*C*H_2); LRMS (ES+) 1233.5 ($[M+K]^+$, 31%), 1217.5 ($[M+Na]^+$, 100%). Data for compound **61**: R_t 40.17; m.p. 168 °C; FTIR (film) ν_{max} 3291, 3062, 2924, 1638, 1607, 1532, 1442, 1429, 1383, 1360, 1294, 1187, 1080, 1034, 974, 950, 818, 753, 732, 698; ^{1}H NMR (400 MHz, MeOD) δ 8.17 (br s, 4H, Ar, C*H*, H_C), 7.94 - 7.92 (m, 8H, Ar, C*H*, H_B), 7.45 (t, *J* = 7.8 Hz, 4H, Ar, C*H*, H_A), 7.28 - 7.27 (m, 6H, Ar, C*H*), 7.14 - 7.13 (m, 6H, Ar, C*H*), 7.05 - 7.04 (m, 4H, Ar, C*H*), 6.98 (s, 16H, Ar, C*H*, H_E), 6.81 - 6.80 (m, 4H, Ar, C*H*), 4.46 - 4.29 (m, 16H, CH_2, H_D), 4.32 - 4.27 (m, 8H, CH_2), 3.25 - 3.22 (m, 4H, CH_2), 1.65 - 1.62 (m, 4H, CH_2), 1.37 - 1.36 (m, 2H, CH_2); ^{13}C NMR (100 MHz, MeOD) δ 168.4 (*C*ON), 160.5 (*C*ON), 160.2 (*C*ONH), 138.3 (Ar, *C*), 136.6 (Ar, *C*), 135.9 (Ar, *C*), 135.1 (Ar, *C*), 132.0 (Ar, *C*H), 130.1 (Ar, *C*H), 130.0 (Ar, *C*H), 129.7 (Ar, *C*H), 129.6 (Ar, *C*H), 129.5 (Ar, *C*H), 129.2 (Ar, *C*H), 128.9 (Ar, *C*H), 128.1 (Ar, *C*H), 126.0 (Ar, *C*H), 51.1 (*C*H_2), 51.0 (*C*H_2), 44.8 (*C*H_2), 42.2 (*C*H_2), 29.5 (*C*H_2), 25.3 (*C*H_2); LRMS (ES+) 1763.8 ($[M+K]^+$, 23%), 1747.8 ($[M+Na]^+$, 100%).

4.4 Experimental for Section 2.4

N^1,*N*^{1},*N*^{6},*N*^{6}-tetrabenzylfumaramide (62)

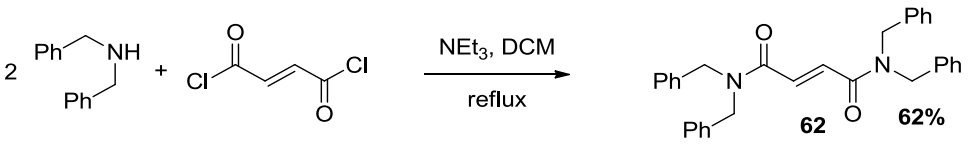

Fumaryl chloride (0.5 mL, 4.6 mmol, 1.0 eq.) was dissolved in dry dichloromethane (20 mL) at RT. A solution of dibenzylamine (1.9 mL, 9.7 mmol, 2.1 eq.) and NEt_3 (1.4 mL, 10.0 mmol, 2.2 eq.) in dry dichloromethane (20 mL) was added using a syringe pump over a period of 1 h at 0 ºC. The reaction was stirred overnight and the solvent was removed *in vacuo*. The crude product was purified by column chromatography with EtOAc / pet (1 / 1) as eluent to afford *N*^{1},*N*^{1},*N*^{6},*N*^{6}-tetrabenzylfumaramide (**62**) as a white solid (1.35 g, 62%). m.p. 98 °C; FTIR (film) ν_{max} 3034, 2923, 1723, 1621, 1493, 1440, 1357, 1315, 1269, 1181, 1080, 950, 750, 695; ^{1}H NMR (300 MHz, $CDCl_3$) δ 7.61 (s, 2H, C*H*), 7.42 – 7.14 (m, 20H, Ar, C*H*), 4.65 (s, 4H, CH_2), 4.59 (s, 4H, CH_2); ^{13}C NMR (100 MHz, $CDCl_3$) δ 166.0 (*C*O), 136.8 (Ar, *C*), 136.1 (Ar, *C*), 132.5 (*C*H), 129.1 (Ar, *C*H), 128.8 (Ar, *C*H), 128.5 (Ar, *C*H), 128.0 (Ar, *C*H), 127.8 (Ar, *C*H), 126.9 (Ar, *C*H), 50.2 (*C*H_2), 48.7 (*C*H_2); HRMS (ES+) calculated for $C_{32}H_{30}N_2O_2Na$ $[M+Na]^+$ 497.2205, found 497.2220.

N^1,N^1,N^6,N^6-tetrabenzylfumaramide [2]rotaxane (63)

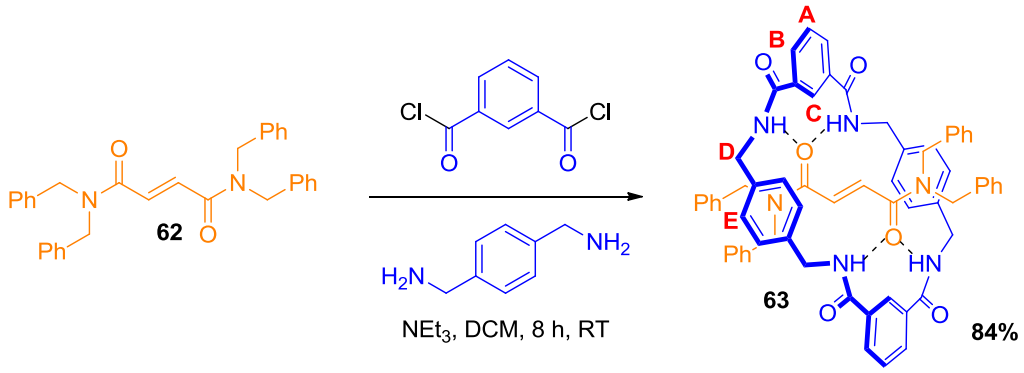

Et_3N (6.7 mL, 48.0 mmol, 24.0 eq.) was added to a stirred solution of N^1,N^1,N^6,N^6-tetrabenzylfumaramide (**62**) (1.3 g, 2.6 mmol, 1.0 eq.) in anhydrous $CHCl_3$ (1000 mL). The solution was stirred vigorously whilst solutions of *p*-xylylene diamine (3.27 g, 24.0 mmol, 12.0 eq.) in anhydrous $CHCl_3$ (95 mL) and isophthaloyl dichloride (4.88 g, 24.0 mmol, 12.0 eq.) in anhydrous $CHCl_3$ (95 mL) were simultaneously added over a period of 4 h using a motor-driven syringe pump. After a further 4 h period the resulting suspension was filtered through a Celite® pad and the solvent removed under reduced pressure. The crude product was purified by column chromatography with $CHCl_3$ / MeOH (96 / 4) as eluent to afford N^1,N^1,N^6,N^6-tetrabenzylfumaramide [2]rotaxane (**63**) as a white solid (2.22 g, 84%). m.p. 182 °C; FTIR (film) ν_{max} 3347, 3030, 1656, 1600, 1525, 1476, 1434, 1363, 1284, 1265, 1195, 1079, 946, 822, 729, 698; ^{1}H NMR (300 MHz, $CDCl_3$) δ 8.43 (s, 2H, Ar, C*H*, H_C), 8.25 (dd, *J* = 7.8, 1.4 Hz, 4H, Ar, C*H*, H_B), 7.56 (t, *J* = 7.8 Hz, 2H, Ar, C*H*, H_A), 7.39 – 7.27 (m, 10H, Ar, C*H*), 7.16 (d, *J* = 7.4 Hz, 2H, Ar, C*H*), 7.05 (t, *J* = 7.4 Hz, 4H, Ar, C*H*), 6.76 (d, *J* = 7.4 Hz, 4H, Ar, C*H*), 6.71 (s, 8H, Ar, C*H*, H_E), 6.04 (s, 2H, C*H*), 5.09 (br s, 4H, CH_2, H_D), 4.49 (s, 4H, CH_2), 4.31 (s,

4H, CH_2), 3.52 – 3.40 (m, 4H, CH_2, H_D); ^{13}C NMR (100 MHz, $CDCl_3$) δ 166.1 (*C*ON), 165.4 (*C*ON), 138.0 (Ar, *C*), 135.7 (Ar, *C*), 134.4 (*C*H), 133.4 (*C*H), 132.3 (Ar, *C*H), 130.0 (Ar, *C*H), 129.9 (Ar, *C*H), 129.5 (Ar, *C*H), 129.2 (Ar, *C*H), 128.5 (Ar, *C*H), 125.8 (Ar, *C*H), 122.2 (Ar, *C*H), 51.9 (*C*H_2), 51.6 (*C*H_2), 43.4 (*C*H_2); HRMS (ES+) calculated for $C_{64}H_{58}N_6O_6Na$ $[M+Na]^+$ 1029.4316, found 1029.4349.

(*E*)-ethyl 4-(dibenzylamino)-4-oxobut-2-enoate (64)

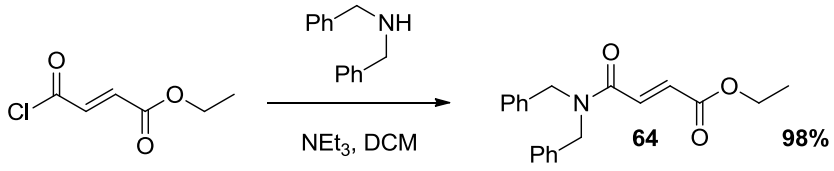

Ethyl fumaroyl chloride (400 mg, 2.5 mmol, 1.0 eq.) was dissolved in dry DCM (25 mL) at RT. A solution of dibenzylamine (0.47 mL, 2.5 mmol, 1.0 eq.) and NEt_3 (0.35 mL, 2.5 mmol, 1.0 eq.) in dry DCM (25 mL) was added using a syringe pump over a period of 2 h. The reaction was stirred overnight and the solvent was removed *in vacuo*. The crude product was purified by column chromatography with $CHCl_3$ / MeOH (98 / 2) as eluent to afford (*E*)-ethyl 4-(dibenzylamino)-4-oxobut-2-enoate (**64**) as a yellow solid (779 mg, 98%). m.p. 98 °C; FTIR (film) ν_{max} 3030, 2982, 1938, 1880, 1719, 1654, 1627, 1432, 1285, 1159, 1082, 1027, 970, 740, 694; ^{1}H NMR (300 MHz, $CDCl_3$) δ 7.33 (d, *J* = 15.2 Hz, 1H, C*H*), 7.23 – 6.96 (m, 10H, Ar, C*H*), 6.82 (d, *J* = 15.2 Hz, 1H, C*H*), 4.49 (s, 2H, CH_2), 4.36 (s, 2H, CH_2), 4.04 (q, *J* = 7.1 Hz, 2H, OCH_2), 1.11 (t, *J* = 7.1 Hz, 3H, CH_3); ^{13}C NMR (100 MHz, $CDCl_3$) δ 165.5 (*C*OO), 165.3 (*C*ONH), 136.7 (Ar, *C*), 136.0 (Ar, *C*), 133.8 (*C*H),

132.2 (*C*H), 129.0 (Ar, *C*H), 128.7 (Ar, *C*H), 128.4 (Ar, *C*H), 128.3 (Ar, *C*H), 128.0 (Ar, *C*H), 127.7 (Ar, *C*H), 127.6 (Ar, *C*H), 126.7 (Ar, *C*H), 61.1 (*C*H_2), 50.2 (*C*H_2), 48.5 (*C*H_2), 14.2 (*C*H_3); HRMS (ES+) calculated for $C_{20}H_{21}NO_3Na$ $[M+Na]^+$ 346.1419, found 346.1429.

(*E*)-4-(dibenzylamino)-4-oxobut-2-enoic acid (65)

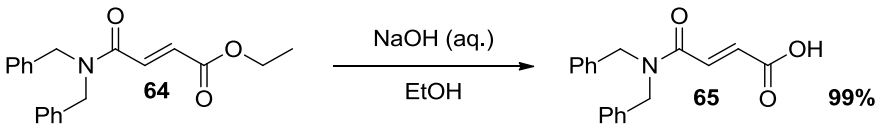

(*E*)-ethyl 4-(dibenzylamino)-4-oxobut-2-enoate (**64**) (468 mg, 1.45 mmol, 1.0 eq.) was dissolved in EtOH (50 mL). A solution of NaOH (70 mg, 1.74 mmol, 1.2 eq.) in water (2.5 mL) was added dropwise. The reaction mixture was stirred for 8 h at RT. The reaction mixture was then acidified with 1 M HCl (10 mL), extracted with DCM (3 x 20 mL) and washed with brine (20 mL). The organic layers were combined, dried over $MgSO_4$ and concentrated under reduced pressure to afford (*E*)-4-(dibenzylamino)-4-oxobut-2-enoic acid (**65**) (427 mg, 99%) as a white solid. m.p. 174 °C; FTIR (film) ν_{max} 3031, 2928, 1607, 1572, 1448, 1401, 1367, 1244, 1169, 1080, 1027, 978, 780, 695; ^{1}H NMR (300 MHz, d_6-DMSO) δ 7.36 – 7.14 (m, 10H, Ar, C*H*), 6.94 (d, *J* = 15.1 Hz, 1H, C*H*), 6.69 (d, *J* = 15.1 Hz, 1H, C*H*), 4.58 (s, 2H, C*H*$_2$), 4.52 (s, 2H, C*H*$_2$); ^{13}C NMR (100 MHz, d_6-DMSO) δ 169.7 (*C*OO), 167.3 (*C*ON), 143.2 (*C*H), 137.5 (Ar, *C*), 129.1 (Ar, *C*H), 128.7 (Ar, *C*H), 128.1 (Ar, *C*H), 127.8 (Ar, *C*H), 127.7 (Ar, *C*H), 127.6 (Ar, *C*H), 126.9 (Ar, *C*H), 126.0 (Ar, *C*H),

50.4 (CH_2), 48.8 (CH_2); HRMS (ES+) calculated for $C_{18}H_{17}NO_3Na_2$ $[M+2Na]^+$ 340.0926, found 340.0932.

(*E*)-N^1,$N^{1'}$-(ethane-1,2-diyl)bis(N^6,N^6-dibenzylfumaramide) (66)

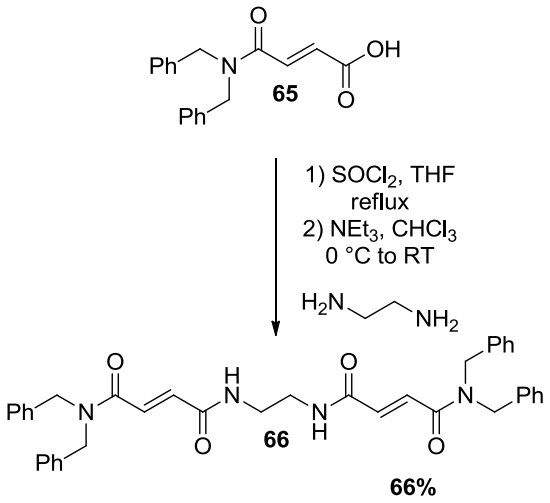

(*E*)-4-(dibenzylamino)-4-oxobut-2-enoic acid (**65**) (300 mg, 1.0 mmol, 3.2 eq.) and thionyl chloride (1 mL) were dissolved in THF (10 mL) and heated at reflux for 3 h. The crude acid chloride formed was evaporated to dryness and the resulting residue was dissolved in $CHCl_3$ (10 mL) and cooled to 0°C. NEt_3 (0.26 mL, 1.9 mmol, 6.4 eq.) and ethylenediamine (32 μL, 0.3 mmol, 1.0 eq.) were added using a motor-driven syringe pump over a period of 2 h. The reaction was stirred overnight and the solvent was removed *in vacuo*. The crude product was purified by column chromatography with $CHCl_3$ / MeOH (95 / 5) as eluent to give the title product as a yellow solid (121 mg, 66%). m.p. 168 °C; FTIR (film) ν_{max} 3294, 3063, 1614, 1539, 1495, 1427, 1295, 1186, 1080, 1029, 966, 729, 695; ^{1}H NMR

(300 MHz, $CDCl_3$) δ 7.34 – 6.96 (m, 20H, Ar, C*H*, 4H, C*H*), 4.49 (s, 4H CH_2), 4.43 (s, 4H, CH_2), 3.17 (s, 4H, CH_2); ^{13}C NMR (100 MHz, $CDCl_3$) δ 166.2 (*C*ON), 165.1 (*C*ON), 136.6 (Ar, *C*), 135.9 (*C*H), 135.7 (*C*H), 129.8 (Ar, *C*H), 128.9 (Ar, *C*H), 128.1 (Ar, *C*H), 127.7 (Ar, *C*H), 126.9 (Ar, *C*H), 50.5 (*C*H_2), 48.7 (*C*H_2), 39.9 (*C*H_2); HRMS (ES+) calculated for $C_{38}H_{38}N_4O_4Na$ $[M+Na]^+$ 637.2791, found 637.2794.

(*E*)-*N*^{1},*N*$^{1'}$-(ethane-1,2-diyl)bis(*N*^{6},*N*^{6}-dibenzylfumaramide) [3]rotaxane (67)

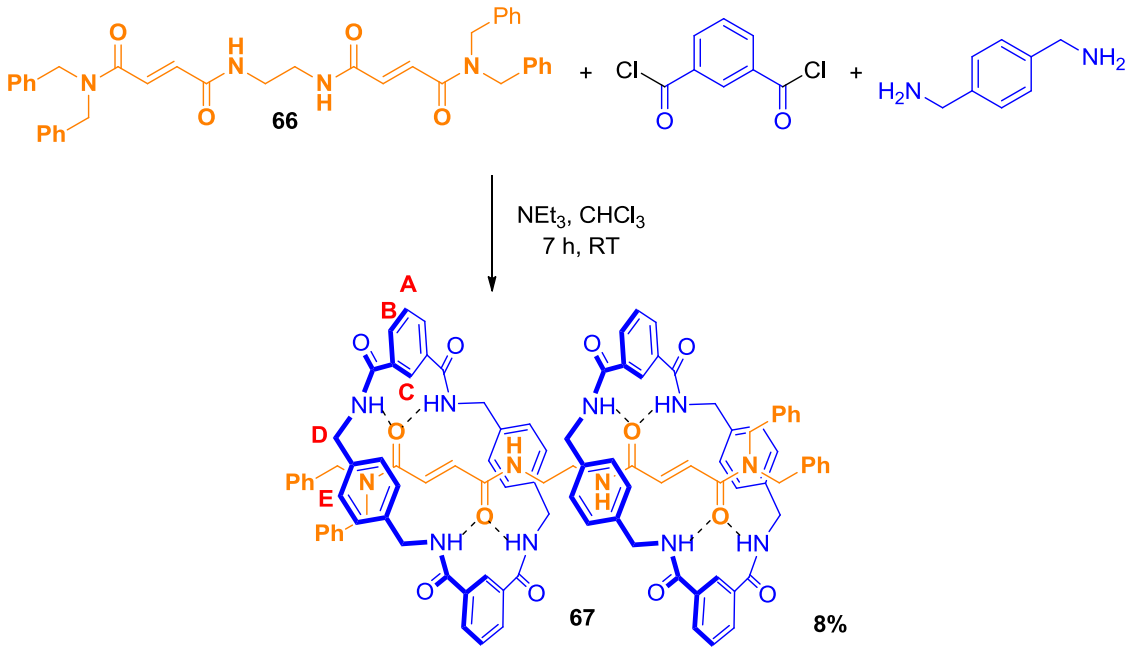

Et_3N (1.3 mL, 9.5 mmol, 48.0 eq.) was added to a stirred solution of (*E*)-*N*^{1},*N*$^{1'}$-(ethane-1,2-diyl)bis(*N*^{6},*N*^{6}-dibenzylfumaramide) (**66**) (121 mg, 0.2 mmol, 1.0 eq.) in anhydrous $CHCl_3$ (100 mL). The solution was stirred vigorously whilst solutions of *p*-xylylene diamine (643 mg, 4.7 mmol, 24.0 eq.) in anhydrous $CHCl_3$ (20 mL) and isophthaloyl dichloride (960 mg, 4.7 mmol, 24.0 eq.) in anhydrous $CHCl_3$

(20 mL) were simultaneously added over a period of 3 h using a motor-driven syringe pump. After a further 4 h period the resulting suspension was filtered through a Celite® pad and the solvent removed under reduced pressure. The crude product was purified by HPLC to afford (*E*)-N^1,$N^{1'}$-(ethane-1,2-diyl)bis(N^6,N^6-dibenzylfumaramide) [3]rotaxane (**67**) as a white solid (25 mg, 8%). HPLC (t = 0 → 60 min, 85 : 15 MeOH : H_2O): R_t 42.45; m.p. 176 °C; FTIR (film) ν_{max} 3300, 3064, 1637, 1601, 1529, 1464, 1423, 1353, 1274, 1079, 956, 818, 753, 729, 695; ^{1}H NMR (400 MHz, d_6-DMSO) δ 8.69 (s, 2H, N*H*), 8.42 (s, 4H, Ar, C*H*, H_C), 8.01 – 7.92 (m, 16H, 8 Ar, C*H*, H_B, 8 N*H*), 7.54 (t, *J* = 7.7 Hz, 4H, Ar, C*H*, H_A), 7.30 – 7.25 (m, 6H, Ar, C*H*), 7.16 – 7.11 (m, 4H, Ar, C*H*), 6.98 – 6.91 (m, 6H, Ar, C*H*), 6.87 (s, 16H, Ar, C*H*, H_E), 6.69 (d, *J* = 7.2 Hz, 4H, Ar, C*H*), 6.00 – 5.88 (m, 4H, C*H*), 4.40 – 4.24 (m, 16H, CH_2, H_D), 4.08 (dd, *J* = 13.9, 4.0 Hz, 8H, CH_2), 3.10 (br s, 4H, CH_2); ^{13}C NMR (100 MHz, d_6-DMSO) δ 165.3 (*C*ON), 165.2 (*C*ON), 164.9 (*C*ON), 136.9 (Ar, *C*), 136.0 (Ar, *C*), 133.7 (Ar, *C*), 132.9 (*C*H), 130.8 (*C*H), 128.5 (Ar, *C*H), 128.3 (Ar, *C*H), 127.5 (Ar, *C*H), 127.1 (Ar, *C*H), 126.0 (Ar, *C*H), 125.5 (Ar, *C*H), 124.0 (Ar, *C*H), 50.7 (*C*H_2), 50.3 (*C*H_2), 43.0 (*C*H_2), 37.7 (*C*H_2); HRMS (ES+) calculated for $C_{102}H_{94}N_{12}O_{12}Na$ $[M+Na]^+$ 1701.7012, found 1701.7054.

(*E*)-*N*^{1},*N*$^{1'}$-(propane-1,3-diyl)bis(*N*^{6},*N*^{6}-dibenzylfumaramide) (68)

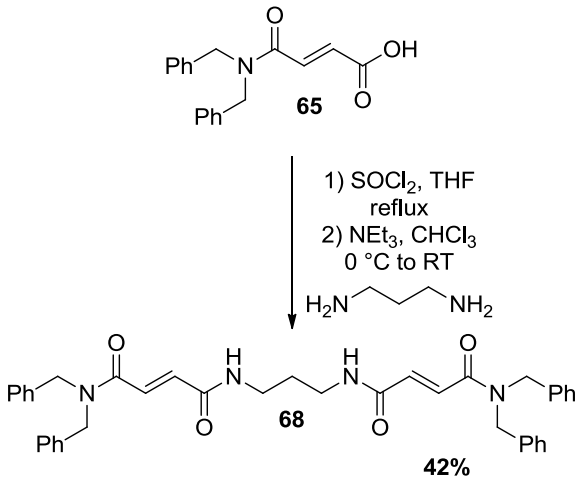

(*E*)-4-(dibenzylamino)-4-oxobut-2-enoic acid (**65**) (300 mg, 1.0 mmol, 3.2 eq.) and thionyl chloride (1 mL) were dissolved in THF (10 mL) and heated at reflux for 3 h. The crude acid chloride formed was evaporated to dryness and the resulting residue was dissolved in $CHCl_3$ (10 mL) and cooled to 0 °C. NEt_3 (0.26 mL, 1.9 mmol, 6.4 eq.) and 1,3-diaminopropane (32 μL, 0.3 mmol, 1.0 eq.) were added using a motor-driven syringe pump over a period of 2 h. The reaction was stirred overnight and the solvent was removed *in vacuo*. The crude product was purified by column chromatography with $CHCl_3$ / MeOH (95 / 5) as eluent to give the title product as a yellow solid (79 mg, 42%). m.p. 146 °C; FTIR (film) ν_{max} 3296, 3064, 3030, 2926, 1612, 1545, 1495, 1428, 1358, 1310, 1186, 1080, 1029, 964; ^{1}H NMR (300 MHz, $CDCl_3$) δ 7.41 – 7.00 (m, 24H, 20 Ar, C*H*, 4 C*H*), 4.56 - 4.48 (m, 8H, CH_2), 3.31 - 3.16 (m, 4H, CH_2), 1.55 (s, 2H, CH_2); ^{13}C NMR (100 MHz, $CDCl_3$) δ 166.1 (*C*ON), 164.8 (*C*ON), 136.7 (Ar, *C*), 136.0 (*C*H), 129.9 (Ar, *C*H), 128. 9 (Ar, *C*H), 128.1 (Ar, *C*H), 127.8 (Ar, *C*H), 126.9 (Ar, *C*H), 50.4 (*C*H_2), 48.7 (*C*H_2), 36.4

(CH_2), 29.5 (CH_2); HRMS (ES+) calculated for $C_{39}H_{40}N_4O_4Na$ $[M+Na]^+$ 651.2947, found 651.2946.

(*E*)-N^1,$N^{1'}$-(propane-1,3-diyl)bis(N^6,N^6-dibenzylfumaramide) [3]rotaxane (69)

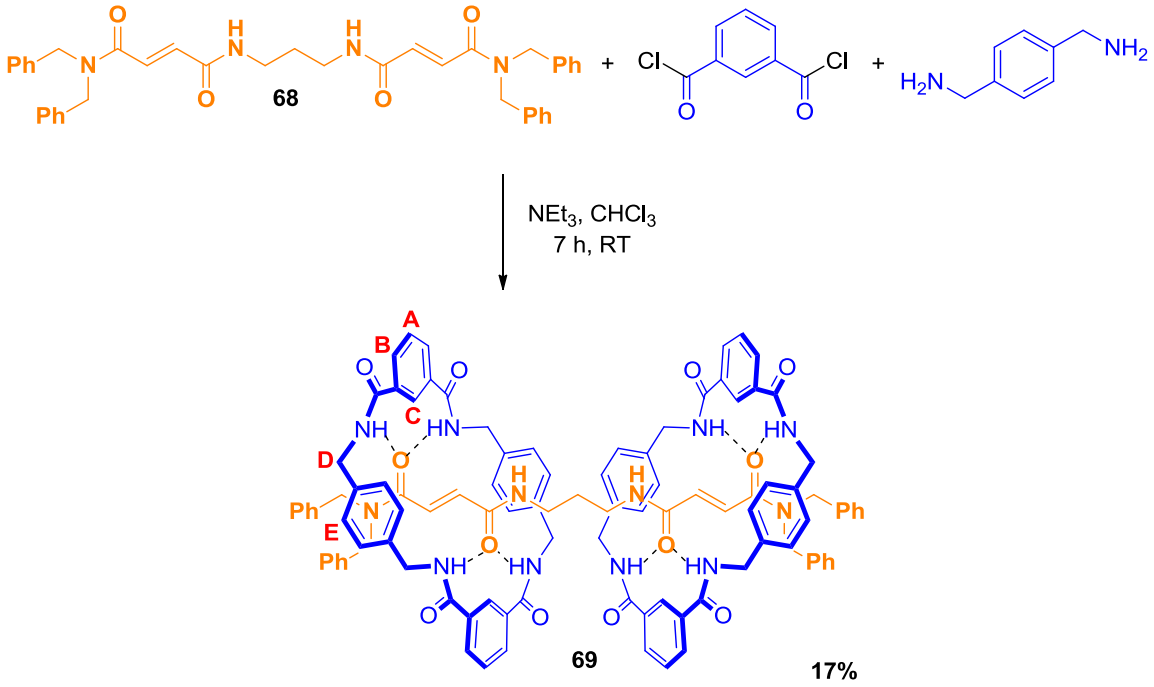

Et_3N (0.87 mL, 6.24 mmol, 48.0 eq.) was added to a stirred solution of (*E*)-N^1,$N^{1'}$-(propane-1,3-diyl)bis(N^6,N^6-dibenzylfumaramide) (**68**) (79 mg, 0.13 mmol, 1.0 eq.) in anhydrous $CHCl_3$ (100 mL). The solution was stirred vigorously whilst solutions of *p*-xylylene diamine (424 mg, 3.12 mmol, 24.0 eq.) in anhydrous $CHCl_3$ (20 mL) and isophthaloyl dichloride (633 mg, 3.12 mmol, 24.0 eq.) in anhydrous $CHCl_3$ (20 mL) were simultaneously added over a period of 3 h using a motor-driven syringe pump. After a further 4 h period the resulting suspension was filtered through a Celite® pad and the solvent removed under reduced pressure. The

crude product was purified by HPLC to afford (*E*)-N^1,$N^{1'}$-(propane-1,3-diyl)bis(N^6,N^6-dibenzylfumaramide) [3]rotaxane (**69**) as a white solid (37 mg, 17%). HPLC (t = 0 → 60 min, 85 : 15 MeOH : H_2O): R_t 46.96; m.p. 187 °C; FTIR (film) ν_{max} 3285, 3061, 2922, 1640, 1528, 1476, 1421, 1358, 1299, 1192, 1080, 1022, 959, 820, 695; ^{1}H NMR (400 MHz, d_6-DMSO) δ 8.48 (s, 1H, N*H*), 8.38 (s, 4H, Ar, C*H*, H_C), 7.97 – 7.99 (m, 12H, 8 Ar, C*H*, H_B, 4 N*H*), 7.56 (t, *J* = 7.7 Hz, 4H, Ar, C*H*, H_A), 7.25 – 7.26 (m, 6H, Ar, C*H*), 7.11 – 7.12 (m, 4H, Ar, C*H*), 7.02 – 6.93 (m, 6H, Ar, C*H*), 6.86 (s, 16H, Ar, C*H*, H_E), 6.71 – 6.73 (m, 4H, Ar, C*H*), 6.00 – 5.82 (m, 4H, C*H*), 4.33 (dd, *J* = 21.1, 14.1 Hz, 16H, CH_2, H_D), 4.09 (d, *J* = 13.9 Hz, 8H, CH_2), 3.11 - 3.15 (m, 4H, CH_2), 1.71 – 1.62 (m, 2H, CH_2); ^{13}C NMR (100 MHz, d_6-DMSO) δ 165.3 (*C*ON), 165.2 (*C*ON), 165.1 (*C*ON), 165.0 (*C*ON), 136.7 (Ar, *C*), 135.8 (Ar, *C*), 133.7 (Ar, *C*), 133.1 (*C*H), 130.7 (*C*H), 128.9 (Ar, *C*H), 128.5 (Ar, *C*H), 128.2 (Ar, *C*H), 127.5 (Ar, *C*H), 127.1 (Ar, *C*H), 125.6 (Ar, *C*H), 124.2 (Ar, *C*H), 50.7 (*C*H_2), 50.2 (*C*H_2), 43.1 (*C*H_2), 37.6 (*C*H_2), 28.4 (*C*H_2); HRMS (ES+) calculated for $C_{103}H_{96}N_{12}O_{12}Na$ $[M+Na]^+$ 1715.7168, found 1715.7144.

(*E*)-ethyl 4-(benzyl(phenyl)amino)-4-oxobut-2-enoate (70)[81]

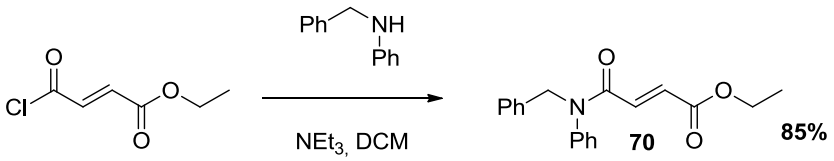

Ethyl fumaroyl chloride (3.2 g, 20.0 mmol, 1.2 eq.) was dissolved in dry DCM (100 mL) at RT. A solution of *N*-benzylaniline (3.0 g, 16.7 mmol, 1.0 eq.) and NEt_3

(2.8 mL, 20.0 mmol, 1.2 eq.) in dry DCM (25 mL) was added using a syringe pump over a period of 2 h. The reaction was stirred overnight and the solvent was removed *in vacuo*. The crude product was purified by column chromatography with hexane / EtOAc (9 / 1) as eluent to afford (*E*)-ethyl 4-(benzyl(phenyl)amino)-4-oxobut-2-enoate (**70**) as a yellow oil (4.37 g, 85%).[1]H NMR (300 MHz, $CDCl_3$) δ 7.30 – 7.03 (m, 8H, Ar, *CH*), 6.95 – 6.65 (m, 4H, 2 Ar, *CH*, 2 C*H*), 4.87 (s, 2H, CH_2), 4.00 (q, *J* = 7.1 Hz, 2H, OCH_2), 1.08 (t, *J* = 7.1 Hz, 3H, CH_3); ^{13}C NMR (100 MHz, $CDCl_3$) δ 165.4 (*C*OO), 163.8 (*C*ON), 141.0 (Ar, *C*), 136.8 (Ar, *C*), 134.3 (*C*H), 131.4 (*C*H), 129.7 (Ar, *C*H), 128.7 (Ar, *C*H), 128.4 (Ar, *C*H), 128.3 (Ar, *C*H), 128.0 (Ar, *C*H), 127.5 (Ar, *C*H), 60.9 (CH_2), 53.4 (CH_2), 14.0 (CH_3); HRMS (ES+) calculated for $C_{19}H_{19}NO_3Na$ $[M+Na]^+$ 332.1263, found 332.1262.

Data were in agreement with those previously reported.[81]

(*E*)-4-(benzyl(phenyl)amino)-4-oxobut-2-enoic acid (71)[81]

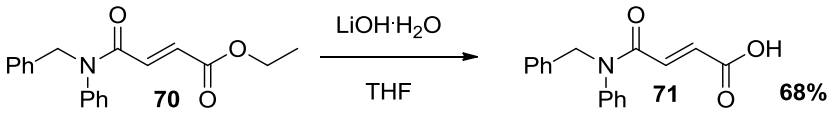

A solution of LiOH·H_2O (1.2 g, 28.0 mmol, 8.0 eq.) in water (29 mL) was added to a solution of (*E*)-ethyl4-(benzyl(phenyl)amino)-4-oxobut-2-enoate (**70**) (4.3 g, 14.0 mmol, 4.0 eq.) in THF (87 mL) at RT. After 36 h, the reaction mixture was poured into 1 M HCl (60 mL). The aqueous layer was extracted with EtOAc (3 x 80 mL) and the combined fractions were dried over $MgSO_4$ and concentrated

under reduced pressure. The crude product was recrystallised from hexane / Et_2O / DCM (29 / 70 / 1) to afford title product as a white solid (2.7 g, 68%). m.p. 95 °C [lit. 95 - 98 °C][81]; ^{1}H NMR (300 MHz, $CDCl_3$) δ 7.43 – 7.17 (m, 8H, Ar, *CH*), 7.03 - 6.93 (m, 2H, Ar, *CH*), 6.94 – 6.80 (m, 2H, C*H*), 5.00 (s, 2H, CH_2); ^{13}C NMR (100 MHz, $CDCl_3$) δ 169.4 (*C*OO), 163.8 (*C*ON), 141.0 (Ar, *C*), 136.4 (Ar, *C*), 130.4 (*C*H), 129.9 (Ar, *C*H), 128.9 (Ar, *C*H), 128.6 (Ar, *C*H), 128.2 (Ar, *C*H), 127.8 (Ar, *C*H), 53.7 (*C*H_2); LRMS (ES-) 280.1 ([M-H]$^-$, 100%).

Data were in agreement with those previously reported.[81]

(*E*)-*N*^{1},*N*$^{1'}$-(propane-1,3-diyl)bis(*N*^{6}-benzyl-*N*^{6}-phenylfumaramide) (72)

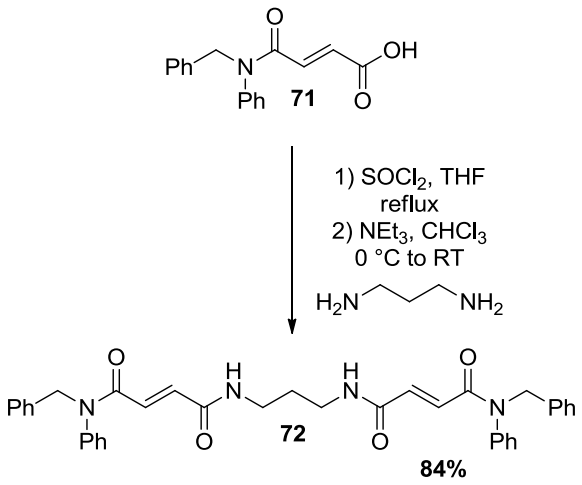

(*E*)-4-(benzyl(phenyl)amino)-4-oxobut-2-enonic acid (**71**) (2.7 g, 9.5 mmol, 4.8 eq.) and thionyl chloride (10 mL) were heated for 3 h at reflux. The crude acid chloride formed was evaporated to dryness and the resulting residue was dissolved in DCM (50 mL). The mixture was cooled to 0 °C. NEt_3 (1.32 mL, 9.5 mmol, 4.8 eq.)

and 1,3-diaminopropane (290 μL, 2.0 mmol, 1.0 eq.) were added using a syringe pump over a period of 2 h. The reaction was stirred overnight and the solvent was removed *in vacuo.* The crude product was purified by column chromatography with EtOAc / pet (1 / 1) as eluent to give the title product as a white solid (1.0 g, 84%). m.p. 128 °C; FTIR (film) ν_{max} 3228, 3062, 2930, 1628, 1593, 1558, 1493, 1391, 1327, 1191, 970, 751, 694; ^{1}H NMR (400 MHz, MeOD / $CDCl_3$) δ 7.37 – 7.30 (m, 6H, Ar, C*H*), 7.25 – 7.19 (m, 6H, Ar, C*H*), 7.17 – 7.13 (m, 4H, Ar, C*H*), 7.03 – 6.97 (m, 4H, Ar, C*H*), 6.89 (d, *J* = 15.0 Hz, 2H, C*H*), 6.71 (d, *J* = 15.0 Hz, 2H, C*H*), 4.97 (s, 4H, CH_2), 3.18 (t, *J* = 6.8 Hz, 4H, CH_2CH_2NH), 1.68 – 1.61 (m, 2H, CH_2); ^{13}C NMR (100 MHz, MeOD / $CDCl_3$) δ 166.5 (*C*O), 142.2 (Ar, *C*), 137.9 (Ar, *C*), 135.6 (*C*H), 131.8 (*C*H), 131.0 (Ar, *C*H), 129.9 (Ar, *C*H), 129.7 (Ar, *C*H), 129.4 (Ar, *C*H), 128.9 (Ar, *C*H), 54.8 (*C*H_2), 38.2 (*C*H_2), 29.9 (*C*H_2); HRMS (ES+) calculated for $C_{37}H_{36}N_4O_4Na$ $[M+Na]^+$ 623.2634, found 623.2629.

(*E*)-N^1,$N^{1'}$-(propane-1,3-diyl)bis(N^6-benzyl-N^6-phenylfumaramide) [2]rotaxane (74) and [3]rotaxane (73)

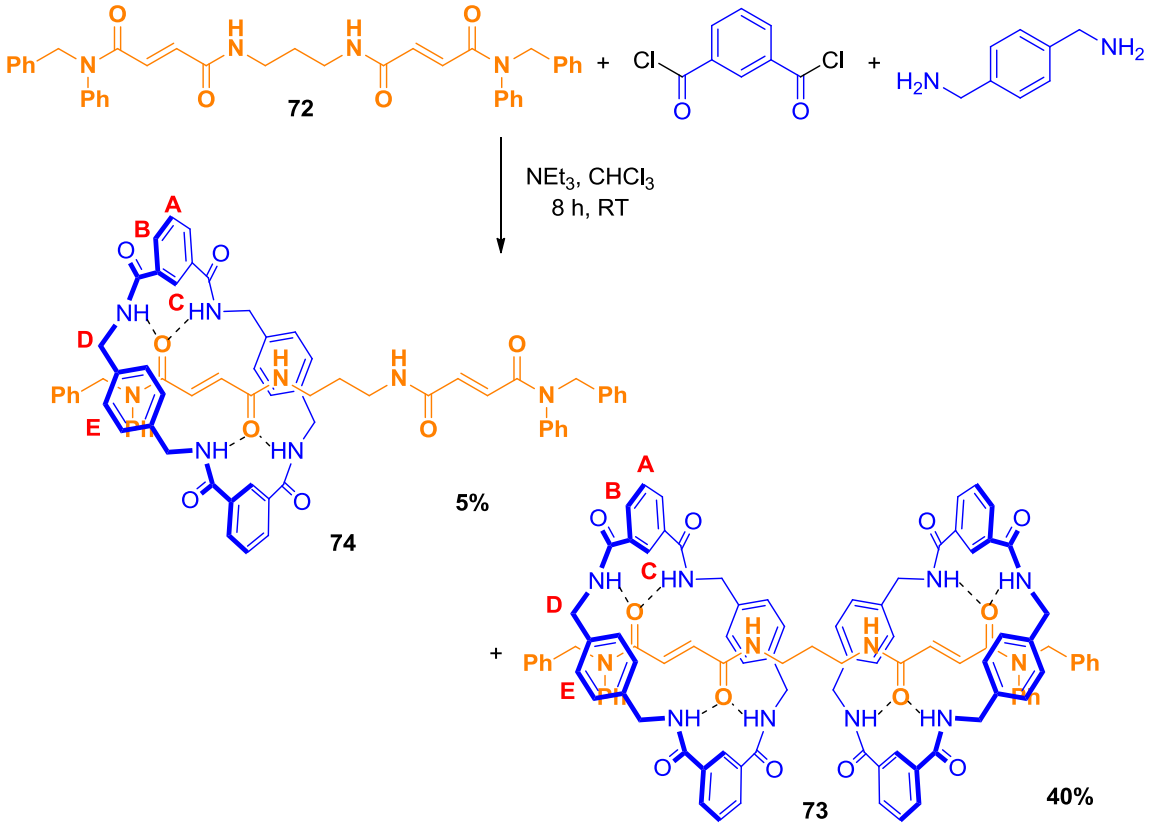

Et_3N (0.7 mL, 4.8 mmol, 48.0 eq.) was added to a stirred solution of (*E*)-N^1,$N^{1'}$-(propane-1,3-diyl)bis(N^6-benzyl-N^6-phenylfumaramide) (**72**) (60 mg, 0.1 mmol, 1.0 eq.) in anhydrous $CHCl_3$ (30 mL). The solution was stirred vigorously whilst solutions of *p*-xylylene diamine (327 mg, 2.4 mmol, 24.0 eq.) in anhydrous $CHCl_3$ (10 mL) and isophthaloyl dichloride (487 mg, 2.4 mmol, 24.0 eq.) in anhydrous $CHCl_3$ (10 mL) were simultaneously added over a period of 4 h using a motor-driven syringe pump. After a further 4 h period the resulting suspension was filtered through a Celite® pad and the solvent removed under reduced pressure. The crude product was purified by column chromatography with EtOAc / MeOH (9

/ 1) as eluent to give the [3]rotaxane (**73**) as a white solid (67 mg, 40%) and the [2]rotaxane (**74**) as a white solid (3 mg, 2%). Data for compound **74**: m.p. 162 °C; FTIR (film) ν_{max} 3301, 3063, 2929, 1639, 1534, 1493, 1420, 1296, 1188, 1110, 1080, 967, 820, 696; ^{1}H NMR (400 MHz, MeOD / $CDCl_3$) δ 8.34 (br s, 2H, Ar, C*H*, H_C), 8.22 – 8.14 (m, 5H, 4 Ar, C*H*, H_B, 1 N*H*), 7.64 (t, *J* = 7.8 Hz, 2H, Ar, C*H*, H_A), 7.27 – 7.16 (m, 6H, Ar, C*H*), 7.09 – 7.00 (m, 8H, Ar, C*H*), 6.95 (s, 8H, Ar, C*H*, H_E), 6.84 (d, *J* = 8.0 Hz, 6H, Ar, C*H*), 6.31 (d, *J* = 14.8 Hz, 2H, C*H*), 6.04 (d, *J* = 14.8 Hz, 2H, C*H*), 4.77 (s, 4H, CH_2), 4.32 (s, 8H, CH_2, H_D), 3.21 (t, *J* = 6.8 Hz, 4H, CH_2CH_2NH), 1.74 – 1.66 (m, 2H, CH_2); ^{13}C NMR (100 MHz, MeOD / $CDCl_3$) δ 166.8 (*C*O), 165.7 (*C*O), 165.1 (*C*O), 140.6 (Ar, *C*), 137.4 (Ar, *C*), 136.4 (Ar, *C*), 134.2 (*C*H), 133.7 (Ar, *C*), 133.4 (*C*H), 131.9 (Ar, *C*H), 129.8 (Ar, *C*H), 129.6 (Ar, *C*H), 129.4 (Ar, *C*H), 129.2 (Ar, *C*H), 128.9 (Ar, *C*H), 128.7 (Ar, *C*H), 128.2 (Ar, *C*H), 127.9 (Ar, *C*H), 124.2 (Ar, *C*H), 54.3 (*C*H_2), 43.9 (*C*H_2), 37.3 (CH_2CH_2NH), 29.0 (*C*H_2); HRMS (ES+) calculated for $C_{69}H_{64}N_8O_8Na$ $[M+Na]^+$ 1155.4745, found 1155.4785. Data for compound **73**: m.p. 178 °C; FTIR (film) ν_{max} 3283, 3066, 2926, 1639, 1609, 1588, 1530, 1495, 1415, 1305, 1272, 1174, 1079, 960, 698; ^{1}H NMR (400 MHz, d_2-DCM / MeOD) δ 8.30 (br s, 4H, Ar, C*H*, H_C), 8.13 (dd, *J* = 7.8, 1.7 Hz, 8H, Ar, C*H*, H_B), 7.64 (t, *J* = 7.8 Hz, 4H, Ar, C*H*, H_A), 7.30 – 7.20 (m, 7H, Ar, C*H*), 7.04 – 6.95 (m, 21H, 16 Ar, C*H*, H_E, 5 m, Ar, C*H*), 6.88 (t, *J* = 7.8 Hz, 4H, Ar, C*H*), 6.81 – 6.75 (m, 4H, Ar, C*H*), 6.44 (br s, 2H, N*H*), 5.86 (d, *J* = 14.9 Hz, 2H, C*H*), 5.46 (d, *J* = 14.9 Hz, 2H, C*H*), 4.66 (s, 4H, CH_2), 4.39 (d, *J* = 14.2 Hz, 8H, CH_2, H_D), 4.22 (d, *J* = 14.2 Hz, 8H, CH_2, H_D), 3.31 – 3.24 (m, 4H, CH_2CH_2NH), 1.91 – 1.75 (m, 2H, CH_2); ^{13}C NMR (100 MHz, d_2-DCM / MeOD) δ 167.3 (*C*O),

166.5 (*C*O), 165.4 (*C*O), 140.8 (Ar, *C*), 137.9 (Ar, *C*), 136.8 (Ar, *C*), 134.3 (Ar, *C*), 133.0 (*C*H), 132.1 (*C*H), 130.0 (Ar, *C*H), 129.9 (Ar, *C*H), 129.8 (Ar, *C*H), 129.7 (Ar, *C*H), 129.1 (Ar, *C*H), 129.0 (Ar, *C*H), 128.7 (Ar, *C*H), 128.1 (Ar, *C*H), 127.7 (Ar, *C*H), 124.9 (Ar, *C*H), 55.0 (CH_2), 44.2 (CH_2), 38.6 (CH_2CH_2NH), 29.5 (CH_2); LRMS (ES+) 1688.8 ($[M+Na]^+$, 25%), 855.9 ($[M+2Na]^{2+}$, 100%).

4.5 Experimental for Section 2.5

N,*N*,*N*',*N*'-tetrakis(2,2-diphenylethyl)-1,2-hydrazodicarboxamide [2]rotaxane (77)

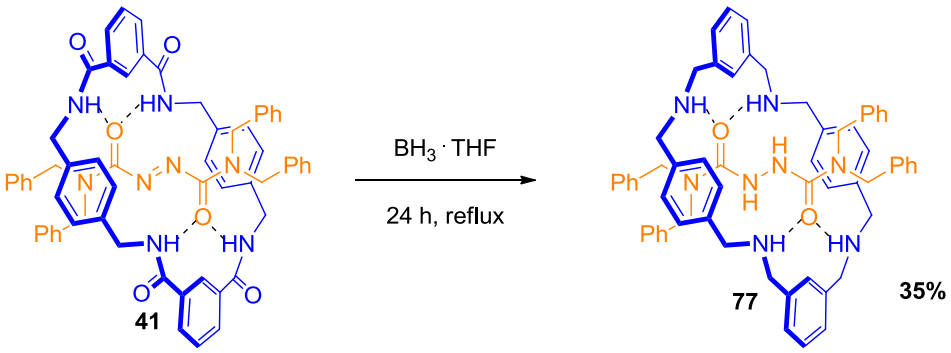

A solution of borane (10.0 mL, 10.0 mmol, 147.0 eq.) in THF was added to rotaxane **41** (69 mg, 0.07 mmol, 1.0 eq.) and the mixture was refluxed for 24 h. Water (5 mL) was added to quench the excess of borane and the mixture was evaporated to dryness. 6 M HCl (2 mL) was added to the residue. The reaction mixture was heated at reflux for 6 h, then made alkaline with aqueous 10% NaOH (10 mL) and extracted with DCM (3 x 20 mL). The combined organic fractions were washed with water (50 mL), dried over $MgSO_4$ and evaporated to dryness.

The crude product was purified by column chromatography with $CHCl_3$ / MeOH (90 / 10) as eluent to afford the title compound (**77**) as a white solid (23 mg, 36%). m.p. 126 °C; FTIR (film) ν_{max} 2924, 2852, 1645, 1495, 1452, 1231, 1077, 1028, 964, 805, 736, 697; ^{1}H NMR (400 MHz, MeOD / $CDCl_3$) δ 7.32 – 7.17 (m, 20H, Ar, C*H*), 7.02 (br s, 8H, Ar, C*H*), 6.96 – 6.88 (m, 8H, Ar, C*H*), 4.21 (br s, 8H, CH_2), 3.83 (br s, 8H, CH_2NH), 3.75 (br s, 8H, CH_2NH); ^{13}C NMR (100 MHz, MeOD / $CDCl_3$) δ 158.5 (*C*ON), 137.1 (Ar, *C*), 129.7 (Ar, *C*H), 129.5 (Ar, *C*H), 129.1 (Ar, *C*H), 128.1 (Ar, *C*H), 127.8 (Ar, *C*H), 53.8 (*C*H_2), 53.7 (*C*H_2), 50.7 (*C*H_2); HRMS (ES+) calculated for $C_{62}H_{67}N_8O_2$ $[M+H]^+$ 955.5387, found 955.5370.

(*E*)-ethyl 4-(diphenylamino)-4-oxobut-2-enoate (81)

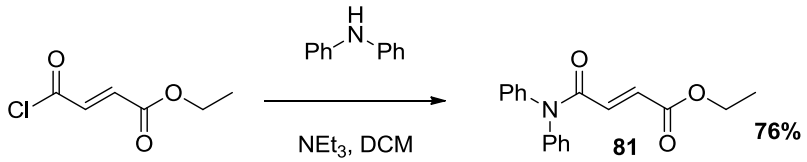

Ethyl fumaroyl chloride (972 mg, 6.0 mmol, 1.2 eq.) was dissolved in dry DCM (20 mL) at RT. A solution of diphenylamine (845 mg, 5.0 mmol, 1.0 eq.) and NEt_3 (0.84 mL, 6.0 mmol, 1.2 eq.) in dry DCM (5 mL) was added using a syringe pump over a period of 2 h. The reaction was stirred overnight and the solvent was removed *in vacuo*. The crude product was purified by column chromatography with pet / EtOAc (8 / 2) as eluent to afford (*E*)-ethyl 4-(diphenylamino)-4-oxobut-2-enoate (**81**) as a yellow oil (1.12 g, 76%). FTIR (film) ν_{max} 3060, 2980, 1716, 1667, 1640, 1590, 1489, 1346, 1295, 1189, 1150, 1025, 970, 760, 692; ^{1}H NMR (300

MHz, $CDCl_3$) δ 7.51 (s, 5H, Ar, *CH*), 7.18 – 6.96 (m, 5H, Ar, *CH*), 6.96 – 6.89 (m, 2H, C*H*), 4.20 (q, *J* = 7.1 Hz, 2H, OCH_2), 1.27 (t, *J* = 7.1 Hz, 3H, CH_3); ^{13}C NMR (100 MHz, $CDCl_3$) δ 165.7 (*C*OO), 164.2 (*C*ON), 143.2 (Ar, *C*), 142.7 (Ar, *C*), 135.4 (*C*H), 131.8 (*C*H), 129.9 (Ar, *C*H), 129.2 (Ar, *C*H), 128.4 (Ar, *C*H), 126.4 (Ar, *C*H), 61.2 (*C*H_2), 14.2 (*C*H_3); HRMS (ES+) calculated for $C_{18}H_{17}NO_3Na$ $[M+Na]^+$ 318.1106, found 318.1107.

(*E*)-4-(diphenylamino)-4-oxobut-2-enoic acid (82)

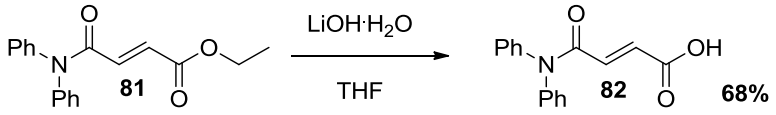

$LiOH·H_2O$ (313 mg, 7.5 mmol, 2.0 eq.) in water (9 mL) was added to a solution of (*E*)-ethyl 4-(diphenylamino)-4-oxobut-2-enoate (**81**) (1.1 g, 3.7 mmol, 1.0 eq.) in THF (38 mL) at RT. After 36 h, the reaction mixture was poured into 1 M HCl (18 mL). The aqueous layer was extracted with EtOAc (3 x 24 mL) and the combined organic fractions were dried over $MgSO_4$ and concentrated under reduced pressure. The crude product was recrystallised from hexane / Et_2O / DCM (29 / 70 / 1) to afford title product as a white solid (680 mg, 68%). m.p. 178 °C; FTIR (film) ν_{max} 3061, 1717, 1656, 1616, 1589, 1452, 1374, 1282, 1254, 1180, 1155, 1075, 974, 861, 797, 756, 693; ^{1}H NMR (300 MHz, $CDCl_3$) δ 10.25 (s, 1H, O*H*), 7.47 - 7.35 (m, 5H, Ar, *CH*), 7.30 - 7.21 (m, 5H, Ar, *CH*), 7.03 (d, *J* = 15.3 Hz, 1H, C*H*), 6.92 (d, *J* = 15.3 Hz, 1H, C*H*); ^{13}C NMR (100 MHz, $CDCl_3$) δ 170.1 (*C*OO), 164.1 (*C*ON), 142.0 (Ar, *C*), 141.5 (Ar, *C*), 137.1 (*C*H), 130.9 (*C*H), 130.0

(Ar, *C*H), 129.2 (Ar, *C*H), 128.4 (Ar, *C*H), 126.9 (Ar, *C*H), 126.4 (Ar, *C*H); HRMS (ES-) calculated for $C_{16}H_{12}NO_3$ $[M-H]^-$ 266.0817, found 266.0815.

(*E*)-*N*^{1},*N*$^{1'}$-(propane-1,3-diyl)bis(*N*^{6} ,*N*^{6}-diphenylfumaramide) (83)

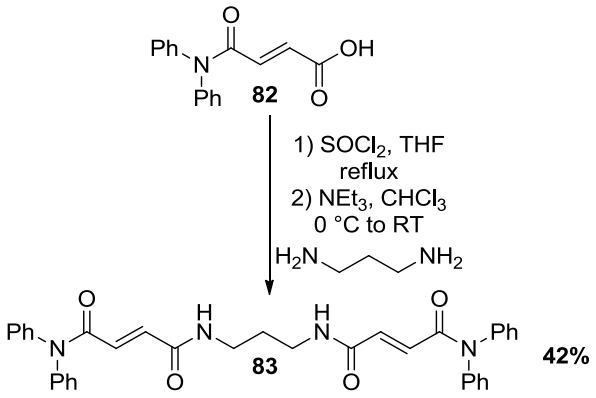

(*E*)-4-(diphenylamino)-4-oxobut-2-enoic acid (**82**) (643 mg, 2.4 mmol, 2.4 eq.) was dissolved in toluene (5 mL). Thionyl chloride (1.2 mL) was added and the mixture was heated at reflux for 3 h. The crude acid chloride formed was evaporated to dryness, the resulting residue was dissolved in DCM (10 mL) and the mixture was cooled to 0°C. NEt_3 (0.3 mL, 2.2 mmol, 2.2 eq.) and 1,3-diaminopropane (84 μL, 1.0 mmol, 1.0 eq.) were added using a syringe pump over a period of 2 h. The reaction was stirred overnight and the solvent was removed *in vacuo*. The crude product was purified by column chromatography with EtOAc / pet (9 / 1) as eluent to give the title product as a white solid (242 mg, 42%). m.p. 241 °C; FTIR (film) ν_{max} 3321, 3059, 2932, 1631, 1593, 1539, 1490, 1357, 1206, 1159, 1075, 974, 763, 698; ^{1}H NMR (400 MHz, MeOD) δ 7.37 (s, 10H, Ar, C*H*), 7.24 – 7.22 (m, 10H, Ar, C*H*), 7.01 (d, *J* = 14.9 Hz, 2H, C*H*), 6.90 (d, *J* = 14.9 Hz, 2H, C*H*), 3.20 – 3.16

(m, 4H, CH_2), 1.62 – 1.59 (m, 2H, CH_2); ^{13}C NMR (100 MHz, MeOD) δ 165.6 (*C*O), 165.3 (*C*O), 141.9 (Ar, *C*), 135.2 (*C*H), 131.4 (*C*H), 130.2 (Ar, *C*H), 129.4 (Ar, *C*H), 128.6 (Ar, *C*H), 127.3 (Ar, *C*H), 126.8 (Ar, *C*H), 37.2 (*C*H_2), 28.9 (*C*H_2); HRMS (ES+) calculated for $C_{35}H_{32}N_4O_4Na$ $[M+Na]^+$ 595.2321, found 595.2314.

(*E*)-*N*^{1},*N*$^{1'}$-(propane-1,3-diyl)bis(*N*^{6} ,*N*^{6}-diphenylfumaramide) [2]rotaxane (85) and [3]rotaxane (84)

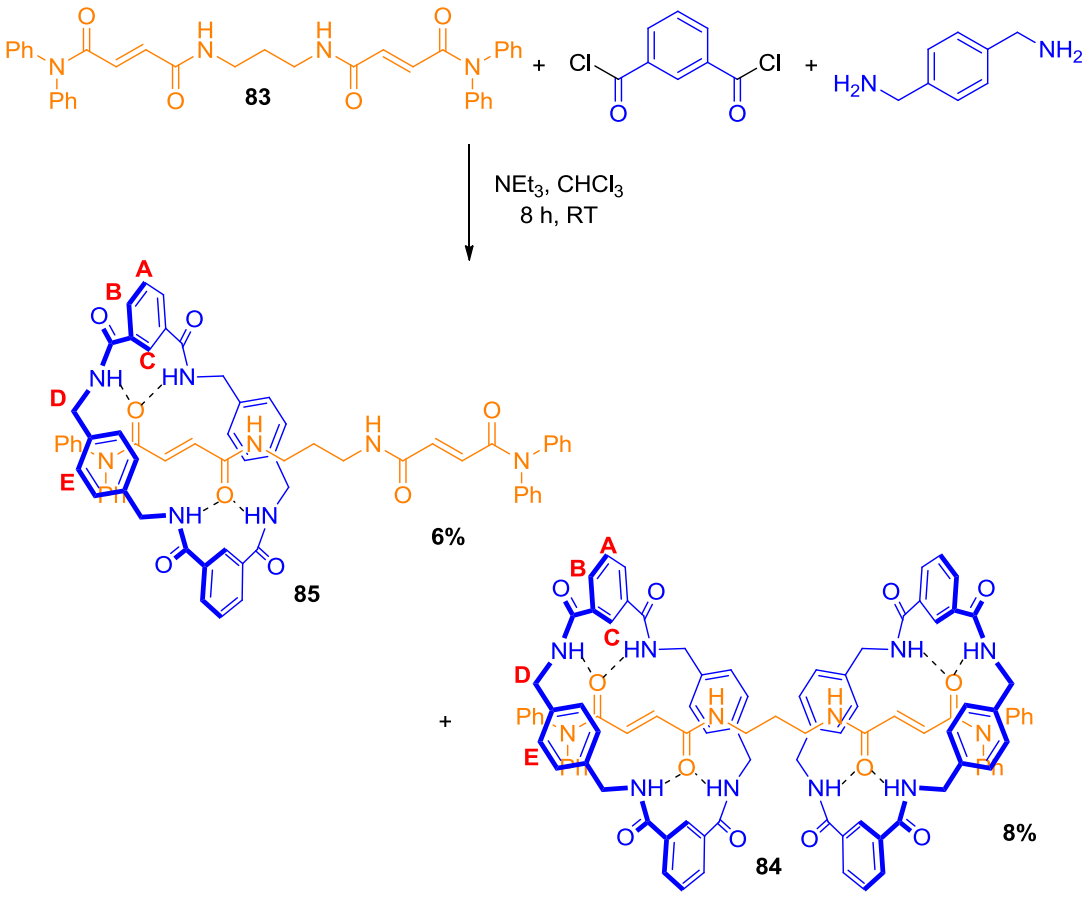

Et_3N (1.14 mL, 8.16 mmol, 48.0 eq.) was added to a stirred solution of (*E*)-*N*^{1},*N*$^{1'}$-(propane-1,3-diyl)bis(*N*^{6} ,*N*^{6}-diphenylfumaramide) (**83**) (97 mg, 0.17 mmol, 1.0 eq.)

in anhydrous $CHCl_3$ (100 mL). The solution was stirred vigorously whilst solutions of *p*-xylylene diamine (555 mg, 4.08 mmol, 24.0 eq.) in anhydrous $CHCl_3$ (20 mL) and isophthaloyl dichloride (828 mg, 4.08 mmol, 24.0 eq.) in anhydrous $CHCl_3$ (20 mL) were simultaneously added over a period of 2 h using a motor-driven syringe pump. After a further 4 h period the resulting suspension was filtered through a Celite® pad and the solvent removed under reduced pressure. The crude product was purified by HPLC to afford the [3]rotaxane (**84**) as a white solid (22 mg, 8%) and the [2]rotaxane (**85**) as a white solid (9 mg, 5%). HPLC (t = 0 → 30 min, 75 : 25 MeOH : H_2O; t = 30 → 40 min, 75 → 95% H_2O in MeOH, t = 40 → 60 min, 95 : 5 MeOH : H_2O): Data for compound **85**: R_t 31.27; m.p. 159 °C; FTIR (film) ν_{max} 3293, 3064, 1635, 1531, 1490, 1355, 1309, 1271, 1211, 1160, 1078, 966, 820, 759, 694; ^{1}H NMR (400 MHz, $CDCl_3$) δ 8.07 – 8.05 (m, 6H, 2 Ar, C*H*, H_C, 4 Ar, C*H*, H_B), 7.78 (t, *J* = 6.1 Hz, 2H, N*H*), 7.49 (t, *J* = 7.7 Hz, 2H, Ar, C*H*, H_A), 7.41 (br s, 4H, N*H*), 7.18 – 7.10 (m, 5H, Ar, C*H*), 7.09 – 6.98 (m, 17H, 8 Ar, C*H*, H_E, 9 Ar, C*H*), 6.93 – 6.92 (m, 4H, Ar, C*H*), 6.85 – 6.83 (m, 2H, Ar, C*H*), 6.62 – 6.57 (m, 2H, C*H*), 6.28 – 6.20 (m, 2H, C*H*), 4.35 (s, 8H, CH_2, H_D), 3.07 – 2.88 (m, 4H, CH_2CH_2NH), 1.38 – 1.24 (m, 2H, CH_2); ^{13}C NMR (100 MHz, $CDCl_3$) δ 166.6 (*C*O), 165.4 (*C*O), 164.9 (*C*O), 141.8 (Ar, *C*), 140.7 (Ar, *C*), 137.6 (Ar, *C*), 134.5 (*C*H), 133.9 (*C*H), 131.6 (Ar, *C*H), 129.9 (Ar, *C*H), 129.4 (Ar, *C*H), 129.2 (Ar, *C*H), 128. 7 (Ar, *C*H), 127.9 (Ar, *C*H), 127.2 (Ar, *C*H), 126.1 (Ar, *C*H), 124.2 (Ar, *C*H), 44.2 (*C*H_2), 36.4 (CH_2CH_2NH), 29.4 (*C*H_2); HRMS (ES+) calculated for $C_{67}H_{60}N_8O_8Na$ $[M+Na]^+$ 1127.4432, found 1127.4442. Data for compound **84**: R_t 37.57; m.p. 185 °C; FTIR (film) ν_{max} 3301, 3065, 1636, 1531, 1490, 1355, 1308,

1161, 1077, 967, 760, 695; ^{1}H NMR (400 MHz, MeOD / $CDCl_3$) δ 8.16 (br s, 4H, Ar, C*H*, H_C), 8.04 (dd, *J* = 7.8, 1.7 Hz, 8H Ar, C*H*, H_B), 7.59 – 7.58 (m, 4H, Ar, C*H*, H_A), 7.22 – 7.10 (m, 19H, 16 Ar, C*H*, H_E, 3 Ar, C*H*), 7.09 – 7.05 (m, 3H, Ar, C*H*), 7.00 - 6.98 (m, 4H, Ar, C*H*), 6.91 – 6.85 (m, 7H, Ar, C*H*), 6.49 – 6.45 (m, 3H, Ar, C*H*), 6.08 (d, *J* = 14.9 Hz, 2H, C*H*), 5.67 (d, *J* = 14.9 Hz, 2H, C*H*), 4.53 (d, *J* = 14.3 Hz, 8H, CH_2, H_D), 4.32 (br s, 8H, N*H*), 4.23 (d, *J* = 14.3 Hz, 8H, CH_2, H_D), 3.35 – 3.33 (m, 4H, CH_2CH_2NH), 1.92 – 1.87 (m, 2H, CH_2); ^{13}C NMR (100 MHz, MeOD / $CDCl_3$) δ 167.8 (*C*O), 166.4 (*C*O), 165.5 (*C*O), 141.8 (Ar, *C*), 140.8 (Ar, *C*), 137.9 (Ar, *C*), 134.4 (Ar, *C*), 134.3 (*C*H), 131.9 (*C*H), 130.2 (Ar, *C*H), 129.8 (Ar, *C*H), 129.7 (Ar, *C*H), 129.0 (Ar, *C*H), 128.3 (Ar, *C*H), 127.9 (Ar, *C*H), 126.3 (Ar, *C*H), 125.4 (Ar, *C*H), 121.2 (Ar, *C*H), 44.5 (*C*H_2), 38.5 (CH_2CH_2NH), 29.3 (*C*H_2); HRMS (ES+) calculated for $C_{99}H_{88}N_{12}O_{12}Na$ $[M+Na]^+$ 1659.6542, found 1659.6563.

(*E*)-ethyl 4-(bis(4-bomophenyl)amino)-4-oxobut-2-enoate (86)

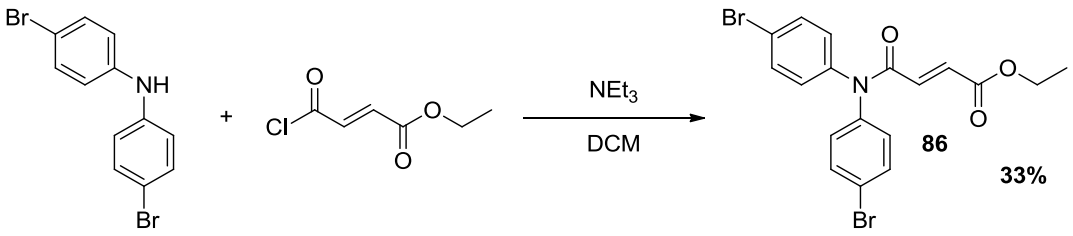

86

33%

Ethyl fumaroyl chloride (468 mg, 3.0 mmol, 1.2 eq.) was dissolved in dry DCM (10 mL) at RT. A solution of bis(4-bromophenyl)amine (800 mg, 2.5 mmol, 1.0 eq.) and NEt_3 (0.4 mL, 3.0 mmol, 1.2 eq.) in dry DCM (5 mL) was added using a syringe pump over a period of 2 h. The reaction was stirred for an additional hour

and the solvent was removed *in vacuo.* The crude product was purified by column chromatography with pet / EtOAc (8 / 2) as eluent to afford (E)-ethyl 4-(bis(4-bromophenyl)amino)-4-oxobut-2-enoate (**86**) as a yellow oil (379 mg, 33%). FTIR (film) ν_{max} 3066, 2981, 1718, 1665, 1639, 1584, 1486, 1333, 1293, 1187, 1151, 1070, 1011, 972, 826, 760, 728, 682; ^{1}H NMR (400 MHz, $CDCl_3$) δ 7.51 (s, 4H, Ar, *CH*), 7.08 – 7.06 (m, 4H, Ar, *CH*), 6.98 – 6.86 (m, 2H, C*H*), 4.20 (q, *J* = 7.1 Hz, 2H, OCH_2), 1.27 (t, *J* = 7.1 Hz, 3H, CH_3); ^{13}C NMR (100 MHz, $CDCl_3$) δ 165.4 (*C*OO), 163.9 (*C*ON), 140.8 (Ar, *C*Br), 140.3 (Ar, *C*Br), 134.5 (*C*H), 133.3 (*C*H), 132.6 (Ar, *C*H), 132.4 (Ar, *C*H), 129.8 (Ar, *C*H), 127.8 (Ar, *C*H), 61.4 (CH_2), 14.2 (CH_3); HRMS (ES+) calculated for $C_{18}H_{15}NO_3Br_2Na$ $[M+Na]^+$ 473.9316, found 473.9318.

(*E*)-4-(bis(4-bromophenyl)amino)-4-oxobut-2-enoic acid (87)

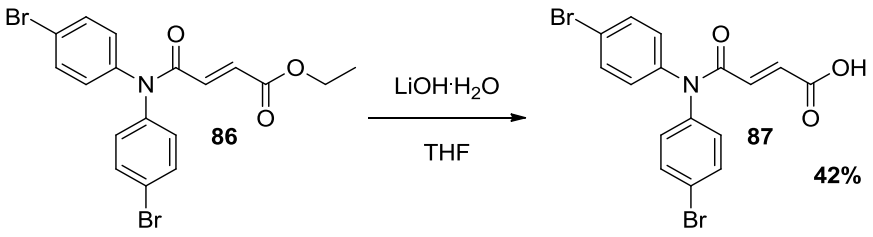

A solution of LiOH·H_2O (71 mg, 1.7 mmol, 2.0 eq.) in water (3 mL) was added to a solution of (*E*)-ethyl 4-(bis(4-bromophenyl)amino)-4-oxobut-2-enoate (**86**) (379 mg, 0.8 mmol, 1.0 eq.) in THF (10 mL) at RT. After 36 h, the reaction mixture was poured into 1 M HCl (6 mL). The aqueous layer was extracted with EtOAc (3 x 8 mL) and the combined fractions were dried over $MgSO_4$ and concentrated under reduced pressure. The crude product was recrystallised from hexane / Et_2O / DCM

(29 / 70 / 1) to afford the title product as a yellow solid (148 mg, 42%). m.p. 168 °C; FTIR (film) ν_{max} 3098, 1702, 1666, 1488, 1412, 1328, 1282, 1205, 1186, 1073, 972, 830, 785, 759, 680; ^{1}H NMR (400 MHz, $CDCl_3$) δ 7.55 – 7.49 (m, 4H, Ar, *CH*), 7.08 – 7.07 (m, 4H, Ar, *CH*), 6.98 (d, *J* = 15.3 Hz, 1H, C*H*), 6.92 (d, *J* = 15.3 Hz, 1H, C*H*); ^{13}C NMR (100 MHz, $CDCl_3$) δ 169.4 (*C*OO), 163.6 (*C*ON), 140.6 (Ar, *C*Br), 136.6 (*C*H), 133.5 (Ar, *C*H), 132.5 (Ar, *C*H), 131.4 (*C*H), 129.8 (Ar, *C*H), 127.9 (Ar, *C*H); HRMS (ES-) calculated for $C_{16}H_{10}NO_3Br_2$ $[M-H]^-$ 423.9184, found 423.9174.

(*E*)-*N*^{1},*N*$^{1'}$-(propane-1,3-diyl)bis(*N*^{6},*N*^{6}-bis(4-bromophenyl)fumaramide) (88)

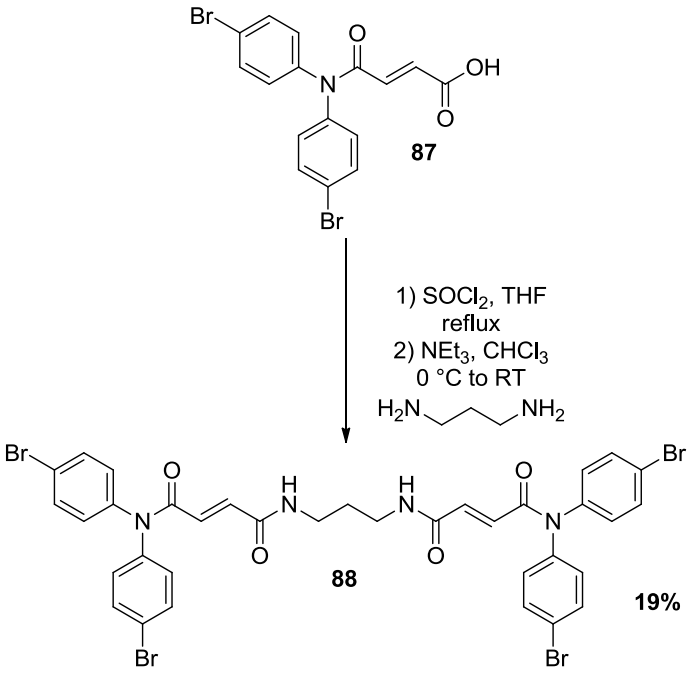

(*E*)-4-(bis(4-bromophenyl)amino)-4-oxobut-2-enoic acid (**87**) (148 mg, 0.35 mmol, 3.5 eq.) was dissolved in toluene (1 mL). Thionyl chloride (0.2 mL) was added and

the mixture was heated at reflux for 3 h. The crude acid chloride formed was evaporated to dryness, the resulting residue was dissolved in DCM (1 mL) and cooled to 0 °C. NEt_3 (30 μL, 0.3 mmol, 3.0 eq.) and 1,3-diaminopropane (8.4 μL, 0.1 mmol, 1.0 eq.) were added using a syringe pump over a period of 2 h. The reaction was stirred overnight and the solvent was removed *in vacuo*. The crude product was purified by column chromatography with EtOAc / MeOH (10 / 1) as eluent to give the title product as a brown solid (17 mg, 19%). m.p. 240 °C; FTIR (film) ν_{max} 3323, 1645, 1543, 1485, 1330, 1070, 1011, 969, 823, 681; ^{1}H NMR (300 MHz, $CDCl_3$) δ 7.45 – 7.39 (m, 8H, Ar, C*H*), 7.15 (d, *J* = 14.9 Hz, 2H, C*H*), 7.11 – 7.05 (m, 8H, Ar, C*H*), 6.72 (d, *J* = 14.9 Hz, 2H, C*H*), 3.02 - 2.96 (m, 4H, CH_2), 1.19 – 1.17 (m, 2H, CH_2); ^{13}C NMR (100 MHz, $CDCl_3$) δ 164.7 (*C*O), 163.9 (*C*O), 142.0 (Ar, *C*Br), 140.3 (Ar, *C*Br), 137.8 (*C*H), 133.6 (Ar, *C*H), 132.2 (Ar, *C*H), 130.3 (*C*H), 128.8 (Ar, *C*H), 128.7 (Ar, *C*H), 38.8 (*C*H_2), 27.3 (*C*H_2); HRMS (ES+) calculated for $C_{35}H_{28}N_4O_4Br_4Na$ $[M+Na]^+$ 910.8701, found 910.8709.

9-[(*N*-benzylamino)methyl]anthracene[121]

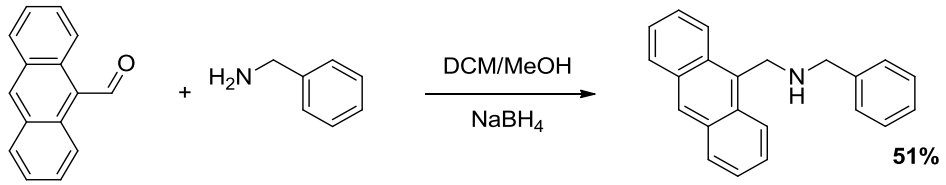

Benzylamine (0.3 mL, 2.5 mmol, 1.0 eq.) was added dropwise using a syringe over a period of 20 min to a stirred solution of 9-anthraldehyde (515 mg, 2.5 mmol, 1.0 eq.) in a mixture of DCM / methanol (1 / 1, 20 mL). The reaction was stirred

overnight and $NaBH_4$ (200 mg, 5.3 mmol, 2.1 eq.) was added to the reaction mixture. The mixture was stirred for 5 h and then concentrated under reduced pressure. The crude product was dissolved in DCM (25 mL) and filtered to remove the excess of $NaBH_4$. The solvent was removed *in vacuo* and the crude product was purified by column chromatography with hexane / EtOAc (2 / 1) as eluent to afford 9-[(*N*-benzylamino)methyl]anthracene as a light brown solid (382 mg, 51%). m.p. 146 °C [lit. 148 - 151 °C][121]; ^{1}H NMR (300 MHz, $CDCl_3$) δ 8.40 (s, 1H, Ar, C*H*), 8.32 – 8.16 (m, 2H, Ar, C*H*), 8.09 – 7.91 (m, 2H, Ar, C*H*), 7.67 – 7.25 (m, 9H, Ar, C*H*), 4.69 (s, 2H, CH_2), 4.05 (s, 2H, CH_2), 1.87 (s, 1H, N*H*); ^{13}C NMR (100 MHz, $CDCl_3$) δ 140.4 (Ar, *C*), 131.6 (Ar, *C*), 130.4 (Ar, *C*), 129.2 (Ar, *C*H), 128.5 (Ar, *C*H), 127.3 (Ar, *C*H), 127.2 (Ar, *C*H), 126.1 (Ar, *C*H), 125.0 (Ar, *C*H), 124.3 (Ar, *C*H), 54.3 (*C*H_2), 44.9 (*C*H_2); LRMS (ES+) 320.2 ([M+Na]$^+$, 100%).

Data were in agreement with those previously reported.[121]

Ethyl 16-benzyl-17-oxo-16-azapentacyclo[6.6.5.0.0.0]nonadeca-2(7),3,5,9(14),10,12-hexaene-19-carboxylate (89)

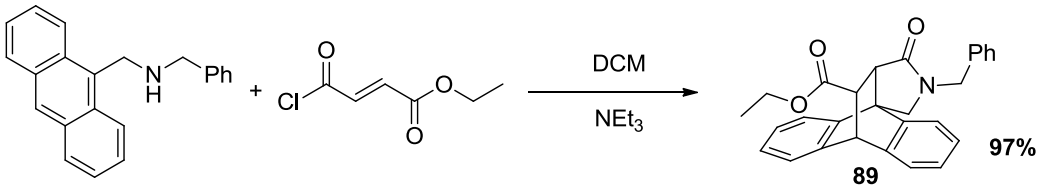

Ethyl fumaroyl chloride (250 mg, 1.5 mmol, 1.2 eq.) was dissolved in dry DCM (10 mL) at RT. A solution of 9-[(*N*-benzylamino)methyl]anthracene (382 mg,

1.3 mmol, 1.0 eq.) and NEt_3 (0.21 mL, 1.5 mmol, 1.2 eq.) in dry DCM (5 mL) was added using a syringe pump over a period of 20 minutes. The reaction was stirred overnight and the solvent was removed *in vacuo*. The crude product was purified by column chromatography with hexane / EtOAc (8 / 2) as eluent to afford ethyl 16-benzyl-17-oxo-16-azapentacyclo[6.6.5.0.0.0]nonadeca-2(7),3,5,9(14),10,12-hexaene-19-carboxylate (**89**) as a white solid (523 mg, 97%). m.p. 78 °C; FTIR (film) ν_{max} 3312, 3064, 2935, 1727, 1690, 1642, 1585, 1538, 1493, 1420, 1304, 1228, 1197, 1028, 820, 754, 698; ^{1}H NMR (400 MHz, $CDCl_3$) δ 7.35 – 7.12 (m, 7H, Ar, C*H*), 7.08 – 6.90 (m, 4H, Ar, C*H*), 6.86 (t, *J* = 7.6 Hz, 1H, Ar, C*H*), 6.58 (d, *J* = 7.6 Hz, 1H, Ar, C*H*), 4.60 - 4.56 (m, 2H, C*H*, CH_2), 4.35 (d, *J* = 14.5 Hz, 1H, CH_2), 4.17 – 3.95 (m, 4H, OCH_2, CH_2), 3.10 (d, *J* = 6.8 Hz, 1H, C*H*), 2.95 (dd, *J* = 6.8, 1.9 Hz, 1H, C*H*), 1.18 (t, *J* = 7.1 Hz, 3H, CH_3); ^{13}C NMR (100 MHz, $CDCl_3$) δ 172.5 (*C*OO), 172.3 (*C*ON), 144.6 (Ar, *C*), 143.2 (Ar, *C*), 139.7 (Ar, *C*), 138.4 (Ar, *C*), 136.4 (Ar, *C*), 129.1 (Ar, *C*H), 128.9 (Ar, *C*H), 128.0 (Ar, *C*H), 126.7 (Ar, *C*H), 126.5 (Ar, *C*H), 126.3 (Ar, *C*H), 126.2 (Ar, *C*H), 125.7 (Ar, *C*H), 123.3 (Ar, *C*H), 121.9 (Ar, *C*H), 119.4 (Ar, *C*H), 61.4 (O*C*H_2), 52.8 (*C*H), 49.5 (*C*), 48.3 (*C*H), 47.4 (*C*H_2), 45.8 (*C*H_2), 44.8 (*C*H), 14.4 (*C*H_3); HRMS (ES+) calculated for $C_{28}H_{25}NO_3Na$ $[M+Na]^+$ 446.1732, found 446.1742.

_N_-tritylaniline[88,122]

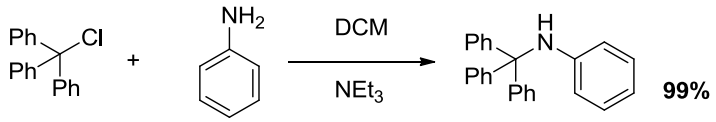

Aniline (4.2 mL, 46.0 mmol, 1.0 eq.) was dissolved in dry DCM (50 mL) at RT. Trityl chloride (14.2 g, 50.0 mmol, 1.1 eq.) and NEt_3 (13.0 mL, 92.0 mmol, 2.0 eq.) were added portionwise over a period of 20 min. The reaction was stirred overnight, diluted with DCM (100 mL), washed with H_2O (3 x 100 mL) and the combined organic fractions were dried over $MgSO_4$. After the solvent was removed *in vacuo* and the crude product was recrystallised from EtOH to afford *N*-tritylaniline as a white solid (16.7 g, 99%). m.p. 146 °C [lit. 151 - 152 °C][88]; ^{1}H NMR (300 MHz, $CDCl_3$) δ 7.40 – 7.13 (m, 15H, Ar, C*H*), 6.90 (t, *J* = 7.4 Hz, 2H, Ar, C*H*), 6.55 (t, *J* = 7.4 Hz, 1H, Ar, C*H*), 6.39 – 6.28 (m, 2H, Ar, C*H*), 5.01 (br s, 1H, N*H*); ^{13}C NMR (100 MHz, $CDCl_3$) δ 146.4 (Ar, *C*), 145.5 (Ar, *C*), 129.4 (Ar, *C*H), 128.3 (Ar, *C*H), 128.0 (Ar, *C*H), 127.4 (Ar, *C*H), 126.9 (Ar, *C*H), 117.4 (Ar, *C*H), 116.2 (Ar, *C*H), 71.6 (*C*); HRMS (ES+) calculated for $C_{25}H_{21}NNa$ $[M+Na]^+$ 358.1572, found 358.1560.

Data were in agreement with previously those reported.[88,122]

Tri(phenyl)methanamine[123,124]

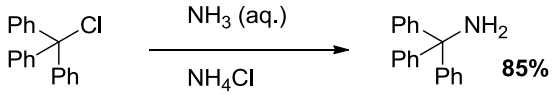

A solution of trityl chloride (27.8 g, 100.0 mmol, 1.0 eq.) in toluene (100 mL) was added dropwise to a vigorously stirred solution of NH_4Cl (5.4 g, 100.0 mmol, 1.0 eq.) in aqueous ammonia (100 mL, 35%). The reaction was stirred for 24 h at RT. The reaction mixture was extracted with EtOAc (3 x 300 mL). The organic combined phases were dried over Na_2SO_4. After the solvent was removed *in vacuo* and the crude product was recrystallised from hexane to afford tri(phenyl)methanamine as a white solid (22 g, 85%). m.p. 100 °C [lit. 102 - 104 °C][123]; ^{1}H NMR (300 MHz, $CDCl_3$) δ 7.47 – 6.82 (m, 15H, Ar, C*H*), 2.18 (br s, 2H, N*H*$_2$); ^{13}C NMR (100 MHz, $CDCl_3$) δ 148.6 (Ar, *C*), 128.1 (Ar, *C*H), 127.9 (Ar, *C*H), 127.3 (Ar, *C*H), 126.6 (Ar, *C*H), 66.3 (*C*); HRMS (ES+) calculated for $C_{19}H_{17}NNa$ $[M+Na]^+$ 282.1259, found 282.1260.

Data were in agreement with those previously reported.[123,124]

(*E*)-ethyl 4-oxo-4-(tritylamino)but-2-enoate (91)

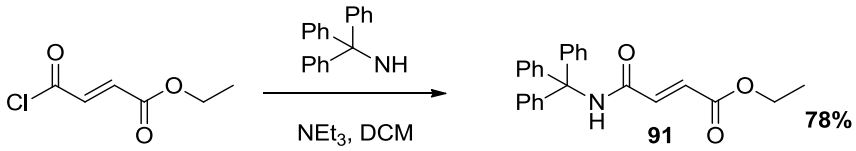

Ethyl fumaroyl chloride (18 mg, 0.11 mmol, 1.1 eq.) was dissolved in dry DCM (10 mL) at RT. A solution of tri(phenyl)methanamine (26 mg, 0.10 mmol, 1.0 eq.) and NEt_3 (15 μL, 0.11 mmol, 1.1 eq.) in dry DCM (0.5 mL) was added using a syringe pump over a period of 2 h. The reaction was stirred overnight and the solvent was removed *in vacuo*. The crude product was purified by column chromatography with pet / EtOAc (9/1) as eluent to afford (*E*)-ethyl 4-oxo-4-(tritylamino)but-2-enoate (**91**) as a white solid (30 mg, 78%). m.p. 138 °C; FTIR (film) ν_{max} 3238, 3050, 3024, 1716, 1681, 1659, 1637, 1525, 1490, 1446, 1293, 1265, 1158, 1036, 905, 767, 730, 697; ^{1}H NMR (300 MHz, $CDCl_3$) δ 7.42 – 7.15 (m, 15H, Ar, C*H*), 7.06 (d, *J* = 15.3 Hz, 1H, C*H*), 7.01 (br s, 1H, N*H*), 6.79 (d, *J* = 15.3 Hz, 1H, C*H*), 4.22 (q, *J* = 7.1 Hz, 2H, OCH_2), 1.31 (t, *J* = 7.1 Hz, 3H, CH_3); ^{13}C NMR (100 MHz, $CDCl_3$) δ 165.7 (*C*OO), 162.7 (*C*ONH), 144.2 (Ar, *C*), 137.0 (*C*H), 131.1 (*C*H), 128.9 (Ar, *C*H), 128.8 (Ar, *C*H), 128.2 (Ar, *C*H), 128.1 (Ar, *C*H), 128.0 (Ar, *C*H), 127.4 (Ar, *C*H), 126.9 (Ar, *C*H), 71.2 (*C*), 61.3 (O*C*H_2), 14.3 (*C*H_3); HRMS (ES+) calculated for $C_{25}H_{23}NO_3Na$ $[M+Na]^+$ 408.1576, found 408.1587.

(*E*)-4-oxo-4-(tritylamino)but-2-enoic acid (92)

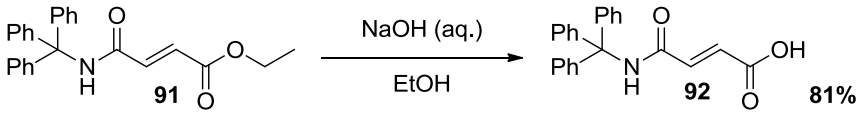

A solution of $LiOH \cdot H_2O$ (1.2 g, 28.3 mmol, 2.0 eq.) in water (29 mL) was added to a solution of (*E*)-ethyl 4-oxo-4-(tritylamino)but-2-enoate (**91**) (4.0 g, 10.6 mmol, 1.0 eq.) in THF (87 mL). The reaction mixture was heated to 60 °C. After 32 h the reaction mixture was cooled and poured into a solution of 1 M HCl (60 mL). The aqueous layer was extracted with Et_2O (3 x 80 mL) and the combined organic fractions were dried over $MgSO_4$ and concentrated under reduced pressure. The resulting solid was recrystallised from hexane / Et_2O / DCM (29 / 70 / 1) to afford (*E*)-4-oxo-4-(tritylamino)but-2-enoic acid (**92**) (3 g, 81%) as a white solid. m.p. 195 °C; FTIR (film) ν_{max} 3029, 1698, 1641, 1522, 1491, 1447, 1311, 1185, 1036, 970, 904, 768, 697; ^{1}H NMR (400 MHz, MeOD / $CDCl_3$) δ 7.30 – 7.11 (m, 15H, Ar, C*H*), 7.07 (d, *J* = 15.4 Hz, 1H, C*H*), 6.64 (d, *J* = 15.4 Hz, 1H, C*H*); ^{13}C NMR (100 MHz, MeOD / $CDCl_3$) δ 167.4 (*C*OOH), 163.2 (*C*ONH), 144.0 (Ar, *C*), 137.2 (*C*H), 130.9 (*C*H), 128.6 (Ar, *C*H), 127.9 (Ar, *C*H), 127.1 (Ar, *C*H), 71.0 (*C*);^{13}C NMR (100 MHz, MeOD / $CDCl_3$) δ 127.1, 127.9 (Ar, *C*H), 128.6 (Ar, *C*H), 130.9 (Ar, *C*H), 137.2 (Ar, *C*H), 144.0, 163.2, 167.4; HRMS (ES+) calculated for $C_{23}H_{19}NO_3Na$ $[M+Na]^+$ 380.1263, found 340.1275.

(*E*)-*N*^{1},*N*$^{1'}$-(propane-1,3-diyl)bis(*N*^{6}-tritylfumaramide) (93)

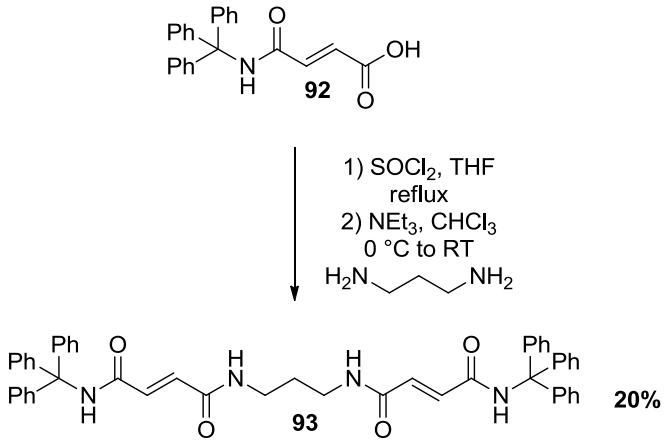

(*E*)-4-oxo-4-(tritylamino)but-2-enoic acid (**92**) (716 mg, 2.0 mmol, 4.0 eq.) and thionyl chloride (1 mL) were dissolved in THF (5 mL) and heated at reflux for 3 h. The crude acid chloride formed was evaporated to dryness, the resulting residue was dissolved in DCM (10 mL) and cooled to 0°C. NEt_3 (0.3 mL, 2.0 mmol, 4.0 eq.) and 1,3-diaminopropane (42 μL, 0.5 mmol, 1.0 eq.) were added using a syringe pump over a period of 2 h. The reaction was stirred overnight and the solvent was removed *in vacuo*. The crude product was purified by column chromatography with EtOAc / MeOH (95 / 5) as eluent to give the title product as a yellow solid (76 mg, 20%). m.p. 208 °C; FTIR (film) ν_{max} 3331, 3251, 3027, 1681, 1635, 1526, 1489, 1448, 1333, 1218, 1181, 978, 903, 770, 699; ^{1}H NMR (400 MHz, d_6-DMSO) δ 9.18 (s, 2H, N*H*), 8.42 – 8.22 (m, 2H, CH_2N*H*), 7.36 – 7.12 (m, 32H, 30 Ar, C*H*, 2 C*H*), 6.65 (d, *J* = 15.2 Hz, 2H, C*H*), 3.15 (dt, *J* = 12.6, 6.5 Hz, 4H, CH_2CH_2NH), 1.68 – 1.47 (m, 2H, CH_2); ^{13}C NMR (100 MHz, d_6-DMSO) δ 163.8 (*C*O), 163.5 (*C*O), 144.4 (Ar, *C*), 133.6 (*C*H), 132.8 (*C*H), 128.5 (Ar, *C*H), 127.5

(Ar, *C*H), 126.4 (Ar, *C*H), 69.6 (*C*), 36.6 (CH_2CH_2NH), 28.9 (CH_2); HRMS (ES+) calculated for $C_{49}H_{44}N_4O_4Na$ $[M+Na]^+$ 775.3226, found 775.3274.

(*E*)-N^1,$N^{1'}$-(propane-1,3-diyl)bis(N^6-tritylfumaramide) [2]rotaxane (94)

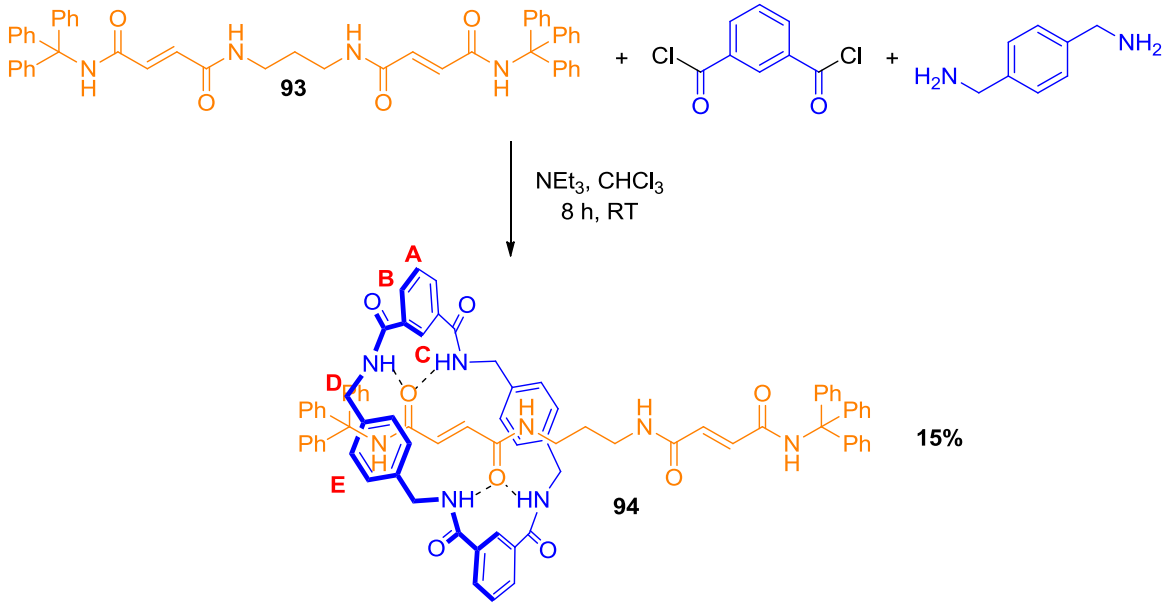

Et_3N (0.5 mL, 3.8 mmol, 48.0 eq.) was added to a stirred solution of (*E*)-N^1,$N^{1'}$-(propane-1,3-diyl)bis(N^4-tritylfumaramide) (**93**) (60 mg, 0.08 mmol, 1.0 eq.) in anhydrous $CHCl_3$ (30 mL). The solution was stirred vigorously whilst solutions of *p*-xylylene diamine (261 mg, 1.9 mmol, 24.0 eq.) in anhydrous $CHCl_3$ (10 mL) and isophthaloyl dichloride (390 mg, 1.9 mmol, 24.0 eq.) in anhydrous $CHCl_3$ (10 mL) were simultaneously added over a period of 4 h using a motor-driven syringe pump. After a further 4 h period the resulting suspension was filtered through a Celite® pad and the solvent removed under reduced pressure. The crude product was purified by HPLC to afford (*E*)-N^1,$N^{1'}$-(propane-1,3-diyl)bis(N^6-

tritylfumaramide) [2]rotaxane (**94**) as a white solid (15 mg, 15%). HPLC (t = 0 → 30 min, 75 : 25 MeOH : H_2O; t = 30 → 40 min, 75 → 95% H_2O in MeOH, t = 40 → 60 min, 95 : 5 MeOH : H_2O): R_t 42.35; m.p. 232 °C; FTIR (film) ν_{max} 3287, 3060, 2925, 2853, 1636, 1520, 1491, 1447, 1316, 1185, 1036, 972, 901, 749, 698; ^{1}H NMR (400 MHz, d_6-DMSO) δ 9.19 (s, 2H, N*H*), 8.42 (br s, 2H, Ar, C*H*, H_C), 8.33 (t, *J* = 5.2 Hz, 6H, N*H*), 8.00 (dd, *J* = 7.7, 1.4 Hz, 4H, Ar, C*H*, H_B), 7.60 (t, *J* = 7.7 Hz, 2H, Ar, C*H*, H_A), 7.28 – 7.11 (m, 30H, Ar, C*H*), 6.92 (s, 8H, Ar, C*H*, H_E), 6.74 (d, *J* = 15.1 Hz, 2H, C*H*), 6.12 (d, *J* = 15.1 Hz, 2H, C*H*), 4.28 (d, *J* = 5.0 Hz, 8H, CH_2, H_D), 3.08 (dd, *J* = 12.7, 6.6 Hz, 4H, CH_2CH_2NH), 1.64 – 1.49 (m, 2H, CH_2); ^{13}C NMR (100 MHz, d_6-DMSO) δ 165.9 (*C*ON), 164.6 (*C*ON), 163.8 (*C*ON), 144.2 (Ar, *C*), 136.7 (Ar, *C*), 134.4 (Ar, *C*), 132.3 (*C*H), 131.3 (*C*H), 130.6 (Ar, *C*H), 128.7 (Ar, *C*H), 128.5 (Ar, *C*H), 127.5 (Ar, *C*H), 126.5 (Ar, *C*H), 125.3 (Ar, *C*H), 69.8 (*C*), 43.1 (*C*H_2), 36.9 (CH_2CH_2NH), 28.5 (*C*H_2); LRMS (ES+) 1308.0 ([M+Na]$^+$, 100%).

(*E*)-ethyl 4-oxo-4-(tritylphenylamino)but-2-enoate (95)

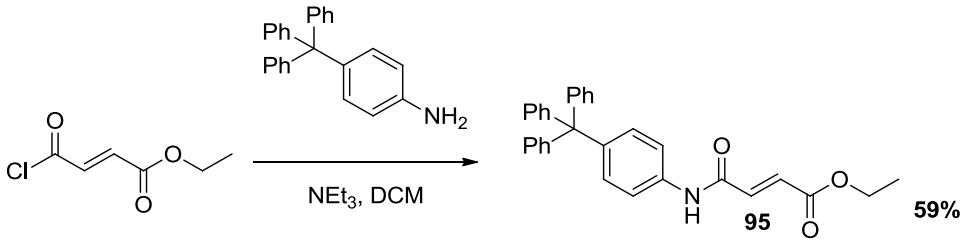

Ethyl fumaroyl chloride (1.0 g, 6.0 mmol, 1.1 eq.) was dissolved in dry DCM (40 mL) at RT. A solution of 4-tritylaniline (1.9 g, 5.5 mmol, 1.0 eq.) and NEt_3 (1.0 mL, 6.0 mmol, 1.1 eq.) in dry DCM (10 mL) was added using a syringe pump

over a period of 2 h. The reaction was stirred overnight and the solvent was removed *in vacuo*. The crude product was purified by column chromatography with pet / EtOAc (9/1) as eluent to afford (*E*)-ethyl 4-oxo-4-(tritylphenylamino)but-2-enoate (**95**) as a white solid (1.5 g, 59%). m.p. 112 °C; FTIR (film) ν_{max} 3031, 1721, 1672, 1654, 1599, 1546, 1491, 1442, 1349, 1277, 1039, 984, 827, 745, 700; ^{1}H NMR (400 MHz, $CDCl_3$) δ 8.25 (s, 1H, N*H*), 7.54 (d, *J* = 8.8 Hz, 2H, Ar, C*H*), 7.39 – 7.09 (m, 18H, 17 Ar, C*H*, 1 C*H*), 6.98 (d, *J* = 15.3 Hz, 1H, C*H*), 4.28 (q, *J* = 7.1 Hz, 2H, OCH_2), 1.33 (t, *J* = 7.1 Hz, 3H, CH_3); ^{13}C NMR (100 MHz, $CDCl_3$) δ 166.0 (*C*OO), 161.8 (*C*ONH), 146.7 (Ar, *C*), 143.8 (Ar, *C*), 137.1 (*C*H), 135.4 (Ar, *C*), 131.9 (Ar, *C*H), 131.3 (*C*H), 131.2 (Ar, *C*H), 127.7 (Ar, *C*H), 126.1 (Ar, *C*H), 119.3 (Ar, *C*H), 64.7 (*C*), 61.6 (O*C*H_2), 14.2 (*C*H_3); HRMS (ES+) calculated for $C_{31}H_{27}NO_3Na$ $[M+Na]^+$ 484.1889, found 484.1887.

(*E*)-4-oxo-4-(tritylphenylamino)but-2-enoic acid (96)

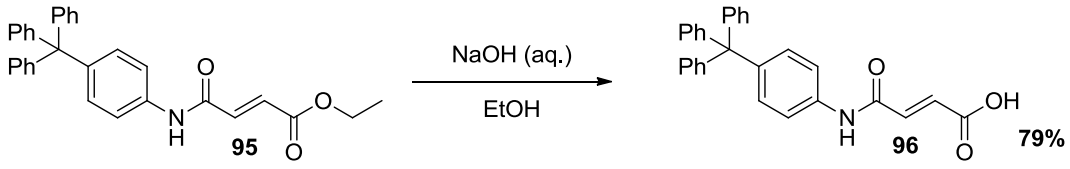

A solution of LiOH·H_2O (271 mg, 6.5 mmol, 2.0 eq.) in water (10 mL) was added to a solution of (*E*)-ethyl 4-oxo-4-(tritylphenylamino)but-2-enoate (**95**) (1.5 g, 3.2 mmol, 1.0 eq.) in THF (43 mL). The reaction mixture was heated to 60 °C. After 32 h, the reaction mixture was cooled and poured into 1 M HCl (30 mL). The aqueous layer was extracted with Et_2O (3 x 40 mL) and the combined organic

fractions were dried over $MgSO_4$ and concentrated under reduced pressure. The resulting solid was recrystallised from hexane / Et_2O / DCM (29 / 70 / 1) to afford (*E*)-4-oxo-4-(tritylphenylamino)but-2-enoic acid (**96**) (1.11 g, 79%) as a white solid. m.p. 216 °C; FTIR (film) ν_{max} 3655, 3300, 3059, 1736, 1703, 1666, 1643, 1597, 1540, 1490, 1441, 1406, 1345, 1290, 1179, 973, 830, 749, 697; ^{1}H NMR (300 MHz, MeOD) δ 7.59 (s, 1H, N*H*), 7.53 (d, *J* = 8.9 Hz, 2H, Ar, C*H*), 7.33 – 7.01 (m, 18H, 17 Ar, C*H*, 1 C*H*), 6.81 (d, *J* = 15.4 Hz, 1H, C*H*), 3.35 (s, 1H, O*H*); ^{13}C NMR (100 MHz, MeOD) δ 168.1 (*C*OOH), 163.6 (*C*ONH), 147.4 (Ar, *C*), 144.1 (Ar, *C*), 137.8 (*C*H), 136.6(Ar, *C*), 132.2 (Ar, *C*H), 131.7 (Ar, *C*H), 128.1 (Ar, *C*H), 126.6 (Ar, *C*H), 119.8 (Ar, *C*H) 65.3 (*C*); HRMS (ES+) calculated for $C_{29}H_{23}NO_3Na$ $[M+Na]^+$ 456.1576, found 456.1588.

(*E*)-*N*^{1},*N*$^{1'}$-(propane-1,3-diyl)bis(*N*^{4}-(4-tritylphenyl)fumaramide) (97)

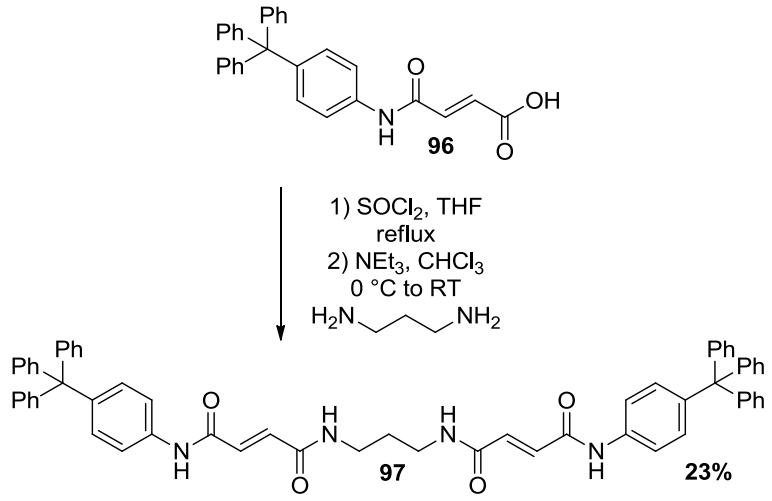

(*E*)-4-oxo-4-(tritylphenylamino)but-2-enoic acid (**96**) (1.1 g, 2.6 mmol, 2.6 eq.) and thionyl chloride (1.5 mL) were dissolved in THF (30 mL) and heated at reflux for 3 h. The crude acid chloride formed was evaporated to dryness, the resulting residue was dissolved in DCM (25 mL) and cooled to 0 °C. NEt_3 (0.4 mL, 2.6 mmol, 2.6 eq.) and 1,3-diaminopropane (83 μL, 1.0 mmol, 1.0 eq.) were added using a syringe pump over a period of 2 h. The reaction was stirred overnight and the solvent was removed *in vacuo*. The crude product was purified by column chromatography with EtOAc / MeOH (95 / 5) as eluent to give the title product as a brown solid (208 mg, 23%). m.p. 154 °C; FTIR (film) ν_{max} 1726, 1689, 1598, 1499, 1456, 1382, 1324, 1305, 1200, 1029, 922, 863, 754, 725, 706, 688; ^{1}H NMR (400 MHz, MeOD) δ 7.53 (s, 4H, Ar, C*H*), 7.51 (s, 2H, N*H*), 7.25 – 7.12 (m, 34H, Ar, C*H*), 7.00 (d, *J* = 15.1 Hz, 2H, C*H*), 6.91 (d, *J* = 15.1 Hz, 2H, C*H*), 3.37 – 3.32 (m, 4H, CH_2CH_2NH), 1.82 - 1.77 (m, 2H, CH_2); ^{13}C NMR (100 MHz, MeOD) δ 166.1 (*C*O), 147.3 (Ar, *C*), 143.9 (Ar, *C*), 136.5 (Ar, *C*), 133.9 (*C*H), 132.2 (*C*H), 131.6

(Ar, *C*H), 128.0 (Ar, *C*H), 126.5 (Ar, *C*H), 119.6 (Ar, *C*H), 65.2 (*C*), 49.7 (CH_2CH_2NH), 37.6 (CH_2); HRMS (ES+) calculated for $C_{61}H_{52}N_4O_4Na$ $[M+Na]^+$ 927.3886, found 927.3902.

4.6 Experimental for Section 2.6

Bis-*p*-xylyl-bis-*m*-xylyldiamine (102)

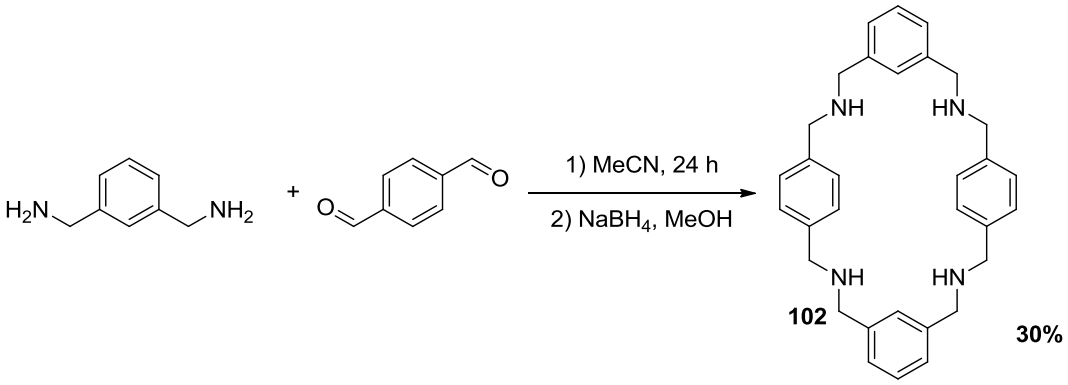

m-Xylylenediamine (1.2 g, 9.0 mmol, 1.0 eq.) in MeCN (280 mL) was added dropwise over a period of 1.5 h using a dropping funnel to a solution of terephthalaldehyde (1.2 g, 9 mmol, 1.0 eq.) in MeCN (150 mL). The mixture was stirred for 24 h at RT. The resulting precipitate was filtered and washed with cold Et_2O (15 mL). The crude tetraimine (1.5 g, 3.2 mmol) was dissolved in MeOH (150 mL) and heated to 45 ºC. $NaBH_4$ (890 mg, 24.0 mmol, 2.7 eq.) was added portionwise and the reaction mixture was stirred for an additional hour. The reaction mixture was concentrated *in vacuo*. Water (10 mL) and DCM (100 mL) were added to the resulting residue and the product was extracted with EtOAc (3 x

200 mL). The combined organic phases were dried over $MgSO_4$ and the solvent was removed *in vacuo* to afford bis-*p*-xylyl-bis-*m*-xylyldiamine (**102**) as a white solid (1.3 g, 30%). m.p. 143 °C; FTIR (film) ν_{max} 3021, 2835, 2806, 1644, 1606, 1587, 1449, 1358, 906, 845, 824, 779, 725, 693; ^{1}H NMR (300 MHz, $CDCl_3$) δ 7.45 (s, 2H, N*H*), 7.34 (s, 8H, Ar, C*H*), 7.32 – 7.28 (m, 3H, Ar, C*H*), 7.22 (d, *J* = 8.0 Hz, 5H, Ar, C*H*), 3.82 (s, 8H, CH_2), 3.79 (s, 8H, CH_2); ^{13}C NMR (100 MHz, $CDCl_3$) δ 140.7 (Ar, *C*), 139.2 (Ar, *C*), 128.5 (Ar, *C*H), 127.6 (Ar, *C*H), 127.1 (Ar, *C*H), 52.7 (*C*H_2), 52.5 (*C*H_2); HRMS (ES+) calculated for $C_{32}H_{37}N_4$ $[M+H]^+$ 477.3018, found 477.3015.

Molecular cage (105)

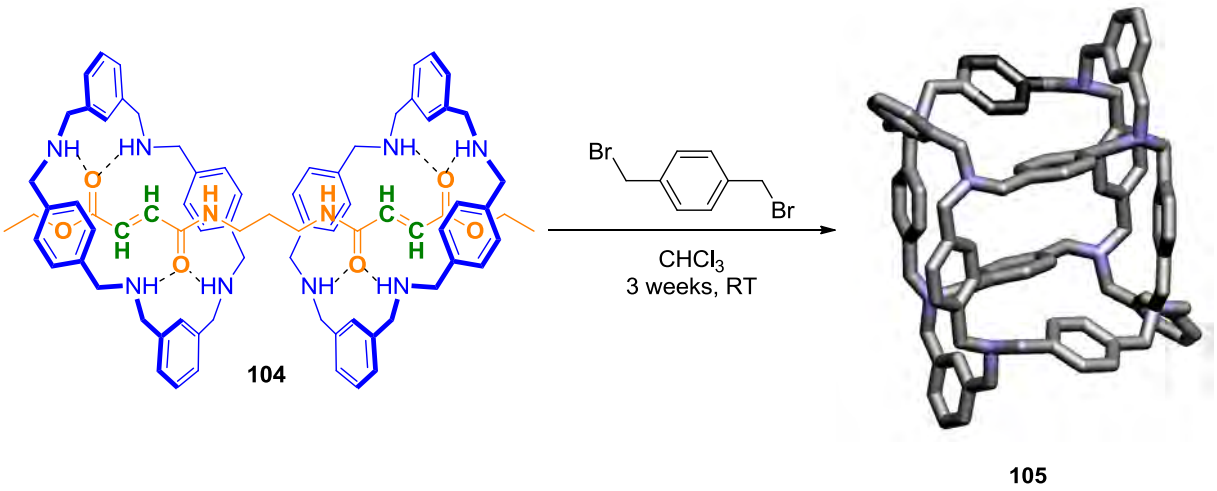

104

105

(2*E*,2'*E*)-diethyl 4,4'-(propane-1,3-diylbis(azanediyl))bis(4-oxobut-2-enoate) (**33**) (33 mg, 0.1 mmol, 1.0 eq.) was dissolved in $CHCl_3$ (10 mL). Bis-*p*-xylyl-bis-*m*-xylyldiamine **102** (95 mg, 0.2 mmol, 2.0 eq.) was added and the solution was stirred for 20 min at RT followed by addition of α,α'-dibromo-*p*-xylene (220 mg,

0.8 mmol, 8.0 eq.). The reaction was monitored via MALDI spectrometry. After 3 weeks the solvent was removed *in vacuo* and the residue was recrystallised from MeCN (10 mL). The solid was purified by column chromatography with $CHCl_3$ / MeOH (95 / 5) as eluent to afford the enriched molecular cage **105** (37 mg, 27%, however not completely pure). m.p. 172 °C; FTIR (film) ν_{max} 3345, 2926, 1717, 1666, 1547, 1436, 1366, 1297, 1163, 1019, 974, 807, 751, 700; ^{1}H NMR (400 MHz, $CDCl_3$) δ 8.03 – 6.89 (m, 48H, Ar, C*H*), 4.32 – 3.08 (m, 48H, CH_2); ^{13}C NMR (100 MHz, $CDCl_3$) δ 140.4 (Ar, *C*), 140.1 (Ar, *C*), 139.9 (Ar, *C*), 138.9 (Ar, *C*), 138.6 (Ar, *C*), 130.3 (Ar, *C*H), 130.1 (Ar, *C*H), 129.4 (Ar, *C*H), 129.0 (Ar, *C*H), 128.6 (Ar, *C*H), 128.0 (Ar, *C*H), 127.7 (Ar, *C*H), 127.1 (Ar, *C*H), 58.9 (*C*H_2), 58.2 (*C*H_2), 58.0 (*C*H_2), 57.8 (*C*H_2). LRMS (MALDI+) 1363.0 ($[M+H]^+$, 100%), 1261.0 (8%).

(2*E*,2'*E*)-di(prop-2-yn-1-yl) 4,4'-(propane-1,3-diylbis(azanediyl))bis(4-oxobut-2-enoate) (111)

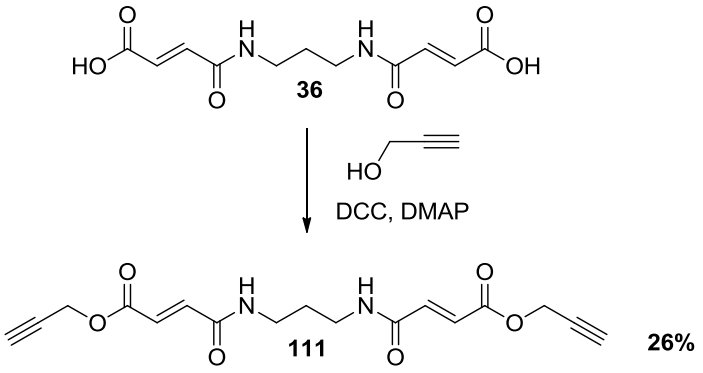

A solution of (2*E*,2'*E*)-4,4'-(propane-1,3-diylbis(azanediyl))bis(4-oxobut-2-enoic acid) (**36**) (270 mg, 1.0 mmol, 1.0 eq.) in DCM (1 mL) was added to a solution of propargyl alcohol (60 μL, 2.0 mmol, 2.0 eq.), *N,N*'-dicyclohexylcarbodiimide (453 mg, 2.2 mmol, 2.2 eq.) and 4-(dimethylamino)pyridine (25 mg, 0.2 mmol, 0.2 eq.) in DCM (10 mL) at 4 ºC. After being stirred for 4 h at 0 ºC, the reaction mixture was allowed to warm to RT. The reaction was stirred overnight and the solvent was removed *in vacuo*. The crude product was purified by column chromatography with EtOAc / pet (1 / 1) as eluent to afford of (2*E*,2'*E*)-di(prop-2-yn-1-yl) 4,4'-(propane-1,3-diylbis(azanediyl))bis(4-oxobut-2-enoate) (**111**) as a white solid (90 mg, 26%). m.p. 145 °C; FTIR (film) ν_{max} 3296, 1718, 1666, 1632, 1547, 1370, 1291, 1158, 1032, 984, 665; ^{1}H NMR (300 MHz, d_6-DMSO) δ 8.60 – 8.58 (m, 2H, N*H*), 7.05 (d, *J* = 15.5 Hz, 2H, C*H*), 6.58 (d, *J* = 15.5 Hz, 2H, C*H*), 4.83 – 4.82 (m, 4H, OCH_2), 3.64 – 3.62 (m, 2H, C*H*), 3.24 – 3.13 (m, 4H, CH_2NH), 1.67 – 1.57 (m, 2H, $CH_2CH_2CH_2$); ^{13}C NMR (100 MHz, MeOD / $CDCl_3$) δ 165.4 (*C*OO), 165.2 (*C*ON), 138.0 (*C*H), 129.3 (*C*H), 77.4 (*C*), 75.9 (*C*H), 53.0 (O*C*H_2),

37.5 (*C*H_2NH), 29.0 (*C*H_2); HRMS (ES+) calculated for $C_{17}H_{18}N_2O_6Na$ $[M+Na]^+$ 369.1063, found 369.1060.

(Azidomethanetriyl)tribenzene[125,126]

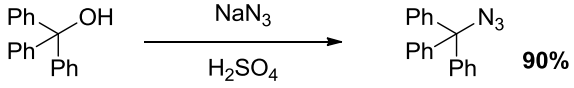

H_2SO_4 (conc., 9 mL) was added dropwise using a pipette to a suspension of sodium azide (4.2 g, 64.5 mmol, 1.7 eq.) in $CHCl_3$ (13 mL) at 0 ºC. The reaction mixture was allowed to warm to RT and a solution of triphenylmethanol (10.0 g, 38.5 mmol, 1.0 eq.) in $CHCl_3$ (40 mL) was added via dropping funnel over a period of 1 h. After additional 30 min of stirring, ice (75 g) was slowly added and the mixture was stirred overnight. The aqueous phase was extracted with Et_2O (3 x 100 mL) and the combined organic layers were dried over $MgSO_4$. The solvent was removed *in vacuo* to afford (azidomethanetriyl)tribenzene as a yellow solid (9.87 g, 90%). m.p. 60 °C [lit. 60 - 62 °C][125]; ^{1}H NMR (300 MHz, $CDCl_3$) δ 7.51 – 7.32 (m, 1H, Ar, C*H*); ^{13}C NMR (100 MHz, $CDCl_3$) δ 143.1 (Ar, *C*), 128.4 (Ar, *C*H), 128.1 (Ar, *C*H), 127.6 (Ar, *C*H), 82.1 (*C*); HRMS (ES+) calculated for $C_{19}H_{16}$ $[M-N_3+H]^+$ 243.1174, found 243.1175.

Data were in agreement with those previously reported.[125,126]

(2*E*,2'*E*)-diethyl 4,4'-(propane-1,3-diylbis(methylazanediyl))bis(4-oxobut-2-enoate) (113)

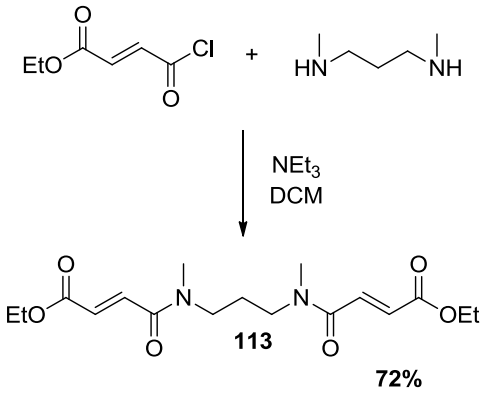

Ethyl fumaroyl chloride (1.8 g, 11.0 mmol, 2.2 eq.) was dissolved in dry DCM (100 mL) at RT. A solution of dimethyl-1,3-propanediamine (0.6 mL, 5.0 mmol, 1.0 eq.) and NEt_3 (1.5 mL, 11.0 mmol, 2.2 eq.) in dry DCM (10 mL) was added using a syringe pump over a period of 2 h. The reaction was stirred overnight and the solvent was removed *in vacuo*. The crude product was purified by column chromatography using $CHCl_3$ / MeOH (94 / 6) as eluent to afford (2*E*,2'*E*)-diethyl 4,4'-(propane-1,3-diylbis(methylazanediyl))bis(4-oxobut-2-enoate) (**113**) as a white solid (2.80 g, 72%). m.p. 168 °C; FTIR (film) ν_{max} 3529, 3469, 2987, 2941, 1718, 1620, 1484, 1415, 1286, 1267, 1174, 1025, 886, 765, 743; ^{1}H NMR (300 MHz, $CDCl_3$) δ 7.26 – 7.11 (m, 2H, C*H*), 6.68 – 6.45 (m, 2H, C*H*), 4.04 (q, *J* = 7.1 Hz, 4H, OCH_2CH$_3$), 3.40 – 3.16 (m, 4H, CH_2NH), 2.97 – 2.82 (m, 6H, NCH_3), 1.76 – 1.66 (m, 2H, CH$_2$CH_2CH$_2$), 1.10 (t, *J* = 7.1 Hz, 6H, CH_3); ^{13}C NMR (100 MHz, $CDCl_3$) δ 165.1 (*C*OO), 164.5 (*C*ON), 133.5 (*C*H), 133.3 (*C*H), 131.1 (*C*H), 130.8 (*C*H), 60.7 (O*C*H$_2$CH$_3$), 47.5 (*C*H$_2$NH), 45.4 (*C*H$_2$NH), 45.0 (*C*H$_2$NH), 35.2 (N*C*H$_3$),

33.5 (N*C*H_3), 26.3 (*C*H_2), 24.2 (*C*H_2), 13.8 (*C*H_3); HRMS (ES+) calculated for $C_{17}H_{26}N_2O_6Na$ $[M+Na]^+$ 377.1689, found 377.1692.

(2*E*,2'*E*)-4,4'-(propane-1,3-diylbis(methylazanediyl))bis(4-oxobut-2-enoic acid) (114)

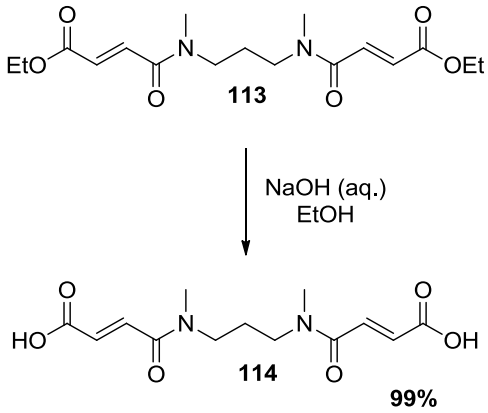

(2*E*,2'*E*)-diethyl 4,4'-(propane-1,3-diylbis(methylazanediyl))bis(4-oxobut-2-enoate) (**113**) (354 mg, 1.0 mmol, 1.0 eq.) was dissolved in EtOH (35 mL). Then NaOH (96 mg, 2.4 mmol, 2.4 eq.) dissolved in water (3 mL) was added dropwise over a period of 5 minutes via a syringe. The reaction was stirred for 16 h at RT and monitored by TLC. The reaction mixture was acidified with 1 M HCl (5 mL), extracted with DCM (3 x 80 mL) and washed with brine (80 mL). The organic layers were combined, dried over $MgSO_4$ and concentrated under reduced pressure to afford (2*E*,2'*E*)-4,4'-(propane-1,3-diylbis(methylazanediyl))bis(4-oxobut-2-enoic acid) (**114**) as a yellow solid (295 mg, 99%). m.p. >256 °C (decomp); FTIR (film) ν_{max} 3322, 2937, 1716, 1613, 1594, 1404, 1271, 1174, 1029, 971, 765; ^{1}H NMR (400 MHz, d_6-DMSO) δ 7.42 – 7.25 (m, 2H, C*H*), 6.59 – 6.41

(m, 2H, C*H*), 3.42 – 3.32 (m, 4H, CH_2NH), 3.07 – 2.90 (m, 6H, NCH_3), 1.77 – 1.68 (m, 2H, $CH_2CH_2CH_2$); ^{13}C NMR (100 MHz, d_6-DMSO) δ 166.4 (*C*OO), 163.9 (*C*ON), 134.4 (*C*H), 134.1 (*C*H), 131.0 (*C*H), 47.1 (CH_2NH), 46.6 (CH_2NH), 45.0 (CH_2NH), 44.6 (CH_2NH), 35.0 (NCH_3), 33.3 (NCH_3), 26.1 (CH_2); HRMS (ES-) calculated for $C_{13}H_{17}N_2O_6$ $[M-H]^-$ 297.1087, found 297.1102.

(2*E*,2'*E*)-di(prop-2-yn-1-yl) 4,4'-(propane-1,3-diylbis(methylazanediyl))bis(4-oxobut-2-enoate) (115)

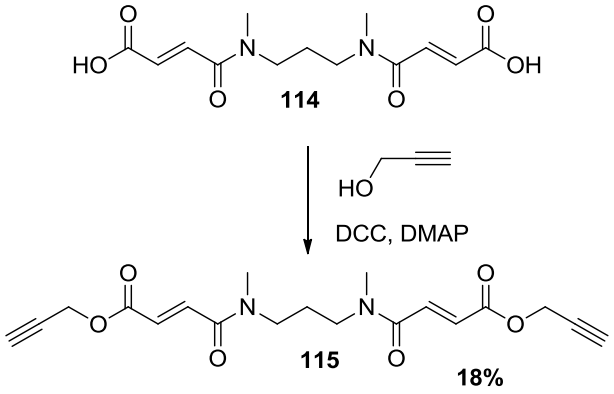

A solution of (2*E*,2'*E*)-4,4'-(propane-1,3-diylbis(methylazanediyl))bis(4-oxobut-2-enoic acid) (**114**) (536 mg, 1.8 mmol, 1.0 eq.) in DCM (1 mL) was added to a solution of propargyl alcohol (0.12 mL, 4.0 mmol, 2.0 eq.), *N,N*'-dicyclohexylcarbodiimide (906 mg, 4.4 mmol, 2.2 eq.) and 4-(dimethylamino) pyridine (50 mg, 0.4 mmol, 0.2 eq.) in DCM (10 mL) at 4 ºC. After being stirred for 4 h at 0 ºC, the reaction mixture was allowed to warm to RT. The reaction was stirred overnight and the solvent was removed *in vacuo*. The crude product was purified by column chromatography with EtOAc / pet (7 / 3) as eluent to afford

(2*E*,2'*E*)-di(prop-2-yn-1-yl) 4,4'-(propane-1,3-diylbis(methylazanediyl)) bis(4-oxobut-2-enoate) (**115**) as a white solid (121 mg, 18%). m.p. 128 °C; FTIR (film) ν_{max} 3266, 2940, 1723, 1649, 1617, 1488, 1404, 1273, 1157, 1029, 970, 763, 696; ^{1}H NMR (300 MHz, $CDCl_3$) δ 7.55 – 7.34 (m, 2H, C*H*), 6.93 – 6.73 (m, 2H, C*H*), 4.82 (br s, 4H, OCH_2), 3.57 – 3.37 (m, 4H, CH_2NH), 3.16 – 3.05 (m, 6H, NCH_3), 2.60 – 2.44 (m, 2H, C*H*), 1.96 – 1.82 (m, 2H, $CH_2CH_2CH_2$); ^{13}C NMR (100 MHz, $CDCl_3$) δ 164.9 (*C*OO), 164.3 (*C*ON), 135.0 (*C*H), 134.6 (*C*H), 130.7 (*C*H), 130.3 (*C*H), 77.3 (*C*), 75.4 (*C*H), 52.7 (O*C*H_2), 48.0 (*C*H_2N), 46.0 (*C*H_2N), 45.6 (*C*H_2N), 35.9 (N*C*H_3), 35.8 (N*C*H_3), 34.2 (N*C*H_3), 26.9 (*C*H_2), 24.7 (*C*H_2); HRMS (ES+) calculated for $C_{19}H_{22}N_2O_6Na$ $[M+Na]^+$ 397.1379, found 397.1376.

1,2-Hydrazodicarboxamide-allyl-thread (117)

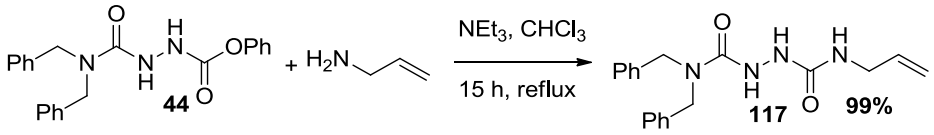

Phenyl *N*,*N*-dibenzylaminocarbonylhydrazinecarboxylate (**44**) (334 mg, 0.9 mmol, 2 eq.) and NEt_3 (0.4 mL, 2.9 mmol, 6.4 eq.) were added to a stirred solution of allylamine (33 μL, 0.45 mmol, 1 eq.) in $CHCl_3$ (25 mL). The reaction mixture was stirred at reflux for 15 h. The reaction mixture was then concentrated under reduced pressure and purified by column chromatography on silica gel using a DCM / MeOH (98 / 2) mixture as eluent to give the title product as a white solid (162 mg, 99%). m.p. 83 °C; FTIR (film) ν_{max} 3245, 3031, 1655, 1533, 1495, 1453,

1405, 1361, 1217, 1079, 1028, 912, 744, 696; ^{1}H NMR (300 MHz, $CDCl_3$) δ 7.09 – 6.90 (m, 10H, Ar, C*H*), 5.57 (s, 1H, N*H*), 5.51 – 5.38 (m, 1H, CH_2CH), 4.89 – 4.67 (m, 2H, CH_2CH), 4.20 (s, 4H, CH_2), 3.45 – 3.31 (m, 2H, $NHCH_2$); ^{13}C NMR (100 MHz, $CDCl_3$) δ 159.7 (*C*ON), 159.4 (*C*ON), 136.9 (Ar, *C*), 135.0 (CH_2CH), 128.8 (Ar, *C*H), 127.5 (Ar, *C*H), 127.4 (Ar, *C*H), 115.3 (CH_2CH), 49.9 (CH_2), 42.3 (CH_2NH); HRMS (ES+) calculated for $C_{19}H_{22}N_4O_2Na$ $[M+Na]^+$ 361.1640, found 361.1646.

(*E*)-N^1-allyl-N^2,N^2-dibenzyldiazene-1,2-dicarboxamide (118)

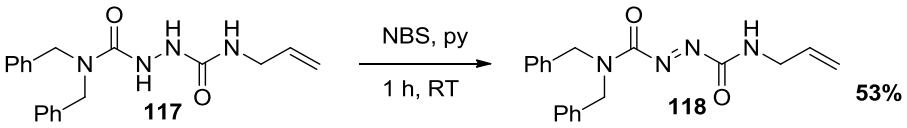

Pyridine (40 μL, 0.47 mmol, 1.1 eq.) and NBS (77 mg, 0.43 mmol, 1.0 eq.) were added to a solution of 1,2-hydrazodicarboxamide-allyl-thread (**117**) (144 mg, 0.42 mmol, 1.0 eq.) in dry DCM (10 mL). The resulting solution was stirred for 1 h at RT. It was then diluted with DCM (5 mL) and sequentially washed with H_2O (2 x 10 mL), a saturated aqueous solution of $Na_2S_2O_3$ (10 mL) and a saturated aqueous solution of $NaHCO_3$ (2 x 10 mL). The combined organic phases were dried over anhydrous $MgSO_4$ and concentrated under reduced pressure. The crude product was purified by column chromatography with DCM / MeOH (98 / 2) as eluent to afford the title product (**118**) as a yellow oil (75 mg, 53%).^{1}H NMR (300 MHz, $CDCl_3$) δ 7.47 – 7.17 (m, 10H, Ar, C*H*), 5.95 – 5.86 (m, 1H, CH_2CH),

5.32 – 5.19 (m, 2H, CH_2CH), 4.66 (s, 2H, CH_2), 4.52 (s, 2H, CH_2), 4.07 (tt, J = 6.0, 1.5 Hz, 2H, NHCH_2). ^{13}C NMR (100 MHz, $CDCl_3$) δ 162.1 (*C*ON), 159.7 (*C*ON), 135.4 (Ar, *C*), 135.2 (Ar, *C*), 132.6 (CH_2*C*H), 128.9 (Ar, *C*H), 128.5 (Ar, *C*H), 128.2 (Ar, *C*H), 127.8 (Ar, *C*H), 117.6 (*C*H_2CH), 49.2 (*C*H_2), 49.1 (*C*H_2), 43.3 (*C*H_2NH); HRMS (ES+) calculated for $C_{19}H_{20}N_4O_2Na$ $[M+Na]^+$ 359.1484, found 359.1481.

Appendix

^{1}H NMR and ^{13}C NMR of [2]rotaxane **49**.

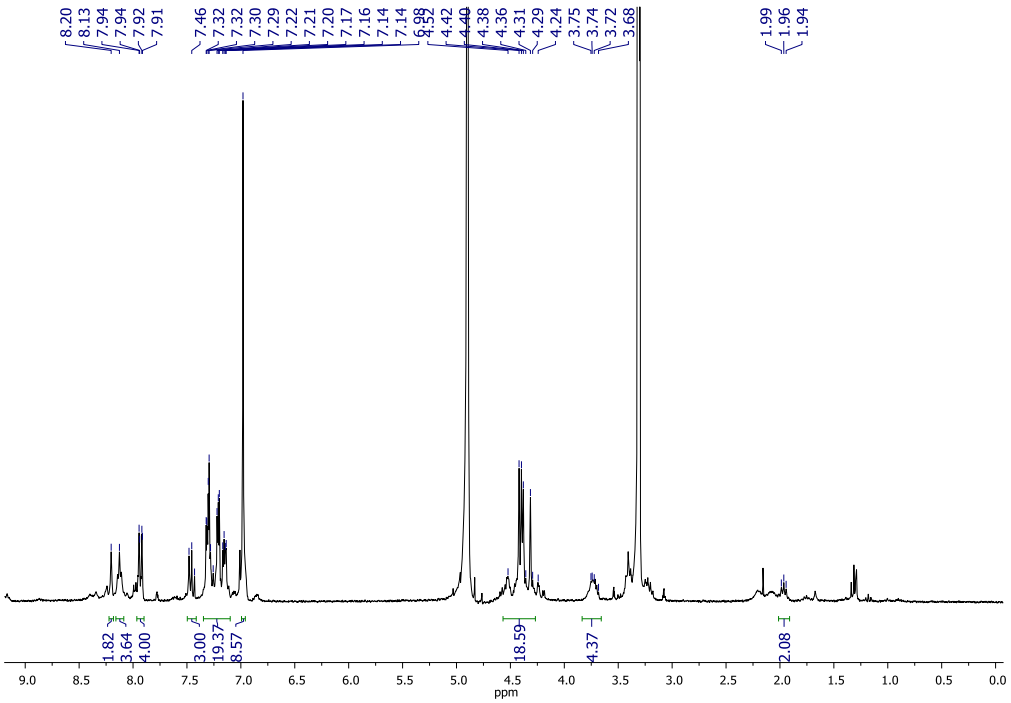

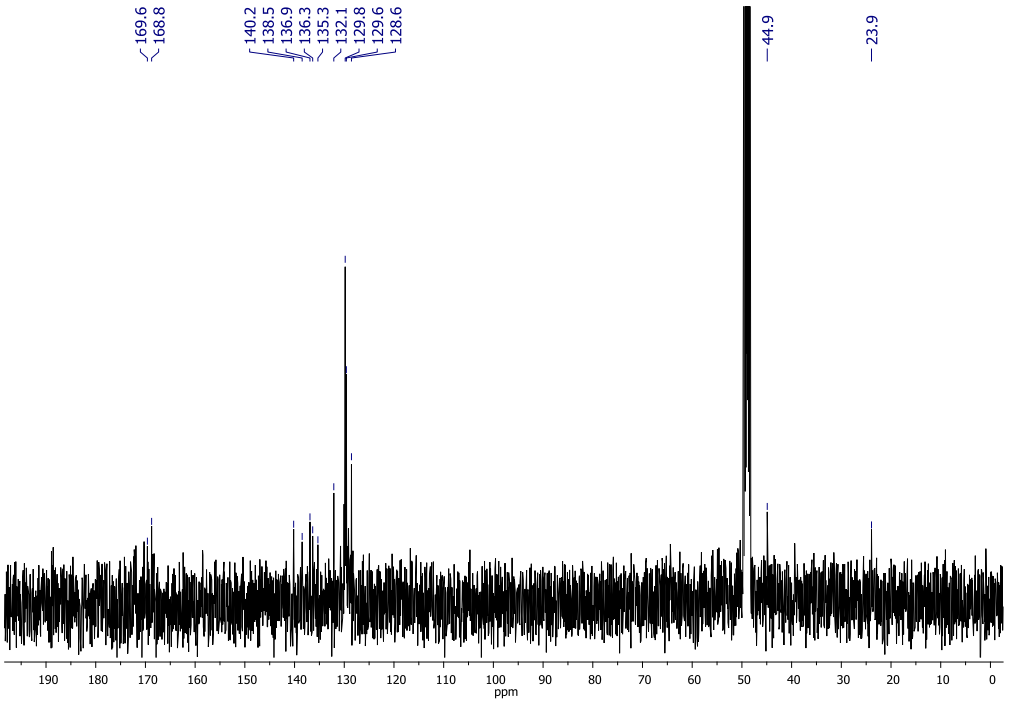

^{1}H NMR and ^{13}C NMR of [2]rotaxane **50**.

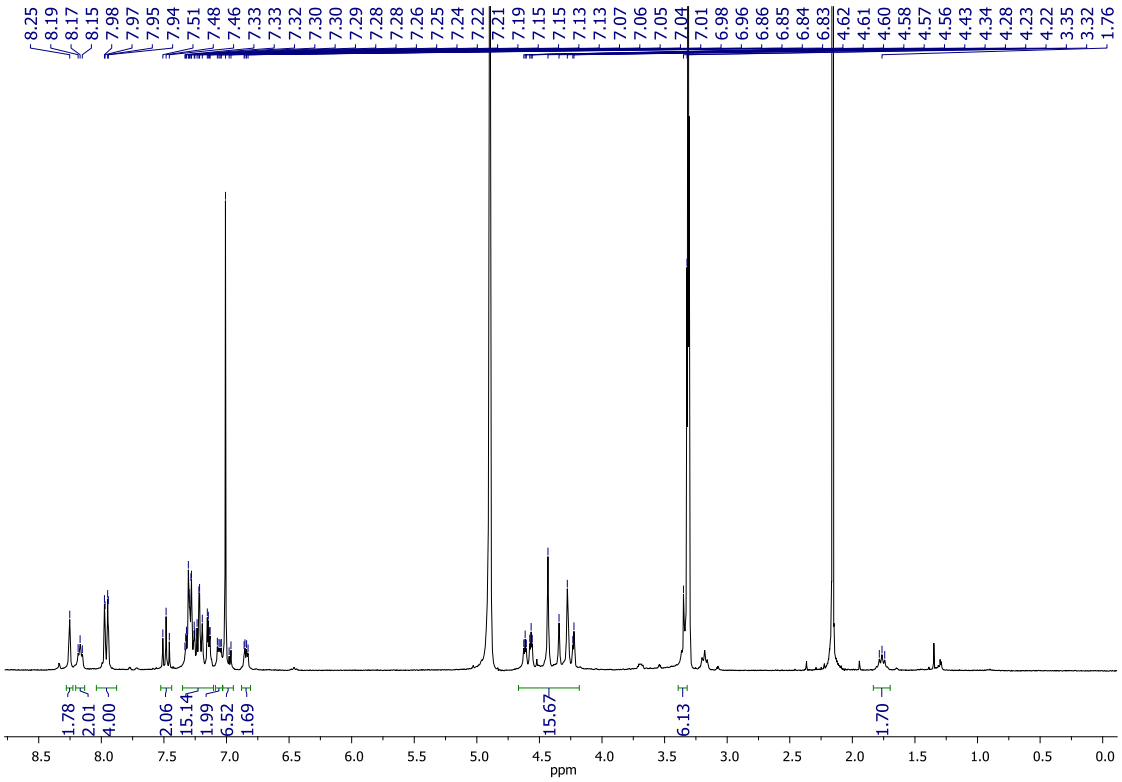

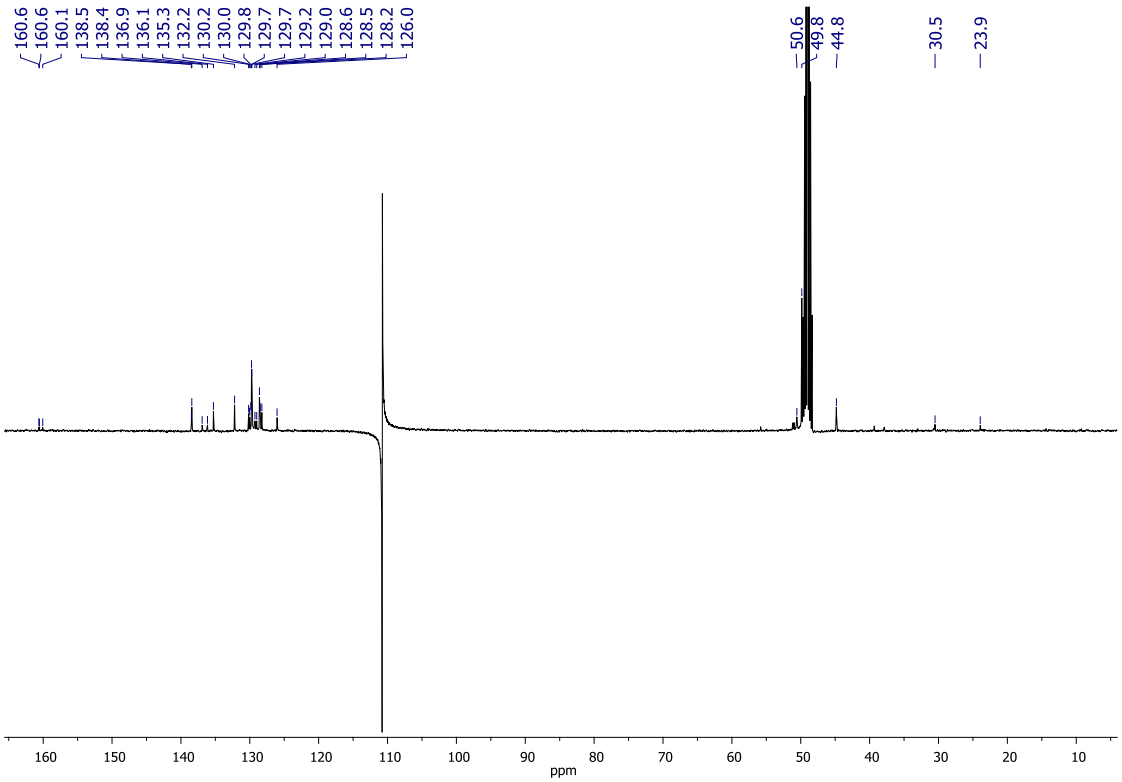

^{1}H NMR and ^{13}C NMR of [2]rotaxane **54**.

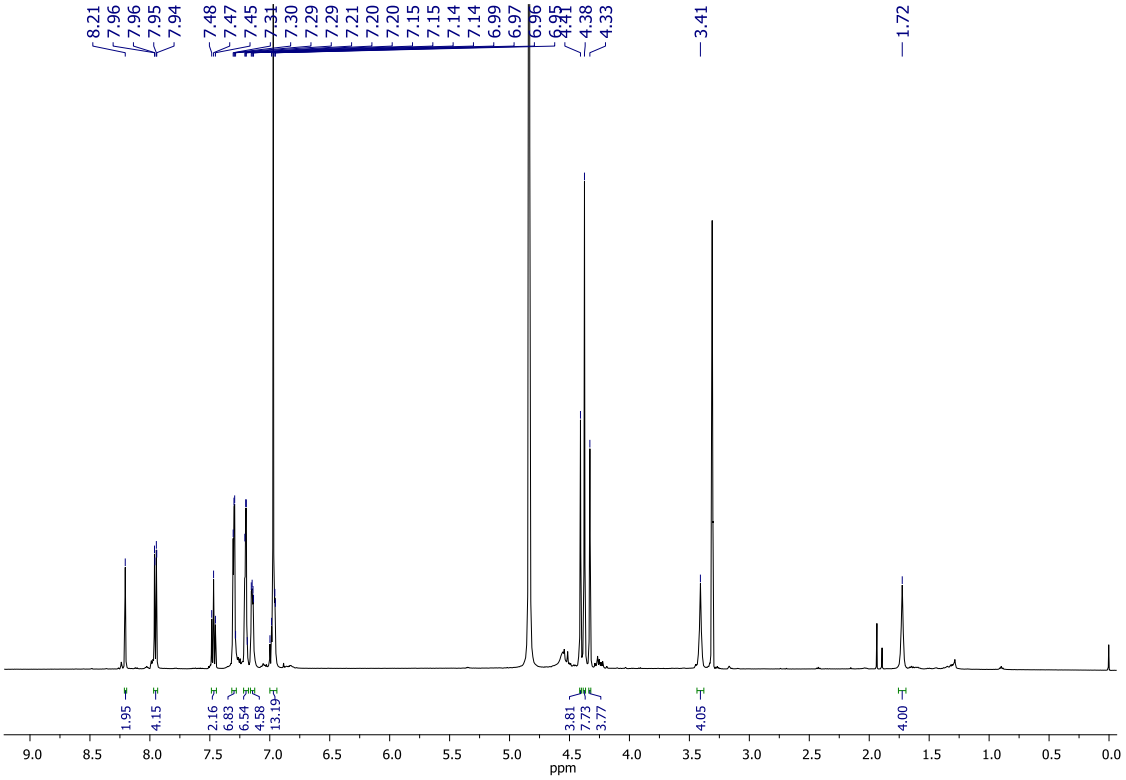

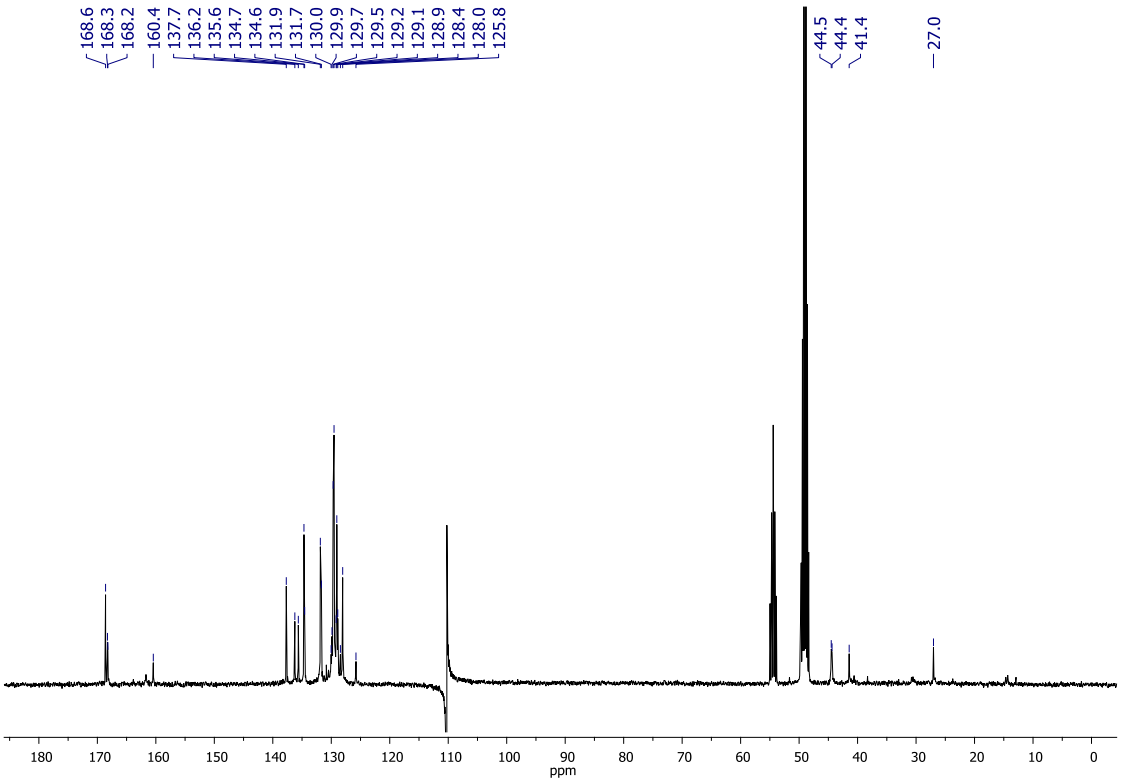

^{1}H NMR and ^{13}C NMR of [2]rotaxane **55**.

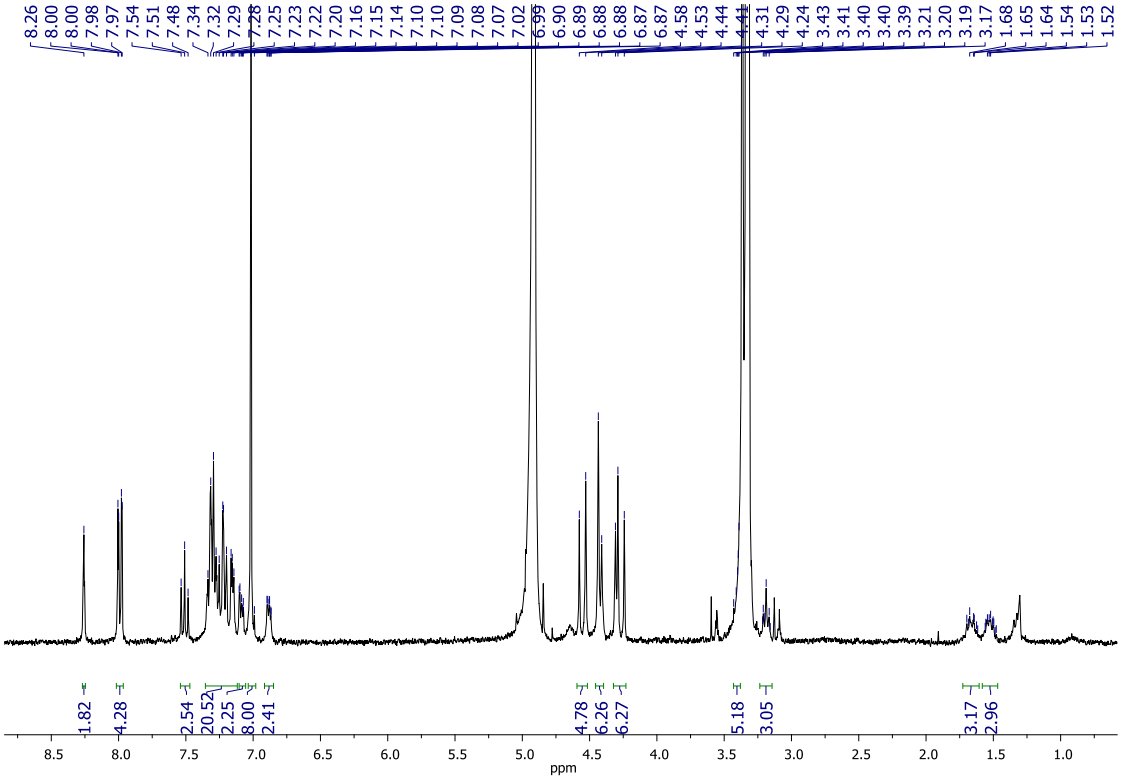

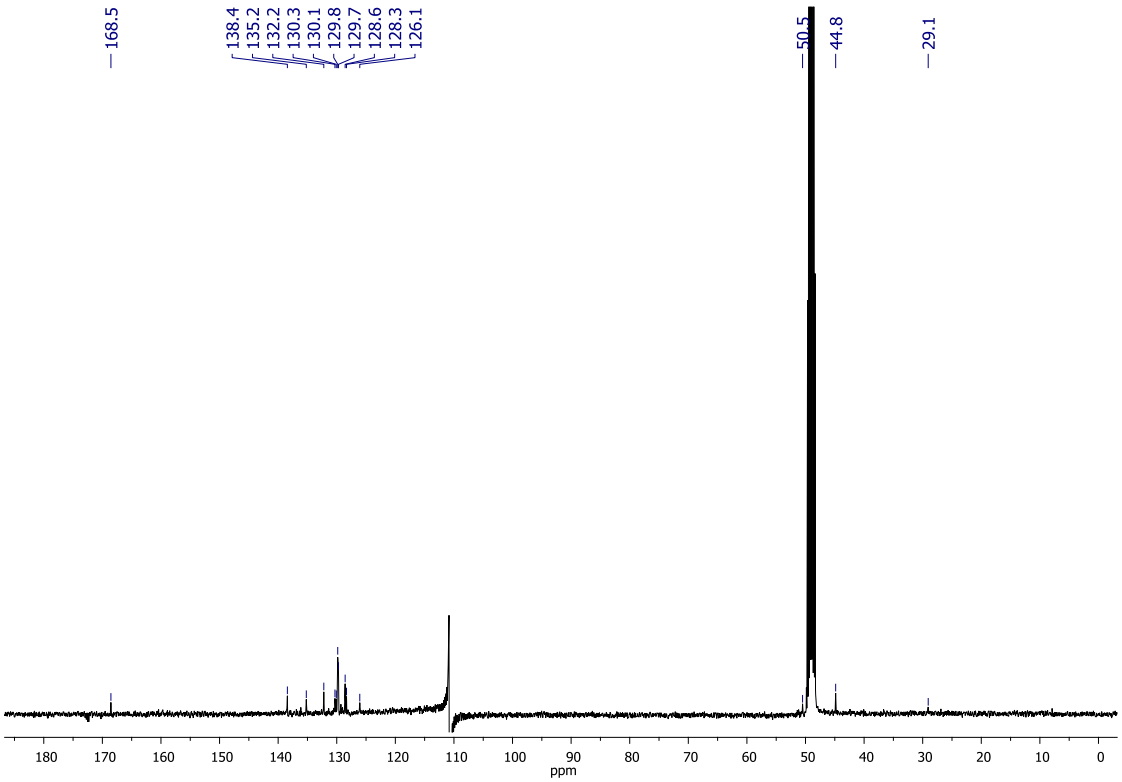

^{1}H NMR and COSY of [2]rotaxane **59**.

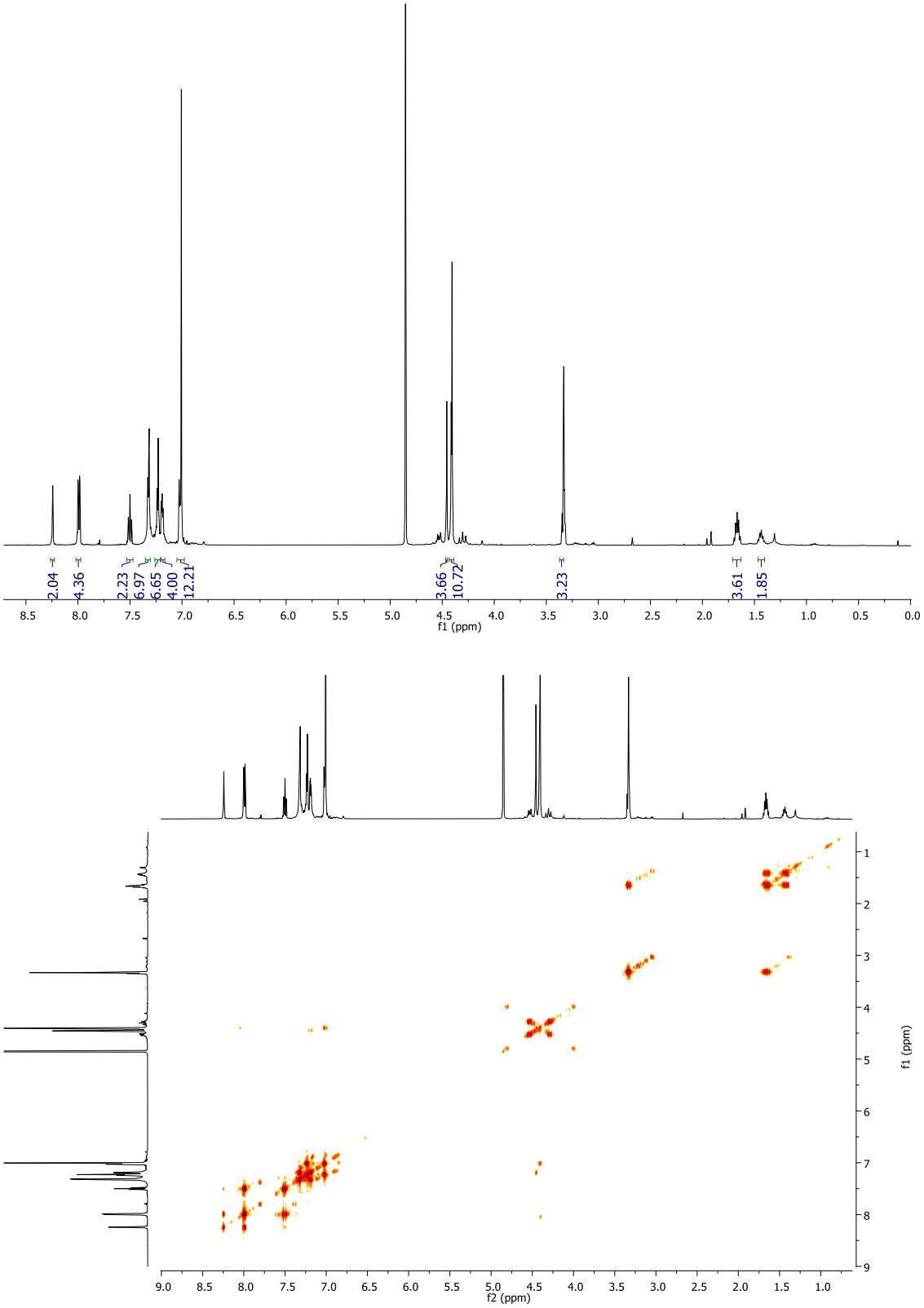

^{13}C NMR and HSQC of [23]rotaxane **59**.

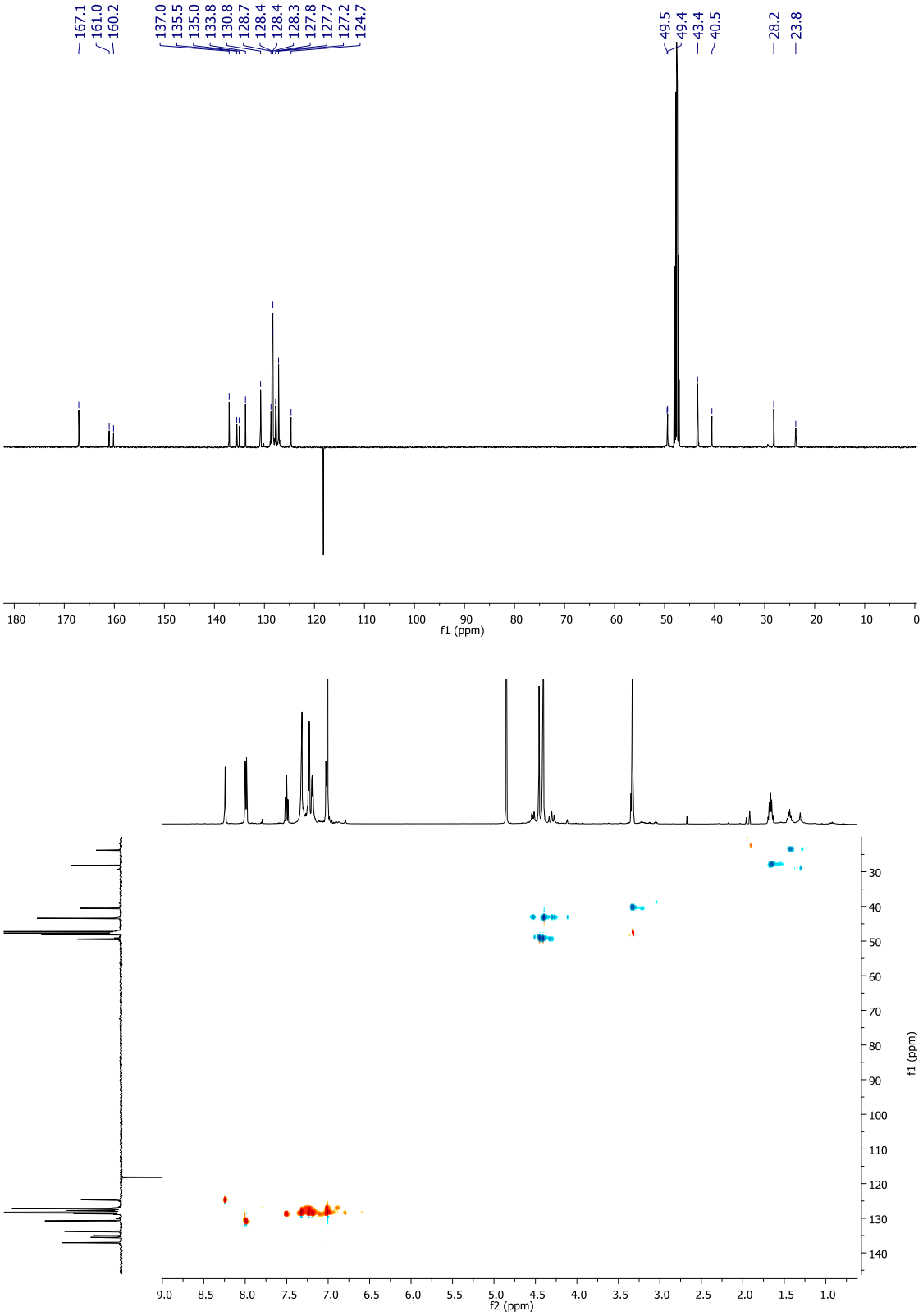

^{1}H NMR and COSY of [2]rotaxane **60**.

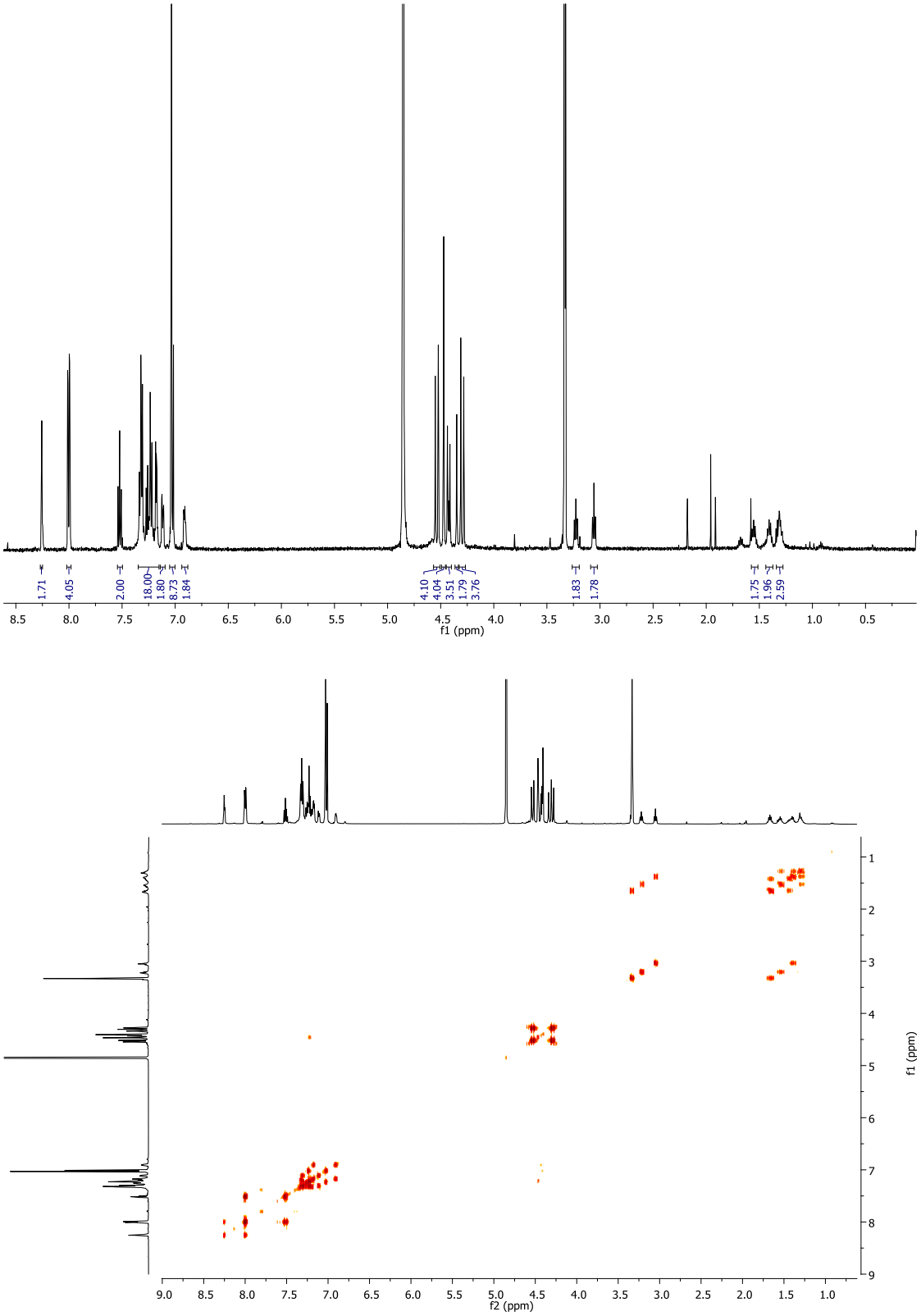

^{13}C NMR and HSQC of [2]rotaxane **60**.

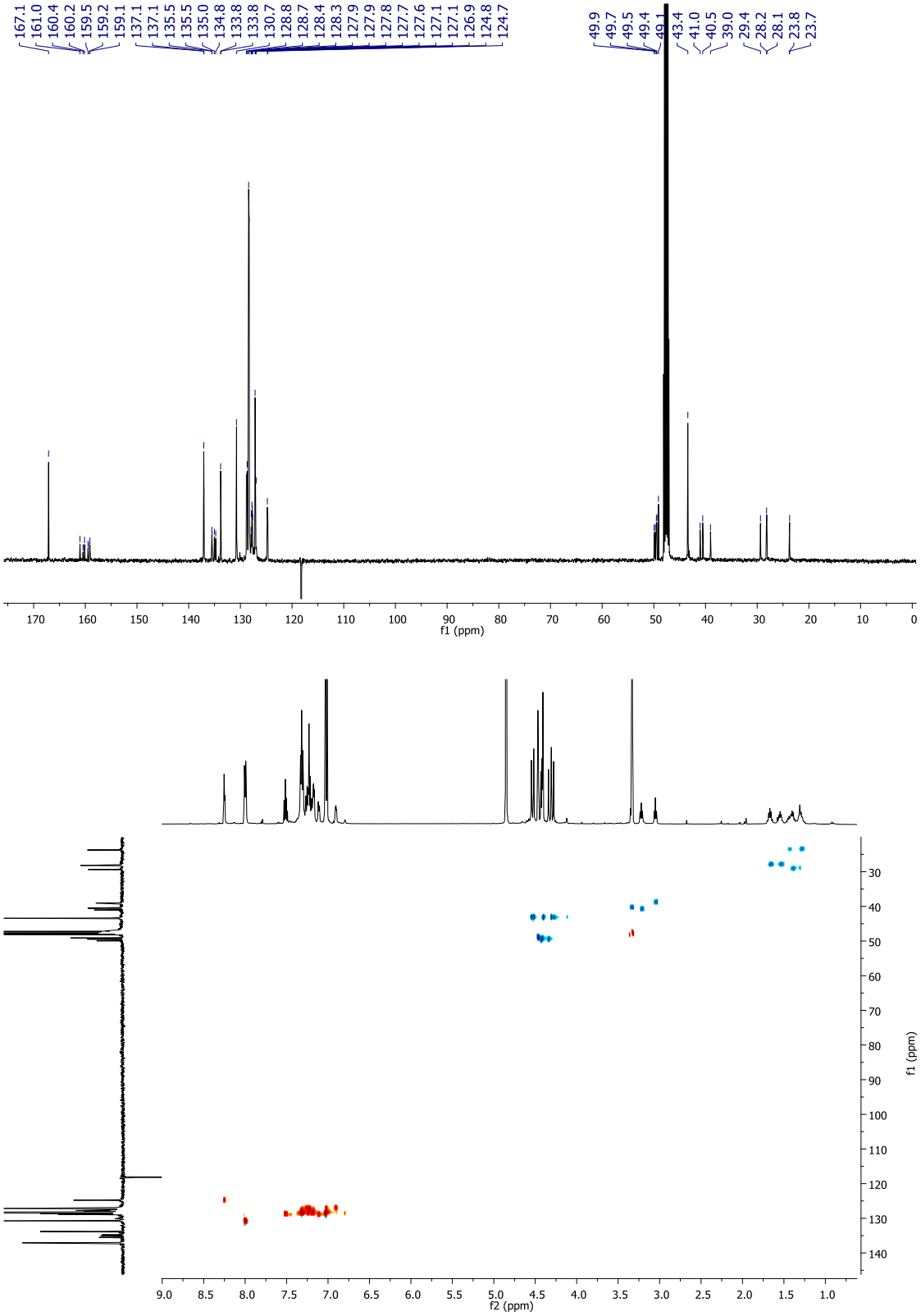

^{1}H NMR and COSY of [3]rotaxane **61**.

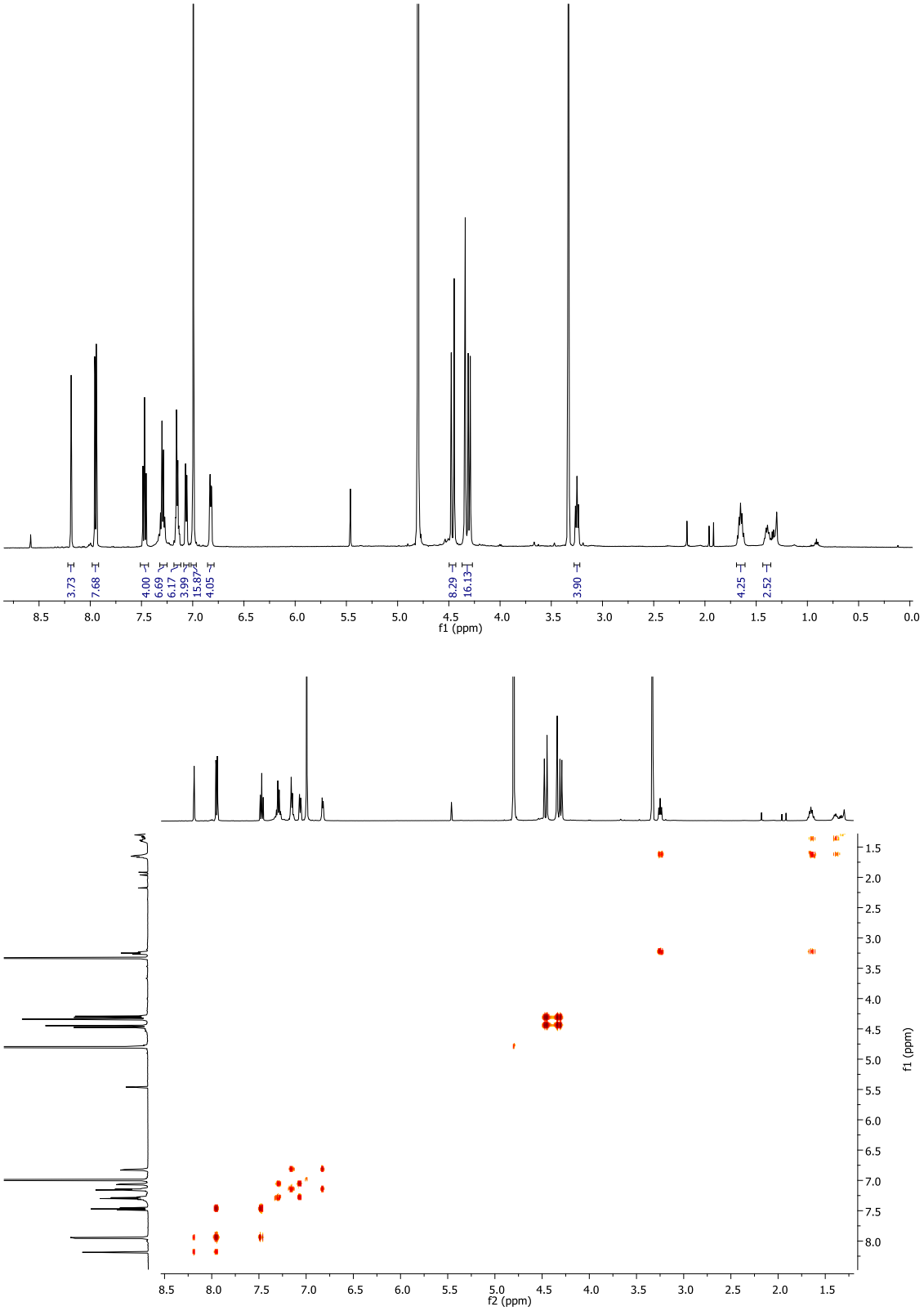

^{13}C NMR and HSQC of [3]rotaxane **61**.

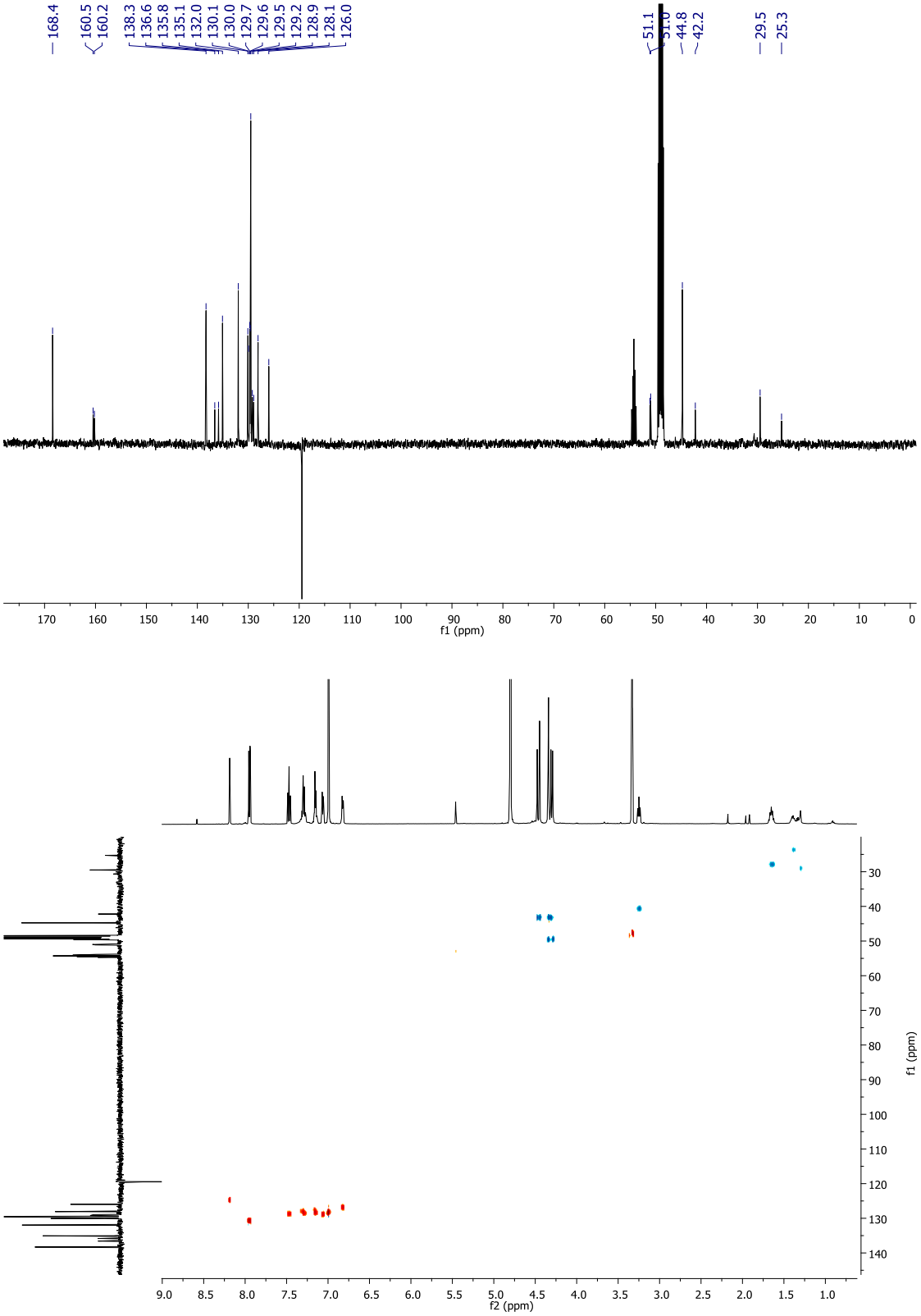

Table 1. Crystal data and structure refinement for [3]rotaxane **61**.

Empirical formula	$C_{37}H_{40}N_8O_4$, 2($C_{32}H_{28}N_4O_4$), 5.55(CH_4O), 1.65(H_2O)	
Formula weight	1933.50	
Temperature	120(2) K	
Wavelength	0.71073 Å	
Crystal system	Triclinic	
Space group	P -1	
Unit cell dimensions	a = 11.4654(3) Å	α= 98.271(1)°
	b = 17.8750(7) Å	β= 97.941(2)°
	c = 25.5552(10) Å	γ = 102.821(2)°
Volume	4974.6(3) $Å^3$	
Z	2	
Density (calculated)	1.291 Mg/m^3	
Absorption coefficient	0.090 mm^{-1}	
F(000)	2053	
Crystal size	0.24 x 0.06 x 0.03 mm^3	
θ range for data collection	2.91 to 25.03°.	
Index ranges	-13<=h<=13, -21<=k<=21, -30<=l<=30	
Reflections collected	54011	
Independent reflections	17271 [R(int) = 0.0938]	
Completeness to θ = 25.03°	98.1 %	
Absorption correction	Semi-empirical from equivalents	
Max. and min. transmission	0.9973 and 0.9787	
Refinement method	Full-matrix least-squares on F^2	
Data / restraints / parameters	17271 / 108 / 1307	
Goodness-of-fit on F^2	1.135	
Final R indices [I>2σ(I)]	R1 = 0.1572, wR2 = 0.2847	
R indices (all data)	R1 = 0.2502, wR2 = 0.3340	
Largest diff. peak and hole	0.753 and -0.446 e.$Å^{-3}$	

Table 2. Hydrogen bonds for [3]rotaxane **61** [Å and °].

D-H...A	d(D-H)	d(H...A)	d(D...A)	<(DHA)
N(4)-H(4A)...O(101)	0.88	1.98	2.834(10)	164.1
N(102)-H(102)...O(1)	0.88	2.08	2.942(9)	167.0
N(103)-H(10C)...O(2)	0.88	2.18	3.032(10)	163.5
N(104)-H(10D)...O(2)	0.88	2.35	3.227(9)	173.0
N(201)-H(201)...O(4)	0.88	2.25	3.115(9)	169.1
N(202)-H(202)...O(4)	0.88	2.48	3.279(9)	150.9
N(203)-H(20E)...O(3)	0.88	2.29	3.046(9)	144.4

^{1}H NMR and ^{13}C NMR of [2]rotaxane **63**.

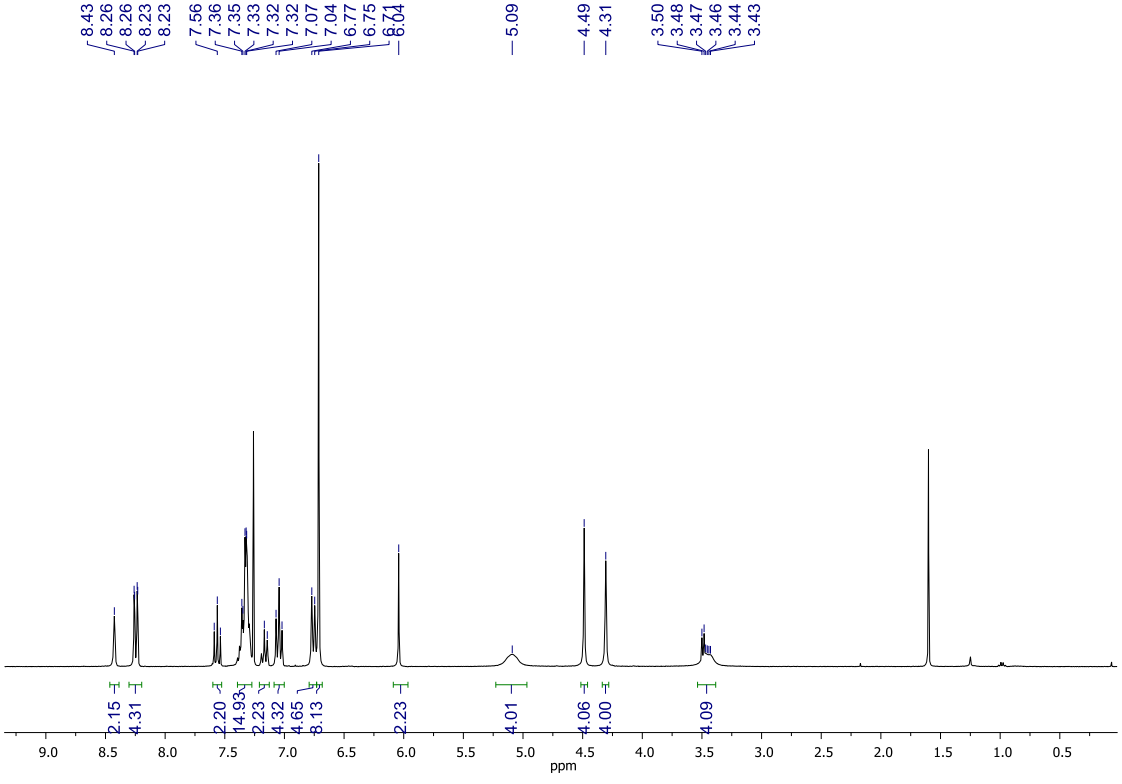

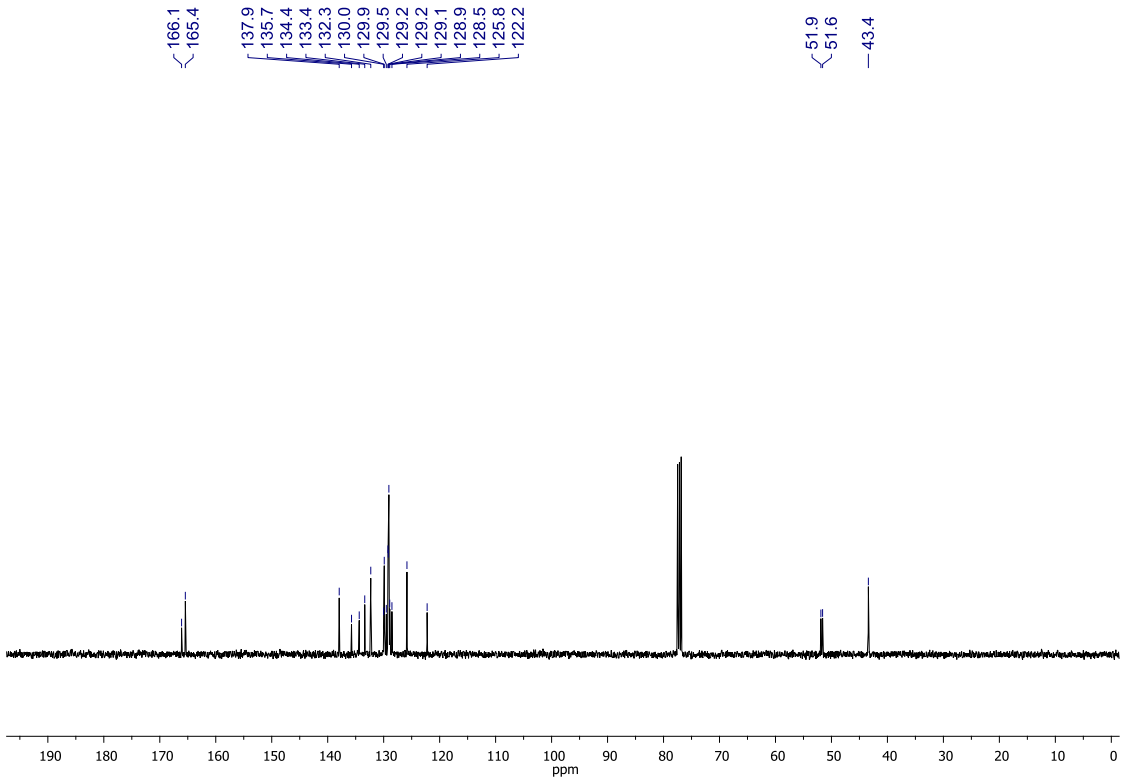

Table 1. Crystal data and structure refinement for [2]rotaxane **63**.

Empirical formula	$C_{32}H_{30}N_2O_2$, $C_{32}H_{28}N_4O_4$, 4($CHCl_3$)	
Formula weight	1484.64	
Temperature	120(2) K	
Wavelength	1.54178 Å	
Crystal system	Monoclinic	
Space group	P 2_1/c	
Unit cell dimensions	a = 10.1643(2) Å	α= 90°
	b = 31.3646(5) Å	β= 112.9800(10)°
	c = 11.6751(2) Å	γ = 90°
Volume	3426.64(10) $Å^3$	
Z	2	
Density (calculated)	1.439 Mg/m^3	
Absorption coefficient	4.897 mm^{-1}	
F(000)	1528	
Crystal size	0.18 x 0.16 x 0.14 mm^3	
θ range for data collection	6.35 to 70.06°.	
Index ranges	-12<=h<=11, -36<=k<=38, -12<=l<=14	

Reflections collected	30442
Independent reflections	6437 [R(int) = 0.0281]
Completeness to θ = 70.06°	98.9 %
Absorption correction	Semi-empirical from equivalents
Max. and min. transmission	0.5472 and 0.4727
Refinement method	Full-matrix least-squares on F^2
Data / restraints / parameters	6437 / 0 / 415
Goodness-of-fit on F^2	1.025
Final R indices [I>2σ(I)]	R1 = 0.0366, wR2 = 0.0950
R indices (all data)	R1 = 0.0406, wR2 = 0.0981
Largest diff. peak and hole	0.511 and -0.415 e.Å^{-3}

Table 2. Hydrogen bonds for [2]rotaxane **63** [Å and °].

D-H...A	d(D-H)	d(H...A)	d(D...A)	<(DHA)
N(101)-H(101)...O(1)#1	0.88	2.42	3.2685(19)	163.2
N(102)-H(102)...O(1)#1	0.88	2.10	2.9772(18)	172.3

^{1}H NMR and ^{13}C NMR of [3]rotaxane **67**.

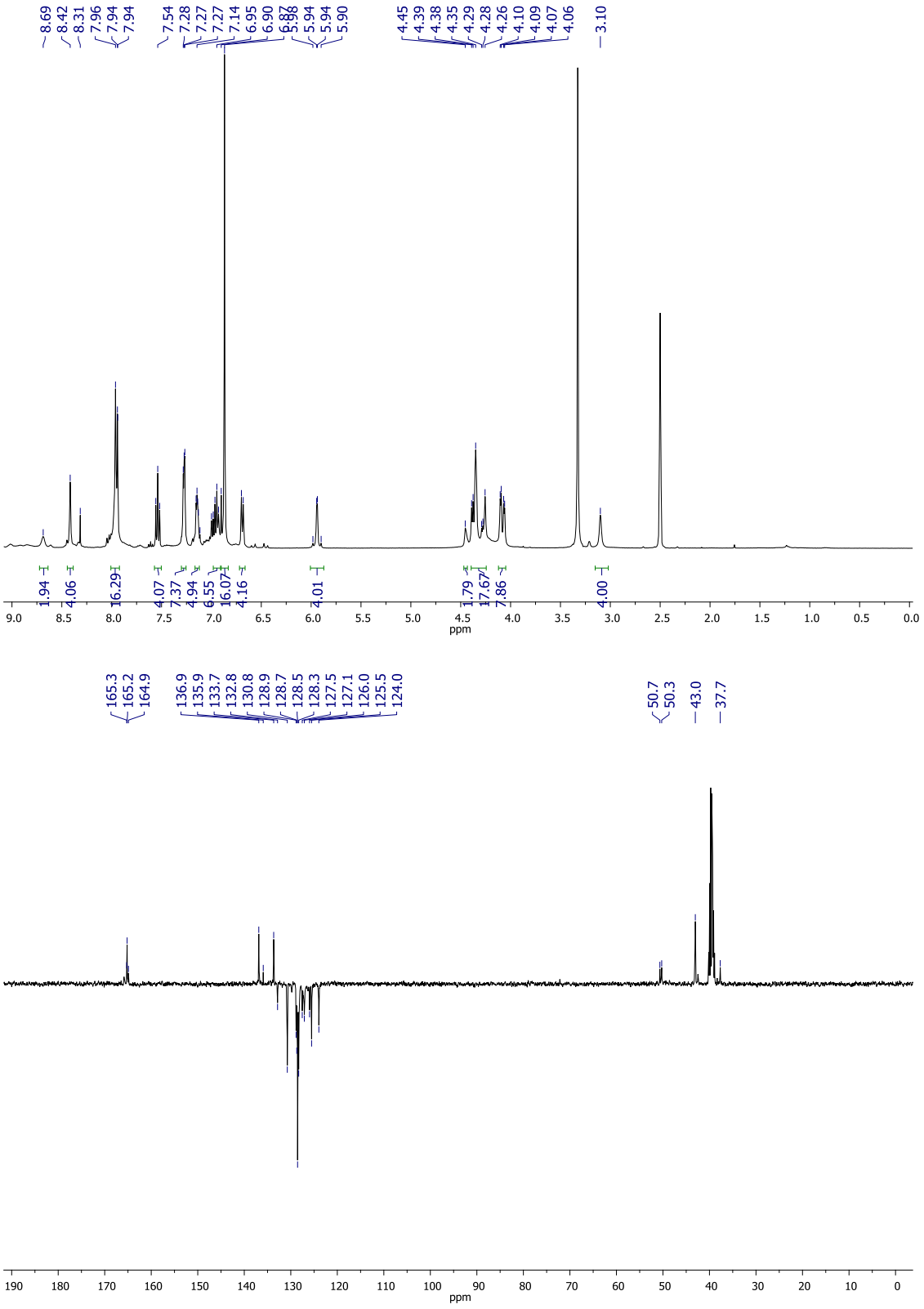

^{1}H NMR and ^{13}C NMR of [3]rotaxane **69**.

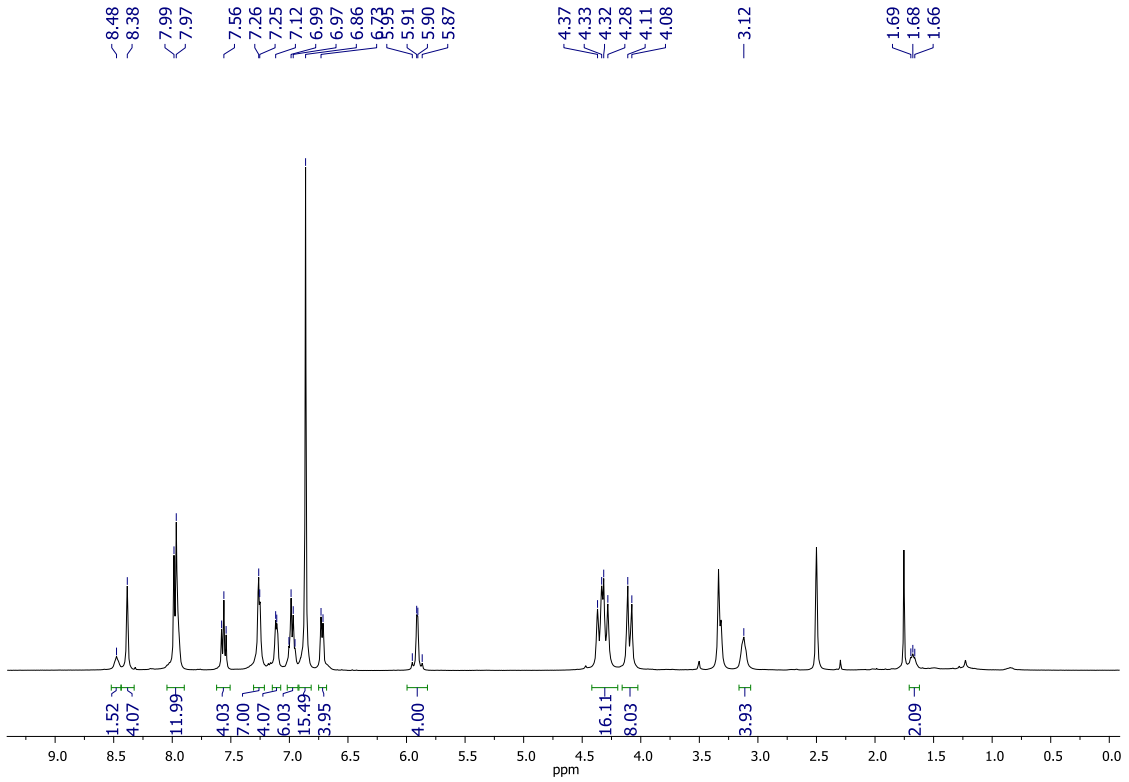

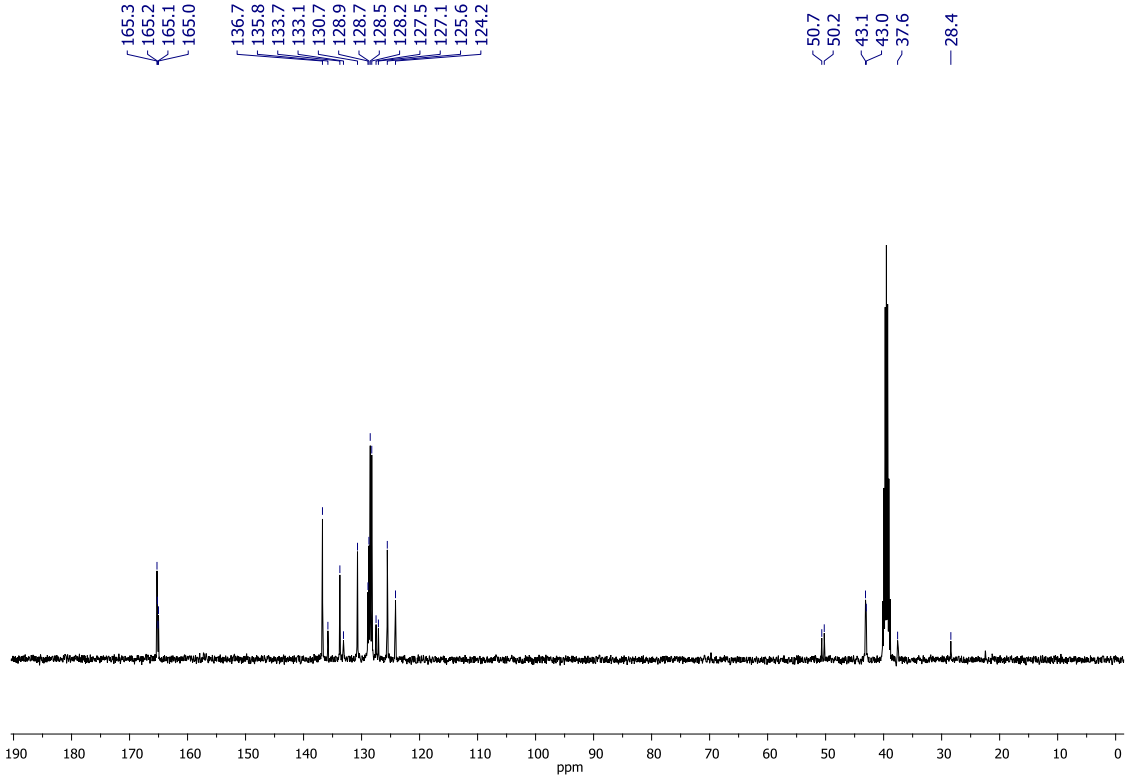

Table 1. Crystal data and structure refinement for [3]rotaxane **69**.

Empirical formula	$C_{110}H_{117}N_{12}O_{15.50}$	
Formula weight	1855.16	
Temperature	100(2) K	
Wavelength	0.71075 Å	
Crystal system	Triclinic	
Space group	*P*–1	
Unit cell dimensions	*a* = 10.8101(6) Å	α = 110.488(8)°
	b = 21.2231(13) Å	β = 97.325(7)°
	c = 22.7870(16) Å	γ = 97.504(7)°
Volume	4770.1(5) Å^3	
Z	2	
Density (calculated)	1.292 Mg / m^3	
Absorption coefficient	0.087 mm^{-1}	
F(000)	1970	
Crystal size	0.20 × 0.03 × 0.02 mm^3	
θ range for data collection	2.99 – 25.03°	
Index ranges	$-10 \le h \le 12$, $-25 \le k \le 25$, $-27 \le l \le 26$	
Reflections collected	33613	
Independent reflections	16656 [R_{int} = 0.0637]	
Completeness to θ = 25.03°	98.9 %	
Absorption correction	Semi–empirical from equivalents	
Max. and min. transmission	0.9983 and 0.9828	
Refinement method	Full-matrix least-squares on F^2	
Data / restraints / parameters	16656 / 405 / 1316	
Goodness-of-fit on F^2	1.053	
Final *R* indices [$F^2 > 2\sigma(F^2)$]	*R1* = 0.0816, *wR2* = 0.1913	
R indices (all data)	*R1* = 0.1513, *wR2* = 0.2292	
Largest diff. peak and hole	0.743 and –0.674 e Å^{-3}	

Table 2. Hydrogen bonds for [2]rotaxane **69** [Å and °].

D-H...A	d(D-H)	d(H...A)	d(D...A)	<(DHA)
N5–H5...O4	0.88	2.05	2.877(5)	155.2
N6–H6N...O3	0.88	2.21	3.080(4)	168.8
N7–H7N...O3	0.88	2.23	3.080(5)	161.0
N9–H9...O1	0.88	2.05	2.889(4)	158.4
N10–H10N...O2	0.88	2.10	2.960(4)	165.2
N11–H11N...O2	0.88	2.52	3.398(5)	176.6

^{1}H NMR of thread **72** (in blue) and [3]rotaxane **73** (in red).

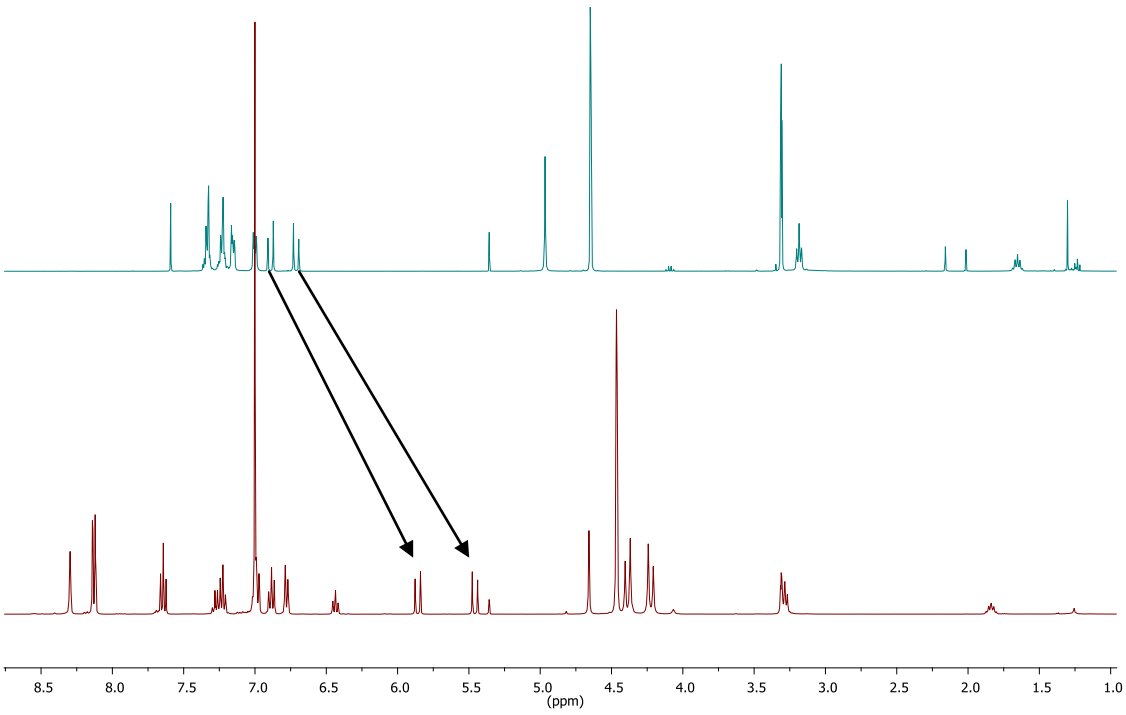

Arrows highlight the shielding of the olefinic protons.

^{1}H NMR and ^{13}C NMR of [3]rotaxane **73**.

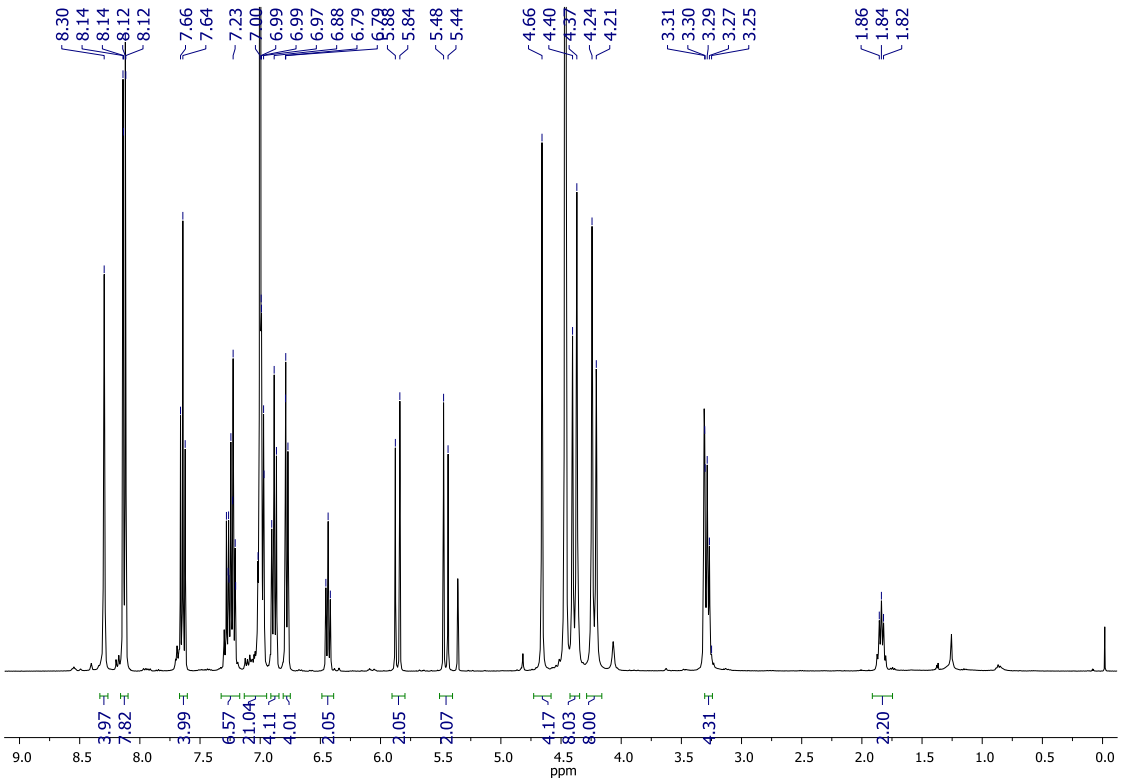

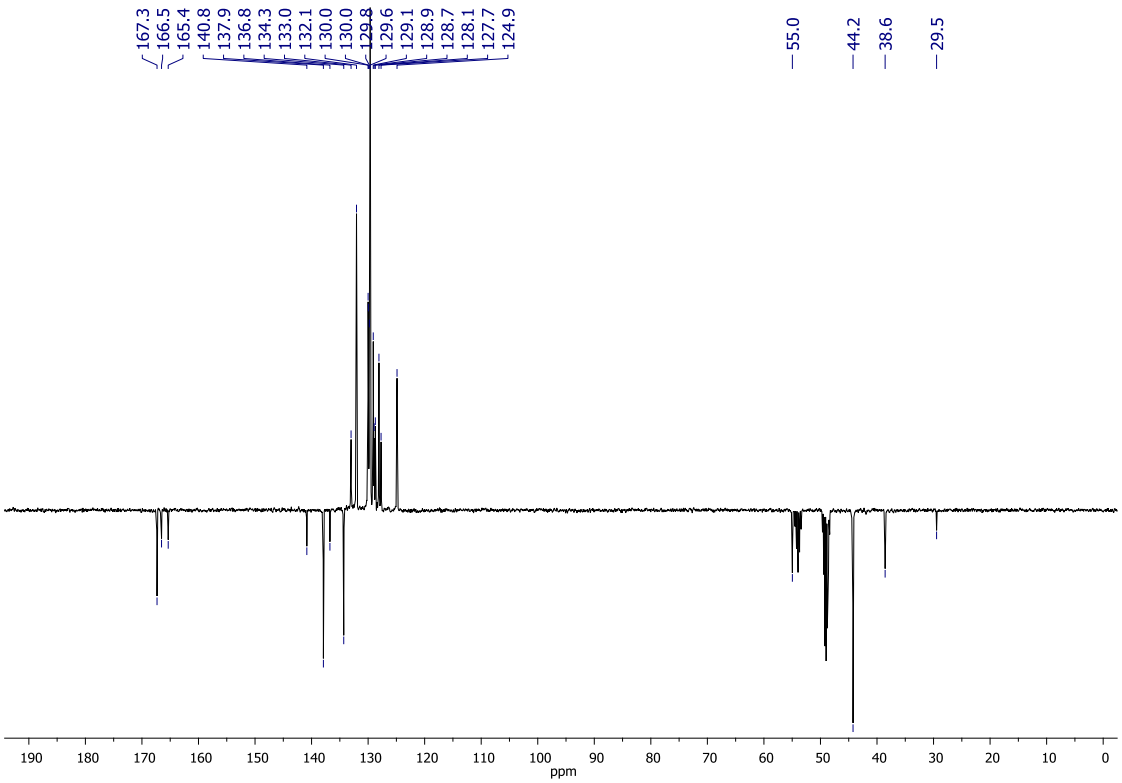

Table 1. Crystal data and structure refinement for [3]rotaxane **73**.

Empirical formula	$C_{101}H_{92}N_{12}O_{12}$, 0.5($C_2H_5OH$), 0.5($CH_3OH$), 2($H_2O$)	
Formula weight	1740.95	
Temperature	120(2) K	
Wavelength	1.54184 Å	
Crystal system	Monoclinic	
Space group	P 2_1	
Unit cell dimensions	a = 10.0536(3) Å	α= 90°
	b = 38.7489(11) Å	β= 92.610(2)°
	c = 11.7046(3) Å	γ = 90°
Volume	4555.0(2) $Å^3$	
Z	2	
Density (calculated)	1.269 Mg/m^3	
Absorption coefficient	0.699 mm^{-1}	
F(000)	1840	
Crystal size	0.21 x 0.13 x 0.06 mm^3	
θ range for data collection	6.35 to 66.58°.	
Index ranges	-11<=h<=11, -46<=k<=46, -13<=l<=13	
Reflections collected	27608	
Independent reflections	13650 [R(int) = 0.0274]	
Completeness to θ = 66.58°	94.9 %	
Absorption correction	Semi-empirical from equivalents	
Max. and min. transmission	0.9593 and 0.8671	
Refinement method	Full-matrix least-squares on F^2	
Data / restraints / parameters	13650 / 6 / 1191	
Goodness-of-fit on F^2	1.075	
Final R indices [I>2σ(I)]	R1 = 0.0509, wR2 = 0.1353	
R indices (all data)	R1 = 0.0549, wR2 = 0.1385	
Absolute structure parameter	0.08(17)	
Largest diff. peak and hole	0.611 and -0.215 e.$Å^{-3}$	

Table 2. Hydrogen bonds for [3]rotaxane **73** [Å and °].

D-H...A	d(D-H)	d(H...A)	d(D...A)	<(DHA)
N(101)-H(101)...O(1)	0.88	2.20	3.072(4)	170.8
N(102)-H(102)...O(1)	0.88	2.09	2.934(4)	161.4
N(103)-H(10C)...O(2)	0.88	2.16	3.002(3)	159.3
N(104)-H(10D)...O(2)	0.88	2.12	2.978(4)	165.5
N(201)-H(201)...O(3)	0.88	2.24	3.082(4)	160.5
N(202)-H(202)...O(3)	0.88	2.22	3.066(4)	162.5
N(203)-H(20E)...O(4)	0.88	2.11	2.969(3)	166.4
N(204)-H(20F)...O(4)	0.88	2.26	3.127(3)	171.0

^{1}H NMR and ^{13}C NMR of [2]rotaxane **74**.

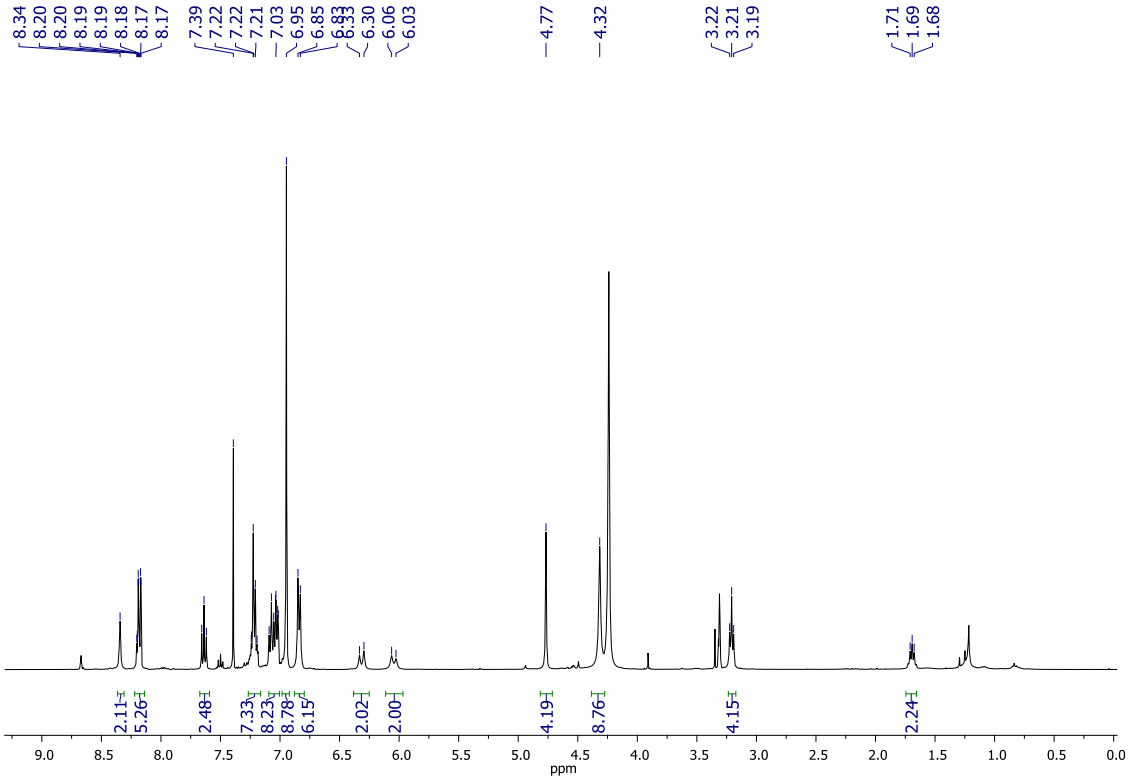

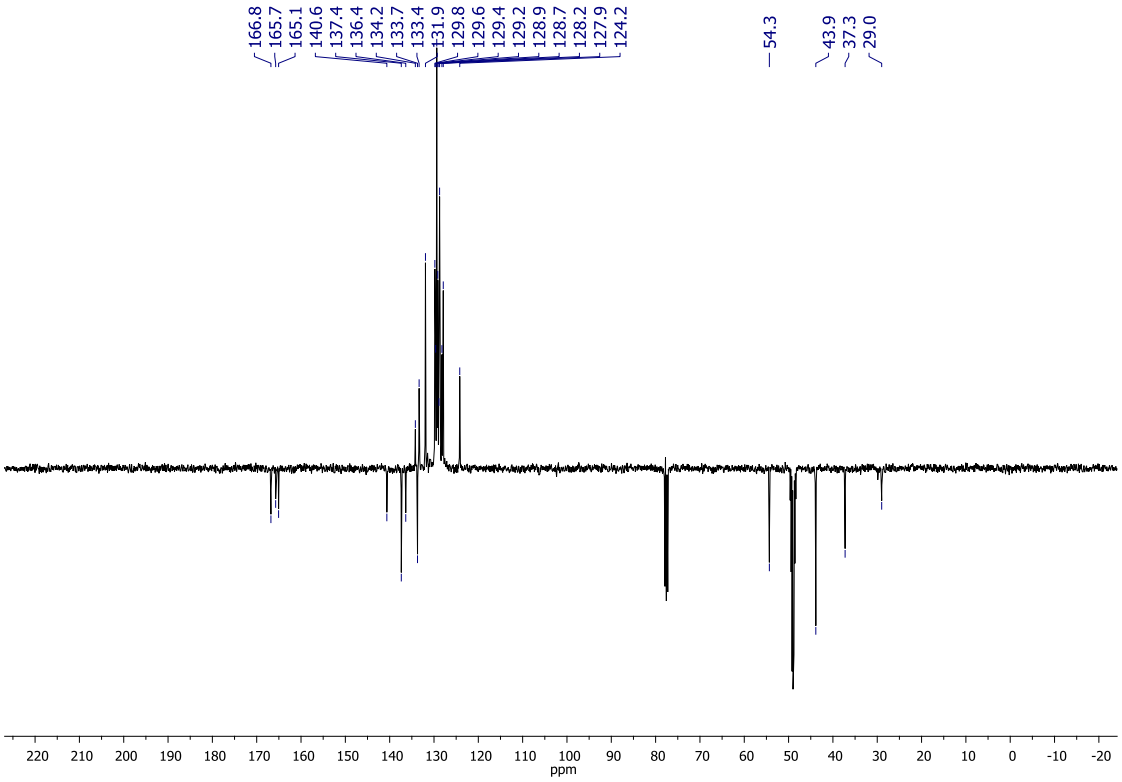
166.8
165.7
165.1
140.6
137.4
136.4
134.2
133.7
133.4
131.9
129.8
129.6
129.4
129.2
128.9
128.7
128.2
127.9
124.2
54.3
43.9
37.3
29.0
220 210 200 190 180 170 160 150 140 130 120 110 100 90 80 70 60 50 40 30 20 10 0 -10 -20
ppm

^{1}H NMR and ^{13}C NMR of [2]rotaxane **77**.

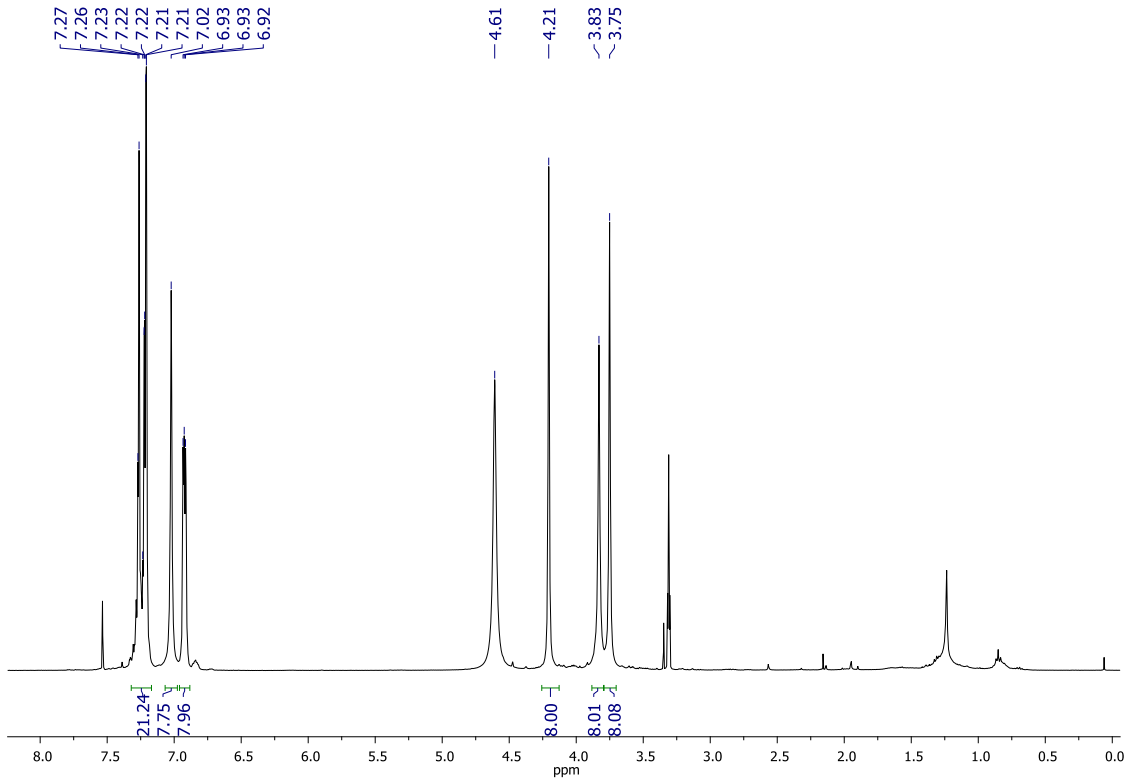

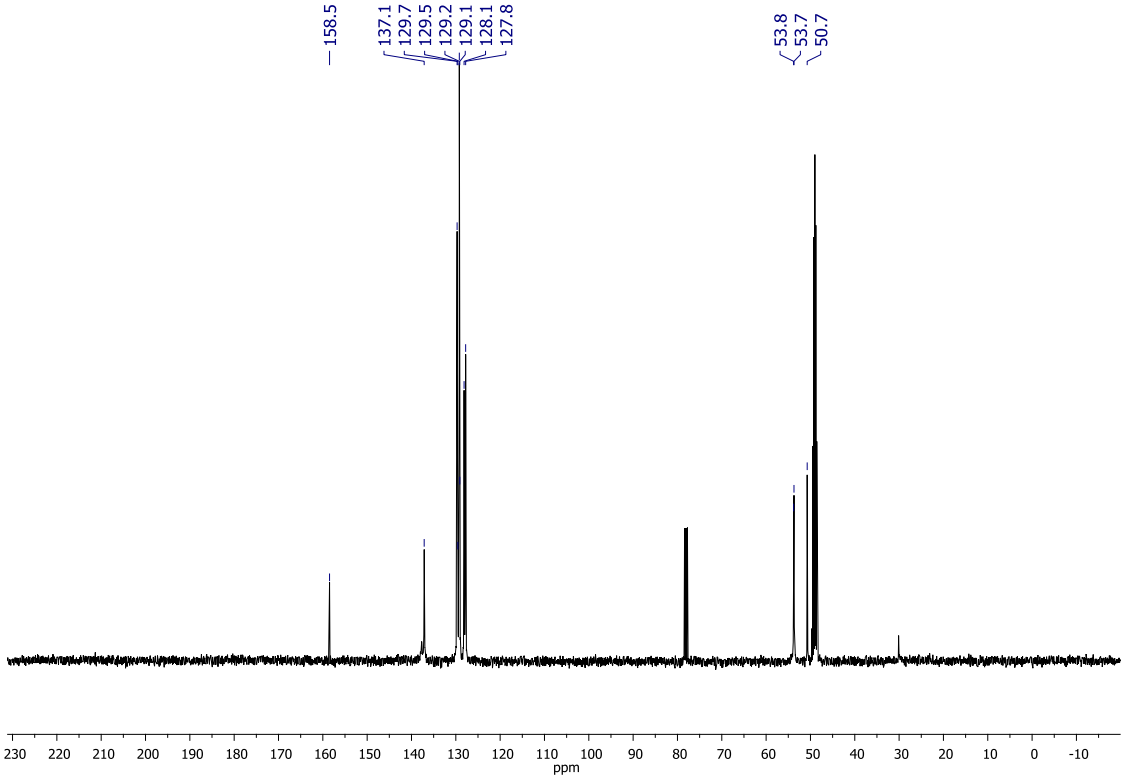

^{1}H NMR and ^{13}C NMR of [3]rotaxane **84**.

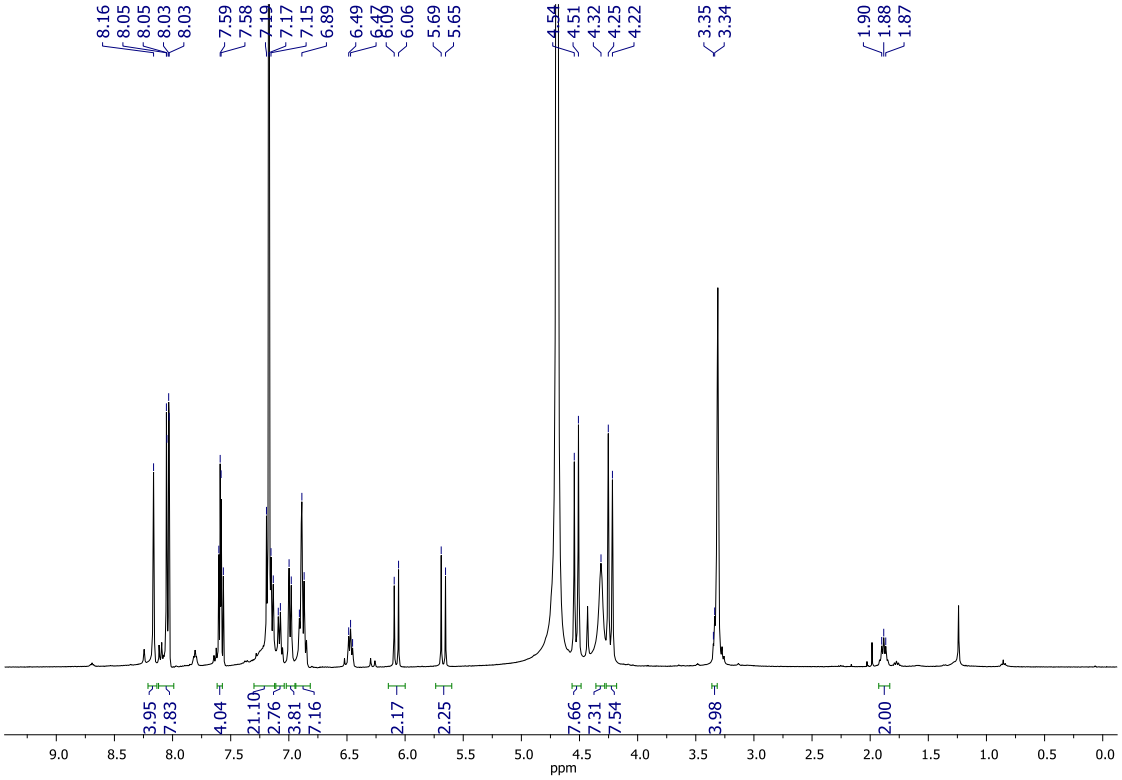

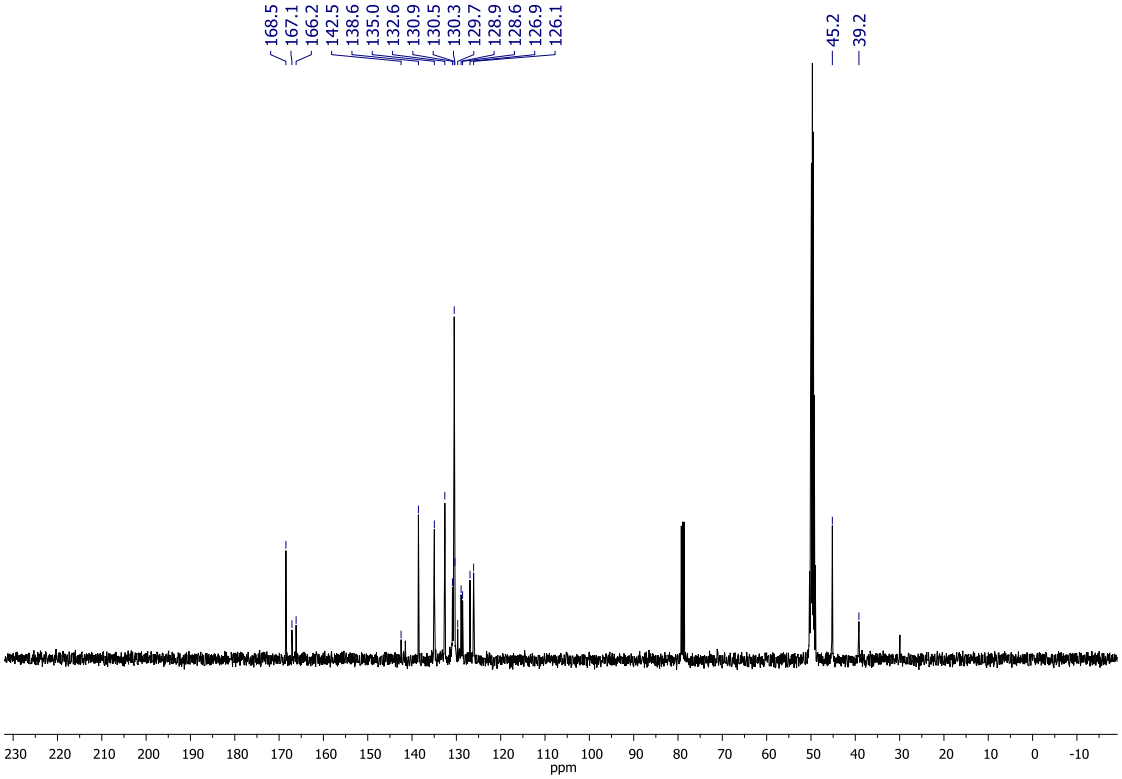

^{1}H NMR and ^{13}C NMR of [2]rotaxane **85**.

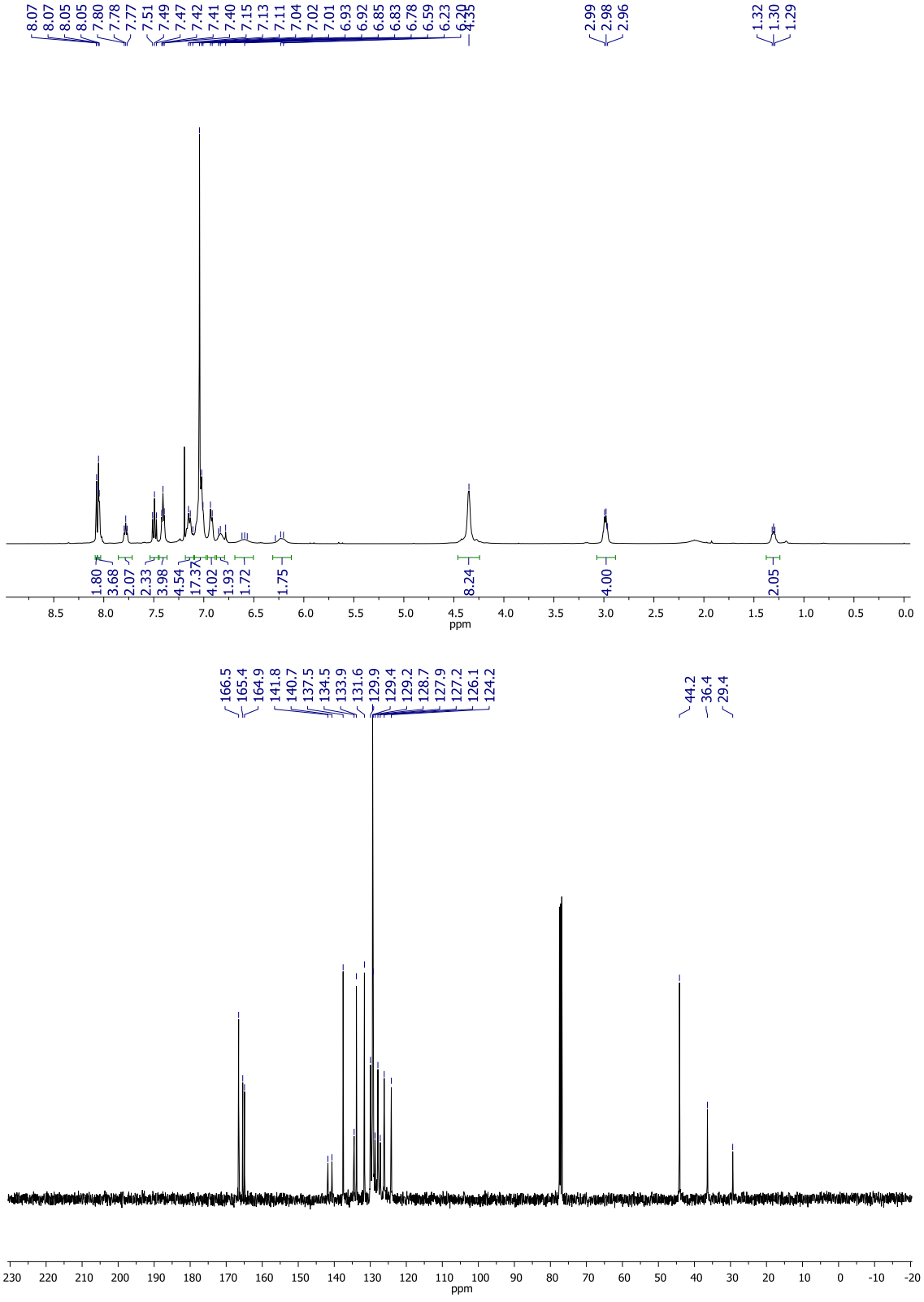

Table 1. Crystal data and structure refinement for Diels-Alder adduct **89**.

Empirical formula	$C_{28}H_{25}NO_3$	
Formula weight	423.49	
Temperature	120(2) K	
Wavelength	1.54184 Å	
Crystal system	Triclinic	
Space group	P -1	
Unit cell dimensions	a = 9.0489(1) Å	α= 67.170(1)°
	b = 10.6951(1) Å	β= 79.463(1)°
	c = 12.5935(2) Å	γ = 81.782(1)°
Volume	1100.87(2) $Å^3$	
Z	2	
Density (calculated)	1.278 mg/m^3	
Absorption coefficient	0.657 mm^{-1}	
F(000)	448	
Crystal size	0.20 x 0.17 x 0.12 mm^3	
θ range for data collection	6.45 to 66.60°.	
Index ranges	-10<=h<=10, -12<=k<=12, -14<=l<=14	
Reflections collected	10832	
Independent reflections	3784 [R(int) = 0.0555]	
Completeness to θ = 66.60°	97.5 %	
Absorption correction	Semi-empirical from equivalents	
Max. and min. transmission	0.9253 and 0.8798	
Refinement method	Full-matrix least-squares on F^2	
Data / restraints / parameters	3784 / 0 / 290	
Goodness-of-fit on F^2	1.028	
Final R indices [I>2σ(I)]	R1 = 0.0581, wR2 = 0.1567	
R indices (all data)	R1 = 0.0616, wR2 = 0.1635	
Largest diff. peak and hole	0.317 and -0.375 e.$Å^{-3}$	

MALDI profile for the formation of box **105** with thread **33** (with the spectrum colour as followed: 1 day shown in red, 2 days shown in brown, 5 days shown in black, 1 week in purple, 2 weeks shown in green and 3 weeks shown in red).

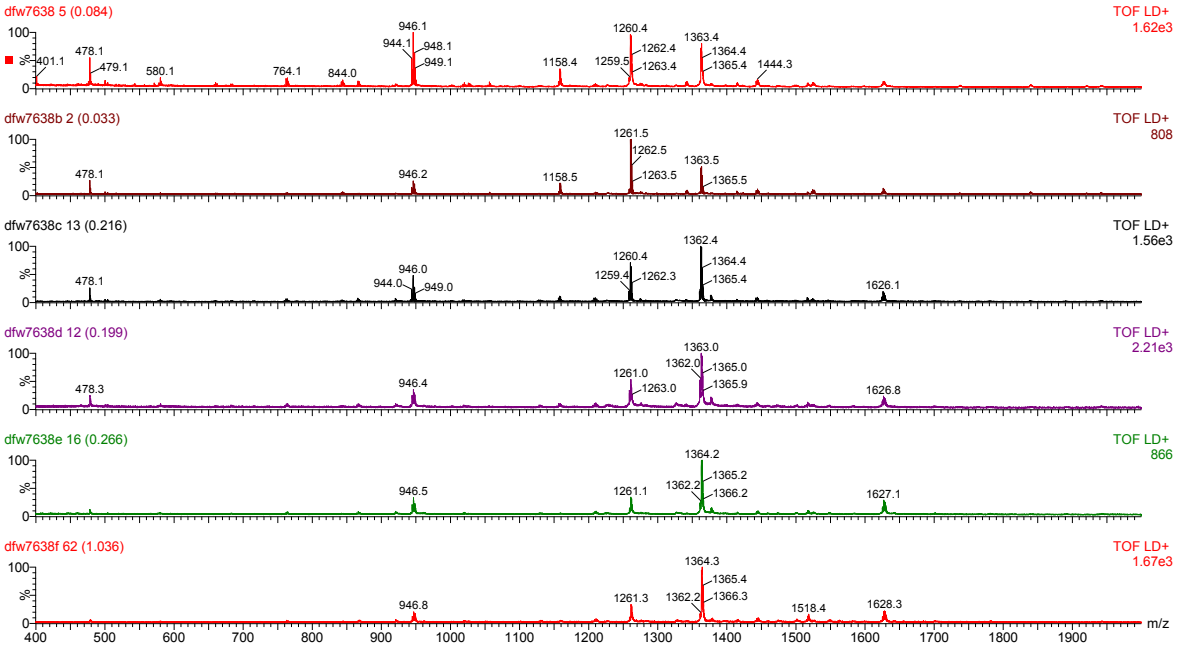

MALDI profile for the formation of box **105** without thread **33** (same colour coded spectra).

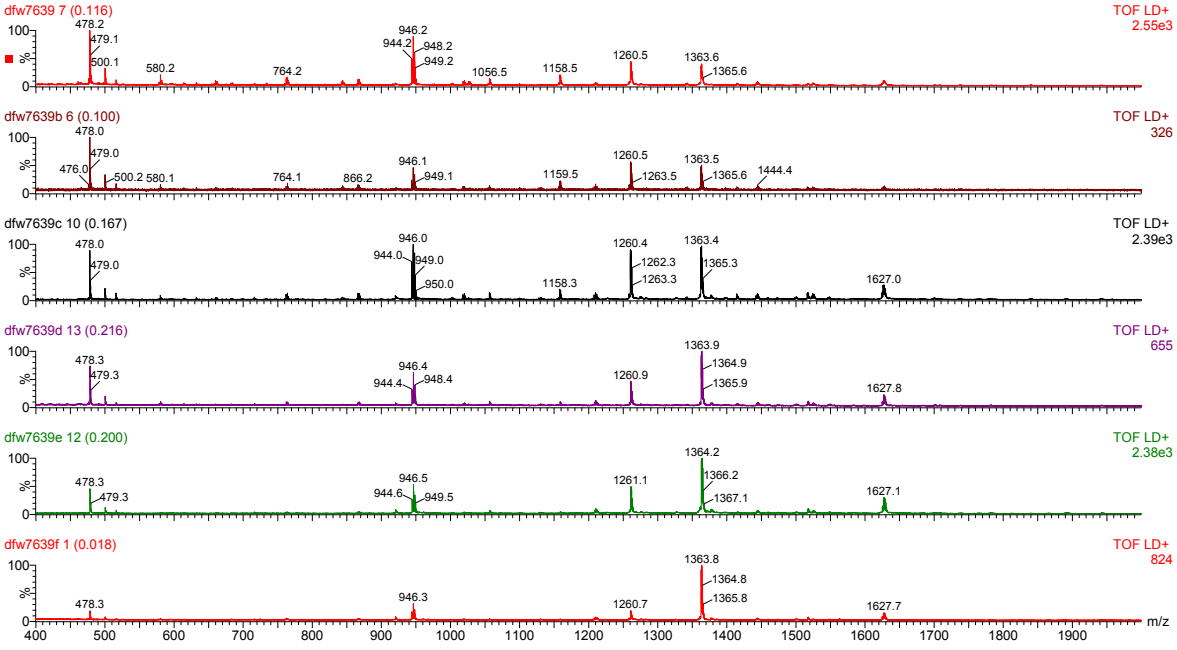

^{1}H NMR and ^{13}C NMR of molecular cage **105**.

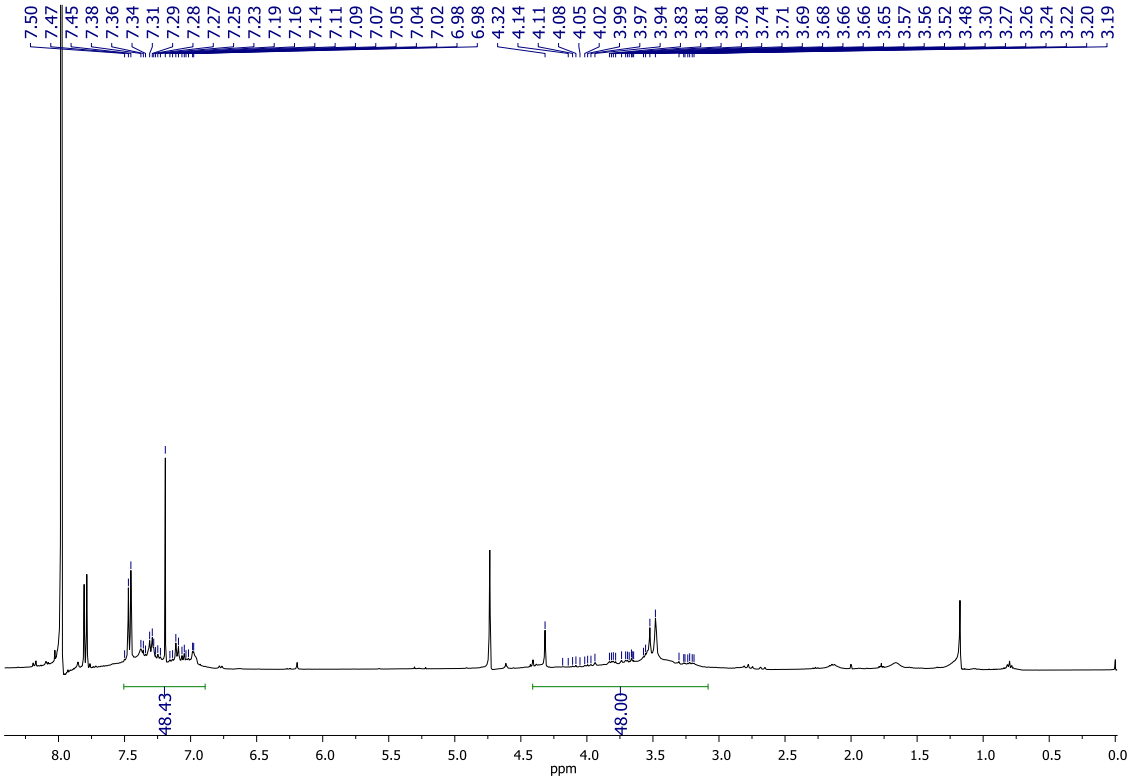

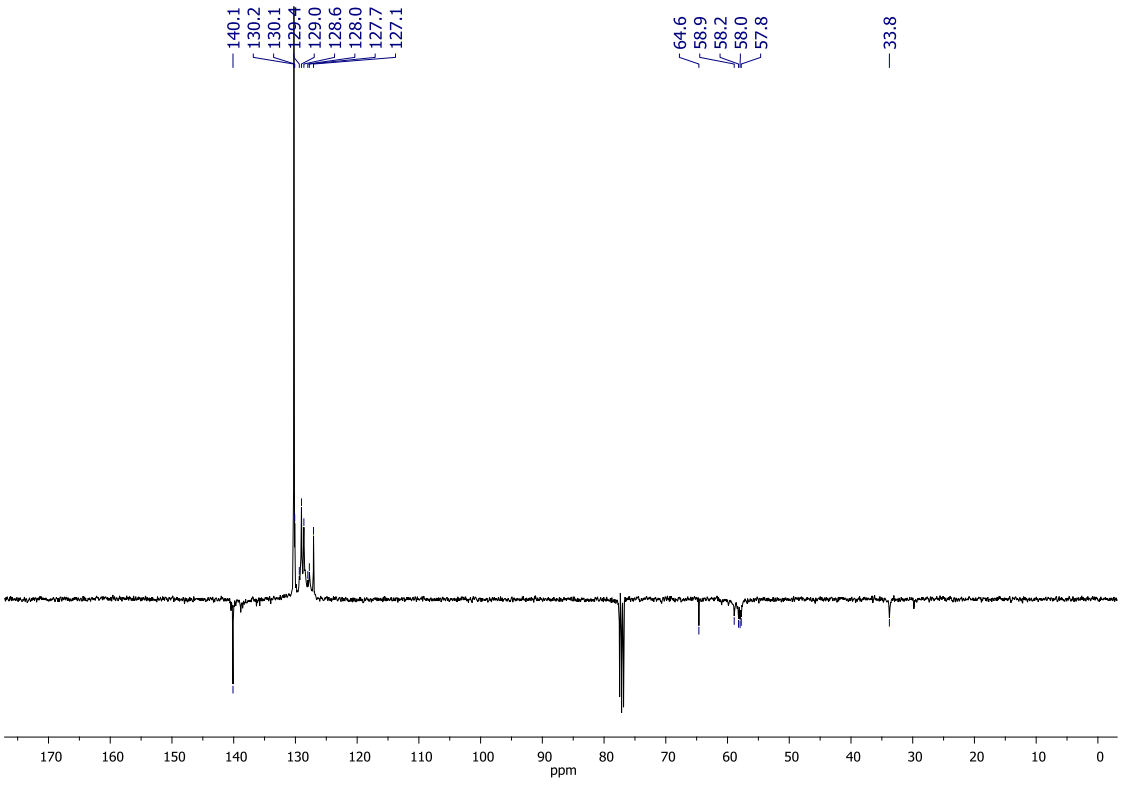

^{1}H NMR of thread **115** (in red) after addition of 1 eq. of macrocycle **102** (in green) and 2 eq. of macrocycle **102** (in blue).

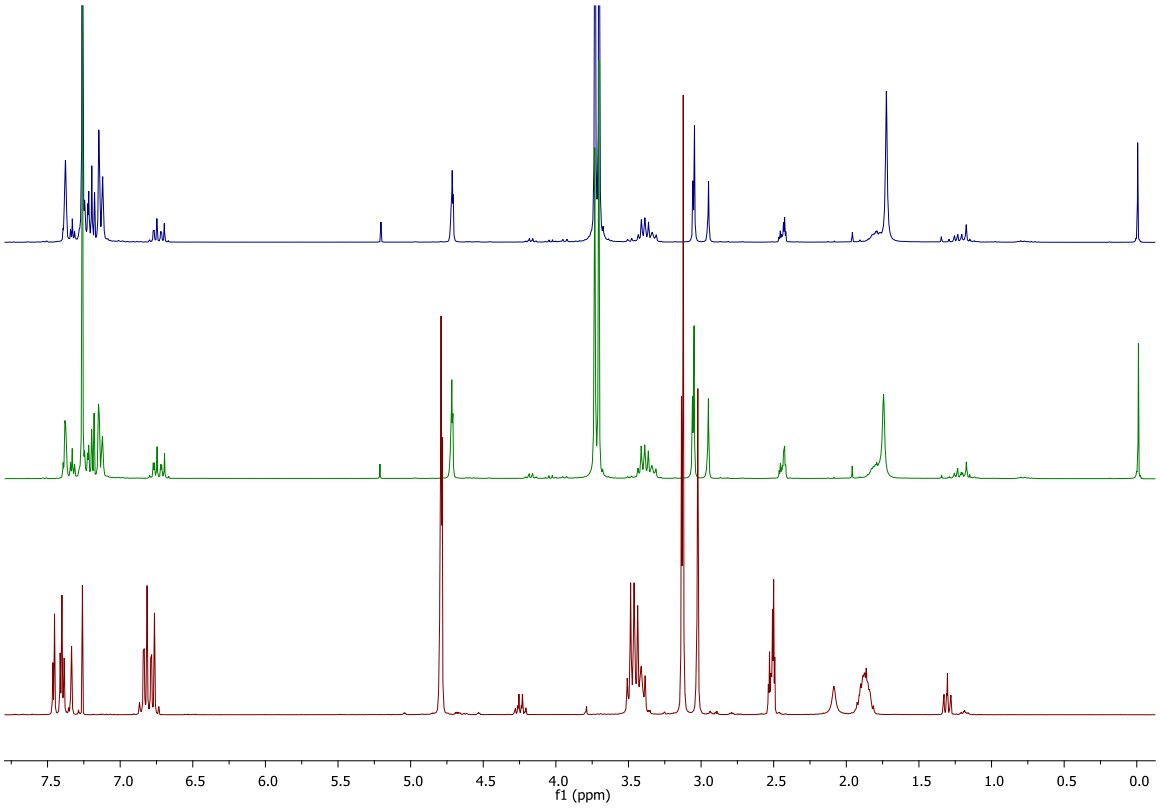

References

(1) Lehn, J. M. *Angew. Chem. Int. Ed.* **1988**, *27*, 89.
(2) Beer, P. D.; Gale, P. A.; Smith, D. K. *Supramolecular Chemistry*; Oxford University Press: Oxford, 2003.
(3) Lichtenthaler, F. W. *Angew. Chem. Int. Ed.* **1995**, *33*, 2364.
(4) Watson, J. D.; Crick, F. H. C. *Nature* **1953**, *171*, 964.
(5) Amabilino, D. B.; Stoddart, J. F. *Chem. Rev.* **1995**, *95*, 2725.
(6) Johnston, A. G.; Leigh, D. A.; Pritchard, R. J.; Deegan, M. D. *Angew. Chem. Int. Ed.* **1995**, *34*, 1209.
(7) Aricó, F.; Badjic, J. D.; Cantrill, S. J.; Flood, A. H.; Leung, K. C.-F.; Liu, Y.; Stoddart, J. F. *Templated Synthesis of Interlocked Molecules*; Springer Berlin / Heidelberg: Los Angeles, 2005; Vol. 249.
(8) Blanco, M.-J.; Chambron, J.-C.; Jimenez, M. C.; Sauvage, J.-P. *Transition-Metal-Templated Synthesis of Rotaxanes*; John Wiley & Sons, Inc.: Illinois, 2003; Vol. Volumen 23.
(9) Harrison, I. T.; Harrison, S. *J. Am. Chem. Soc.* **1967**, *89*, 5723.
(10) Schill, G.; Zollkopf, H. *Nachr. Chem. Techn.* **1967**, *15*, 149.
(11) Cao, J.; Fyfe, M. C. T.; Stoddart, J. F.; Cousins, G. R. L.; Glink, P. T. *J. Org. Chem.* **2000**, *65*, 1937.
(12) Tachibana, Y.; Kihara, N.; Ohga, Y.; Takata, T. *Chem. Lett.* **2000**, 806.
(13) Cantrill, S. J.; Fulton, D. A.; Heiss, A. M.; Pease, A. R.; Stoddart, J. F.; White, A. J. P.; Wiliams, D. J. *Chem. Eur. J.* **2000**, *6*, 2274.
(14) Asakawa, M.; Brancato, G.; Fanti, M.; Leigh, D. A.; Shimizu, T.; Sawin, A. M. Z.; Wong, J. K. Y.; Zerbetto, F.; Zhang, S. *J. Am. Chem. Soc.* **2002**, *124*, 2939.
(15) Wisner, J. A.; Beer, P. D.; Drew, M. G. B.; Sambrook, M. R. *J. Am. Chem. Soc.* **2002**, *124*, 12469.
(16) Glink, P. T.; Oliva, A. I.; Stoddart, J. F.; White, A. J. P.; Wiliams, D. J. *Angew. Chem. Int. Ed.* **2001**, *40*, 1870.
(17) Cantrill, S. J.; Preece, J. A.; Stoddart, J. F.; Wang, Z.-H.; White, A. J. P.; Wiliams, D. J. *Tetrahedron* **2000**, *56*, 6675.
(18) Ashton, P. R.; Baxter, I.; Fyfe, M. C. T.; Raymo, F. M.; Spencer, N.; Stoddart, J. F.; White, A. J. P.; Wiliams, D. J. *J. Am. Chem. Soc.* **1998**, *120*, 2297.
(19) Händel, M.; Plevoest, M.; Gestermann, S.; Vögtle, F. *Angew. Chem. Int. Ed.* **1997**, *36*, 1199.
(20) Dietrich-Buchecker, C. O.; Sauvage, J. P. *Tetrahedron Lett.* **1983**, *24*, 5091.
(21) Ashton, P. R.; Ballardini, R.; Balzani, V.; Belohradsky, M.; Gandolfi, M. T.; Philip, D.; Prodi, L.; Raymo, F. M.; Reddington, M. V.; Spencer, N.; Stoddart, J. F.; Venturi, M.; Wiliams, D. J. *J. Am. Chem. Soc.* **1996**, *118*, 4931.
(22) Ashton, P. R.; Glink, P. T.; Stoddart, J. F.; Tasker, P. A.; White, A. J. P.; Wiliams, D. J. *Chem. Eur. J.* **1996**, 729.
(23) Browne, W. R.; Feringa, B. L. *Nature nanotechnology* **2006**, *1*, 25.
(24) Anelli, P. L.; Spencer, N.; Stoddart, J. F. *J. Am. Chem. Soc.* **1991**, *113*, 5131.

(25) Pons, M.; Millet, O. *Prog. Nucl. Magn. Reson. Spectrosc.* **2001**, *38*, 267.
(26) Hunter, C. A. *J. Am. Chem. Soc.* **1992**, *114*, 5303.
(27) Vögtle, F.; Händel, M.; Meier, S.; Ottens-Hildebrandt, S.; Ott, F.; Schmidt, T. *Liebigs Annalen* **1995**, 739.
(28) Parham, A. H.; Windisch, B.; Vögtle, F. *Eur. J. Org. Chem.* **1999**, 1233.
(29) Brancato, G.; Coutrot, F.; Leigh, D. A.; Murphy, A.; Wong, J. K. Y.; Zerbetto, F. *PNAS* **2002**, *99*, 4967.
(30) Carver, F. J.; Hunter, C. A.; Shannon, R. J. *J. Chem. Soc., Chem. Commun.* **1994**, 1277.
(31) Johnston, A. G.; Leigh, D. A.; Pritchard, R. J.; Deegan, M. D. *Angew. Chem. Int. Ed.* **1995**, *34*, 1209.
(32) Gatti, F. G.; Leigh, D. A.; Nepogodiev, S. A.; Slawin, A. M. Z.; Teat, S. J.; Wong, J. K. Y. *J. Am. Chem. Soc.* **2001**, *123*, 5983.
(33) Belowich, M. E.; Valente, C.; Smaldone, R. A.; Friedman, D. C.; Thiel, J.; Cronin, L.; Stoddart, J. F. *J. Am. Chem. Soc.* **2012**, *134*, 5243.
(34) Moonen, N.; Flood, A.; Fernández, J.; Stoddart, J. *Molecular Machines* **2005**, 99.
(35) Fyfe, M. C. T.; Stoddart, J. F. *Acc. Chem. Res.* **1997**, *30*, 393.
(36) Lane, A. S.; Leigh, D. A.; Murphy, A. *J. Am. Chem. Soc.* **1997**, *119*, 11092.
(37) Keaveney, C. M.; Leigh, D. A. *Angew. Chem. Int. Ed.* **2004**, *43*, 1222.
(38) Murakami, H.; Kawabuchi, A.; Matsumoto, R.; Ido, T.; Nakashima, N. *J. Am. Chem. Soc.* **2005**, *127*, 15891.
(39) Kay, E.; Leigh, D. *Molecular Machines* **2005**, 133.
(40) Tian, H.; Wang, Q. C. *Chem. Soc. Rev.* **2006**, *35*, 361.
(41) Yang, W.; Li, Y.; Liu, H.; Chi, L.; Li, Y. *Small* **2012**, *8*, 504.
(42) Langton, M. J.; Beer, P. D. *Chem. Eur. J.* **2012**, *18*, 14406
(43) Davis, J. J.; Beer, P. D. *Org. Biomol. Chem.* **2009**, *7*, 415.
(44) Williams, A. R.; Northrop, B. H.; Chang, T.; Stoddart, J. F.; White, A. J. P.; Williams, D. J. *Angew. Chem. Int. Ed.* **2006**, *45*, 6665.
(45) Chichak, K. S.; Cantrill, S. J.; Pease, A. R.; Chiu, S. H.; Cave, G. W. V.; Atwood, J. L.; Stoddart, J. F. *Science* **2004**, *304*, 1308.
(46) Radha Kishan, M.; Parham, A.; Schelhase, F.; Yoneva, A.; Silva, G.; Chen, X.; Okamoto, Y.; Vögtle, F. *Angew. Chem. Int. Ed.* **2006**, *45*, 7296.
(47) Lukin, O.; Vögtle, F. *Angew. Chem. Int. Ed.* **2005**, *44*, 1456.
(48) Fujita, M.; Ogura, K. *Bull. Chem. Soc. Jpn.* **1996**, *69*, 1471.
(49) Fujita, M.; Oguro, D.; Miyazawa, M.; Oka, H.; Yamaguchi, K.; Ogura, K. *Nature* **1995**, *378*, 469.
(50) Murase, T.; Horiuchi, S.; Fujita, M. *J. Am. Chem. Soc.* **2010**, *131*, 2866.
(51) Nishiyabu, R.; Kubo, Y.; James, T. D.; Fossey, J. S. *Chem. Commun.* **2011**, *47*, 1124.
(52) Nishiyabu, R.; Kubo, Y.; James, T. D.; Fossey, J. S. *Chem. Commun.* **2011**, *47*, 1106.
(53) Nishimura, N.; Kobayashi, K. *Angew. Chem. Int. Ed.* **2008**, *47*, 6255.
(54) Icli, B.; Sheepwash, E.; Riis-Johannessen, T.; Schenk, K.; Filinchuk, Y.; Scopelliti, R.; Severin, K. *Chem. Sci.* **2011**, *2*, 1719.

(55) Hasell, T.; Schmidtmann, M.; Stone, C. A.; Smith, M. W.; Cooper, A. I. *Chem. Commun.* **2012**, *48*, 4689.
(56) Ariga, K.; Vinu, A.; Miyahara, M.; Hill, J. P.; Mori, T. *J. Am. Chem. Soc.* **2007**, *129*, 11022.
(57) Varpness, Z.; Peters, J.; Young, M.; Douglas, T. *Nano Lett.* **2005**, *5*, 2306.
(58) Meeuwissen, J.; Reek, J. N. H. *Nat. Chem.* **2010**, *2*, 615.
(59) Hart-Cooper, W. M.; Clary, K. N.; Toste, F. D.; Bergman, R. G.; Raymond, K. N. *J. Am. Chem. Soc.* **2012**, *134*, 17873.
(60) Balaji, T.; El Safty, S. A.; Matsunaga, H.; Hanaoka, T.; Mizukami, F. *Angew. Chem.* **2006**, *118*, 7360.
(61) Horcajada, P.; Serre, C.; Vallet-Regí, M.; Sebban, M.; Taulelle, F.; Férey, G. *Angew. Chem.* **2006**, *118*, 6120.
(62) Crowley, J. D.; Lewis, J.; Gavey, E.; Cameron, S. A. *Chem. Sci.* **2012**, *3*, 778.
(63) Han, S. S.; Choi, S.-H.; van Duin, A. C. T. *Chem. Commun.* **2010**, *46*, 5713.
(64) Farrusseng, D. *Metal-Organic Frameworks*; Wiley-VCH, 2011.
(65) Vukotic, V. N.; Harris, K. J.; Zhu, K.; Schurko, R. W.; Loeb, S. J. *Nat. Chem.* **2012**, *4*, 456.
(66) Yang, J.; Ma, J. F.; Batten, S. R. *Chem. Commun.* **2012**, *48*, 7899.
(67) Lin, Z.; Sun, J.; Efremovska, B.; Warmuth, R. *Chem. Eur. J.* **2012**, *18*, 12864.
(68) Kang, J.; Rebek, J. *Nature* **1997**, *385*, 50.
(69) Stang, P. J. *J. Am. Chem. Soc.* **2012**, *134*, 11829.
(70) Feng, X.; Ding, X.; Jiang, D. *Chem. Soc. Rev.* **2012**, *41*, 6010.
(71) Thompson, M. A. *Planaria Software LLC, Seattle, WA* **2004**.
(72) Macrae, C. F.; Bruno, I. J.; Chisholm, J. A.; Edgington, P. R.; Mccabe, P.; Pidcock, E.; Rodriguez-Monge, L.; Taylor, R.; Streek, J.; Wood, P. A. *J. Appl. Crystallogr.* **2008**, *41*, 466.
(73) Allen, C. L.; Williams, J. M. J. *Chem. Soc. Rev.* **2011**, *40*, 3405.
(74) Katritzky, A. R.; Avan, I.; Tala, S. R. *J. Org. Chem.* **2009**, *74*, 8690.
(75) Han, C.; Lee, J. P.; Lobkovsky, E.; Porco, J. A. *J. Am. Chem. Soc.* **2005**, *127*, 10039.
(76) ern , .; la ar n, M.; Orenes, R. A. *J. Am. Chem. Soc.* **2010**, *132*, 10741.
(77) Kenner, G. W.; Seely, J. H. *J. Am. Chem. Soc.* **1972**, *94*, 3259.
(78) Johnston, A. G.; Leigh, D. A.; Murphy, A.; Smart, J. P.; Deegan, M. D. *J. Am. Chem. Soc.* **1996**, *118*, 10662.
(79) Berná, J.; Alajarín, M.; Marín-Rodríguez, C.; Franco-Pujante, C. *Chem. Sci.* **2012**, *3*, 2314.
(80) Gatti, F. G.; Leigh, D. A.; Nepogodiev, S. A.; Slawin, A. M. Z.; Simon, J.; Wong, J. K. Y. *J. Am. Chem. Soc.* **2001**, *123*, 5983.
(81) Alvarez-Pérez, M.; Goldup, S. M.; Leigh, D. A.; Slawin, A. M. Z. *J. Am. Chem. Soc.* **2008**, *130*, 1836.
(82) Watanabe, N.; Furusho, Y.; Kihara, N.; Takata, T.; Kinbara, K.; Saigo, K. *Bull. Chem. Soc. Jpn.* **2001**, *74*, 149.
(83) Furusho, Y.; Shoji, J.; Watanabe, N.; Kihara, N.; Adachi, T.; Takata, T. *Bull. Chem. Soc. Jpn.* **2001**, *74*, 139.

(84) Fu, N.; Gassensmith, J. J.; Smith, B. D. *Supramol. Chem.* **2009**, *21*, 118.
(85) Ciganek, E. *J. Org. Chem.* **1980**, *45*, 1497.
(86) Hahn, W. E.; Szalecki, W.; Boszczyk, W. *Pol. J. Chem.* **1978**, *52*, 2497.
(87) Schalley, C. A.; Beizai, K.; Vögtle, F. *Acc. Chem. Res.* **2001**, *34*, 465.
(88) Maender, O. W.; Janzen, E. G. *J. Org. Chem.* **1969**, *34*, 4072.
(89) Theodorou, V.; Ragoussis, V.; Strongilos, A.; Zelepos, E.; Eleftheriou, A.; Dimitriou, M. *Tetrahedron Lett.* **2005**, *46*, 1357.
(90) Goldeman, W.; Soroka, M. *ARKIVOC* **2010**, *11*, 360.
(91) Semlyen, J. A. *Large ring molecules*; John Wiley & Son Ltd, 1996.
(92) Atkinson, I. M.; Lindoy, L. F. *Self assembly in supramolecular systems*; Royal Society of Chemistry, 2000; Vol. 7.
(93) Anelli, P. L.; Ashton, P. R.; Spencer, N.; Slawin, A. M. Z.; Stoddart, J. F.; Williams, D. J. *Angew. Chem. Int. Ed.* **1991**, *30*, 1036.
(94) Ashton, P. R.; Odell, B.; Reddington, M. V.; Slawin, A. M. Z.; Stoddart, J. F.; Williams, D. J. *Angew. Chem. Int. Ed.* **1988**, *27*, 1550.
(95) Ashton, P. R.; Philip, D.; Spencer, N.; Stoddart, J. F. *J. Chem. Soc., Chem. Commun.* **1991**, 1677.
(96) Gong, C.; Balanda, P. B.; Gibson, H. W. *Macromolecules* **1998**, *31*, 5278.
(97) Trabolsi, A.; Hmadeh, M.; Khashab, N. M.; Friedman, D. C.; Belowich, M. E.; Humbert, N.; Elhabiri, M.; Khatib, H. A.; Albrecht-Gary, A. M.; Stoddart, J. F. *New J. Chem.* **2009**, *33*, 254.
(98) McNitt, K. A.; Parimal, K.; Share, A. I.; Fahrenbach, A. C.; Witlicki, E. H.; Pink, M.; Bediako, D. K.; Plaisier, C. L.; Le, N.; Heeringa, L. P. *J Am Chem Soc* **2009**, *131*, 1305.
(99) Schalley, C. A. *Analytical Methods in Supramolecular Chemistry*; John Wiley & Sons, 2007.
(100) Huang, Y. L.; Hung, W. C.; Lai, C. C.; Liu, Y. H.; Peng, S. M.; Chiu, S. H. *Angew. Chem. Int. Ed.* **2007**, *46*, 6629.
(101) Leigh, D. A.; Thomson, A. R. *Org. Lett.* **2006**, *8*, 5377.
(102) Chen, M.; Han, S.; Jiang, L.; Zhou, S.; Jiang, F.; Xu, Z.; Liang, J.; Zhang, S. *Chem. Commun.* **2010**, *46*, 3932.
(103) Kaufmann, L.; Dzyuba, E. V.; Malberg, F.; Loew, N. L.; Groschke, M.; Brusilowskij, B.; Huuskonen, J.; Rissanen, K.; Kirchner, B.; Schalley, C. *Org. Biomol. Chem.* **2012**, *10*, 5954.
(104) Chen, D.; Martell, A. E. *Tetrahedron* **1991**, *47*, 6895.
(105) Murakami, Y.; Kikuchi, J.; Ohno, T.; Hirayama, T.; Hisaeda, Y.; Nishimura, H.; Snyder, J. P.; Steliou, K. *J. Am. Chem. Soc.* **1991**, *113*, 8229.
(106) Murakami, Y.; Ohno, T.; Hayashida, O.; Hisaeda, Y. *J. Chem. Soc., Chem. Commun.* **1991**, 950.
(107) Vidonne, A.; Philp, D. *Tetrahedron* **2008**, *64*, 8464.
(108) Hassan, N. I.; del Amo, V.; Calder, E.; Philp, D. *Org. Lett.* **2011**, *13*, 458.
(109) Gololobov, Y. G.; Zhmurova, I.; Kasukhin, L. *Tetrahedron* **1981**, *37*, 437.
(110) Huisgen, R.; Knorr, R.; Möbius, L.; Szeimies, G. *Chem. Ber.* **1965**, *98*, 4014.
(111) Rostovtsev, V. V.; Green, L. G.; Fokin, V. V.; Sharpless, K. B. *Angew. Chem. Int. Ed.* **2002**, *41*, 2596.

(112) Tornøe, C. W.; Christensen, C.; Meldal, M. *J. Org. Chem.* **2002**, *67*, 3057.
(113) Dzyuba, . .; aufmann, L.; L w, N. L.; Meyer, A. K.; Winkler, H. D. F.; Rissanen, K.; Schalley, C. A. *Org. Lett.* **2011**, *13*, 4838.
(114) Alcaide, B.; Almendros, P.; Alonso, J. M. *Chem. Eur. J.* **2003**, *9*, 5793.
(115) Gildersleeve, J.; Pascal Jr, R. A.; Kahne, D. *J. Am. Chem. Soc.* **1998**, *120*, 5961.
(116) Fernandes, A.; Viterisi, A.; Coutrot, F.; Potok, S.; Leigh, D. A.; Aucagne, V.; Papot, S. *Angew. Chem. Int. Ed.* **2009**, *48*, 6443.
(117) Gottlieb, H. E.; Kotlyar, V.; Nudelman, A. *J. Org. Chem.* **1997**, *62*, 7512.
(118) Bottari, G.; Leigh, D. A.; Pérez, E. M. *J. Am. Chem. Soc.* **2003**, *125*, 13360.
(119) Quirós, M.; Astorga, C.; Rebolledo, F.; Gotor, V. *Tetrahedron* **1995**, *51*, 7715.
(120) Harris, J. M.; McDonald, R.; Vederas, J. C. *J. Chem. Soc., Perkin Trans. 1* **1996**, 2669.
(121) Gray, C. W.; Johnson, L. L.; Walker, B. T.; Sleevi, M. C.; Campbell, A. S.; Plourde, R.; Houston, T. A. *Bioorg. Med. Chem. Lett.* **2005**, *15*, 5416.
(122) Pattanayak, S.; Sinha, S. *Tetrahedron Lett.* **2011**, *52*, 34.
(123) Branchaud, B. P. *J. Org. Chem.* **1983**, *48*, 3531.
(124) Canle, M.; Clegg, W.; Demirtas, I.; Elsegood, M. R. J.; Maskill, H. *J. Chem. Soc., Perkin Trans. 2* **1999**, 85.
(125) Kricheldorf, H. R. *Chem. Ber.* **1973**, *106*, 3765.
(126) Kitamura, M.; Yano, M.; Tashiro, N.; Miyagawa, S.; Sando, M.; Okauchi, T. *Eur. J. Org. Chem.* **2011**, *2011*, 458.